

New Substrate Classes in Iridium-Catalyzed Asymmetric Hydrogenation

Inauguraldissertation

zur

Erlangung der Würde eines Doktors der Philosophie

vorgelegt der

Philosophisch-Naturwissenschaftlichen Fakultät

der Universität Basel

von

Maurizio Bernasconi

aus Riva San Vitale, Ticino

Basel, 2014

Genehmigt von der Philosophisch-Naturwissenschaftlichen Fakultät
auf Antrag von

Prof. Dr. Andreas Pfaltz

Prof. Dr. Karl Gademann

Basel, den 10.12.2013

Prof. Dr. Jörg Schibler
Dekan

Acknowledgements

I would like to thank my supervisor, Prof. Dr. Andreas Pfaltz for giving me the privilege to carry out my doctoral studies in his research group and for the freedom of research given to me.

I am very thankful to Prof. Dr. Karl Gademann for accepting to co-examine this work, and to Prof. Dr. Dennis Gillingham for chairing the defense.

A very, very big thanks goes to Dr. Paolo Tosatti, not only for correcting and restyling this manuscript, but also for his suggestions and constructive discussions regarding my research and chemistry in general. Grazie mille!!

For their motivation in carrying out research under my supervision and for their synthetic contribution during their Master Theses, I would like to thank my Master students Vincenzo Ramella, Annina Wehrle and Baptiste Barré as well as Christophe Daeppen for his contribution during his Wahlpraktikum.

I wish to express my gratitude to Prof. Dr. Gademann, Fabian Schmid, Dr. Andreas Schumacher, Dr. Paolo Tosatti, Marc-André Müller and Raphaël Liffert for the successful collaborations we had in the course of the last years.

I am very grateful to Dr. Michael Parmentier for fruitful discussions and for keeping my French language skills at a decent level.

For their help in solving numerous computer-related problems I had in the course of my stay in Basel I wish to thank Dr. Paolo Tosatti, Dr. Adrian von der Höh, Dr. York Schramm and Dr. Jaroslav Padevet.

I am grateful to Dr. Heinz Nadig and Dr. Xiangyang Zhang (ETH Zürich) for recording EI and ESI mass spectra as well as Werner Kirsch for performing elemental analyses. A big thank you goes also to the members of the workshop for their technical support.

For the friendly working atmosphere, and the numerous scientific and non-scientific discussions, in Lab 202 during the last four years I thank Dr. Pablo Mauleon, Dr. Andreas Schumacher, Dr. René Tannert, Larissa Pauli, Robin Scheil and Esther Hörmann. It has been a great time with you all!

Furthermore I am thankful to all the former and present Pfaltz group members, especially Marina Mambelli–Johnson, for their contribution to the group social activities.

Desidero ringraziare i miei genitori Laura e Pierre e i miei fratelli Francesco e Alessandro per il loro sostegno e per il loro affetto. Un ringraziamento a Ines, Pia, Arturo e Tödi per avermi fatto sentire a mio agio fin dal nostro primo incontro, é sempre un piacere trascorrere il fine settimana da voi!

Infine, desidero ringraziare mia moglie Jasmine per rendere facili anche le cose più difficili, per la sua pazienza e per il suo immenso sostegno quotidiano, sappi che senza tutto ciò questo lavoro non sarebbe stato possibile.....sei semplicemente fantastica!

ACKNOWLEDGEMENTS	I
LIST OF ABBREVIATIONS	VII
CHAPTER 1.....	1
INTRODUCTION	1
1.1 TRANSITION METAL-CATALYZED ASYMMETRIC HYDROGENATION: A BRIEF INTRODUCTION ^[1]	1
1.2 Iridium-CATALYZED ASYMMETRIC HYDROGENATION ^[18,19]	4
1.2.1 Counterion Effect	6
1.2.2 N,P-Ligands for Asymmetric Hydrogenation	6
1.2.3 NHC Ligands for Asymmetric Hydrogenation	11
1.2.4 Catalytic Cycle ^[66]	12
1.2.5 Drawbacks and Future Challenges in Iridium-Catalyzed Asymmetric Hydrogenation	13
1.2.6 Aim of This Work.....	14
CHAPTER 2.....	15
IRIDIUM-CATALYZED ASYMMETRIC HYDROGENATION OF VINYLSILYL DERIVATIVES ..	15
2.1 INTRODUCTION	15
2.2 RESULTS AND DISCUSSION	20
2.2.1 Vinylsilanes	20
2.2.2 Vinylsiloxanes	34
2.2.3 Vinylsiletanes.....	41
2.2.4 Trifluorovinylsilanes.....	44
2.3 SUMMARY.....	45
CHAPTER 3.....	47
IRIDIUM-CATALYZED ASYMMETRIC HYDROGENATION OF MALEIC ACID DIMETHYLESTERS.....	47
3.1 INTRODUCTION	47
3.1.1 State of the Art	48
3.2 RESULTS AND DISCUSSION	49
3.2.1 Iridium-Catalyzed Asymmetric Hydrogenation of Maleic Anhydrides.....	49

3.2.2 Iridium-Catalyzed Asymmetric Hydrogenation of Maleic Acid Dimethyldiesters	53
3.2.3 Synthetic Applications of the Hydrogenation Products	58
3.3 SUMMARY	60
CHAPTER 4	63
IRIDIUM-CATALYZED ASYMMETRIC HYDROGENATION OF 3,3-DISUBSTITUTED ALLYLIC ALCOHOLS IN ETHERAL SOLVENTS	63
4.1 INTRODUCTION	63
4.2 RESULTS AND DISCUSSION	65
4.2.1 Substrate Synthesis	65
4.2.2 Attempted Iridium-Catalyzed Chemoselective Asymmetric Hydrogenation of α,β -Unsaturated Aldehydes	66
4.2.3 Iridium-Catalyzed Asymmetric Hydrogenation of 3,3-Disubstituted Allylic Alcohols in Etheral Solvents	70
4.3 SUMMARY	76
CHAPTER 5	79
CHIRAL N-HETEROCYCLIC CARBENE/PYRIDINE LIGANDS FOR THE IRIDIUM-CATALYZED ASYMMETRIC HYDROGENATION OF OLEFINS	79
5.1 INTRODUCTION: N-HETEROCYCLIC CARBENES IN TRANSITION METAL CATALYSIS ^[146]	79
5.1.1 N-Heterocyclic Carbenes in Asymmetric Hydrogenation Reactions	80
5.2 RESULTS AND DISCUSSION	84
5.2.1 Iridium-Catalyzed Asymmetric Hydrogenation of Acid-Labile Substrates	84
5.2.2 Catalyst Loading Screening in the Asymmetric Hydrogenation of trans-Methyl Stilbene	86
5.3 SUMMARY ^[167]	87
CHAPTER 6	89
EXPERIMENTAL SECTION	89
6.1 GENERAL INFORMATION	89
6.1.1 Working techniques	89

6.2.1 Analytical methods	89
6.2 Iridium-Catalyzed Asymmetric Hydrogenation of Vinylsilyl Derivatives	92
6.2.1 Synthesis and analytical data of trimethylsilyl- and dimethylphenyl- substituted vinylsilanes.....	92
6.2.2 Synthesis and analytical data of vinylsiloxanes.....	103
6.2.3 Synthesis and analytical data of vinylsiletane 63	105
6.2.4 Synthesis and analytical data of trifluorovinylsilane 67	106
6.2.5 Analytical data for hydrogenation compounds.....	106
6.3 Iridium-Catalyzed Asymmetric Hydrogenation of Maleic Acid Dimethyldiester	112
6.3.1 Synthesis and analytical data of maleic anhydrides.....	112
6.3.2 Synthesis and analytical data of maleic acid dimethylesters.....	114
6.3.3 Analytical data of the hydrogenation products.....	126
6.4 Iridium-Catalyzed Asymmetric Hydrogenation of 3,3-Disubstituted Allylic Alcohols.....	135
6.4.1 Synthesis and analytical data of 3,3-disubstituted α,β -unsaturated esters ...	135
6.4.2 Synthesis and analytical data of 3,3-disubstituted allylic alcohols	136
6.4.3 Synthesis and analytical data of 3,3-disubstituted unsaturated aldehydes....	138
6.4.3 Analytical data of the hydrogenation products.....	139
6.5 Chiral N-Heterocyclic Carbene/Pyridine Ligands for the Iridium-Catalyzed Asymmetric Hydrogenation of Olefins	141
6.5.1 Synthesis and analytical data of the substrates.....	141
6.5.2 Analytical data of the hydrogenation products.....	143
REFERENCES	145

List of Abbreviations

1-Ad	1-adamantyl
α	alpha
Ac	acetyl
aq.	aqueous
Ar	aryl
β	beta
BAr _F	tetrakis[3,5-bis(trifluoromethyl)phenyl]borate
BINAP	2,2'-bis(diphenylphosphino)-1,1'-binaphtyl
Boc	<i>tert</i> -butyloxycarbonyl
Bn	benzyl, phenylmethyl
br	broad
b.p.	boiling point
Bu	butyl
°C	degrees centigrade
<i>c</i>	concentration
calc.	calculated
cat.	catalyst
COD	1,5-cyclooctadiene
conv.	conversion
Cp*	pentamethylcyclopentadienyl
Cy	cyclohexyl
d	doublet
δ	chemical shift (NMR)
DBU	1,8-diazabicyclo[5.4.0]undec-7-ene
DCE	dichloroethane
DIBAL-H	diisobutylaluminium hydride
DIPEA	<i>N,N</i> -diisopropylethylamine
DMAD	dimethylacetylenedicarboxylate
DMAP	4- <i>N,N</i> -dimethylaminopyridine

DMF	<i>N,N</i> -dimethylformamide
DMSO	dimethylsulfoxide
dppf	1,1'-bis(diphenylphosphino)ferrocene
(DHQD) ₂ AQN	hydroquinidine (anthraquinone-1,4-diyl)diether
EA	elemental analysis
<i>ee</i>	enantiomeric excess
EI	electron-impact ionization
Et	ethyl
EtOAc	ethyl acetate
eq.	equivalent(s)
ESI	electron spray ionization
eV	electron volt
GC	gas chromatography
h	hour(s)
HRMS	high resolution mass spectrometry
HPLC	high performance liquid chromatography
Hz	hertz
<i>i</i>	iso
IR	infrared spectroscopy
<i>J</i>	coupling constant
L	ligand
L*	enantiopure ligand
L-DOPA	L-3,4-dihydroxyphenylalanine
LRMS	low resolution mass spectrometry
M	molarity (mol/L)
m	medium (IR)
<i>m</i>	<i>meta</i>
Me	methyl
min.	minutes
MMP	matrix metalloproteinase inhibitor
mL	milliliter
m.p.	melting point

MS	mass spectrometry
Ms	mesityl
ms	molecular sieves
MTBE	methyl- <i>tert</i> -butyl ether
<i>m/z</i>	mass to charge ratio
<i>n</i>	<i>normal</i>
n.d.	not determined
NHC	<i>N</i> -heterocyclic carbene
NMR	nuclear magnetic resonance
o/n	overnight
<i>o</i>	<i>ortho</i>
<i>p</i>	<i>para</i>
kPa	kilopascal, 10 ⁵ Pascal (N/m ²)
Pd/C	palladium on charcoal
pin	pinacol
Ph	phenyl
PHOX	phosphine-oxazoline
PMP	<i>para</i> -methoxyphenyl
ppm	parts per million, 10 ⁻⁶
PPTS	pyridinium <i>para</i> -toluenesulfonate
PTSA	<i>para</i> -toluenesulfonic acid
Py	pyridine
quant.	quantitative
<i>rac</i>	racemic
R _f	retention factor
rt	room temperature
s	strong (IR)
TBAF	tetrabutylammonium fluoride
<i>tert</i>	tertiary
Tf	Trifluoromethanesulfonyl
THF	tetrahydrofuran
TLC	thin layer chromatography

TMEDA	<i>N,N,N',N'</i> -tetramethylethylenediamine
TMS	trimethylsilyl
TOF	turn over frequency
Tol	toluene
t_R	retention time
Ts	tosyl, 4-toluenesulfonyl
UV	ultraviolet
w	weak
xylyl	methylbenzyl
$\tilde{\nu}$	wave number (cm^{-1})

Chapter 1

Introduction

1.1 Transition Metal-Catalyzed Asymmetric Hydrogenation: A Brief Introduction^[1]

After the pioneering work by Wilkinson and Coffey, who discovered that a phosphine-based rhodium catalyst ($[\text{RhCl}(\text{PPh}_3)_3]$) was able to catalyze the reduction of unsaturated carbon-carbon bonds,^[2] metal-catalyzed hydrogenation has attracted increasing interest and has been developed into an extremely powerful method in the organic chemist's repertoire. In particular the preparation and deployment of chiral catalysts that enable the enantioselective hydrogenation of prochiral, unsaturated compounds to give highly enantioenriched molecules has been the object of numerous studies. The quest for chiral transition metal complexes to be used as homogeneous catalysts for hydrogenation started in the late 1960s. A milestone in this discovery process is the work of Knowles, who developed a chiral version of the Wilkinson catalyst by replacing the triphenylphosphine with a chiral phosphine (CAMP, Figure 1)^[3] and, later on, with a bisphosphine ligand (DIPAMP) inspired by Kagan (DIOP).^[4]

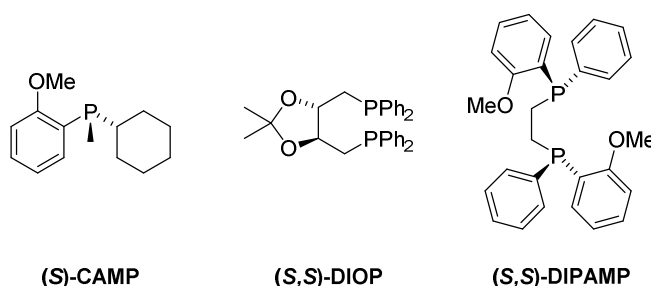


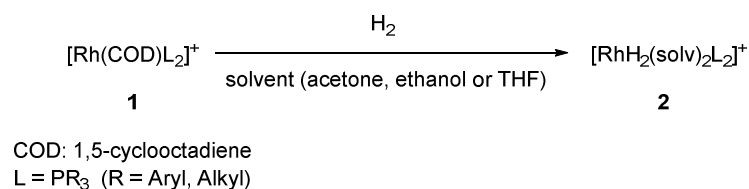
Figure 1: Structure of the first generation phosphine and biphosphines used in rhodium-catalyzed asymmetric hydrogenation.

Following these seminal studies, a plethora of chiral phosphine-based ligands were developed in a short period of time for the rhodium-catalyzed asymmetric hydrogenation of C=C bonds.^[5] The substrate scope of this reaction though was limited to α -dehydroamino acids,^[4d] until the discovery that the BINAP-ruthenium system developed

by Noyori could be used to catalyze the asymmetric hydrogenation of a broader range of functionalized alkenes and, subsequently, ketones.^[6]

The fundamental work carried out by Knowles and Noyori in this field was awarded with the Nobel Prize for Chemistry in 2001.^[6d,7]

Besides the use of neutral rhodium complexes, like the Wilkinson's catalyst, in transition metal-catalyzed hydrogenation, Schrock and Osborn^[8] showed that also cationic species can catalyze this transformation. They found out that rhodium complex **1**, bearing two phosphines and a diene as ligands, reacted under hydrogenation conditions in the presence of a coordinating solvent like acetone, methanol or tetrahydrofuran to afford bis-solvated species **2** (Scheme 1). Such species could be isolated and turned out to be catalytically active.



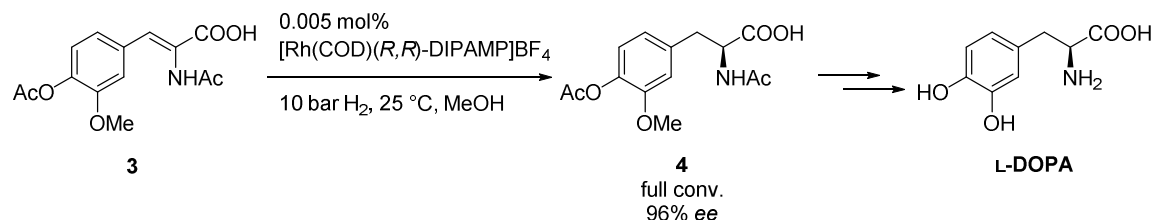
Scheme 1: Study of the activity of cationic rhodium complexes by Schrock and Osborn.

These experiments demonstrated that the dissociation of a solvent molecule from complex **2** is required to allow the coordination of the olefin substrate to the metal center and to start the catalytic cycle. This rate-determining step was found to be fast for these rhodium catalysts,^[9] but it was not for the corresponding iridium analogs, which were almost inactive.^[8a]

The pioneering work of Schrock and Osborn^[8] represents the first application of dienes, and in particular 1,5-cyclooctadiene (COD), as ligands for stabilizing the precatalyst. In the presence of hydrogen the COD ligand is reduced and leaves the coordination sphere of the complexes generating a cationic, coordinatively unsaturated catalyst precursor.

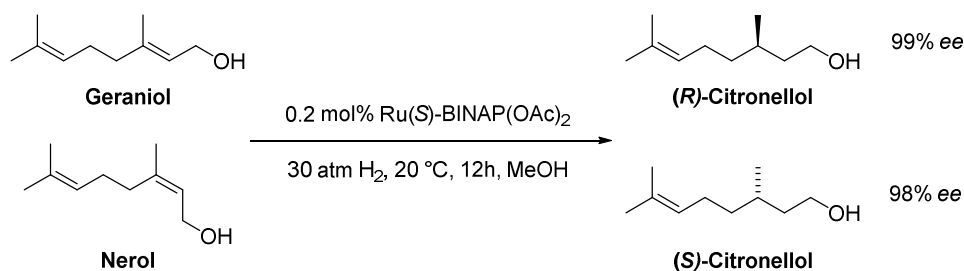
Nowadays, asymmetric hydrogenation is a powerful tool for the stereoselective synthesis of chiral molecules which find widespread application in both academia and industry. In fact, this reaction is characterized by numerous advantages, such as very high enantioselectivities, low catalyst loading, perfect atom economy and high conversions. All these features can be observed in the archetypal rhodium-catalyzed asymmetric

hydrogenation depicted in Scheme 2, where the stereogenic center of **4** is installed by hydrogenation of **3** affording a key intermediate in the synthesis of L-DOPA,^[10] a drug used in the treatment of Parkinson's disease.



Scheme 2: Key step in the synthesis of L-DOPA (Monsanto L-DOPA process).

Another classic example of asymmetric hydrogenation is the synthesis of (*R*)-citronellol, an intermediate in the preparation of vitamin E, or (*S*)-citronellol starting from geraniol or nerol respectively and using Ru(*S*)-(BINAP)(OAc)₂ as the catalyst (Scheme 3).^[11]



Scheme 3: Ru catalyzed asymmetric hydrogenation of allylic alcohols.

The major drawback of Rh- and Ru- catalyzed asymmetric hydrogenation is the need for a coordinating group like an alcohol, a carboxylic acid, an amine or an ester, that directs the hydrogenation process, as shown in Scheme 2 and Scheme 3. This feature explains the chemoselectivity observed in Scheme 3, where the trisubstituted olefin adjacent to the alcohol is reduced, while the other double bond at C6 remains untouched. In fact, only a few Ru and Rh complexes bearing chiral bisphosphorous ligands gave successful results in the hydrogenation of unfunctionalized olefins.^[12] This limitation could be overcome by the use of chiral catalysts based on other transition metals, like platinum,^[13] zirconium or titanium. Indeed, after some pioneering work by Kagan,^[14] Vollhardt^[15] and Paquette,^[16] Buchwald described the use of chiral titanium^[17] and zirconium^[18] cyclopentadienyl derivatives for the asymmetric hydrogenation of unfunctionalized olefins. Despite the high enantioselectivities and conversions achieved using this methodology, the catalysts

developed by Buchwald were not broadly used in either academia or industry. Such metal complexes indeed present several disadvantages as they are moisture- and air-sensitive, require harsh reaction conditions and are effective only with a low substrate/catalyst ratio.^[17-18] Moreover, the catalyst precursors need activation by reaction with *n*-BuLi to generate the low-valent titanocene^[17] and zirconocene^[18] complexes.

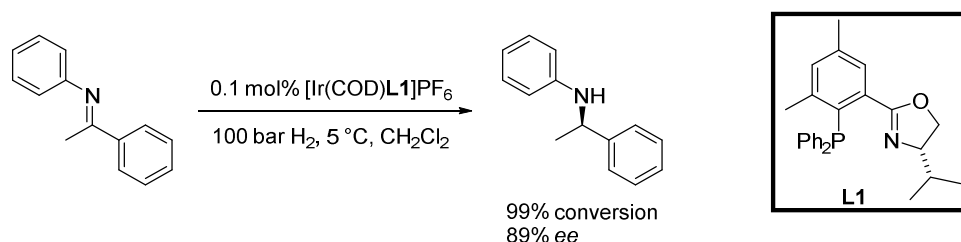
1.2 Iridium-Catalyzed Asymmetric Hydrogenation^[1b,19]

The first report of the use of iridium in hydrogenation reactions has been published by Crabtree,^[20] roughly ten years after the discovery of the Wilkinson catalyst. At that time, the research community was not interested in applying iridium for such transformation, since the iridium analogs of the Wilkinson catalyst, $[\text{IrCl}(\text{PPh}_3)_3]$ was known to react irreversibly with dihydrogen to form the stable $[\text{IrClH}_2(\text{PPh}_3)_3]$ complex. This species, unlike the Wilkinson catalyst, fails to undergo dissociation of a phosphine ligand to allow the binding of the olefin to the metal and thus starting the catalytic cycle.^[9] Similarly, the cationic iridium complexes $[\text{Ir}(\text{COD})\text{PR}_3]^+$ synthesized by Schrock and Osborn^[8], showed weak activity toward hydrogenation of olefins in coordinating solvents (see Scheme 1). Crabtree and coworkers recognized that this low activity was related to the binding strength of the solvent molecules bound to the metal center. They postulated that the strong coordinating solvents used in these experiments inhibit the dissociation of the latter from the active catalyst species, avoiding the coordination of the olefin and thus impeding the catalytic cycle. In order to circumvent catalysts deactivation, Crabtree decided to investigate the activity of $[\text{Ir}(\text{COD})(\text{PR}_3)_2]\text{PF}_6$ complexes in a non-coordinating solvent. After discouraging results in benzene, toluene and hexane, the use of dichloromethane and chloroform resulted in high activities. It was somewhat surprising that chlorinated media were the solvent of choice, since it was known that they might oxidize and deactivate low-valent complexes used in hydrogenation and were therefore avoided in Rh- and Ru-catalyzed hydrogenation.^[2a]

Among many related complexes, $[\text{Ir}(\text{COD})\text{PCy}_3(\text{Py})]\text{PF}_6$, the so-called Crabtree catalyst, turned out to be the most active catalyst for the hydrogenation of di-, tri- and tetra-substituted unfunctionalized olefins in non-coordinating solvents.^[8b,21] The disadvantage

of such complex is the competitive degradation to inactive dimers or trimers during the course of the reaction, which explains the low levels of conversion observed in spite of the high initial turnover frequency (TOF) observed.^[22]

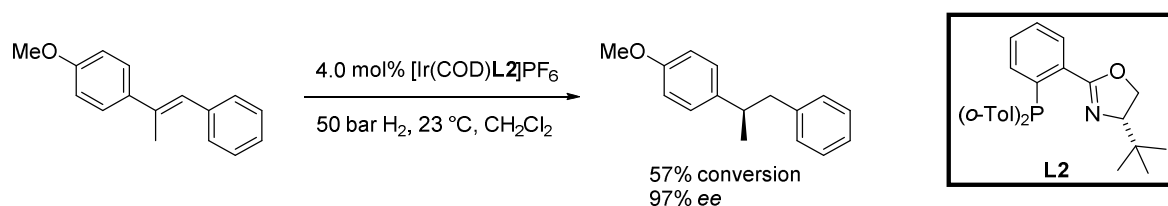
While the first chiral version of the Wilkinson catalyst was developed in a relatively short time,^[3] it took almost 20 years before the first chiral version of the Crabtree catalyst was disclosed. In 1997, our group published the first iridium-catalyzed asymmetric hydrogenation using bidentate N,P-ligands as chirality source (Scheme 4).^[23]



Scheme 4: First example of iridium-catalyzed asymmetric hydrogenation.

This catalyst class, named PHOX, is based on chiral oxazolines, which are derived from chiral amino acids and a tertiary phosphine.^[24] These ligands have found application also in palladium^[24a,24b,24d] and iridium^[24c] catalyzed allylic substitution reactions as well as other transition metals-catalyzed reactions.

In 1998 another reports by our group showed the power of this catalyst class in the hydrogenation of unfunctionalized olefins (Scheme 5).^[25]



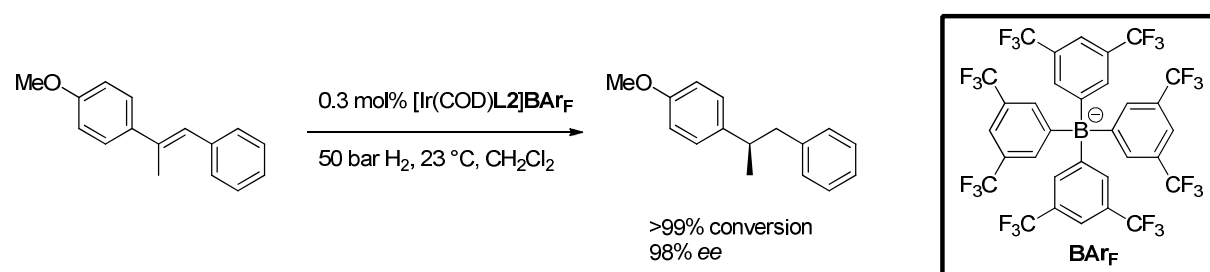
Scheme 5: Application of PHOX ligand L2 in the asymmetric hydrogenation of unfunctionalized olefins.

A variety of unfunctionalized olefins could be reduced with very good enantioselectivities but, unfortunately, high catalyst loading was required to achieve good conversions.^[25] Despite the high initial TOF, the catalyst underwent deactivation in a short period of time. Addition of molecular sieves and the use of dry solvents resulted beneficial, although not

sufficient to reach full conversion. The cause of this deactivation, like in the case of Crabtree's catalyst, was found to be the irreversible formation of an inactive trinuclear complex.^[26]

1.2.1 Counterion Effect

When the hexa fluoro phosphate (PF_6^-) counteranion was replaced by the bulky tetrakis[3,5-bis(trifluoromethyl)phenyl]borate (BAR_F^-),^[27] only a very low catalyst loading (0.3 mol%) was necessary to achieve full conversion in the asymmetric hydrogenation of unfunctionalized olefins (compare Scheme 5 and Scheme 6).^[25]



Scheme 6: Counterion effect on the iridium-catalyzed asymmetric hydrogenation.

The BAR_F anion is considerably less coordinating than the previously used counteranions and therefore does not compete with the substrate in binding to the metal center.^[1b,19,28] This stabilizes the key intermediate in the catalytic process, a bishydride olefin complex, thus promoting the hydrogenation pathway over the deactivation process.^[28a] Nowadays the vast majority of the catalysts used for asymmetric hydrogenation have a cationic iridium metal center, a COD ligand, a BAR_F counterion and an N,P-ligand (in some cases a C,P-ligand with and N-heterocyclic carbene is used, see Section 1.2.3).

1.2.2 N,P-Ligands for Asymmetric Hydrogenation

After the report of the phosphine-oxazolines as good N,P-ligands in the iridium-catalyzed asymmetric hydrogenation, a plethora of other catalysts has been synthesized. In most cases, a six membered ring is formed between the N,P-ligand and the iridium center. The phosphorus moiety is normally a phosphine^[25,29] or a phosphinite^[30] but also some phosphites^[31] have been used.

Contribution by the Pfaltz group

Since 1998 our group has developed a multitude of new N,P-ligands for the iridium-catalyzed asymmetric hydrogenation, of which the most efficient are depicted in Figure 2.

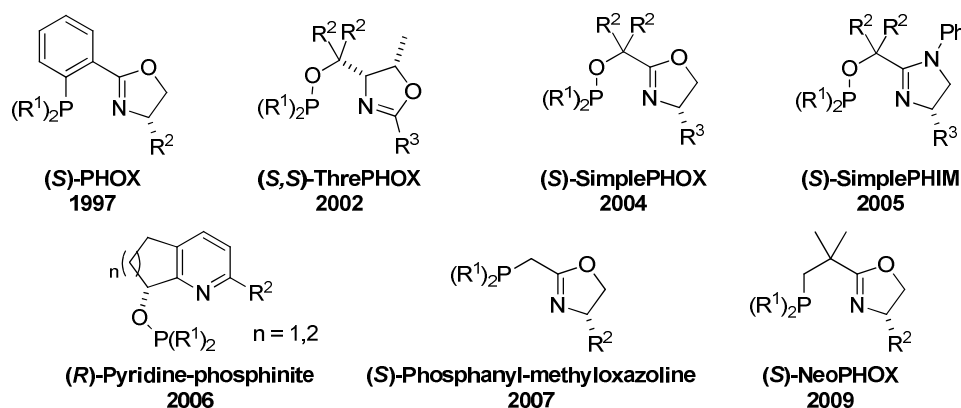
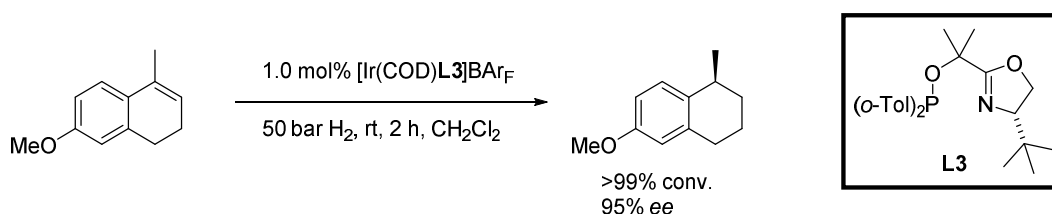


Figure 2: Selection of N,P-ligands developed in the Pfaltz laboratories.

In 2002 the ThrePHOX ligands class was developed.^[30b] This class is substantially different from the PHOX ligands. In fact, besides the use of a phosphinite as P-moiety, the stereogenic information was moved to the center of the backbone. A unique property of this ligand class is the presence of a second stereogenic center on the oxazoline moiety. The ThrePHOX ligands have been successfully applied to the reduction of terminal olefins,^[30b] and later on of 4*H*-chromenes.^[32]

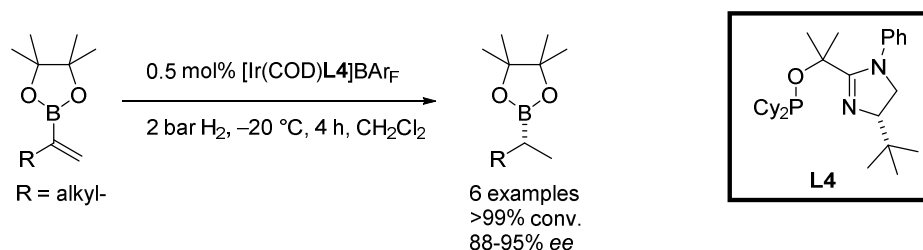
Some years later, the easily synthesized SimplePHOX family^[30c] was applied to the asymmetric hydrogenation of functionalized olefins like acrylic esters, allylic alcohols, and, most importantly, cyclic substrates like 1-methyl-3,4-dihydronaphthalene (Scheme 7).^[30c]



Scheme 7: Application of the SimplePHOX ligand **L3** to the asymmetric hydrogenation of cyclic substrates.

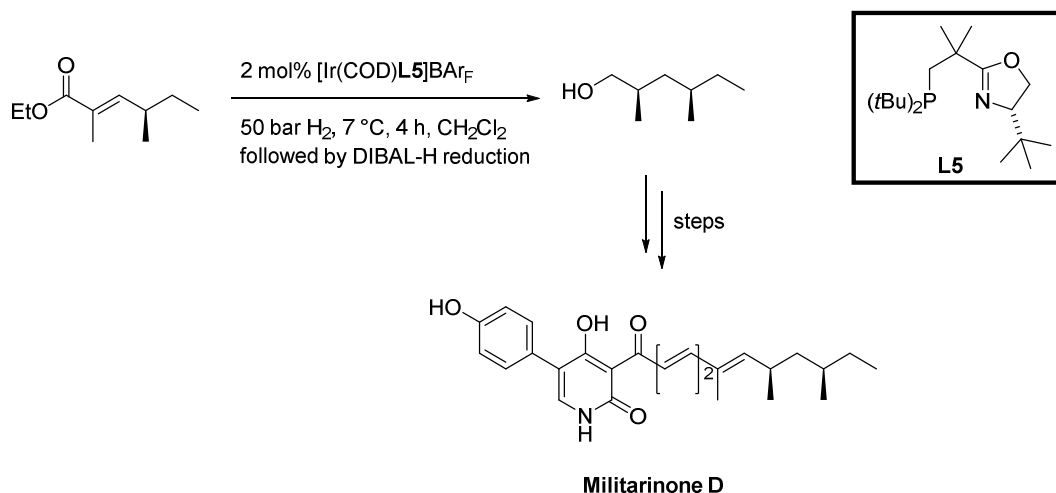
The success of this ligand structure paved the way to the synthesis of related ligand families, like the SimplePHIM^[30f] and the NeoPHOX.^[29d] The usefulness of the SimplePHIM ligands has been recently shown in the asymmetric hydrogenation of terminal vinyl

boronates^[33] to yield chiral boronates, highly versatile building blocks in organic synthesis (Scheme 8).



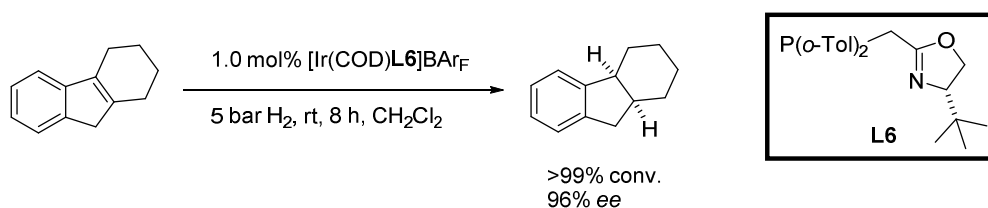
Scheme 8: Application of SimplePHIM ligand **L4** to the asymmetric hydrogenation of terminal vinyl boronates.

NeoPHOX ligands found application in the reduction of a broader range of substrates, among others in the synthesis of the precursors of some natural products. Noteworthy is the use of catalysts based on this ligand class in the synthesis of the key intermediate of Militarinone D,^[34] a pyridone alkaloid isolated from an entomopathogenic fungus that shows general neurotogenic activity (Scheme 9).



Scheme 9: Key step in the total synthesis of Militarinone D.

All the ligands described so far form a six-membered chelate ring with the metal center. However, this property is not a must and indeed also five-membered chelate structures like phosphanyl-methyloxazoline^[29b,35] have been shown to catalyze hydrogenation reactions in a very efficient way.^[36] Using such catalyst class the asymmetric hydrogenation of unfunctionalized tetrasubstituted double bonds became more accessible (Scheme 10).^[29b,36-37]



Scheme 10: Asymmetric hydrogenation of tetrasubstituted double bonds.

In addition to ligands that possess an oxazoline moiety as a source of chirality, another N,P-ligand structure proved to be very useful for the iridium-catalyzed asymmetric hydrogenation of several substrates: the pyridine-phosphinite ligand class.^[30g] Chiral molecules of this type were first synthesized in 2006 in our group and closely mimic the structure of the Crabtree catalyst. Moreover the rigid conformation given by the bicyclic core seems to be crucial for achieving high enantioselectivities.^[30d]

Nowadays this is one of the most powerful ligand classes in the field of iridium-catalyzed asymmetric hydrogenation, mainly due to their broad substrate scope. Indeed, not only unfunctionalized olefins, but also furan derivatives,^[30g] α,β -unsaturated esters^[38] and vinyl borates^[33] could be reduced with excellent results using iridium catalysts based on this ligand class (Figure 3).

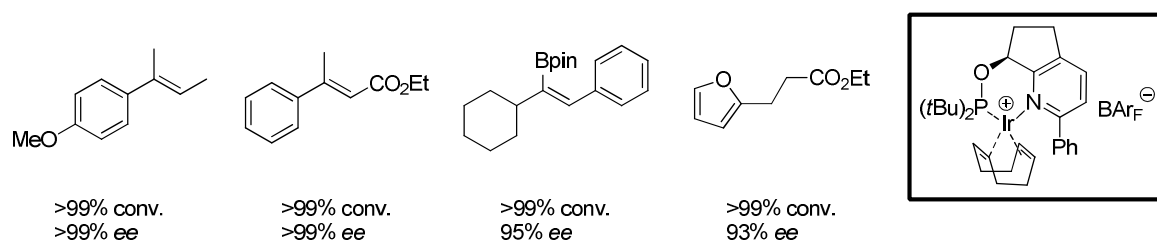


Figure 3: Selection of substrates that can be reduced by a bicyclic pyridine phosphinite-derived iridium catalyst.

In recent years these iridium complexes have found broad application in the asymmetric hydrogenation of key intermediates of many natural products.^[34,39]

Contribution by other laboratories

Besides our group, many other researchers have been interested in the synthesis of novel, powerful N,P-ligands for iridium-catalyzed asymmetric hydrogenation. The Andersson group focused its attention on the development of new PHOX-derived ligands, as well as bicyclic thiazole complexes for the asymmetric hydrogenation of functionalized^[40] and unfunctionalized olefins^[41] and imines.^[42]

The Ding and Zhou laboratories on the other hand showed that larger chelate rings with the metal center are also promising ligands for this transformation. More precisely, seven^[43] (SpinPHOX, Ding), or even nine^[44] (SiPHOX, Zhou) membered systems can act as catalysts in the reduction process of α,β -unsaturated carboxylic acids achieving excellent results.^[44-45] The main characteristic of these ligands is given by the spirocyclic core which keeps the structure rigid allowing for efficient enantiodiscrimination (Figure 4).

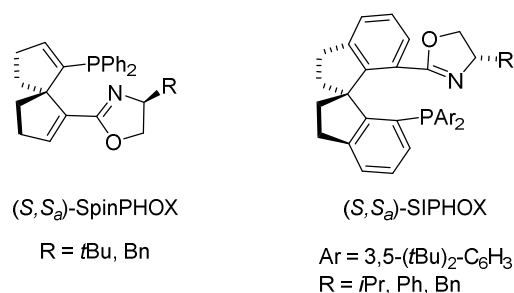
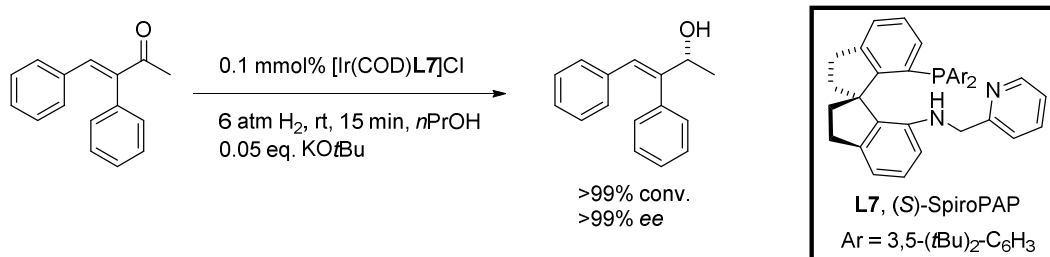


Figure 4: Structures of the spirocyclic ligands SpinPHOX and SiPHOX.

Interestingly, SpinPHOX-derived catalysts are able, besides the hydrogenation of C=C, also to catalyze the asymmetric hydrogenation of imines with remarkably high yield and selectivity.^[43]

In general the asymmetric hydrogenation of C=N bonds, among others quinolines, can also be carried out with N,P-^[46] and P,P-ferrocenyl-based^[47] complexes.

More rare is the enantioselective reduction of C=O bonds catalyzed by iridium complexes. Only in the last few years an efficient catalyst based on an N,P-ligand has been developed for this reaction by the Zhou group.^[48] This methodology is noteworthy as it can be applied to the chemoselective reduction of carbonyl groups leaving olefins situated in close proximity untouched (Scheme 11).^[49]

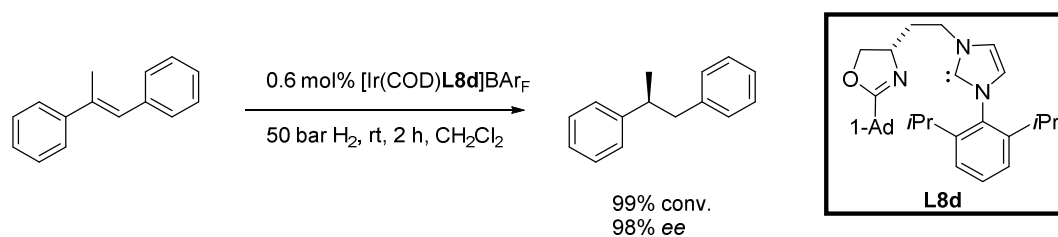


Scheme 11: Chemoselective carbonyl reduction in presence of an olefin.

1.2.3 NHC Ligands for Asymmetric Hydrogenation

N-Heterocyclic carbenes (NHCs) were developed independently by Wanzlick^[50] and Öfele^[51] in the 1960s. However, such complexes have not been used in transition metal catalysis until the mid 1990s, when NHC-based complexes were used as ligands in asymmetric reactions by Enders^[52] and Herrmann.^[53] These particular carbenes are known for stabilizing the low oxidation states of transition metals because of their strong σ -donating and weak π -accepting properties which render the metal center more electron-rich compared to the corresponding phosphine complexes.^[54] Another interesting property of NHC-based complexes is their stability toward air and moisture^[54a,55] that, together with their high activity, makes this class of ligands very interesting for a multitude of different transformations, such as other alkene metathesis,^[56] hydrogenations,^[57] C-C^[53a,58] and C-N^[58e,59] bond formation.

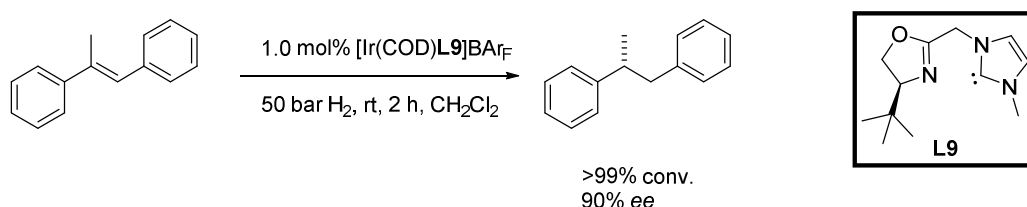
Despite the considerable potential of NHC-based metal complexes, there have been very few applications of them in asymmetric catalysis^[53b,60] before 2001, when Burgess^[54b,61] developed imidazolyli-dine-oxazoline-based NHC complexes such as **L8d** for iridium-catalyzed asymmetric hydrogenation. This was the first report of high enantioselective induction using electron-rich carbene ligands in any catalytic process.^[61] Best results were obtained using ligands containing a seven membered chelate ring, with the *N*-heterocyclic carbene replacing the phosphine of the classical N,P-ligands, and two bulky group, such as 1-adamantyl on the oxazoline moiety and 2,6-di-*isopropyl*phenyl on the imidazolidine (Scheme 12). These ligands could be synthesized using a modular combination of imidazoles and oxazoline electrophiles, giving access to a large library of iridium catalysts.^[54b]



Scheme 12: Hydrogenation of *trans*-methylstilbene using Burgess NHC ligand **L8d**.

Ligand **L8d** found then broad application in the asymmetric hydrogenation of functionalized olefins^[62] and in natural product synthesis.^[63] Moreover, it has been demonstrated that the acidity of this catalyst class is lower compared to known iridium N,P-complexes. Therefore these catalysts are well suited for the hydrogenation of acid-labile substrates like, for example, vinyl ethers.^[64]

Since the best results using N,P-ligands were obtained using six-membered chelate rings, our group became interested in evaluating the efficacy of oxazoline based NHC ligands forming a ring of the same size with the iridium center.^[65] The results obtained were inferior, in terms of enantioselectivity and catalyst loading, compared to those achieved with the seven-membered catalyst developed by Burgess (Scheme 13).^[65]

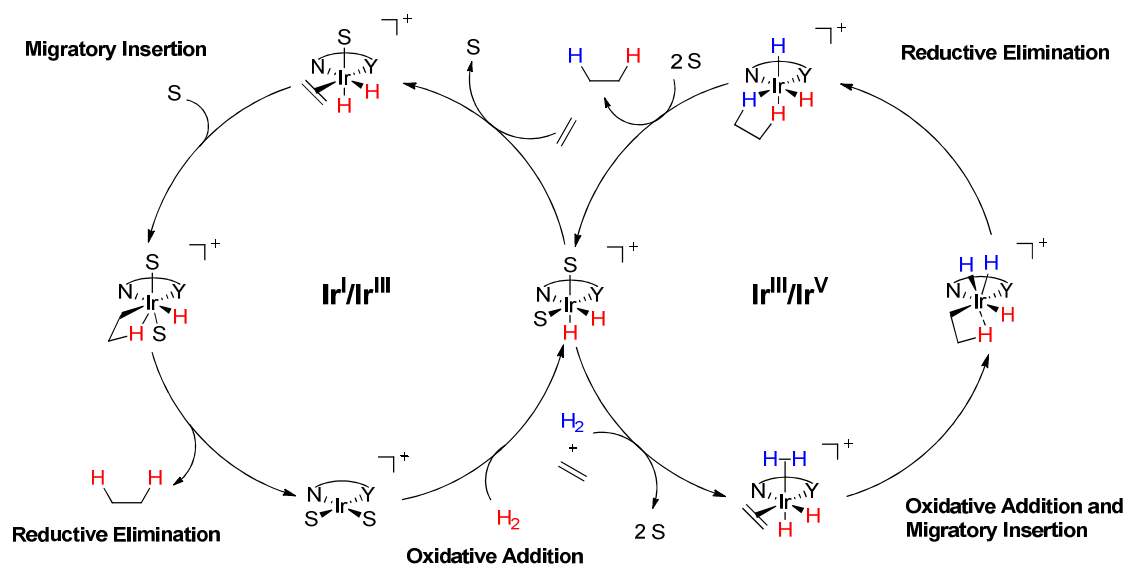


Scheme 13: Hydrogenation of *trans*-methylstilbene using Pfaltz oxazoline-based NHC carbenes.

1.2.4 Catalytic Cycle^[66]

The activation of iridium-catalysts bearing an N,P-ligand by hydrogenation of the cyclooctadiene moiety has been extensively studied^[67] and the mechanism is nowadays unanimously accepted. In contrast, the exact mechanism of the iridium-catalyzed asymmetric hydrogenation is still under debate. Some researchers believe that an $\text{Ir}^{\text{III}}\text{-Ir}^{\text{V}}$ catalytic cycle is responsible for this reaction,^[68] others believe that an $\text{Ir}^{\text{I}}\text{-Ir}^{\text{III}}$ cycle, like the one established in rhodium-catalyzed hydrogenations,^[69] is more plausible.^[70] The first hypothesis is based on computational studies, the second on gas-phase reactivity data^[70b] of a PHOX-catalyst, and polarization NMR spectroscopy.^[70a]

Unfortunately, each experimental and theoretical study on this process has been carried out using various models, different catalysts, substrates and reaction conditions. Therefore, it is almost impossible to compare these results and state clearly which cycle is favored. It might be even possible that depending on the substrate, the conditions and the catalyst of choice, either an $\text{Ir}^{\text{I}}\text{-Ir}^{\text{III}}$ or an $\text{Ir}^{\text{III}}\text{-Ir}^{\text{V}}$ cycle can operate.



Scheme 14: The $\text{Ir}^{\text{I}}/\text{Ir}^{\text{III}}$ (left) and $\text{Ir}^{\text{III}}/\text{Ir}^{\text{V}}$ (right) catalytic cycles for iridium catalyzed hydrogenation of olefins; S = solvent; Y = phosphine or carbene.^[66]

1.2.5 Drawbacks and Future Challenges in Iridium-Catalyzed Asymmetric Hydrogenation

At the beginning of this chapter the advantages of the transition metal-catalyzed asymmetric hydrogenation were listed. However, some drawbacks for this reaction can still be found and represent important challenges in current research. Arguably, one of the major issues is the preferential use of dichloromethane as a solvent for the iridium-catalyzed hydrogenation. Besides being a volatile and toxic solvent, it dissolves the fatty layer of the skin and can cause dermatitis.

Since Crabtree's findings^[2a] only a few reports of iridium-catalyzed asymmetric hydrogenation in non-chlorinated solvents have been published^[49,71] and for some of them additives were required to achieve high activity.^[44]

Although the field of iridium-catalyzed asymmetric hydrogenation has expanded vastly over the last fifteen years, there is still the need to improve catalyst efficiency by new ligand design in order to successfully reduce an even broader range of challenging

substrates for which there is currently no efficient asymmetric hydrogenation methodology available.

1.2.6 Aim of This Work

The main aim of the research presented in this thesis was to expand the current scope of the iridium-catalyzed asymmetric hydrogenation to challenging substrates. Chapter 2 deals with the enantioselective reduction of vinylsilanes while the results of the asymmetric hydrogenation of maleic acid dimethyldiesters are the subject of Chapter 3. The second goal of the research presented herein was the deployment of environmentally advantageous solvents for iridium-catalyzed asymmetric hydrogenations. The outcome of the efforts made in this directions are described in Chapter 4, where ethereal solvents like THF and 2-MeTHF have been successfully used as solvents in the asymmetric hydrogenation of allylic alcohols.

Additionally, some time was devoted to the development of new NHC ligands for the asymmetric hydrogenation of acid-labile substrates, as reported in Chapter 5.

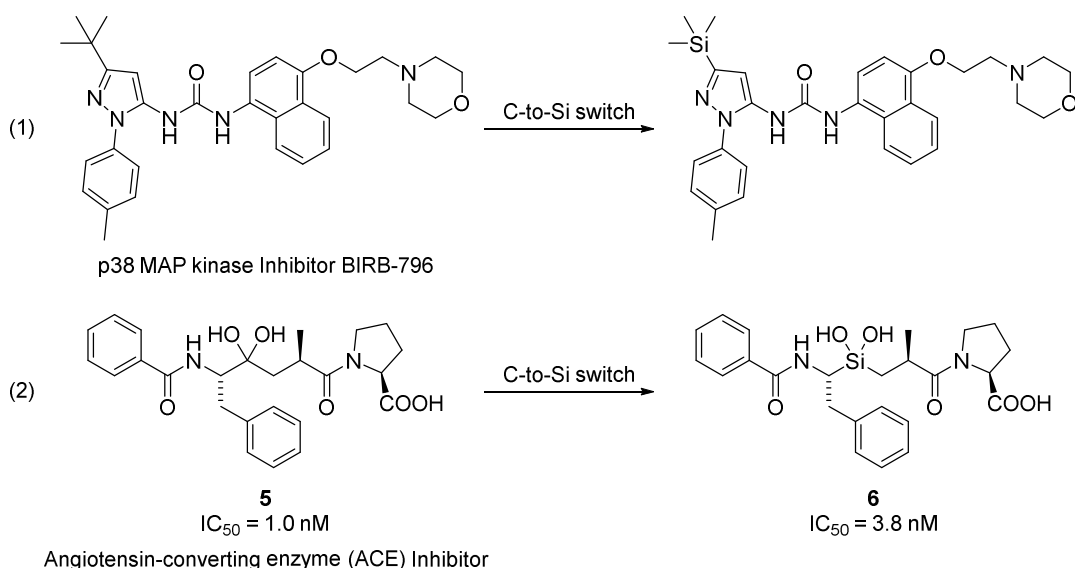
Chapter 2

Iridium-Catalyzed Asymmetric Hydrogenation of Vinylsilyl Derivatives

2.1 Introduction

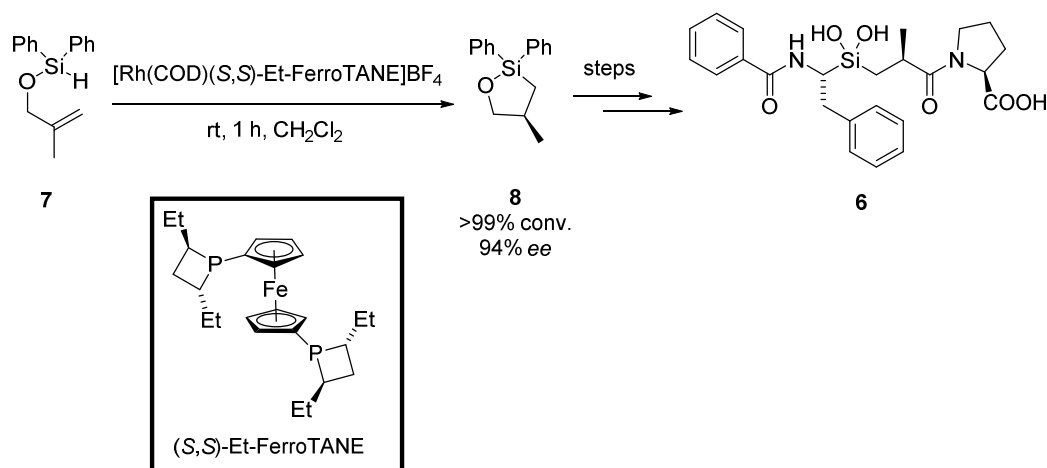
Despite several similarities between silicon and carbon, these two elements are characterized by substantial differences.^[72] Besides the higher atomic weight and the reduced electronegativity, the higher lipophilicity of silicon compounds compared to related carbon analogs plays an important role in the *in vivo* effects of the molecules.^[73] A small increase in lipophilicity can markedly increase the volume of distribution of the molecule reflecting increased tissue penetration, making the silicon-based drugs less prone to hepatic metabolism.^[72]

These properties together with non-toxicity of organosilanes, availability and cheapness have long stimulated the interest of scientists in silicon as a replacement for carbon, particularly in biologically active molecules.^[74] This element has been mainly applied in the design of bioactive organosilanes starting with a molecule of known biological activity and replacing a carbon atom with a silicon atom or derivate. This procedure, called carbon-to-silicon switch,^[74e,75] has found broad application in developing organosilane pesticides^[74b,74c] and recently in the fine tuning of the pharmacological or pharmacokinetic properties of marketed drugs.^[72,76] The two most common carbon-to-silicon switches are depicted in Scheme 15. In the first case a quaternary carbon is replaced by a silicon atom in order to increase hydrophobicity,^[77] whereas in the second example the unstable hydrate was replaced by a stable silicon analog exhibiting similar inhibitory effect as the parent compound (eq. 2).^[74g,78] However, an important drawback in the use of silicon analog **6** as ACE inhibitor was represented by the long synthetic sequence required for its preparation and the use of expensive chiral reagents for the synthesis of the intermediate enantioenriched siladiol.^[74g]



Scheme 15: Most common carbon-to silicon switches.

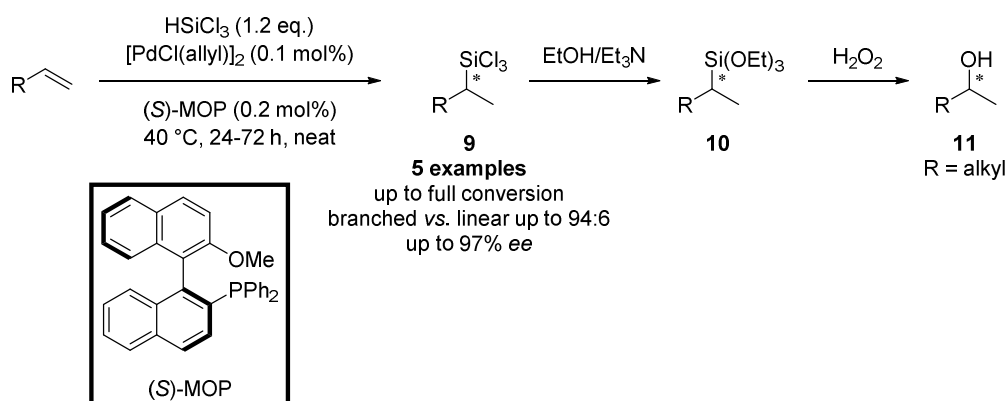
In 2011, the research group of Prof. Sieburth solved this issue by developing an intramolecular asymmetric rhodium-catalyzed hydrosilylation of compound **7** to afford the cyclic enantioenriched silane **8** in good yield and selectivity. This intermediate could then be applied to the synthesis of the target molecule **6** (Scheme 16).^[79]



Scheme 16: Rhodium-catalyzed asymmetric hydrosilylation to afford compound **8** by Sieburth *et al.*^[79]

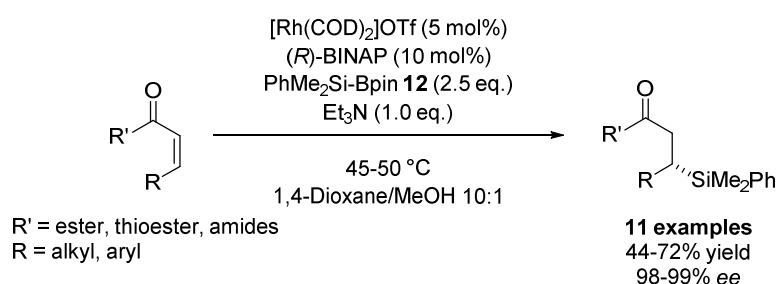
In general, the development of asymmetric methodologies aimed at affording enantioenriched silanes has been neglected for a long time. Only in recent years the need for more efficient synthetic routes to these molecules has stimulated the interest of various research groups.^[80] Although the most frequently used transformations are undoubtedly represented by palladium-,^[80a,80b] copper-,^[80g-j] rhodium-^[80c-e] or *N*-heterocyclic carbene-catalyzed^[80f] conjugated 1,4-additions as well as copper catalyzed

allylic substitutions,^[80k-n] the first method applied to the synthesis of enantioenriched silanes was the asymmetric hydrosilylation of terminal olefins developed by Hayashi and coworkers (Scheme 17).^[80o] This powerful reaction gives access to trichlorosilanes **9** in good yield and selectivity and using low catalyst loadings. Trichlorosilanes **9** can then be transformed into the corresponding vinylsiloxanes **10**, that can subsequently undergo Tamao–Fleming oxidation^[81] to the related enantioenriched alcohols **11**.



Scheme 17: First asymmetric hydrosilylation by Hayashi *et al.*^[80o]

The majority of the available methodologies for the synthesis of enantioenriched silanes involve the use of (dimethylphenylsilyl)boronic acid pinacol ester **12** as the silicon source, limiting the nature of the substituents on the silicon atom to the dimethylphenyl group (a representative example is shown in Scheme 18).



Scheme 18: Application of reagent **12** in the synthesis of enantioenriched dimethylphenylsilanes.^[80d]

Reports of enantioenriched silanes bearing substituents other than the dimethylphenyl group are scarce.^[80c,80r,82] One of such examples is represented by the iridium-catalyzed asymmetric hydrogenation of trisubstituted vinylsilanes to afford enantioenriched trimethylsilanes (Table 1).^[80r] Despite the good conversion, this transformation suffered

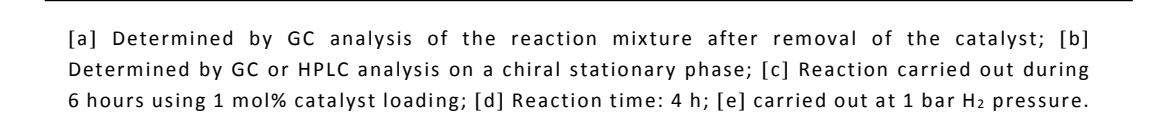
from poor to moderate enantioselectivities (28-58% *ee*). Indeed only for the specific substrate **13** excellent enantiomeric excess could be achieved (Table 1).

Given the lack of generality of the current methods for the preparation of enantioenriched silanes, our group became interested in broadening the substrate scope of the asymmetric hydrogenation of vinylsilanes using N,P-based iridium catalysts. Aie Wang, a former member of the Pfaltz group, started this project by comparing the performance of our catalysts with those of Andersson's catalyst, [Ir(COD)**L10**] BAR_F (Table 2).^[83]

Table 1: Iridium-catalyzed asymmetric hydrogenation of trimethylvinylsilanes **13-18**.^[80r]

13-18		L10	
13 >99% conv. 98% <i>ee</i> (<i>R</i>)	14 >99% conv. 28% <i>ee</i> (<i>S</i>)	15 >99% conv. 58% <i>ee</i> (<i>S</i>)	16 >99% conv. 48% <i>ee</i> (–)
		17 >99% conv. 55% <i>ee</i> (+)	18 >99% conv. 55% <i>ee</i> (<i>S</i>)

After an extensive catalyst screening in which all the different ligand classes were tested, Wang figured out which ligands allowed to achieve best results in terms of selectivity and yield for every test substrate (Table 2). Unfortunately, none of the N,P-ligands tested resulted to be consistently the ligand of choice for a variety of substrates, but, in general ligands **L3** and **L11** performed best. Indeed, six out of the nine vinylsilanes depicted in Table 2 could be hydrogenated using catalysts bearing one of these two ligands. Despite the lack of a universal ligand for the asymmetric hydrogenation of vinylsilanes, the enantiomeric excesses obtained were promising and better than the reference values reported by Andersson using the phosphine/thiazole ligand **L10** (compare Table 1 vs. Table 2). For example vinylsilane **15** could be reduced with full conversion and excellent enantiomeric excess in only two hours, whilst in the previous example of Andersson twelve hours were required to reach full conversion with a poor optical yield (28% *ee*). Moreover, outstanding results were achieved also in the hydrogenation of alkyl,alkyl



2.2 Results and Discussion

2.2.1 Vinylsilanes

2.2.1.1 Synthesis of Vinylsilanes

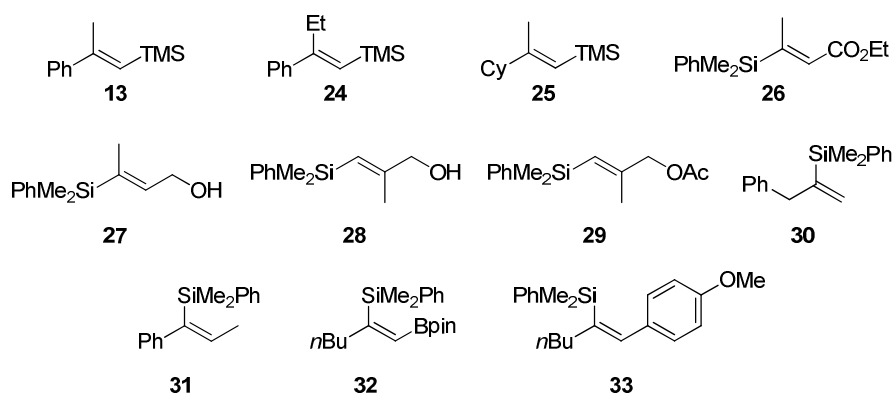
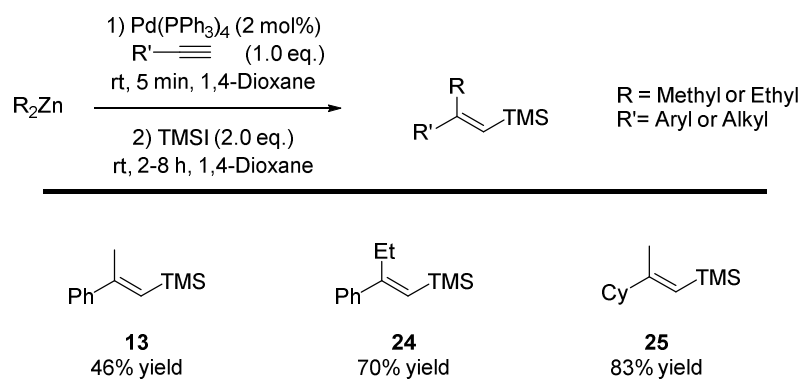


Figure 5: Synthesized vinylsilanes.

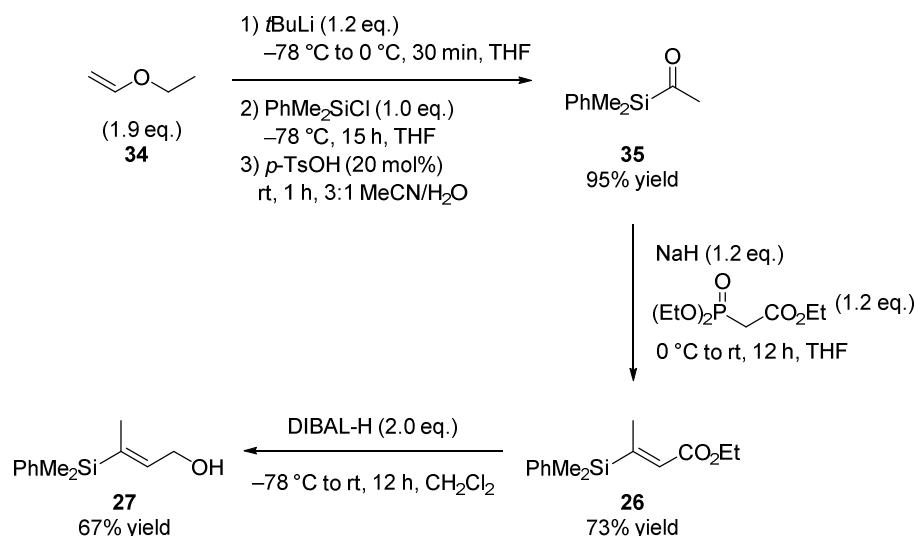
Different synthetic pathways have been followed for the synthesis of dimethylphenylvinylsilanes, but only one method was used for the synthesis of the trimethylsilyl analogs, which were synthesized starting from commercially available terminal alkynes *via* palladium-catalyzed coupling reaction with iodotrimethylsilane and an organozinc reagent (Table 3).^[84]

Table 3 Synthesis of trimethylvinylsilanes following the procedure developed by Chatani *et al.*^[84]



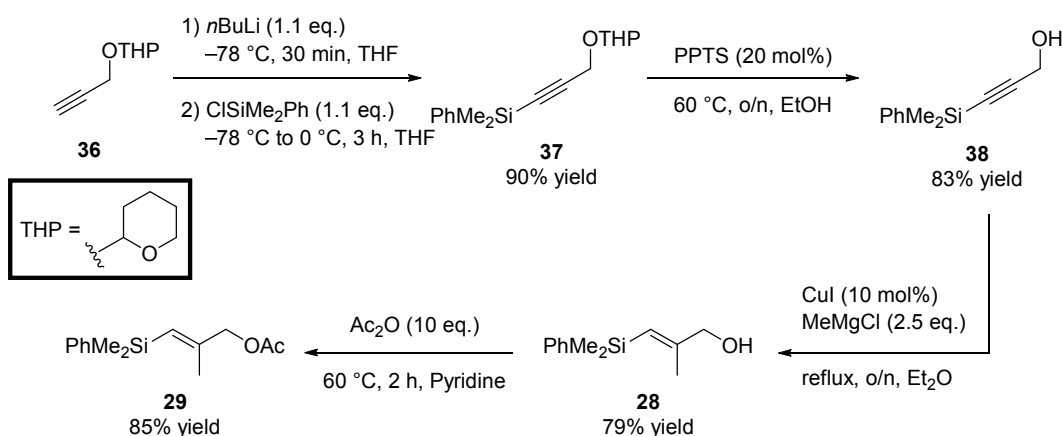
Despite some problems of regioselectivity in the synthesis of vinylsilane **13**, which resulted in moderate yield, substrates **24** and **25** could be prepared under the same reaction conditions in perfect stereo- and regioselectivity.

In order to expand the substrate scope of the hydrogenation and considering the considerable amount of trimethylsilanes already synthesized and tested by Wang, the focus of the project was moved to the related dimethylphenylvinylsilanes. The two step synthesis of α,β -unsaturated ester **26** started from vinyl ether **34**, which was transformed into acylsilane **35**. After Horner–Wadsworth–Emmons reaction and DIBAL-H reduction allylic alcohol **27** was afforded in good yield (Scheme 19).



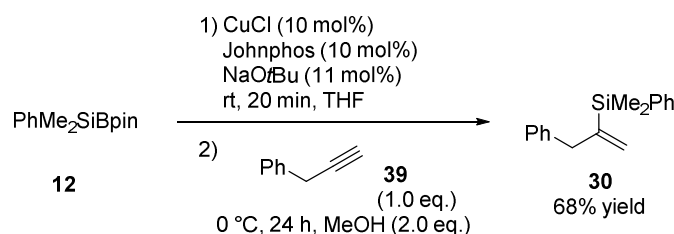
Scheme 19: Synthetic pathway to vinylsilanes **26** and **27**.

The isomeric allylic alcohol **28** was obtained through a four steps synthesis. Silylation of protected propargylic alcohol **36**^[85] followed by acidic cleavage of the tetrahydropyran protecting group^[86] resulted in the formation of free alcohol **38**, that was subjected to organocupration using methylmagnesium chloride to give allylic alcohol **28** in 83% yield and perfect regioselectivity.



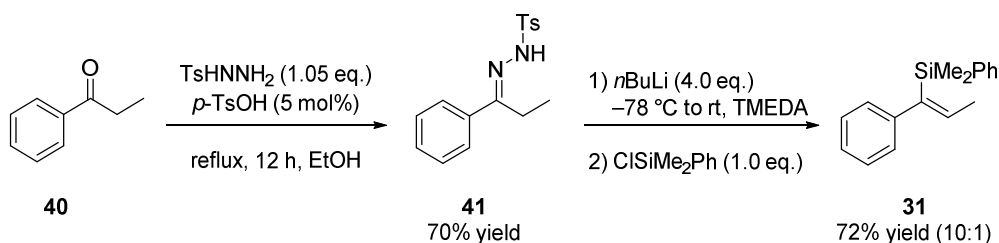
Scheme 20: Synthesis of vinylsilanes **28** and **29**.

Acetalization using acetic anhydride^[87] yielded vinylsilane **29** (Scheme 20). Recent advances in the field of copper catalysis allowed for the synthesis of substrate **30** *via* a highly regioselective silylcupration of terminal alkyne **39** using (dimethylphenylsilyl)boronic acid pinacol ester **12** as a silicon source (Scheme 21).^[88]



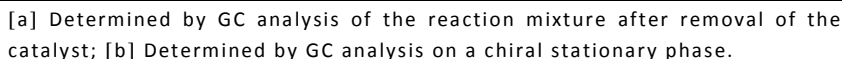
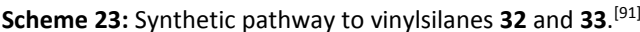
Scheme 21: Synthesis of vinylsilane **30** following the procedure published by Loh *et al.*^[88]

One of the best known synthetic methods for synthesizing vinylsilanes is the Shapiro reaction. In this reaction, discovered in 1967,^[89] a tosylhydrazone bearing an α -hydrogen reacts with an excess of *n*-butyllithium to generate a vinyllithium that can be trapped by a broad variety of electrophiles, generating olefins which may be difficult to prepare by other means. Using this methodology, vinylsilane **31** could be obtained in good yield starting from propiophenone **40** in 2 steps (Scheme 22).^[90]



Scheme 22: Synthesis of vinylsilanes **31** *via* Shapiro reaction.

Finally, vinylsilane **32** was obtained by palladium-catalyzed regio- and stereoselective silaboration of 1-hexyne **42**, using reagent **12** in good yield. This compound could then easily be transformed into compound **33** under Suzuki–Miyaura conditions (Scheme 23).^[91]



The outcome of the reaction using this ligand class seemed to be rather independent of either the size of the carbocyclic ring and the substituent on the phosphine moiety. Indeed, the results summarized in Table 4 show that stirring the substrate in the presence of 0.5 mol% catalyst under 50 bar hydrogen afforded silane **43** in similar enantioselectivities (90%-94% *ee*), independently of the pyridine phosphinite ligand used. Encouraged by the results obtained, the influence of the hydrogen pressure as well as the reaction temperature was examined using the best ligand out of the initial screening, **L17**.

Table 5: Pressure and temperature screening in the hydrogenation of compound **13**.

Reaction scheme: **13** $\xrightarrow[\text{Pressure H}_2, \text{ Temperature, 2 h, CH}_2\text{Cl}_2]{0.5 \text{ mol\% [Ir(COD)L17]BARF}}$ **43**

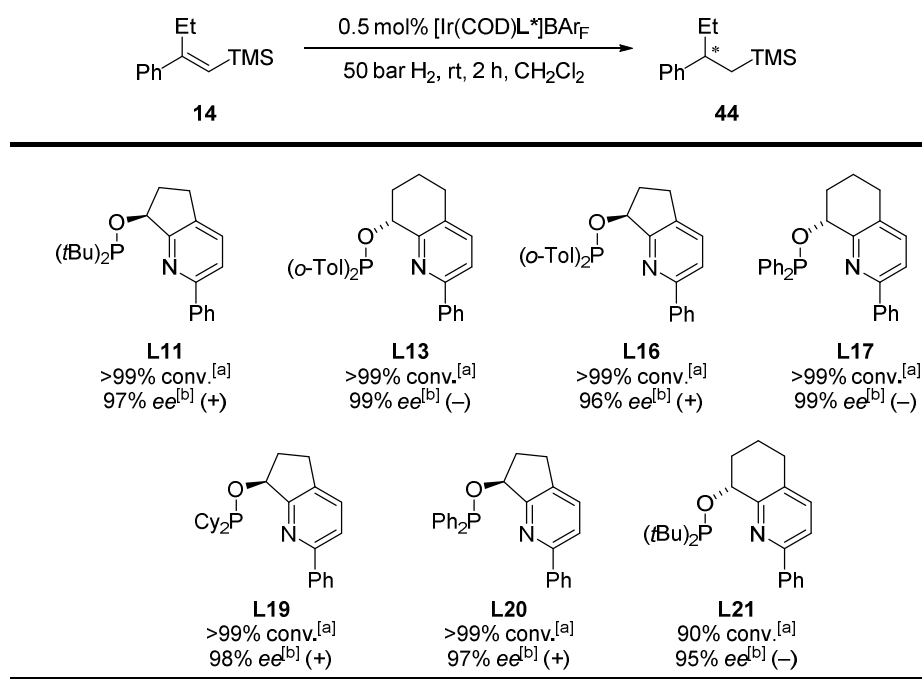
Entry	Pressure (bar)	Temperature (°C)	Conv. ^[a] (%)	<i>ee</i> ^[b] (%)
1	50	rt	>99	94 (–)
2	50	–20	93	96 (–)
3 ^[c]	10	rt	>99	95 (–)
4 ^[d]	10	–20	74	72 (–)

[a] Determined by GC analysis of the reaction mixture after removal of the catalyst; [b] Determined by GC analysis on a chiral stationary phase; [c] Reaction time: 4 h; [d] Reaction time: 7 h.

As shown in Table 5, lowering either the reaction temperature to –20 °C resulted in a slight improvement of the enantioselectivity (96 vs. 94% *ee*) but incomplete conversion (entry 2). On the other hand, with a reduced hydrogen pressure silane **43** could be obtained with 95% *ee* while keeping full conversion (entry 3). However, lowering both parameters at the same time had a negative influence on both yield and selectivity (entry 4). Once established that pyridine-phosphinite ligands were the most suited for the hydrogenation of vinylsilanes, a further screening of a selection of such ligands was carried out using compound **14** as test substrate (Table 6). As expected, excellent results were obtained both in terms of yield and selectivity. An analysis of the performance of different catalysts showed that while the nature of phosphinite moiety in the five membered carbocyclic ring scaffolds exhibited little influence on the enantioselectivity of the reaction, six-membered

carbocyclic ring pyridine phosphinite ligands performed better with diarylphosphinites than dialkyl ones (*cf.* results with **L13**, **L17** and **L21**, Table 6).

Table 6: Ligand screening in the hydrogenation of vinylsilane **14**.

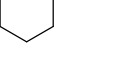


[a] Determined by GC analysis of the reaction mixture after removal of the catalyst; [b] Determined by GC analysis on a chiral stationary phase.

In the hydrogenation of alkyl/alkyl-disubstituted vinylsilane **25** the difference between the results achieved using catalysts bearing a pyridine-phosphinite ligand and the catalysts possessing other N,P-ligand classes was even more striking.

Indeed, all the other N,P-ligand classes tested in the iridium-catalyzed asymmetric hydrogenation of substrate **25** yielded silane **45** in excellent yield but poor enantiomeric excess, whereas pyridine-phosphinites resulted the ligands of choice also for purely alkyl-substituted substrates (Table 7). It should also be noted that the enantiomeric excess of silane **45** could be enhanced to 97% by carrying out the hydrogenations under 10 bar hydrogen pressure with catalyst [Ir(COD)**L17**]BAR_f, maintaining all other parameters fixed.

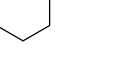
Table 7: Ligand screening in the hydrogenation of vinylsilane **25**.



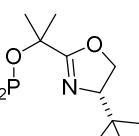
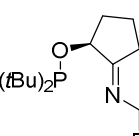
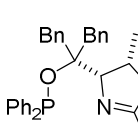
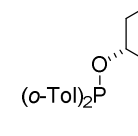
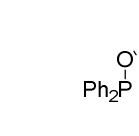
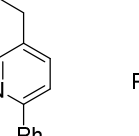
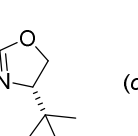
25

0.5 mol% [Ir(COD)**L**]⁺BAR_F⁻

50 bar H₂, rt, 4 h, CH₂Cl₂



45

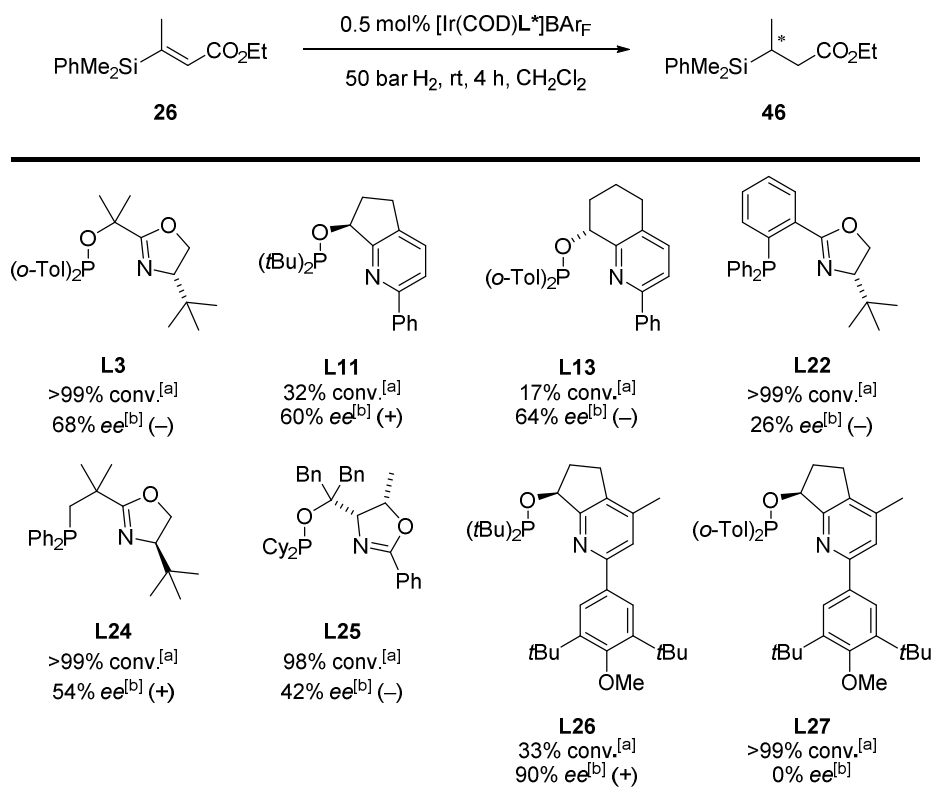
 <p>L3 >99% conv.^[a] 5% ee^[b] (+)</p>	 <p>L11 >99% conv.^[a] 92% ee^[b] (-)</p>	 <p>L12 >99% conv.^[a] 11% ee^[b] (-)</p>	 <p>L13 >99% conv.^[a] 91% ee^[b] (+)</p>
 <p>L17 >99% conv.^[a] 95% ee^[b] (+)</p>	 <p>L22 >99% conv.^[a] 30% ee^[b] (-)</p>	 <p>L23 >99% conv.^[a] 2% ee^[b] (-)</p>	

[a] Determined by GC analysis of the reaction mixture after removal of the catalyst; [b] Determined by GC analysis on a chiral stationary phase.

Although good to excellent results could be obtained in the asymmetric hydrogenation of trimethylvinylsilanes, thus demonstrating the viability of vinylsilanes as substrates for this transformation with our catalysts, the products obtained find little application in organic synthesis. For instance, the trimethylsilyl- group cannot undergo Tamao–Fleming oxidation to the corresponding alcohols, as for this transformation the presence of a heteroatom, a hydrogen an aryl or heteroaryl-group on the silicon atom is required,^[81] although some exceptions are known.^[92] For this reason, the hydrogenation of easily oxidized dimethylphenylvinylsilanes became the main focus of the project.

The first substrate of this kind that was tested in the iridium-catalyzed asymmetric hydrogenation was α,β -unsaturated ester **26** (Table 8). In contrast to the vinylsilanes evaluated earlier, for this specific compound various N,P-ligands yielded the desired product **46** with full conversion while catalysts bearing a pyridine-phosphinite ligand like **L11**, **L13**, **L26** and **L27** proved to be either poorly active or selective or both.

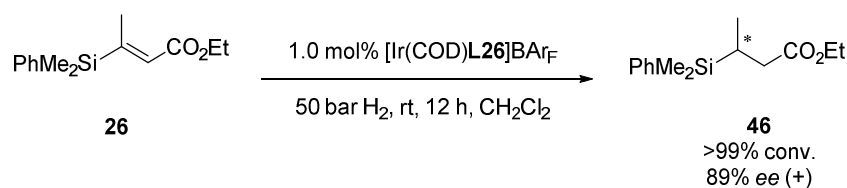
Table 8: Ligand screening for the hydrogenation of vinylsilane **26**.



[a] Determined by GC analysis of the reaction mixture after removal of the catalyst; [b] Determined by HPLC analysis on a chiral stationary phase.

In particular the catalyst based on ligand **L26** afforded the product **46** with poor conversion but 90% *ee*, the best enantioselectivity registered among the catalysts screened. Most surprisingly the related *ortho*-tolyl phosphine analog **L27** gave opposite results with full conversion but giving silane **46** as a racemic mixture.

In order to achieve full conversion of **26** with catalyst [Ir(COD)**L26**]BAR_F, the reaction was carried out for a prolonged time and with 1.0 mol% of catalyst. In this case the substrate was completely transformed into **46** with negligible erosion of enantioselectivity (Scheme 24).

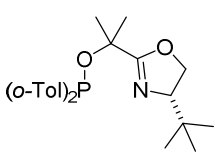
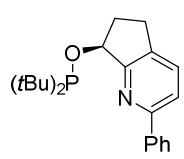
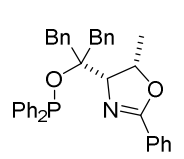
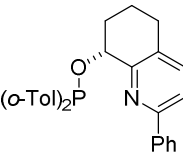
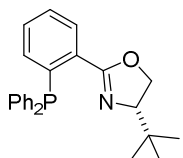
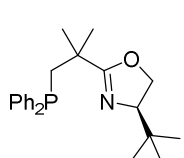
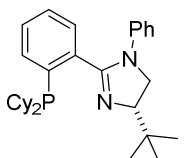
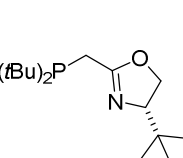


Scheme 24: Optimized reaction conditions for the reduction of substrate **26**.

The level of enantioselectivity obtained is slightly inferior to the benchmark of 95% *ee* achieved *via* copper-catalyzed asymmetric hydrosilylation, however, milder, more practical reaction conditions were required for the hydrogenation compared to the hydrosilylation reaction that had to be performed at $-78\text{ }^{\circ}\text{C}$.^[80q]

From these first investigations it seemed that the reduction of trimethyl substituted vinylsilanes proceeded with better levels of enantioselectivity compared to the reduction of dimethylphenyl substituted analogs. This impression was also confirmed when allylic alcohol **27** was used as a test substrate for the hydrogenation. Despite the good conversions only poor selectivities were achieved (Table 9).

Table 9: Ligand screening in the asymmetric hydrogenation of vinylsilane **27**.

$\text{PhMe}_2\text{Si}-\text{CH}=\text{CH}-\text{CH}_2\text{OH} \xrightarrow[50\text{ bar H}_2, \text{rt, 12 h, CH}_2\text{Cl}_2]{0.5\text{ mol\% [Ir(COD)L}^*\text{]BARf}} \text{PhMe}_2\text{Si}-\text{CH}^*(\text{H})-\text{CH}_2\text{CH}_2\text{OH}$ <div style="display: flex; justify-content: space-around; width: 100%;"> 27 47 </div>			
 <p>L3 24% conv.^[a] 4% <i>ee</i>^[b] (–)</p>	 <p>L11 22% conv.^[a] 32% <i>ee</i>^[b] (+)</p>	 <p>L12 98% conv.^[a] 37% <i>ee</i>^[b] (–)</p>	 <p>L13 4% conv.^[a] n.d. <i>ee</i></p>
 <p>L22 >99% conv.^[a] 26% <i>ee</i>^[b] (–)</p>	 <p>L24 >99% conv.^[a] 16% <i>ee</i>^[b] (+)</p>	 <p>L28 >99% conv.^[a] 15% <i>ee</i>^[b] (–)</p>	 <p>L29 >99% conv.^[a] 16% <i>ee</i>^[b] (–)</p>

n.d. = not determined; [a] Determined by GC analysis of the reaction mixture after removal of the catalyst; [b] Determined by HPLC analysis on a chiral stationary phase.

Since in general superior enantioselectivities were obtained with substrates bearing the silyl group at the less substituted carbon atom, the isomeric allylic alcohol **28** was synthesized and tested in the iridium-catalyzed asymmetric hydrogenation (Table 10). Interestingly, only a few complexes were able to catalyze in this case. Moreover, the results obtained with ligands **L3** and **L23** showed that the presence of *ortho*-tolyl

$$\text{PhMe}_2\text{Si}-\text{CH}=\text{CH}-\text{CH}_2\text{OH} \xrightarrow[50 \text{ bar H}_2, \text{ rt, 12 h, CH}_2\text{Cl}_2]{1.0 \text{ mol\% [Ir(COD)L}^*\text{]BAR}_\text{F}} \text{PhMe}_2\text{Si}-\text{CH}_2-\text{CH}^*(\text{H})-\text{CH}_2\text{OH}$$

28 **48**

L3
67% conv.^[a]
74% ee^[b] (+)

L11
0% conv.^[a]

L21
0% conv.^[a]

L22
0% conv.^[a]

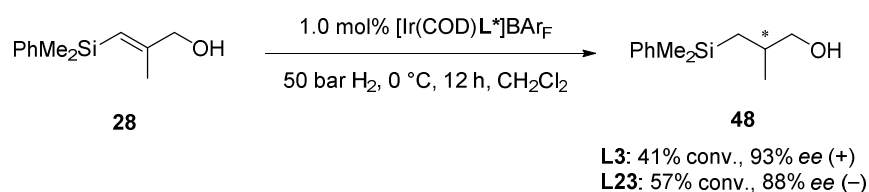
L23
>99% conv.^[a]
86% ee^[b] (–)

L24
17% conv.^[a]
62% ee^[b] (–)

L28
0% conv.^[a]

L30
1% conv.^[a]
n.d. ee

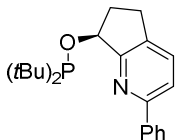
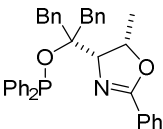
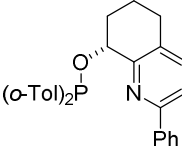
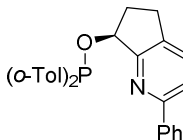
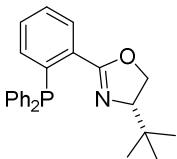
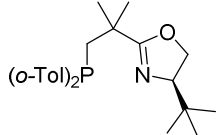
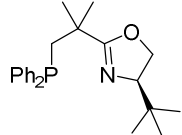
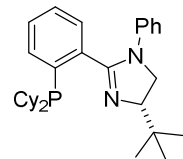
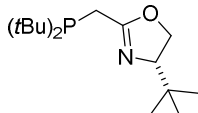
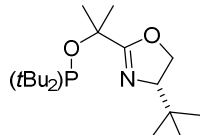
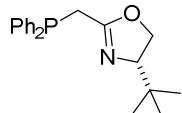
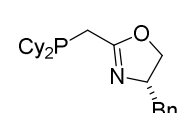
In order to improve the enantioselectivity, the hydrogenation of alcohol **28** was carried out at lower temperature using the most promising ligands, **L3** and **L23** (Scheme 25).



Although performing the reaction at 0 °C rather than room temperature resulted in higher enantiomeric excess of silane **48**, in particular when ligand **L3** was used (*cf.* Table 10 and Scheme 25), the conversion was drastically diminished. However, a comparison of the enantiomeric excesses achieved in the reduction of vinylsilanes **27** and **28** confirmed the hypothesis that vinylsilanes having the silyl group adjacent to the prostereogenic center are better substrates than those bearing the silicon atom directly attached to the

prostereogenic center. It should be noted though that not all the vinylsilanes featuring this substitution pattern could be hydrogenated with satisfactory level of enantioselectivity, as shown in the reduction of acetate **29** (Table 11).

Table 11: Ligand screening in the hydrogenation of vinylsilane **29**.

$\text{PhMe}_2\text{Si}-\text{CH}=\text{CH}-\text{CH}_2\text{OAc} \xrightarrow[50 \text{ bar H}_2, \text{ rt, 2 h, CH}_2\text{Cl}_2]{0.5 \text{ mol\% [Ir(COD)L}^*\text{]BARf}} \text{PhMe}_2\text{Si}-\text{CH}_2-\text{CH}_2-\text{CH}_2\text{OAc}$			
29			49
 <p>L11 86% conv.^[a] 14% ee^[b] (–)</p>	 <p>L12 >99% conv.^[a] 10% ee^[b] (–)</p>	 <p>L13 >99% conv.^[a] 50% ee^[b] (+)</p>	 <p>L16 >99% conv.^[a] 14% ee^[b] (–)</p>
 <p>L22 79% conv.^[a] 12% ee^[b] (+)</p>	 <p>L23 >99% conv.^[a] 55% ee^[b] (–)</p>	 <p>L24 62% conv.^{[a][c]} 64% ee^[b] (–)</p>	 <p>L28 >99% conv.^[a] 45% ee^[b] (+)</p>
 <p>L29 >99% conv.^[a] 58% ee^[b] (+)</p>	 <p>L30 >99% conv.^[a] 28% ee^[b] (+)</p>	 <p>L31 62% conv.^{[a][c]} 22% ee^[b] (+)</p>	 <p>L32 62% conv.^{[a][d]} 3% ee^[b] (+)</p>

[a] Determined by GC analysis of the reaction mixture after removal of the catalyst;

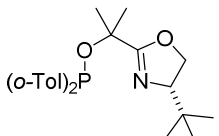
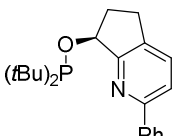
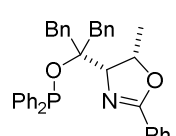
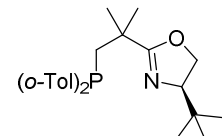
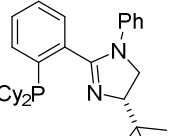
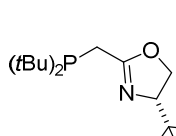
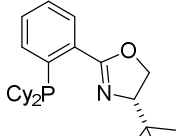
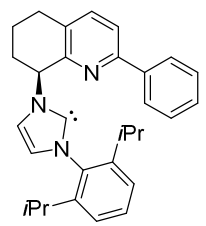
[b] Determined by HPLC analysis on a chiral stationary phase; [c] 5% of the (Z)-isomer of the starting material were detected; [d] 10% of the (Z)-isomer of the starting material were detected.

Indeed, despite the good yields, the enantioselectivities were not as high as for the free alcohol **28** (*cf.* Table 10 and Table 11). One possible reason for the moderate selectivity could be ascribed to partial *cis/trans*-isomerization of the starting material occurring during the hydrogenation process. This hypothesis was supported by the detection of some traces of (**Z**)-**29** in cases where full conversion was not achieved, for example when ligands **L24**, **L31** or **L32** were employed.

After having tested some functionalized dimethylphenylvinylsilanes, the reduction of more unfunctionalized substrates such as **30-31** was investigated.

The results summarized in Table 12 show that regardless of the ligands used for the hydrogenation of **30**, the product **50** could be obtained only in poor enantiomeric excess although complete conversion was achieved in all cases using 0.5 mol% of any catalyst.

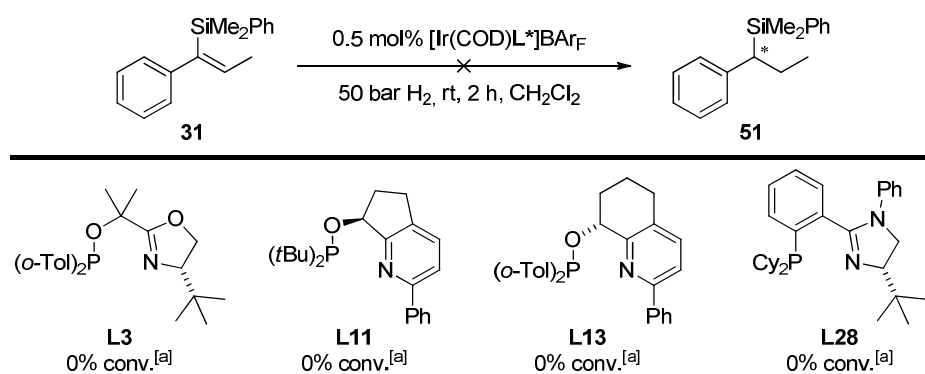
Table 12: Ligand screening for the asymmetric hydrogenation of vinylsilane **30**.

$ \begin{array}{c} \text{SiMe}_2\text{Ph} \\ \\ \text{Ph}-\text{CH}=\text{CH}_2 \\ \mathbf{30} \end{array} \xrightarrow[50 \text{ bar H}_2, \text{ rt, 4 h, CH}_2\text{Cl}_2]{0.5 \text{ mol\% [Ir(COD)L}^*\text{]BAR}_\text{F}} \begin{array}{c} \text{SiMe}_2\text{Ph} \\ \\ \text{Ph}-\text{CH}-\text{CH}_2 \\ \mathbf{50} \end{array} $			
 <p>L3 >99% conv.^[a] 42% ee^[b] (+)</p>	 <p>L11 >99% conv.^[a] 30% ee^[b] (–)</p>	 <p>L12 >99% conv.^[a] 22% ee^[b] (+)</p>	 <p>L23 >99% conv.^[a] 8% ee^[b] (–)</p>
 <p>L28 >99% conv.^[a] 36% ee^[b] (+)</p>	 <p>L29 >99% conv.^[a] 6% ee^[b] (+)</p>	 <p>L33 >99% conv.^[a] 15% ee^[b] (+)</p>	 <p>L34b >99% conv.^[a] 10% ee^[b] (–)</p>

[a] Determined by GC analysis of the reaction mixture after removal of the catalyst;

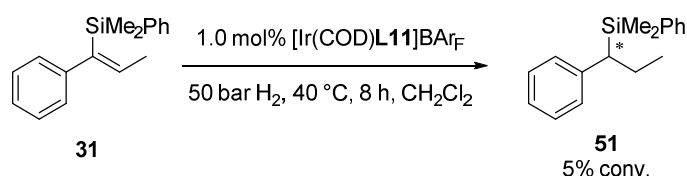
[b] Determined by HPLC analysis on a chiral stationary phase.

In an effort to achieve higher levels of enantioselectivity than those registered with vinylsilane **30**, a trisubstituted substrate bearing a phenyl group directly bound to the prostereogenic center (**31**) was tested in the iridium-catalyzed asymmetric hydrogenation. However, no conversion into **51** was observed (Table 13). The use of higher hydrogen pressure (70 bar), additives (NaI, I₂, KI, NBu₄I), or different solvents (THF, MTBE or toluene) did not improve the results.

Table 13: Ligand screening for the hydrogenation of vinylsilane **31**.

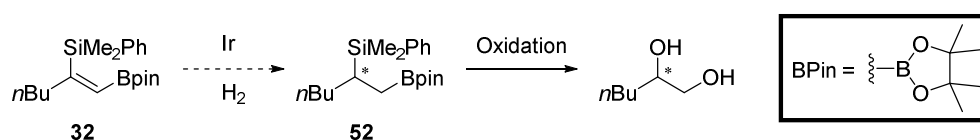
[a] Determined by GC analysis of the reaction mixture after removal of the catalyst.

Only with 1.0 mol% catalyst loading, prolonged reaction time and higher reaction temperature traces of the desired product could be detected (Scheme 26).

**Scheme 26:** Reduction of vinylsilane **31** at higher reaction temperature and prolonged reaction time.

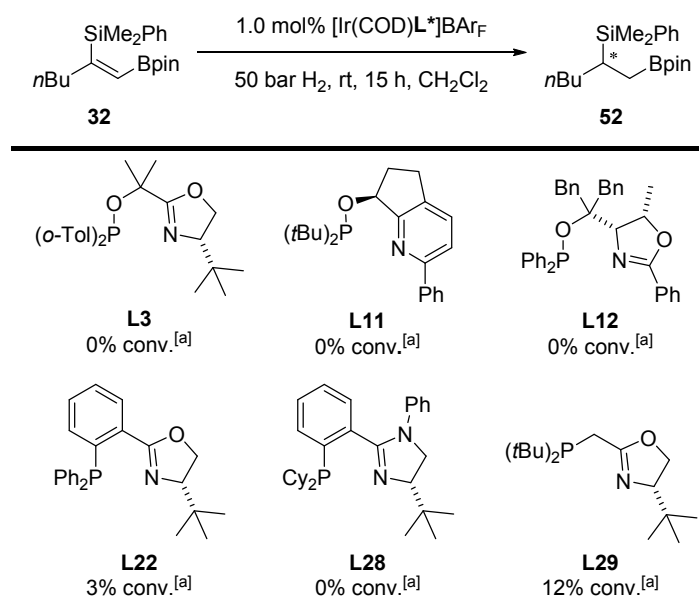
These results were discouraging since Wang^[83] showed that compound **14**, the trimethylsilylvynylsilane analog of **31** could be reduced in perfect yield and high enantioselectivity using ligand **L11** (cf. Table 2 and Table 13). Such observations are consistent with the poor ability of the olefin to coordinate to the metal center, likely due to the steric bulk of the two phenyl groups in the substrates.

Another interesting structural motif is represented by *cis*- β -silylalkenylborates such as **32**, whose reduced product could give access to 1,2-diols after oxidation (Scheme 27). The interest for this type of compounds raised after the recent progress in the iridium-catalyzed hydrogenation of vinylboronates and bisboronic esters^[33] reported by our group.

**Scheme 27:** Potential Applications of *cis*- β -silylalkenylborate **32**.

Also in this occasion the steric bulk of the substrate proved to be too demanding, hampering the reactivity of the catalyst and yielding compound **32** with only poor conversion (Table 14).

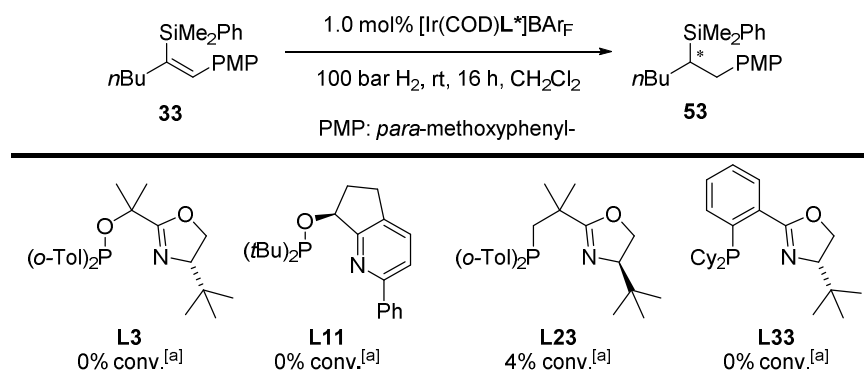
Table 14: Ligand screening for the hydrogenation of vinylsilaboronate **32**.



[a] Determined by GC analysis of the reaction mixture after removal of the catalyst.

The best ligand for this transformation was found to be the phosphinomethyloxazoline ligand **L29**, which afforded compound **52** in 12% yield. Further attempts to achieve higher turnover using the catalyst based on such ligand and different reaction conditions were unsuccessful. Replacing the boronic ester moiety with an arguably less sterically hindered

Table 15: Ligand screening for the hydrogenation of vinylsilane **33**.

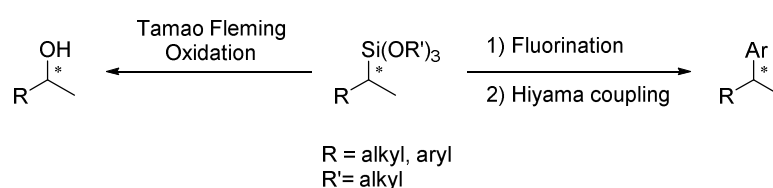


[a] Determined by GC analysis of the reaction mixture after removal of the catalyst.

para-methoxyphenyl group did not show any influence on the conversion under forcing reaction conditions (100 bar H₂), high catalyst loading and prolonged reaction time (Table 15). In general the presence of a dimethylphenylsilyl group compared to the trimethylsilyl substituent seems to drastically reduce the range of substrates that are suitable for a successful hydrogenation using the iridium catalysts developed in our group. For example aryl groups on the C=C bond of trimethylvinylsilane substrates posed no particular challenge to the effective iridium-catalyzed asymmetric hydrogenation, while they were no longer tolerated on dimethylphenylvinylsilanes. This effect is likely to be attributed to the enhanced steric bulk caused by the presence of the phenyl group on the silicon atom. After these discouraging results in the hydrogenation of dimethylphenylvinylsilanes the effect of other silicon substituents at the C=C bond were investigated.

2.2.2 Vinylsiloxanes

After careful analysis, vinylsiloxanes were chosen as a valid alternative to dimethylphenylvinylsilane. Regarding the possible applications of the hydrogenation products, in addition to the aforementioned Tamao–Fleming oxidation, enantioenriched siloxanes can be transformed in one step into the corresponding trifluorosilanes. The latter hold particular interest as they represent the only silanes that can undergo an sp²-sp³ Hiyama cross coupling (Scheme 28).^[93]



Scheme 28: Applications of enantioenriched vinylsiloxanes.

2.2.2.1 Synthesis of Vinylsiloxanes

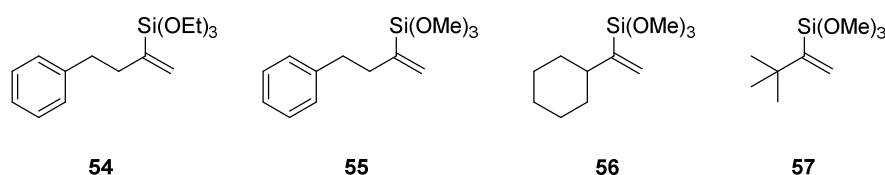
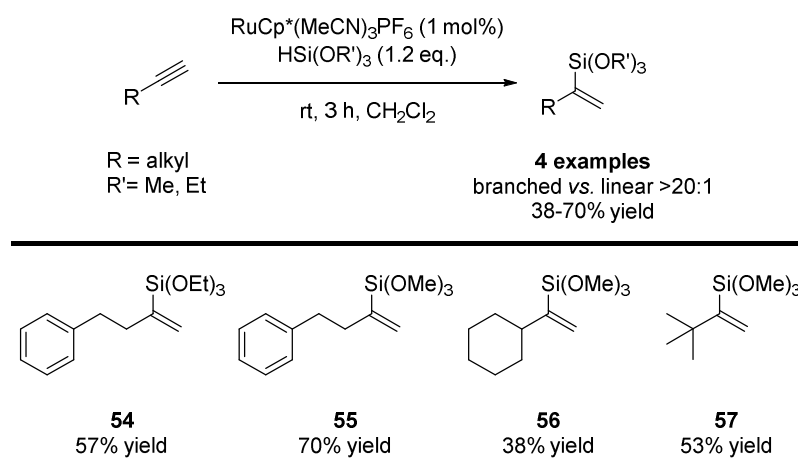


Figure 6: Synthesized vinylsiloxanes.

While the preparation of dimethylphenylvinylsilanes required several different synthetic routes depending on the desired product, the ruthenium-catalyzed hydrosilylation of terminal alkynes^[94] provided a general entry into vinylsiloxanes **54-57** (Table 16). Indeed, the use of commercially available $\text{RuCp}^*(\text{MeCN})_3\text{PF}_6$ allowed for the synthesis of the desired vinylsiloxanes in moderate to good yield after purification by column chromatography.

Table 16: Hydrosilylation of terminal alkynes following the procedure developed by Trost *et al.*^[94]

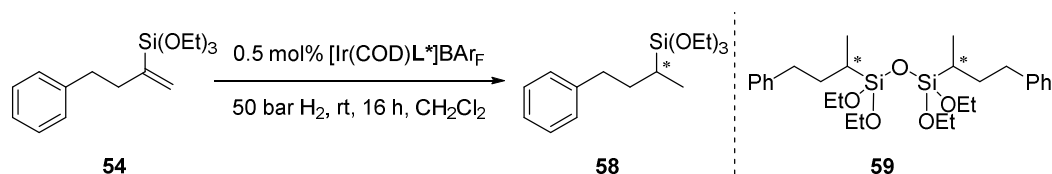


2.2.2.2 Iridium-Catalyzed Asymmetric Hydrogenation of Vinylsiloxanes

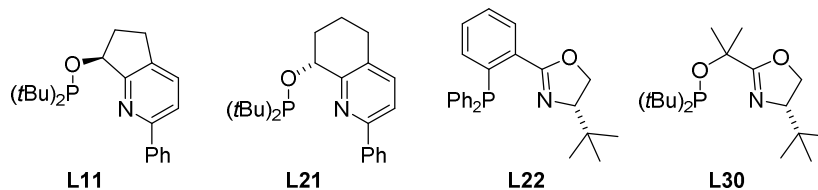
An initial catalyst screening was carried out using vinylsiloxane **54** as test substrate and three N,P-ligand classes under standard reaction conditions (50 bar H_2 , 0.5 mol% catalyst loading, Table 17). As a result, the desired siloxane **58** was formed together with a side product, whose structure was assigned as **59** on the basis of ^1H -NMR and GC-MS analyses. Compound **59** could likely result from an acid promoted dimerization of product **58**. The acidic species necessary for such a reaction to take place could be the iridium-hydrido intermediates formed in the course of the hydrogenation. Indeed Burgess *et al.*^[64] showed that intermediates of N,P-ligand-based iridium catalysts are rather acidic. When phosphine-based ligands such as **L22** are used, the corresponding iridium intermediates should be less acidic than those derived from catalysts bearing phosphinite-based ligands such as **L11**, **L21** or **L30**. The fact that the catalyst based on phosphinoxazoline ligand **L22** afforded the lowest amount of side product compared to phosphinite complexes

underpinned this hypothesis (cf. entry 3 with entries 1, 2 and 4).

Table 17: Ligand screening for the hydrogenation of vinylsiloxane **54**.



Entry	L*	Conv. to 58 ^[a] (%)	Conv. to side product ^[a] (%)
1	L11	87	13
2	L21	79	21
3	L22	95	5
4	L30	53	47



[a] Determined by GC analysis of the reaction mixture after removal of the catalyst.

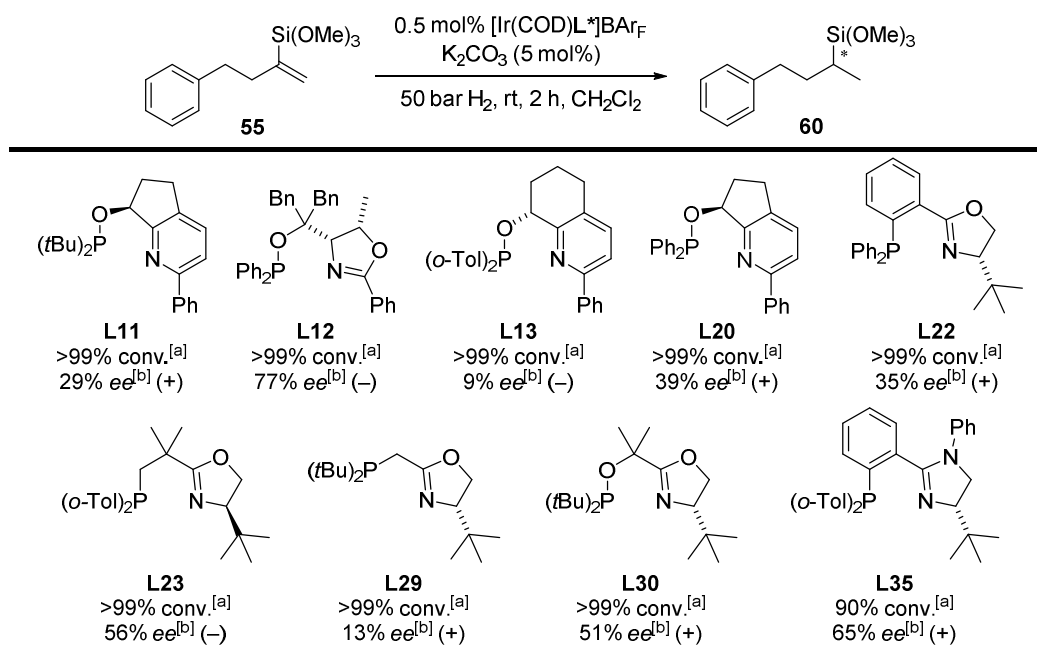
Unfortunately, the level of selectivity of the hydrogenation could not be determined by HPLC, since the side product **59** had the same retention time as the two enantiomers of **58**. In an attempt to circumvent the formation of undesired side products, three inorganic bases were added to the reaction mixture as additives (Table 18).

Table 18: Use of inorganic bases in the hydrogenation of vinylsiloxane **54**.



Entry	Base	Conv. to 58 ^[a] (%)	ee ^[b] (%)
1	K₂CO₃	>99	15 (+)
2	Na₂CO₃	>99	15 (+)
3	Cs₂CO₃	>99	15 (+)

[a] Determined by GC analysis of the reaction mixture after removal of the catalyst; [b] Determined by HPLC analysis on a chiral stationary phase.

Table 20: Ligand screening for the hydrogenation of vinylsiloxane **55**.

[a] Determined by GC analysis of the reaction mixture after removal of the catalyst;

[b] Determined by HPLC analysis on a chiral stationary phase.

Ligands **L35** and **L30**, which performed best in the hydrogenation of vinylsiloxane **54**, yielded inferior results compared to ThrePhox ligand **L12** in the hydrogenation of **55**. In order to enhance the selectivity of the reaction a pressure and temperature screening was carried out using this ligand class (Table 21).

Table 21: Pressure and temperature screening **55**.

<div style="display: flex; align-items: center; justify-content: space-around;"> <div style="text-align: center;"> </div> <div style="border: 1px solid black; padding: 5px;"> L25 </div> </div>					
Entry	L*	Pressure (bar)	Temperature (°C)	Conv. ^[a] (%)	ee ^[b] (%)
1	L25	5	rt	>99	55 (-)
2	L12	5	rt	>99	80 (-)
3 ^[c]	L12	1	rt	>99	79 (-)
4	L12	5	-20	>99	81 (-)

[a] Determined by GC analysis of the reaction mixture after removal of the catalyst; [b] Determined by HPLC analysis on a chiral stationary phase; [c] Reaction time: 13 h.

Paralleling the observations made for the hydrogenation of vinylsilanes (see Subchapter 2.2.1.2), no marked effect on the selectivity of the reduction of vinylsiloxane **55** was registered when the hydrogenation was carried out under 5 bar hydrogen pressure (entry 2) or at lower temperature (entry 4). In contrast, the presence of aryl substituents on the phosphorus atom proved to be crucial for the selectivity of the transformation (*cf.* entry 1 and 2).

To compare the reactivity of vinylsiloxanes with that of the related vinylsilanes in the hydrogenation reaction, compound **56** was synthesized and subjected to iridium-catalyzed asymmetric hydrogenation. This compound was of particular interest as it represents the *tris*-methoxy analog of vinylsilanes **21** and **23**.

Table 22: Ligand screening for the hydrogenation of vinylsiloxane **56**.

<hr/>			
<p>L3 >99% conv.^[a] 14% ee^[b] (–)</p>	<p>L12 >99% conv.^[a] 44% ee^[b] (+)</p>	<p>L11 >99% conv.^[a] 28% ee^[b] (–)</p>	<p>L22 >99% conv.^[a] 53% ee^[b] (–)</p>
<p>L24 >99% conv.^[a] 64% ee^[b] (+)</p>	<p>L28 >99% conv.^[a] 79% ee^[b] (–)</p>	<p>L29 >99% conv.^[a] 34% ee^[b] (–)</p>	
<p>L30 >99% conv.^[a] 89% ee^[b] (–)</p>	<p>L36 >99% conv.^[a] 51% ee^[b] (–)</p>	<p>L37 >99% conv.^[a] 22% ee^[b] (–)</p>	

[a] Determined by GC analysis of the reaction mixture after removal of the catalyst; [b] Determined by GC analysis on a chiral stationary phase.

Like in the previous ligand screening carried out with vinylsiloxanes, the ligands belonging to the SimplePHOX and PHIM classes, such as **L30** and **L28**, gave the best enantioselectivities affording siloxane **61** with 89% and 79% *ee* respectively. As shown in Figure 7, while the best results were obtained in the hydrogenation of compound **21** the hydrogenation of vinylsiloxane **56** and dimethylphenylvinylsilane **22** still gave comparable high levels of enantioselectivity at full conversion, demonstrating the versatility of this methodology.

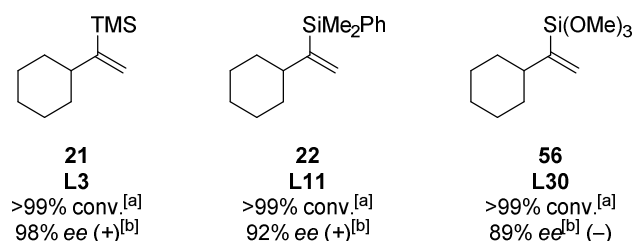
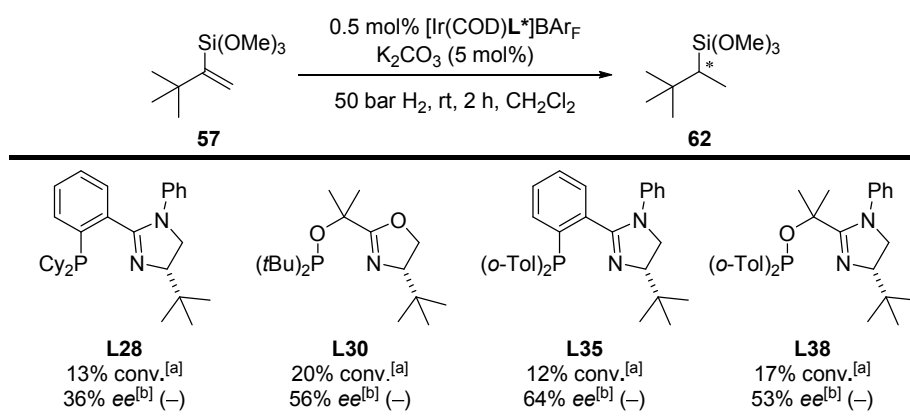


Figure 7: Comparison of the outcome of the hydrogenation of compounds **21**, **22** and **56**.

A further investigation of the iridium-catalyzed asymmetric hydrogenation of vinylsiloxanes was conducted using compound **57**. Unfortunately, though, substrate **57** was reduced to siloxane **62** with low conversion and low to moderate enantioselectivity under the conditions shown in Table 23.

Table 23: Ligand screening for the hydrogenation of vinylsiloxane **57**.

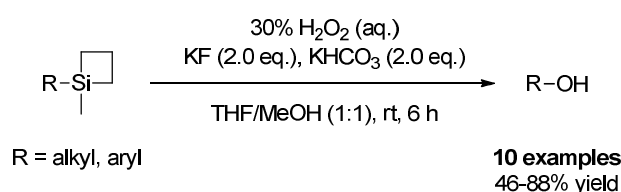


[a] Determined by GC analysis of the reaction mixture after removal of the catalyst; [b] Determined by GC analysis on a chiral stationary phase.

This lack of reactivity is likely due to the sterically demanding *tert*-butyl group in close proximity to the C=C bond, that hampers the coordination of the olefin to the iridium center.

2.2.3 Vinylsiletanes

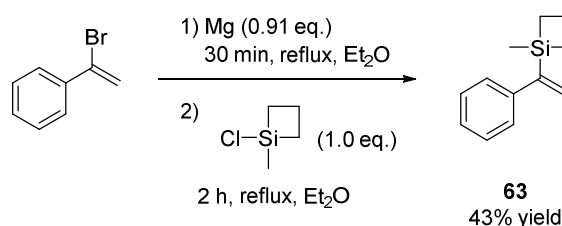
Since superior results were obtained using trimethylsilanes as test substrates (see Figure 7), a search for alternative silicon groups having similar size was undertaken. In this regard vinylsiletanes represented a starting point. Although so far the use of siletanes for synthetic applications has been limited,^[95] these compounds have the advantage over trimethylsilanes to be easily oxidized, and therefore more useful for subsequent chemical transformations such as, for instance, the preparation of alcohols as shown in Scheme 29.^[96]



Scheme 29: Oxidation of siletanes by Dudley.^[96]

2.2.3.1 Iridium-Catalyzed Asymmetric Hydrogenation of Vinylsiletane **63**

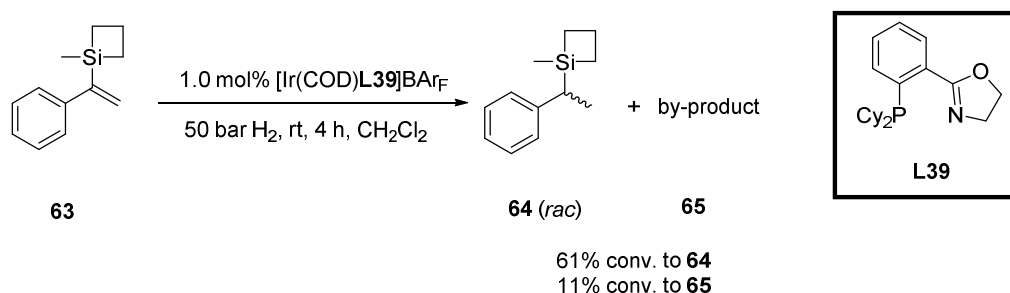
The synthesis of strained, yet stable and easy to handle, silacycle **63** was achieved by Grignard substitution starting from α -bromostyrene in moderate yield (Scheme 30). This compound served as a test substrate for the hydrogenation reaction with several iridium catalysts.



Scheme 30: Synthesis of vinylsiletane **63**.^[96]

Given the impossibility to reduce vinylsiletane **63** to afford siletane **64** in a non-enantioselective fashion using standard palladium on charcoal reduction, the iridium catalyst bearing achiral PHOX ligand **L39** was employed. Hydrogenation with this metal

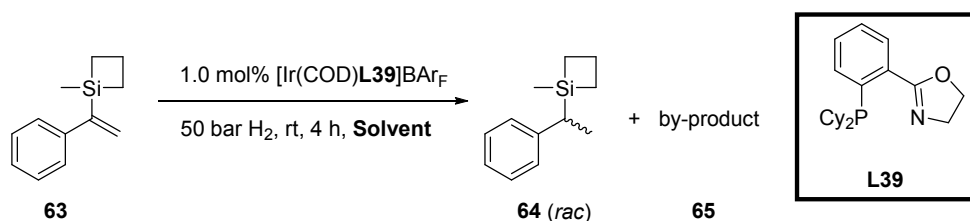
catalyst afforded a mixture of the desired racemic product and an unidentified side product (**65**) (Scheme 31).



Scheme 31: Hydrogenation of vinylsiletane **63** with an achiral catalyst. (conversions determined by GC-MS analysis of the reaction mixture after removal of the catalyst).

The structure of the by-product was not elucidated, but GC-MS (m/z 355) and ^1H NMR analysis suggested that the compound was likely generated from the interaction of two product molecules. This result resembles the previous outcome of the hydrogenation of vinylsiloxanes **54** (*cf.* Table 17), where the addition of a base was crucial to circumvent by-product formation. As a consequence many bases were screened as additives in order to avoid side product formation, but in this occasion the addition of 5 mol% of inorganic (K_2CO_3 , Cs_2CO_3 , KHCO_3) or organic bases (DBU, DIPEA) resulted in a complete loss of catalytic activity. Last, the solvent was changed to THF or MTBE in the hope to avoid the formation of the undesired side product (Table 24). Unfortunately, in this case silane **64** was formed as the minor component.

Table 24: Use of ethereal solvents for the hydrogenation of vinylsiletane **63** with $[\text{Ir}(\text{COD})\text{L39}]\text{BARf}$.



Entry	Solvent (0.2 M)	Conv. to 64 ^[a] (%)	Conv. to 65 ^[a] (%)
1	MTBE	26	52
2	THF	7	22

[a] Determined by GC-MS analysis of the reaction mixture after removal of the catalyst.

Given the low activity and the enhanced ratio of side product obtained in THF and MTBE, dichloromethane remained the solvent of choice for the further experiments.

When vinylsiletane **63** was hydrogenated with other catalysts, in addition to the desired compound **64** and the previously detected side product **65**, two further unidentified by-products were observed. The formation of these two further by-products could be avoided only when PHOX ligands were applied (Table 25).

Table 25: PHOX-ligands for the asymmetric hydrogenation of vinylsiletane **63**.

$$\text{63} \xrightarrow[50 \text{ bar H}_2, \text{rt, 13 h, CH}_2\text{Cl}_2]{1.0 \text{ mol\% [Ir(COD)L}^*\text{]BARf}} \text{64 (rac)} + \text{by-product 65}$$

Entry	L*	Conv. to 64 ^[a] (%)	ee 64 ^[b] (%)	Conv. to 65 ^[a] (%)
1	L2	57	56 (–)	43
2	L22	40	80 (–)	60
3	L33	61	8 (–)	39
4	L39	93	75 (–)	7
5	L40	88	78 (–)	12

L2

L22

L33

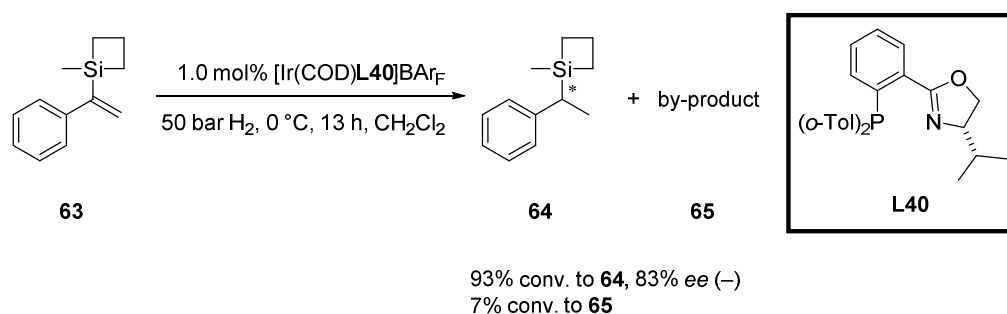
L40

L41

[a] Determined by GC-MS analysis of the reaction mixture after removal of the catalyst; [b] Determined by HPLC analysis on a chiral stationary phase.

Although, as shown in Table 25, generation of by-product could not be completely avoided, when ligand **L40** was applied only 7% conversion to **65** was detected, yielding the desired compound good yield and moderate enantiomeric excess.

Attempts to decrease the formation of side product **65** and simultaneously enhance the enantioselectivity by lowering the reaction temperature only led to a modest increase of the enantioselectivity, but the side product was still formed to the same extent (Scheme 32).



Scheme 32: Hydrogenation of vinylsiletane **63** at lower temperature.

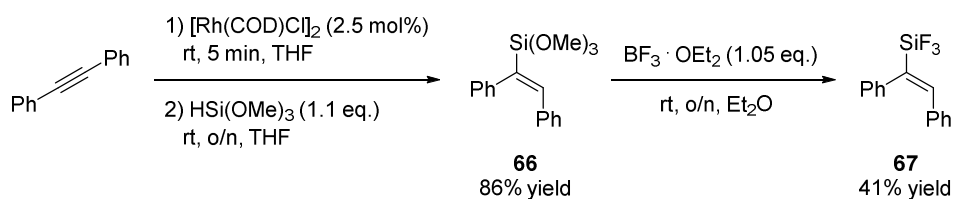
Since the formation of side product **65** could not be completely avoided and the level of enantioselectivity was not excellent, the focus of the project turned to trifluorovinylsilanes.

2.2.4 Trifluorovinylsilanes

To conclude the survey of possible vinylsilyl derivatives to be reduced in the presence of chiral iridium catalysts, the suitability of fluorine as a substituent on the silicon atom was considered. The small size of this halogen atom should enable facile substrate coordination to the metal center, allowing for the reduction of sterically demanding substrates. Moreover, as mentioned already earlier, the resulting trifluorosilanes are interesting target compounds, since they could be used in the modular synthesis of different building blocks *via* Hiyama cross-coupling (see Scheme 28).^[93]

2.2.4.1 Iridium-Catalyzed Asymmetric Hydrogenation of Trifluorovinylsilane 67

The synthesis of trifluorovinylsilane **67** was achieved starting from commercially available diphenylacetylene in two synthetic steps. Hydrosilylation^[97] followed by fluorination^[98] with boron trifluoride diethyl etherate afforded the desired compound in moderate yield (Scheme 33).



Scheme 33: Synthesis of trifluorovinylsilane **67**.

The substrate synthesized was then tested in the iridium-catalyzed hydrogenation using a selection of N,P-ligands as summarized in Table 26. Despite the forcing reaction conditions (100 bar H₂, 1 mol% catalyst loading, 14 hours) no reaction took place. Given the absence of reactivity, no further trifluorovinylsilane was investigated.

Table 26: Ligand screening for the hydrogenation of trifluorovinylsilane **67**.

67 **68**

Entry	L*	Conv. to 68 ^[a] (%)
1	L3	0
2	L11	0
3	L22	0
4	L24	0

L3

L11

L22

L24

[a] Determined by ¹H NMR analysis of the reaction mixture after removal of the catalyst.

2.3 Summary

To conclude, various compounds bearing a vinylsilyl moiety were prepared in moderate to good yields. While the synthesis of a series of trimethylvinylsilanes required several different synthetic routes, dimethylphenyl- and trialkoxy- vinylsilanes were synthesized following only one synthetic pathway for each substituent pattern.

These substrates were then subjected to iridium-catalyzed asymmetric hydrogenation using N,P-ligands. The outcome of this transformation confirmed that, as shown in Wang's preliminary results (Table 2),^[83] trimethyl-substituted vinylsilanes performed better than the corresponding dimethylphenyl and trialkoxy analogs (see Figure 7). Adding the results

of Wang^[83] to the ones achieved in the course of this investigation, 12 trimethyl- and dimethylphenyl-vinylsilanes could be hydrogenated affording the desired compounds with up to full conversion and enantiomeric excesses ranging between 83% and 99% *ee*. These levels of enantioselectivity exceeded the benchmark set by Andersson *et al.* in 2006 (see Table 1).^[80r]

The hydrogenation of vinylsiloxanes yielded a mixture of the desired product and an unidentified side product, which could be circumvented by adding 5 mol% of potassium carbonate to the reaction mixture. In this way 3 vinylsiloxanes were reduced with full conversion and good enantiomeric excesses (70-89% *ee*).

Despite the generally good levels of enantioselectivity obtained, the major drawback of this process was represented by the lack of an universal iridium complex able to successfully catalyze the hydrogenation of this substrate class. Indeed, for each substrate a ligand screening had to be carried out in order to figure out the most promising ligand scaffold.

At the end of the project the hydrogenation of vinylsiletanes and trifluorovinylsilanes was considered, but due to unavoidable formation of side products and the absence of reactivity, the substrate scope was not investigated further.

Chapter 3

Iridium-Catalyzed Asymmetric Hydrogenation of Maleic Acid Dimethylesters

3.1 Introduction

Prochiral fumarates and maleates, as well as the corresponding anhydrides, represent an interesting class of unsaturated compounds for iridium-catalyzed asymmetric hydrogenation. The enantioselective hydrogenation of such compounds would provide access to highly valuable 2-substituted succinic acid derivatives that find applications as chiral building blocks and whose basic structure can be found in a variety of biologically active molecules like matrix metalloproteinase inhibitors (MMP, **69** and **70**), caspase 1 inhibitors (**71**) and mitiglinide (**72**), a drug used in the treatment of diabetes^[99] (Figure 8).

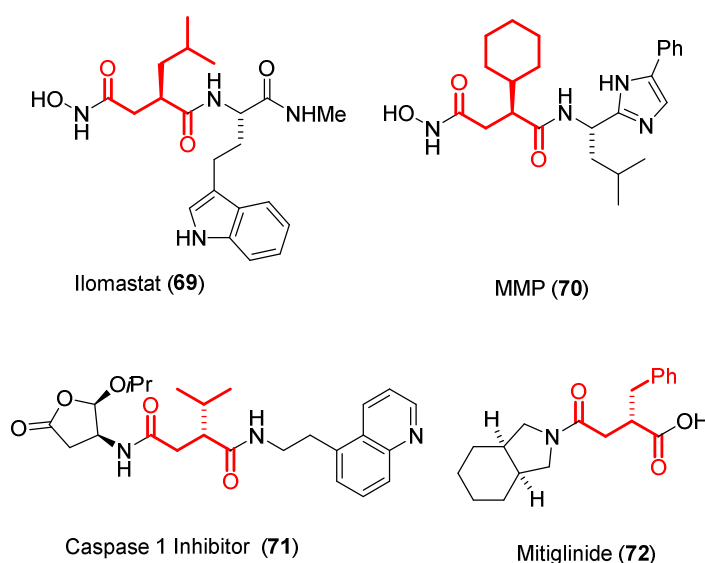


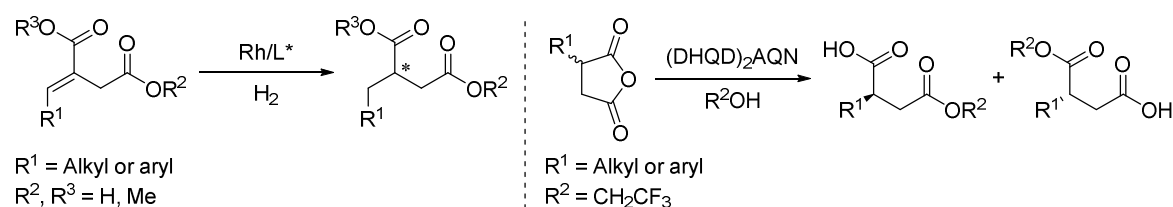
Figure 8: Structures of biologically active compounds containing the 2-substituted succinic acid moiety.

In addition, the versatility of the functional groups that are present in the reduced products allows a broad array of subsequent chemical transformations (see section 3.2.3)

3.1.1 State of the Art

Several reports on the asymmetric hydrogenation of itaconic acid derivatives have been published over the last decades^[1a,100] but none of these deals with the hydrogenation of the corresponding isomeric fumarates or maleates. Similarly, only one example of asymmetric hydrogenation of an α -alkylidene succinic anhydride has been reported in the literature,^[101] while asymmetric hydrogenations of 2-substituted maleic anhydrides are extremely rare. Indeed, only one method for the Rh-catalyzed hydrogenation of citraconic anhydride **73a** has been published and, although excellent conversion could be achieved for this substrate, the enantioselectivity achieved was very poor (26% ee).^[102] According to the results of Shimoda and Kubota, currently the most efficient method for the enantioselective reduction of citraconic anhydride is an enzymatic reduction using a reductase from *Marchantia polymorpha*.^[103] This methodology has not been applied to more complex maleic anhydrides and therefore, it seems evident that more general methods that allow for the efficient and selective preparation of 2-substituted succinic anhydrides or acid derivatives are of interest.

Arguably, the lack of enantioselective reductions of fumarates, maleates and substituted maleic anhydrides is a consequence of their poor reactivity toward hydrogenation, due to the conjugation of the C=C bond with the two carboxylic groups. Therefore, enantioenriched 2-substituted succinic acid derivatives have been synthesized *via* the rhodium-catalyzed asymmetric hydrogenation of the parent β -substituted itaconic acid,^[104] or its methyl ester,^[104b,105] or by organocatalytic parallel kinetic resolution of monosubstituted succinic anhydrides^[106] (Scheme 34).



Scheme 34: Enantioselective routes to chiral 2-substituted succinic acid derivatives.

While the latter method is limited to a maximum yield of 50%, the hydrogenation of itaconic acid derivatives cannot be performed efficiently when the target C=C bond is

tetrasubstituted, as would be required for the synthesis of **70** and **71** (Figure 8). Moreover, the reduction of itaconic acid derivatives does not allow to access 2-aryl-succinic acid derivatives.

3.2 Results and Discussion

3.2.1 Iridium-Catalyzed Asymmetric Hydrogenation of Maleic Anhydrides

Initial investigations focused on the iridium-catalyzed asymmetric hydrogenation of maleic anhydrides. As a test substrate, commercially available citraconic anhydride **73a** was chosen and its hydrogenation carried out with several catalysts that have been developed in the past in the Pfaltz research group. The results of such catalyst screening are summarized in Table 27.

Table 27. Ligand screening for the hydrogenation of citraconic anhydride **73a**.

73a
74a

<p>L11 59% conv.^[a] 89% ee^[b] (R)</p>	<p>L12 10% conv.^[a] 71% ee^[b] (S)</p>	<p>L20 10% conv.^[a] 3% ee^[b] (R)</p>	<p>L22 28% conv.^[a] 50% ee^[b] (S)</p>
<p>L23 >99% conv.^[a] 86% ee^[b] (R)</p>	<p>L24 >99% conv.^[a] 91% ee^[b] (R)</p>	<p>L30 14% conv.^[a] 58% ee^[b] (S)</p>	<p>L34b >99% conv.^[a] 39% ee^[b] (R)</p>
<p>L42 >99% conv.^[a] 55% ee^[b] (S)</p>	<p>L43 30% conv.^[a] 73% ee^[b] (S)</p>	<p>L44 36% conv.^[a] 61% ee^[b] (S)</p>	<p>L35 >99% conv.^[a] 71% ee^[b] (S)</p>

[a] Determined by GC analysis of the reaction mixture after removal of the catalyst; [b] Determined by GC analysis on a chiral stationary phase.

In the initial screening all the different ligand classes were tested. Under standard conditions (50 bar H₂, rt, 18 h, CH₂Cl₂), the ligands which performed best were **L23** and **L24**, belonging to the NeoPHOX family.^[29d] The presence of an aryl moiety on the phosphine as well as a bulky *tert*-butyl group on the oxazoline seemed necessary to achieve good results in terms of both conversion and selectivity, as the results with ligands **L42**, **L43** and **L44** show.

The opposite effect can be observed when using the pyridine-phosphinite based catalysts. Ligand **L20** bearing a diphenylphosphine gave worse results compared to the *ditert*-butyl phosphine analogs **L11**, which yielded the desired product with 59% conversion and 89% *ee*. Among the other complex classes, only a few catalysts gave full conversion, and usually moderate enantioselectivities were observed (**L34b**, **L35**).

These initial results were very encouraging since, as mentioned earlier, only one example of metal-catalyzed asymmetric hydrogenation of citraconic anhydride was known in the literature, affording **74a** in only 26% *ee*.^[102] To further improve the results outlined in Table 27, the effect of temperature and pressure was scrutinized using the three most

Table 28: Pressure and temperature screening for the hydrogenation of citraconic anhydride **73a**.

Entry	L*	Pressure (bar)	Temperature (°C)	Conv. ^[a] (%)	<i>ee</i> ^[b] (%)
1	L11	50	−10	11	87
2	L11	10	r.t.	22	86
3	L23	50	−10	27	83
4	L23	10	r.t.	>99	88
5	L24	50	−10	35	88
6	L24	10	r.t.	99	93

L11

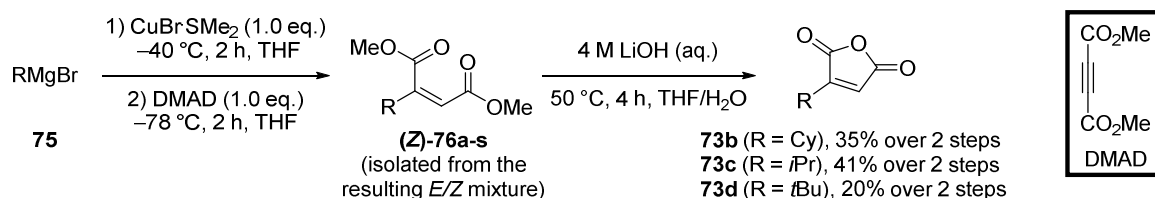
L23

L24

[a] Determined by GC analysis of the reaction mixture after removal of the catalyst;

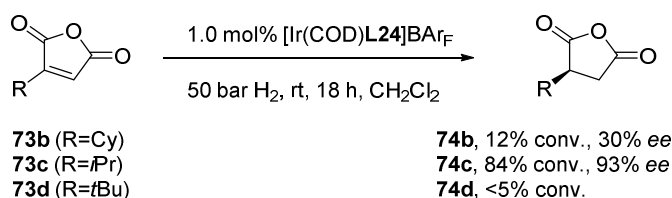
[b] Determined by GC analysis on a chiral stationary phase.

promising catalysts of the ligand screening (**L11**, **L23**, **L24**). A decrease of the reaction temperature did not furnish the expected results. In fact only poor conversion could be achieved after 18 hours at $-10\text{ }^{\circ}\text{C}$ (Table 28, entries 1, 3, 5). A slightly positive influence on the enantiomeric excess was observed when the hydrogenation reaction was carried out at 10 bar hydrogen pressure (Table 28, entries 4 and 6). With a promising selection of catalysts for the hydrogenation of citraconic anhydride, it was decided to test the substrate scope of the reaction on a series of more sterically hindered compounds. Therefore, the compounds shown in Scheme 35 were synthesized in two steps in moderate yields by copper-catalyzed Michael addition of Grignard reagents to dimethylacetylenedicarboxylate (DMAD), followed by condensation of the corresponding maleic acid dimethylesters using an aqueous solution of lithium hydroxide.



Scheme 35: Synthesis of maleic anhydrides.

Given the foreseen lower reactivity of maleic anhydrides **73b-d** compared to citraconic anhydride, it was decided to test them first under the conditions outlined in Table 27 (50 bar H_2), seeing that probably more forcing conditions would be needed to drive the hydrogenations to completion. Indeed, even carrying out the hydrogenation of **73c** under 50 bar of hydrogen full conversion could not be achieved, as shown in Scheme 36.



Scheme 36: Results of the hydrogenation of substrates **73b-d** using ligand **L24**.

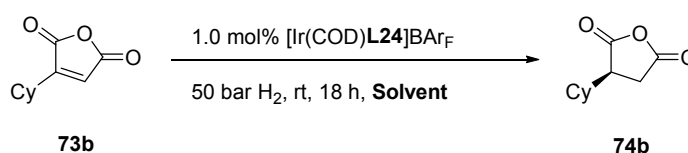
In the case of maleic anhydrides **73b** and **73d** some solubility issues were also encountered. These substrates were poorly soluble in dichloromethane, resulting in only poor results in the catalytic reaction (Scheme 36). For this reason a solvent screening

(Table 29) was carried out in order to enhance the solubility of the substrates without affecting the solubility of the catalyst and ideally achieving good levels of conversion and enantioselectivity. Polar solvents did not furnish the desired effects (Table 29, entries 1 to 4), while in methyl-*tert*-butyl ether the maleic anhydrides were well soluble, but the catalyst was not.

In an attempt to dissolve both the substrate and the catalyst, a 1:1 mixture of dichloromethane and methyl-*tert*-butyl ether was employed as solvent. In this case 40% conversion and 79% enantiomeric excess were achieved for the reduction of **73b**. Carrying out the reaction at 40 °C improved the conversion to 64% while keeping almost the same enantioselectivity (77% vs. 79% *ee*, entries 6 and 7).

Given the moderate levels of enantioselectivity observed in the case of **73b** and to circumvent the solubility issues observed with this substrate, it was chosen to use maleic acid dimethyldiesters as alternative substrates. These compounds are even easier to prepare than maleic anhydrides, as they are precursors in the synthesis of the maleic anhydrides.

Table 29: Solvent screening for the hydrogenation of maleic anhydride **73b**.



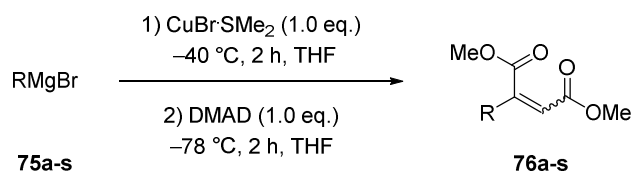
Entry	Solvent (0.2 M)	Conv. ^[a] (%)	<i>ee</i> ^[b] (%)
1	Ethylacetate	10	n.d.
2	Methanol	9	n.d.
3	Propylene Carbonate	0	-
4	Acetone	9	n.d.
5	MTBE	12	n.d.
6	MTBE:CH ₂ Cl ₂ (1:1)	40	79
7 ^[c]	MTBE:CH ₂ Cl ₂ (1:1)	64	77

[a] Determined by GC analysis of the reaction mixture after removal of the catalyst; [b] Determined by GC analysis on a chiral stationary phase; [c] The reaction was carried out at 40 °C.

3.2.2 Iridium-Catalyzed Asymmetric Hydrogenation of Maleic Acid Dimethyldiesters

To investigate the suitability of maleic acid dimethylesters as substrates for iridium-catalyzed asymmetric hydrogenation, a series of these compounds was synthesized *via* a one-step procedure starting from dimethylacetylenedicarboxylate (DMAD).^[107] This copper-catalyzed Michael addition reaction gave access to a broad array of maleic acid dimethyldiester by simple variation of the Grignard reagent. The yield of the transformation was often low due to the difficult separation of the two stereoisomers formed by flash chromatography (yields reported in Table 30 are based on the amount of pure *E*- or *Z*-isomers isolated from the purification process).

Table 30. Substrates synthesized *via* organocupration reaction starting from DMAD.



Entry	R	Yield (%)	Entry	R	Yield (%)
1	(<i>Z</i>), Me (76a)	15	11	(<i>Z</i>), 2-Me-C ₆ H ₄ (76j)	9
2	(<i>E</i>), Me (76a)	17	12	(<i>Z</i>), 4-OMe-C ₆ H ₄ (76k)	24
3	(<i>Z</i>), Cy (76b)	50	13	(<i>Z</i>), 4-F-C ₆ H ₄ (76l)	28
4	(<i>Z</i>), <i>i</i> Pr (76c)	77	14	(<i>Z</i>), 3-F-C ₆ H ₄ (76m)	13
5	(<i>Z</i>), <i>t</i> Bu (76d)	38	15	(<i>Z</i>), 4-Cl-C ₆ H ₄ (76n)	8
6	(<i>Z</i>), <i>n</i> Bu (76e)	88	16	(<i>Z</i>), 4-CF ₃ -C ₆ H ₄ (76o)	4
7	(<i>Z</i>), <i>i</i> Bu (76f)	31	17	(<i>Z</i>), 4-Ph-C ₆ H ₄ (76p)	12
8	(<i>Z</i>), Ph (76g)	24	18	(<i>Z</i>), 4-TMS-C ₆ H ₄ (76q)	5
9	(<i>Z</i>), 4-Me-C ₆ H ₄ (76h)	14	19	(<i>Z</i>), 4-SMe-C ₆ H ₄ (76r)	15
10	(<i>Z</i>), 3-Me-C ₆ H ₄ (76i)	15	20	(<i>Z</i>), 3-thiophenyl (76s)	15

To find out the most promising catalyst class for the iridium-catalyzed asymmetric hydrogenation of maleic acid dimethyldiesters, a ligand screening was carried out employing compound **76b** as the test substrate (Table 31).

Like for the related anhydrides, not many complexes were able to catalyze such transformation to completion. Ligands **L23** and **L24**, which previously performed best, gave good enantioselectivity but poor conversion. For this transformation the best ligands were those belonging to the pyridine phosphinite class. Important features for this class of ligands to perform well are the size of the carbocyclic ring fused to the pyridine and the substituents on the phosphinite moiety. As shown in Table 29 ligand **L11** bearing a five membered carbocyclic ring performed much better than its six membered analog **L21**, and the use of a di-*tert*-butyl-phosphinite was crucial for both conversion and selectivity (compare the results obtained with **L11** and **L20** in Table 31).

Table 31: Ligand screening for the hydrogenation of maleic acid dimethyldiester **76b**.

<p>L11 96% conv.^[a] 92% ee^[b] (+)</p>		<p>L20 41% conv.^[a] 77% ee^[b] (+)</p>	
<p>L24 26% conv.^[a] 90% ee^[b] (+)</p>		<p>L25 86% conv.^[a] 77% ee^[b] (-)</p>	
<p>L30 27% conv.^[a] 1% ee^[b] (-)</p>		<p>L45 98% conv.^[a] 96% ee^[b] (+)</p>	
<p>L21 30% conv.^[a] 29% ee^[b] (+)</p>		<p>L26 >99% conv.^[a] 77% ee^[b] (+)</p>	
<p>L46 >99% conv.^[a] >99% ee^[b] (+)</p>		<p>L23 34% conv.^[a] 65% ee^[b] (+)</p>	
<p>L28 63% conv.^[a] 19% ee^[b] (-)</p>			

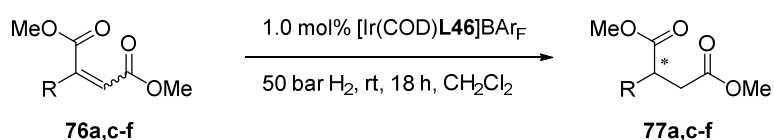
[a] Determined by GC analysis of the reaction mixture after removal of the catalyst; [b] Determined by GC analysis on a chiral stationary phase.

With the excellent results obtained with **L11** in hand, further catalysts from this family were tried (**L26**, **L45**, **L46**). The particularities of these ligands are the different electronic and steric properties of the pyridine ligand-core. Small changes on the pyridine ring (**L45**) and bulky substituents on the phenyl ring in proximity to the pyridine (**L26**) do have only a small influence on selectivity and conversion, but when the phenyl ring on the pyridine was exchanged for a 2,6-difluorophenyl group, the results achieved were outstanding (>99% conversion and *ee* using **L46**).

Ligand **L46** has been recently synthesized in our laboratory^[108] reasoning that the 2,6-difluorophenyl moiety could play an important role in preventing the C-H insertion process that often occurs with complexes of iridium and ligands bearing a phenyl substituent on the pyridine ring. In fact, such a C-H insertion is an undesirable side reaction that is known to reduce the catalyst activity.^[109]

Encouraged by the results obtained with substrate **76a**, other 2-alkyl-substituted maleic acid dimethyldiesters were tested in the iridium-catalyzed asymmetric hydrogenation reaction (Table 32).

Table 32: Substrate scope of the hydrogenation of 2-Alkyl substituted maleic acid dimethyldiester **76a,c-f**.



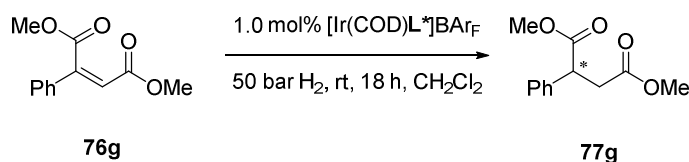
Entry	Substrate (R)	Conv. ^[a] (%)	<i>ee</i> ^[b] (%)
1	(Z)- 76a (Me)	>99	97 (+)
2	(E)- 76a (Me)	>99	98 (+)
3 ^[c]	76a (Me)	>99	98 (+)
4	(Z)- 76c (<i>i</i> Pr)	>99	99 (+)
5	(Z)- 76d (<i>t</i> Bu)	99	98 (+)
6	(Z)- 76e (<i>n</i> Bu)	97	96 (+)
7	(Z)- 76f (<i>i</i> Bu)	>99	95 (+)

[a] Determined by GC analysis of the reaction mixture after removal of the catalyst; [b] Determined by GC analysis on a chiral stationary phase; [c] A 1.5:1 mixture of (**Z**)-**76a** and (**E**)-**76a** was used in this case.

Interestingly, either reducing or increasing the steric bulk of the substituent on the C=C bond had no major impact on the outcome of the hydrogenation. In fact, substrates bearing either linear and branched alkyl substituents such as **(Z)**-**76a**, **c-f** were reduced with excellent conversion and with enantiomeric excesses ranging from 95 to 98% under the same conditions used for the hydrogenation of **76b**. Remarkably, the reduction of the fumarate derivative **(E)**-**76a** with the catalyst used for this study led to the formation of **77a** which has the same configuration as that deriving from maleate **(Z)**-**76a** (*cf.* entries 1 and 2). Therefore, even mixtures of maleates and fumarates could be hydrogenated in an enantioconvergent fashion (entry 3). This represents a highly desirable feature for the reaction, especially when the separation of the two geometric isomers of the starting material is difficult. More sterically demanding substituents as those present on substrate **(Z)**-**76c** and **(Z)**-**76d** were reduced with very high level of conversion and nearly perfect enantioselectivity (98-99% *ee*).

To further explore the generality of this method aryl-substituted dimethyl maleates, were examined. Compound **76g** was chosen as the test substrate for these investigations and its hydrogenation was attempted with iridium catalysts based on ligands **L11**, **L25**, **L45** and **L46** (Table 33).

Table 33: Ligand screening in the hydrogenation of maleic acid dimethyldiester **76g**.



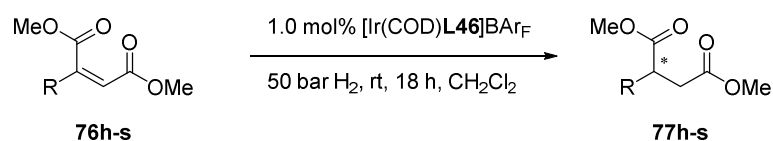
Entry	L*	Conv. ^[a] (%)	ee ^[b] (%)
1	L11	16	92 (+)
2	L25	>99	79 (–)
3	L45	14	89 (+)
4	L46	95	96 (+)

[a] Determined by GC analysis of the reaction mixture after removal of the catalyst; [b] Determined by GC analysis on a chiral stationary phase.

The novel pyridyl phosphinite ligand **L46** outperformed the first generation ligand **L11**. While both catalysts reduced **76g** to **77g** with similar enantioselectivities (95% vs. 92% *ee*), the new generation catalyst achieved much higher conversion (95% vs. 16%, *cf.* entries 1 and 4). These results are consistent with the hypothesis that the 2,6-difluorophenyl moiety decreases the poisoning rate of the catalyst, allowing a longer catalyst activity. In addition, like for the 2-alkyl substituted maleates, it was found that the methyl group on the pyridyl ring in **L45** has no major influence on the outcome of the reaction (*cf.* entries 1 and 3).

Further to these encouraging results, a broader set of substrates was tested using catalyst [Ir(COD)**L46**]BAr_F (Table 34).

At the beginning, in order to gain an insight on the steric and electronic effects of the substituents on the outcome of the reaction, different tolyl-substituents were considered (entries 1-3). The reaction proceeded smoothly for **76h** with complete conversion and excellent enantioselectivity. Moving the methyl group of the tolyl substituent to the *meta* (**76i**) and then to the *ortho* position (**76j**) resulted in decreased reactivity of the substrates toward hydrogenation. In fact, in the case of **76i** the catalyst loading had to be increased to 2 mol% to achieve full conversion (entry 3), whilst sterically hindered **76j** was essentially not active under the same reaction conditions. With regard to the electronic effect of the substituents, both electron-rich and electron-poor aromatic groups at the C=C bond were well tolerated (entries 5-10), and no clear trend in either reactivity or selectivity could be observed. The presence of a trimethylsilyl group at the *para* position of the aromatic substituent was somehow problematic, requiring a higher catalyst loading (2.0 mol%) to achieve full conversion of **75q** into **76q** (entries 11 and 12). In terms of functional group compatibility, while the presence of a thioether in the molecule (entry 13) was not tolerated, 3-thiophenyl dimethyl maleate could be hydrogenated in good conversion (88%, entry 14) and selectivity (84% *ee*), showing the broad substrate scope of this methodology.

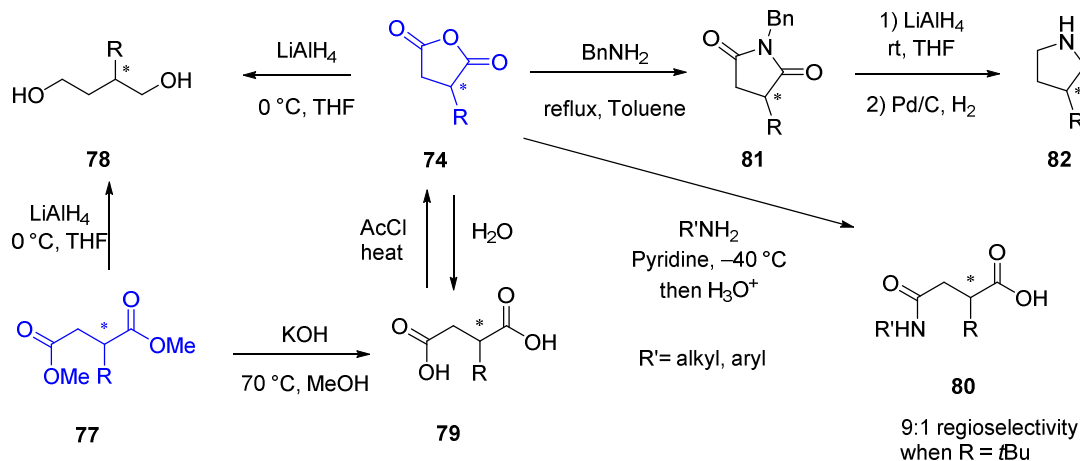
Table 34: Substrate scope of the hydrogenation of 2-Aryl substituted maleic acid dimethyldiester **76h-s**.

Entry	Substrate (R)	Conv. ^[a] (%)	ee ^[b] (%)
1	76h (4-Me-C ₆ H ₄)	>99	97 (+)
2	76i (3-Me-C ₆ H ₄)	52	95 (+)
3 ^[c]	76i (3-Me-C ₆ H ₄)	>99	96 (+)
4	76j (2-Me-C ₆ H ₄)	2	n.d.
5	76k (4-OMe-C ₆ H ₄)	>99	94 (+)
6	76l (4-F-C ₆ H ₄)	>99	96 (+)
7	76m (3-F-C ₆ H ₄)	99	95 (+)
8	76n (4-Cl-C ₆ H ₄)	>99	92 (+)
9	76o (4-CF ₃ -C ₆ H ₄)	>99	91 (+)
10	76p (4-Ph-C ₆ H ₄)	>99	97 (+)
11	76q (4-TMS-C ₆ H ₄)	30	n.d. ^[d]
12 ^[c]	76q (4-TMS-C ₆ H ₄)	>99	96 (+)
13	76r (4-SMe-C ₆ H ₄)	0	-
14	76s (3-thiophenyl)	88	84 (+)

n.d. = not determined; [a] Determined by GC analysis of the reaction mixture after removal of the catalyst; [b] Determined by GC or HPLC analysis on a chiral stationary phase; [c] 2 mol% of catalyst loading were used; [d] Enantiomeric excess could not be determined because of the overlapping peaks of unreacted **76q** and one of the enantiomers of the product in the HPLC chromatogram.

3.2.3 Synthetic Applications of the Hydrogenation Products

As mentioned in the introduction of this chapter, the products of the iridium-catalyzed hydrogenation of maleic acid dimethyldiesters **77** or maleic anhydrides **74** are useful building blocks as they can be transformed into a variety of interesting compounds in a few synthetic steps (Scheme 37).

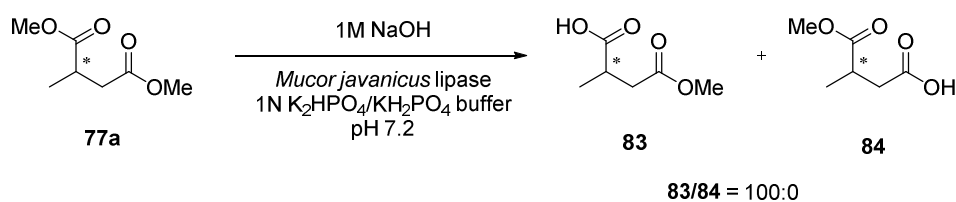


Scheme 37: Possible applications of maleic acid dimethyldiester **77** and maleic anhydrides **74**.

As is known both succinic diesters and anhydrides can be readily converted into the corresponding diols **78**^[110] and diacids **79**^[111] without loss of enantioselectivity.

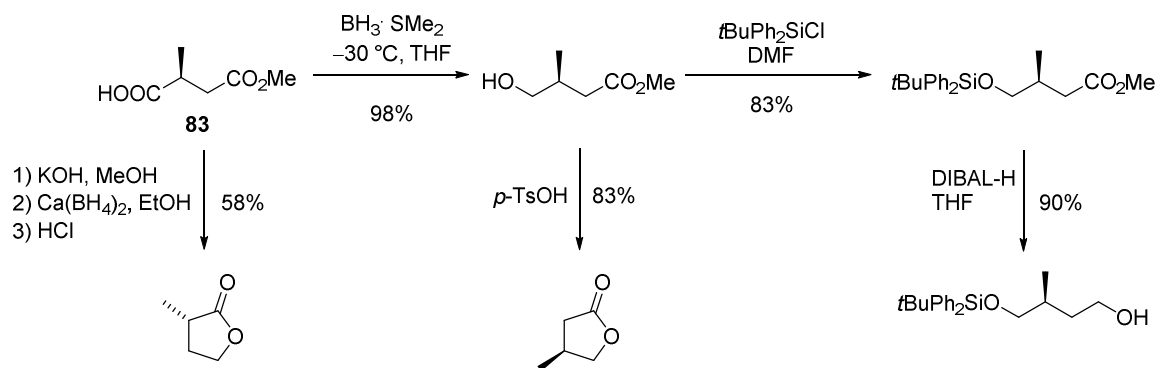
Fortunately, since the hydrogenation of anhydrides was not as general as hoped for, products **74** can be anyway accessed from **79**.^[111] Such succinic anhydrides are highly versatile compounds, since they can be used as starting materials for the synthesis of γ -aminoacids **80**,^[112] succinimide (**81**)^[113] and pyrrolidine derivatives (**82**).^[113] It should be noted that, some succinimide derivatives were so far accessible *via* iridium-catalyzed asymmetric hydrogenation of α -alkylidene succinimides,^[113b] but this transformation does not allow to access enantiopure 2-aryl succinimides. These can now be synthesized with the methodology presented herein. In fact, 2-aryl succinimide derivatives can be easily prepared from the enantioenriched succinic anhydrides.^[114]

Furthermore, in order to serve as useful intermediates in the synthesis of the biologically active molecules like **69** to **72**, the succinic dimethyldiester should undergo a selective saponification of one ester moiety. One example on this transformation was reported in 2003 by Helmchen and co-workers.^[115] In this report dimethyl 2-methylsuccinate underwent an enzyme-catalyzed semi-saponification to give mono ester **83** in quantitative yield and excellent regioselectivity (Scheme 38).



Scheme 38: Enzyme-catalyzed semisaponification of **77a**.

This transformation gives access to the important building block class of the chiral C₅-bifunctional compounds that are widely used in the synthesis of terpenoid natural products (Scheme 39).



Scheme 39: Preparation of C₅-building blocks.^[115]

In order to expand the range of applications of succinic diesters **77 b-s** to the synthesis of these enantioenriched C₅-synthons, the semisaponification reaction of **77f** was attempted. Despite the previous report,^[115] the employment of *Mucor javanicus* lipase as an enzyme failed to provide the desired product. Instead a complex mixture of both mono esters as well as succinic acid was obtained. Similar results were obtained when treating **77f** with sterically hindered bases like *t*BuOK. Unfortunately, the enzyme-catalyzed semi-saponification reaction seemed to be very substrate-specific, impeding a broader substrate scope. Due to these disappointing results, the selective hydrolysis of succinic diesters **77 b-s** was shelved.

3.3 Summary

In summary, the preparation of alkyl- and aryl-substituted maleic acid dimethyldiesters as well as some alkyl-substituted maleic anhydrides was achieved in moderate yield starting from commercially available dimethylacetylenedicarboxylate (DMAD).

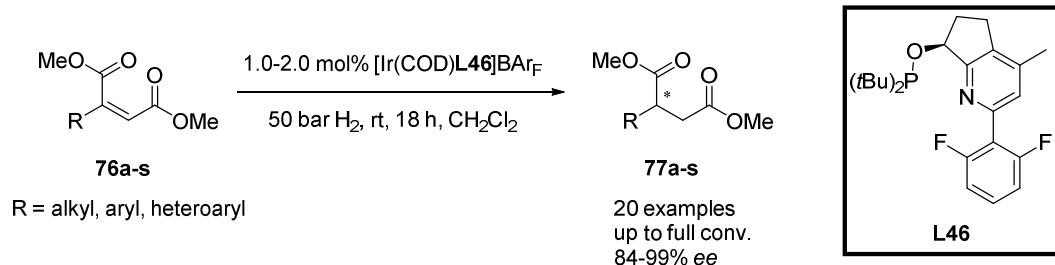
The compounds prepared were tested as novel substrates for the iridium-catalyzed asymmetric hydrogenation.

The initial idea of enantioselectively reducing substituted maleic anhydrides met with only partial success due to major solubility problems of these substrates. For this reason the

focus of the project moved to the hydrogenation of the parent maleic acid dimethyldiesters. Such compounds proved to be more suited to this transformation, reacting smoothly in the presence of pyridine-phosphinite based iridium complexes to afford the desired succinic dimethyldiesters in good yields and selectivities.

Within this class of catalysts, the most active was that based on ligand **L46**, bearing a di-*tert*-butyl phosphinite and a 2,6-difluorophenyl group on the pyridine ring. The latter is thought to play an important role in preventing deactivation of the catalyst. Indeed, as already mentioned earlier, pyridine phosphinite iridium complexes bearing a phenyl substituent on the pyridine ring are known to undergo C–H insertion that lowers the catalyst activity.

The iridium-catalyzed asymmetric hydrogenation presented in this chapter features a broad substrate scope (Scheme 40), as alkyl-, heteroaryl- and aryl groups were tolerated as substituents of the maleic acid diesters. In total 20 examples of these new substrates could be reduced with excellent yields (up to full conversion) and enantioselectivities (from 84 up to 99% *ee*).



Scheme 40: iridium-catalyzed asymmetric hydrogenation of maleic acid dimethyldiesters **76a-s**.

The products of this process can be used for a variety of transformations to afford succinic acids,^[111] diols,^[110] γ -aminoacids derivatives^[112] as well as succinic anhydrides,^[111] succinimides,^[113] pyrrolidines.^[113]

Chapter 4

Iridium-Catalyzed Asymmetric Hydrogenation of 3,3-Disubstituted Allylic Alcohols in Etheral Solvents

4.1 Introduction

During the last decades the asymmetric hydrogenation of many functionalized olefins such as α -substituted acrylic acids,^[45,116] enamides,^[117] α,β -unsaturated carboxylic acids^[44,118] and esters^[37,62,119] could be successfully achieved using ruthenium-, rhodium- or iridium-based complexes. More recently, further examples of unsaturated carbonyl compounds, like enones, have been successfully chemoselectively reduced at the C=C bond in good yield and enantioselectivity.^[37,101,120] These reactions show that in the field of transition metal-catalyzed hydrogenation in general higher reactivity is observed for C=C compared to C=O bonds.^[6d,121] Some important exceptions are the iridium catalysts developed in the Takaya^[122] and Zhou^[48-49] group (see Chapter 1, Scheme 11) as well as Noyori's ruthenium-based catalyst,^[123] which preferentially reduce C=O bonds in the presence of C=C bonds.

Despite the recent progress in this field, the chemoselective, metal-catalyzed asymmetric hydrogenation of the C=C bonds of α,β -unsaturated aldehydes is unexplored. The major issue with this kind of transformation is the enhanced reactivity of the C=O bond which favors over-reduction, yielding the saturated alcohols rather than the saturated aldehydes as final products.^[124]

An alternative synthetic approach to α - and β -substituted chiral aldehydes is represented by the transfer hydrogenation of the parent enals. In recent years many organocatalysts have been reported^[125] to catalyze such reaction in good yield and chemoselectivity but unfortunately relatively low levels of enantiomeric excesses and high catalyst loading render this synthetic route less attractive for large scale syntheses.

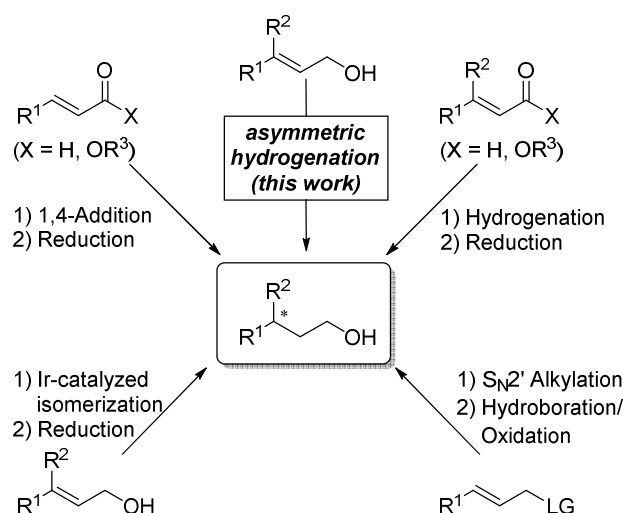
The need for a general method for the highly enantioselective reduction of enals occurring selectively at the C=C bond set a challenge that could potentially be tackled using iridium-

catalyzed asymmetric hydrogenation by judicious choice of catalyst and reaction conditions.

Unfortunately, this goal could not be attained. Generally a mixture of the desired product, the related allylic alcohol and the corresponding saturated alcohol were obtained (see subsection 4.2.1). Nonetheless, the latter was formed in excellent enantioselectivity when β,β -disubstituted enals were employed as a substrates. This observation and the impossibility to selectively reduce the C=C bond of α,β -unsaturated aldehydes under the reaction conditions investigated, shifted the focus of the study on the reduction of allylic alcohols. It was discovered that, under similar reaction conditions to those tested for enals, the corresponding 3,3-disubstituted allylic alcohols could be reduced to afford the same product in similar yield and enantioselectivity, indicating that the aldehyde moiety is not crucial for the outcome of the reaction.

The interest in prochiral allylic alcohols in the field of asymmetric hydrogenation started with Noyori's first report in 1987, when the use of Ru-BINAP catalysts for the asymmetric hydrogenation of geraniol and nerol was unveiled.^[126] Since then, many studies have been reported on the selective hydrogenation of 2,3-disubstituted allylic alcohols and, in particular, α -methyl cinnamyl alcohol has become a standard substrate for the evaluation of new metal complexes for asymmetric hydrogenation. Nevertheless, the currently available methodologies for the enantioselective reduction of this substrate class, lack in generality.^[1b,127]

For instance, the hydrogenation of their 3,3-disubstituted allylic alcohols proved considerably more difficult to achieve with high degrees of stereoselectivity and for a wide range of substrates,^[1b,127] and only a few specific compounds could be successfully deployed for this reaction.^[126,128] Therefore, state-of-the-art asymmetric methodologies for the preparation of 3,3-disubstituted chiral primary alcohols are mainly based on multi-step syntheses that rely on a first enantioselective transformation carried out on a functionalized substrate, followed by an adjustment of the oxidation state of the resulting product. As summarized in Scheme 41 asymmetric S_N2' allylic alkylation,^[129] 1,4-addition onto α,β -unsaturated carbonyl compounds,^[130] asymmetric isomerization of allylic alcohols to aldehydes,^[131] asymmetric hydrogenation of α,β -unsaturated carboxylic acids,^[132] esters^[132] and aldehydes^[125] all afford products that require further redox transformations to yield the target molecules.



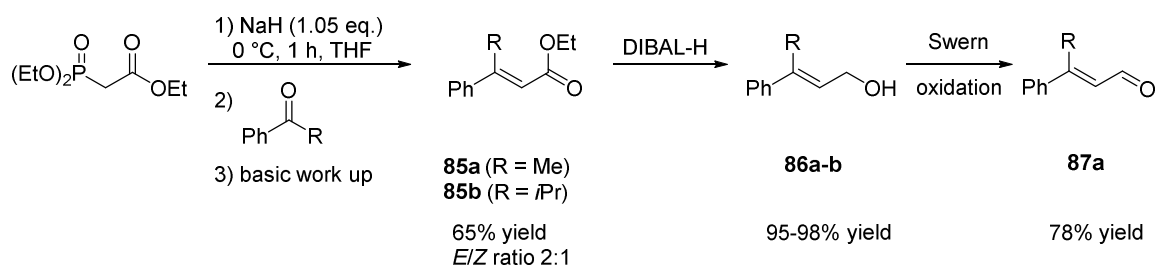
Scheme 41: Synthetic routes to enantioenriched 3,3-disubstituted primary alcohols.

Therefore, a more direct approach to the synthesis of these alcohols, that affords the product in the right oxidation state with no need for further functional group manipulation would be highly desirable.

4.2 Results and Discussion

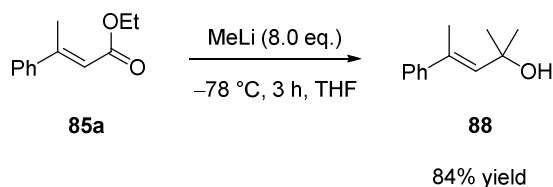
4.2.1 Substrate Synthesis

The substrates needed for the investigations shown in this Chapter were easily obtained in a three steps synthetic sequence. While ester **85a** was commercially available, compound **85b** was synthesized via Horner–Wadsworth–Emmons reaction of *iso*-butyrophenone with triethyl phosphonoacetate yielding the desired α,β -unsaturated ester in good yield. Subsequent DIBAL-H reduction led to 3,3-disubstituted allylic alcohols **86a-b**, which could then be oxidized under Swern conditions^[133] to the related aldehydes **87a** (Scheme 42).



Scheme 42: Synthesis of allylic alcohols **86a,b** and α,β -unsaturated aldehyde **87a**.

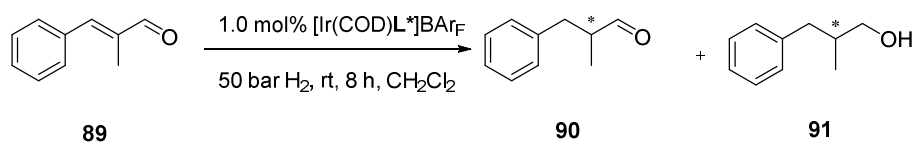
The synthesis of tertiary alcohol **88** was achieved following the procedure described by Weinreb *et al.*^[134] Methylolithium addition to ester **85a**, yielded the desired compound **88** in 84% yield (Scheme 43).



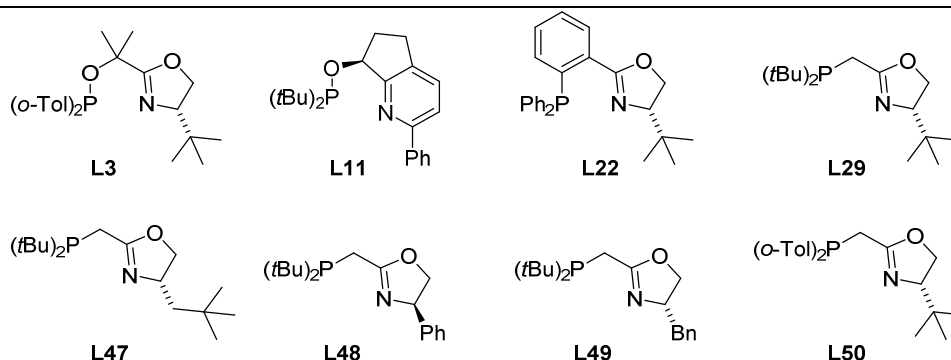
Scheme 43: Synthesis of tertiary allylic alcohol **88**.

4.2.2 Attempted Iridium-Catalyzed Chemoselective Asymmetric Hydrogenation of α,β -Unsaturated Aldehydes

As mentioned earlier, the original aim of the project described in this Chapter was the chemoselective reduction of the C=C bond of α,β -unsaturated aldehydes. Initial experiments were aimed at identifying the most promising class of chiral iridium catalysts for the hydrogenation of commercially available *trans*- α -methyl-cinnamaldehyde **89** (Table 35). The results outlined in Table 35 show that, regardless of the catalyst used, under screening conditions (50 bar H₂, rt, CH₂Cl₂), the major product observed was the saturated alcohols **91**, resulting from the reduction of both C=C and C=O bonds. In contrast, the desired aldehyde **90** could only be detected in some cases and always as the minor product. Among the catalysts tried, those based on ligands **L29** and **L47**, belonging to the phosphinomethyloxazoline family, proved to be the most active (entries 4 and 5), whereas poor activity was observed for other iridium N,P-ligand complexes (Table 35, entries 1-3). The phosphinomethyloxazoline ligand class has proven particularly effective for the hydrogenation of tetrasubstituted olefins^[29b,36,135] but so far has not found use for the hydrogenation of other substrate classes. Catalysts derived from **L29** or the likes of are attractive because the chiral ligands are readily accessible through several short synthetic routes^[29b,35-36,135] (See also Section 1.2.2). In the examples reported in Table 35, the presence of a sterically hindered *tert*-butyl group on the phosphine and an alkyl group on the oxazoline seemed necessary to achieve full conversion, as the results with ligands **L48**, **L49** and **L50** show (entries 6-8).

Table 35: Ligand screening in the chemoselective hydrogenation of aldehyde **89**.

Entry	L*	Conversion to 90 ^[a] (%)	Conversion to 91 ^[a] (%)	ee 91 ^[b] (%)
1	L3	5	9	n.d.
2	L11	2	2	n.d.
3	L22	0	0	-
4	L29	0	>99	26 (–)
5	L47	0	>99	28 (–)
6	L48	4	39	19 (+)
7	L49	9	27	15 (–)
8	L50	6	2	n.d.



n.d. = not determined; [a] Determined by GC analysis of the reaction mixture after removal of the catalyst; [b] Determined by GC analysis on a chiral stationary phase.

The outcome of this series of experiments clearly indicated that the olefin and the aldehyde moiety possess similar reactivity, rendering the chemoselective hydrogenation of such substrates with the catalysts developed in the Pfaltz group difficult to achieve. Given the poor enantiomeric excess obtained with aldehyde **89**, and in order to explore the generality of this method, its β,β -disubstituted isomer **87a** was synthesized and tested in the catalytic process (Table 36). Like in the previous example, only the catalysts based on **L29**, **L47** and **L51** were able to promote the hydrogenation. While catalysts bearing **L47** and **L51** gave only traces of the corresponding allylic alcohol **86a**, ligand **L29** afforded a mixture of allylic alcohol **86a**, saturated alcohol **93a** and the desired product **92a**. It is

worth highlighting that, despite the low conversion, very high enantiomeric excess (98%) for aldehyde **92a** was achieved. This is remarkable since, as mentioned earlier, the asymmetric reduction of β,β -disubstituted α,β -unsaturated aldehydes has been proven to be more challenging in terms of selectivity and substrate scope than the corresponding α,α -disubstituted analogs.^[1b,127] On the other hand, the results summarized in Table 36 confirm the difficulty in developing a chemoselective reduction of substrates like **87a** or **89**. In this regard it seems that little changes on the ligand structure have a major impact on the outcome of the catalysis. Indeed, when catalysts bearing **L47** or **L51** were used, C=O bond reduction was faster than olefin reduction. The opposite effect was observed with ligand **L29**.

Table 36. Ligand screening for the chemoselective hydrogenation of **87a**.

Entry	L*	Conv. to 92a ^[a] (%)	Conv. to 86a ^[a] (%)	Conv. to 93a ^[a] (%)
1	L11	0	0	0
2	L13	0	0	0
3	L29	12 (–98% ee) ^[b]	8	5
4	L47	0	9	0
5	L50	0	0	0
6	L51	0	19	0

L11

L13

L29

L47

L50

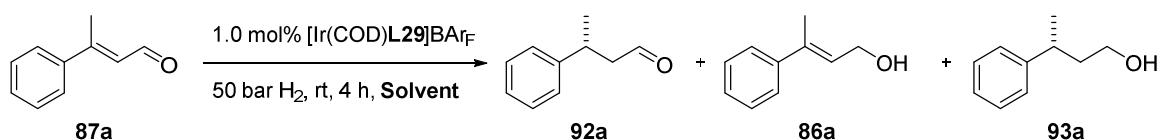
L51

[a] Determined by GC analysis of the reaction mixture after removal of the catalyst; [b] Determined by GC analysis on a chiral stationary phase.

In an attempt to improve the results obtained with the most successful iridium complex bearing ligand **L29**, the effect of the solvent was scrutinized as summarized in Table 37.

Unfortunately, the solvents tested did not improve the conversion to the saturated aldehyde **92a**. In contrast, in toluene exclusive reduction of the C=O bond took place, leaving the olefin untouched (Table 37, entry 1). A similar outcome could be observed in etheral solvents such as methyl-*tert*-butyl-ether or diethylether, with the C=O reduction being considerably faster than the hydrogenation of the C=C bond (entries 2 and 3).

Table 37: Solvent screening in the chemoselective hydrogenation of **87a**.



Entry	Solvent	Conv. 92a ^[a] (%)	Conv. 86a ^[a] (%)	Conv. 93a ^[a] (%)	ee 93a ^[b] (%)
1	Toluene	0	21	0	-
2	MTBE	1	34	12	95 (–)
3	Et ₂ O	2	52	14	96 (–)
4	THF	0	0	>99	97 (–)
5	PhCl	0	0	>99	98 (–)

[a] Determined by GC analysis of the reaction mixture after removal of the catalyst; [b] Determined by GC analysis on a chiral stationary phase.

In tetrahydrofuran (THF) as well as in chlorobenzene (entries 4 and 5 respectively), full conversion to the saturated alcohol **93a** was detected. Despite the lack of chemoselectivity, it was surprising to notice that the transformation could be carried out with high degrees of enantioselectivity in several solvents. In fact, enantiomeric excesses above 95% were achieved regardless of the solvent used (entries 2–5). Several reports on the iridium-catalyzed hydrogenation in dichloromethane^[19] or methanol^[116c,136] have been published, but none of them documents the use of THF for such transformation. In fact, this solvent has been avoided for iridium-catalyzed asymmetric hydrogenations since it is known to coordinate to the metal center, thus deactivating the catalyst (See Chapter 1.2).^[137] However, the use of THF would have several advantages over the routinely used dichloromethane, in particular, low toxicity and higher boiling point play in favor of tetrahydrofuran.

The excellent enantiomeric excesses obtained in THF for the asymmetric reduction of **87a**, as well as the lack of chemoselectivity of this transformation, rose the question about the importance of the aldehyde moiety for the outcome of the catalysis. To answer this question, related 3,3-disubstituted allylic alcohols **86a,b** were synthesized and tested as substrates for the iridium-catalyzed asymmetric hydrogenation.

4.2.3 Iridium-Catalyzed Asymmetric Hydrogenation of 3,3-Disubstituted Allylic Alcohols in Ethereal Solvents

The results of the iridium-catalyzed asymmetric hydrogenation of substrates **86a,b** using various phosphinomethyloxazoline ligands are outlined in Table 38. Similarly to what was observed previously, the electronic and steric properties of the ligand were found to have a major impact on the activity and selectivity of the catalyst. The presence of an alkyl phosphine was crucial for good performances (**L51** and **L29**). Indeed, despite the lower catalyst loading (0.5 vs. 1.0 mol% for the related α,β -unsaturated aldehydes), alcohols **93a** and **93b** were obtained in excellent enantiomeric excesses using ligand **L51** and **L29**. In contrast, ligands bearing aryl-phosphines yielded reduced activity as well as poor enantioselectivities (entries 5-8).

Table 38: Phosphinomethyloxazoline ligands in the hydrogenation of 3,3-disubstituted allylic alcohols **86a,b**.^[a,b]

<p>86a (R = Me) 86b (R = <i>i</i>Pr)</p>		<p>93a,b</p>			
L51		L29		L31	
95a , >99% conv., 95% ee (–)		95a , 7% conv., ee n.d. ^[c]		95a , 15% conv., 29 ee (–) ^[c]	
95b , >99% conv., 71% ee (–)		95b , 85% conv., 24% ee (–)		95b , 70% conv., 69% ee (–)	
				L52	
				95a , 17% conv., 58 ee (–) ^[c]	
				95b , >99% conv., 14% ee (–)	

n.d. = not determined; [a] Conversions determined by GC analysis of the reaction mixture after removal of the catalyst; [b] Enantiomeric excesses determined by GC analysis on a chiral stationary phase; [c] 3% of the (*Z*)-isomer of the starting material was detected.

A comparison between the results summarized in Table 37 and Table 38, shows that, under these reaction conditions, the aldehyde moiety has no major influence on the outcome of this transformation. The iridium catalysts bearing a phosphinomethyloxazoline ligand are able to catalyze the hydrogenation of α,β -unsaturated aldehydes as well as allylic alcohols with excellent conversion and enantiomeric excesses. Therefore, the focus of the project shifted toward the asymmetric hydrogenation of the related 3,3-disubstituted allylic alcohols.

By careful analysis of the results from the reduction of substrate **86a**, an unexpected reactivity was discovered. Indeed, the reaction catalyzed by ligands **L29**, **L31** and **L52**, afforded traces of the (Z)-regioisomer of the starting material (Table 38). This observation raised some concerns regarding the mechanism of the transformation. Instead of the classical hydrogenation mechanism (see Chapter 1.2.4), it was envisaged that another reaction pathway related to that recently proposed by Mazet *et al.*^[131] could take place (Figure 9).

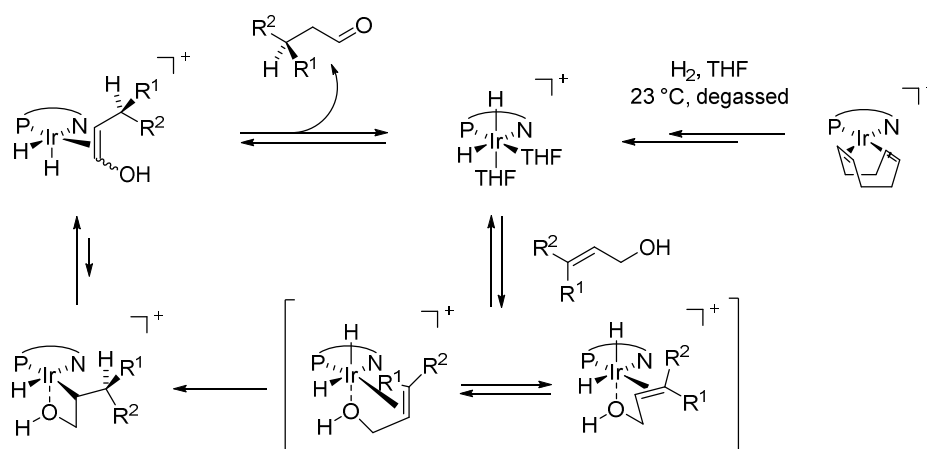
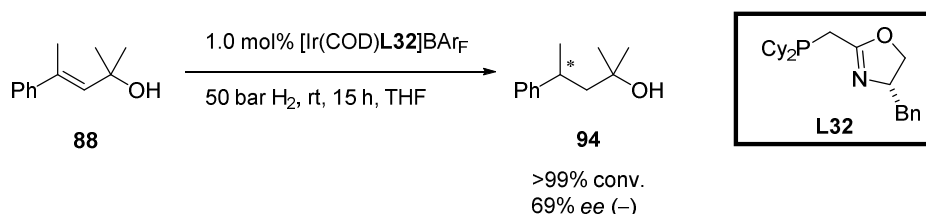


Figure 9: Proposed mechanism for the isomerisation of allylic alcohols by Mazet.^[131]

Mazet and co-workers demonstrated that, under similar reaction conditions to those used in this study, phosphinemethyloxazoline-based catalysts can promote the isomerization of allylic alcohols to the corresponding saturated aldehydes.^[1b,127]

In order to ascertain what reaction pathway did take place in the case of the hydrogenation described herein, the reduction of tertiary allylic alcohol **88**, was investigated under similar reaction conditions to those described in Table 38. Surprisingly, when catalysts bearing ligands **L29** and **L51** were applied to this transformation in addition

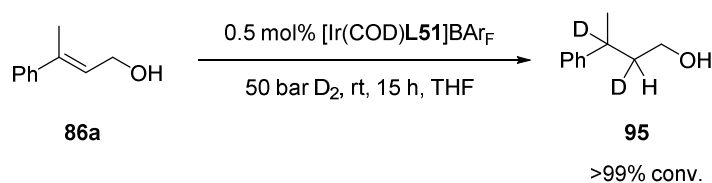
to the product, a mixture of three unidentified side products could be observed. The latter could not be assigned to side product derived from any isomerization reactions or from an elimination process. Nevertheless, judicious choice of the iridium catalyst made it possible to achieve full conversion and 69% *ee* for the formation of **94**, avoiding the formation of any unidentified by-products (Scheme 44).



Scheme 44: Asymmetric hydrogenation of allylic alcohol **88** using an iridium catalyst bearing ligand **L32**.

The outcome of the experiment shown in Scheme 44 supports the hypothesis that direct hydrogenation of the C=C bond occurs, since alcohol **88** could not react according to the mechanism proposed by Mazet and thus forming an aldehyde. However, the different behavior of the substrate with different catalysts and the formation of unidentified by-products in some cases called for further investigations aimed to clarify the reaction mechanism.

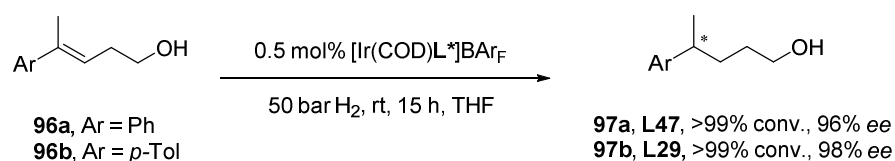
Vincenzo Ramella^[138] and Paolo Tosatti^[139] from our group, carried out further experiments which support the proposition that, under these reaction conditions, the classical hydrogenation pathway is favored. Ramella^[138] showed that when the reduction of substrate **86a** was ran under 50 bar of D₂, complete deuterium incorporation (>90%) at the C2 and C3 positions was obtained, whereas no deuteration occurred at the C1 position (Scheme 45).



Scheme 45: Deuteration experiment on allylic alcohol **86a** carried out by Vincenzo Ramella.

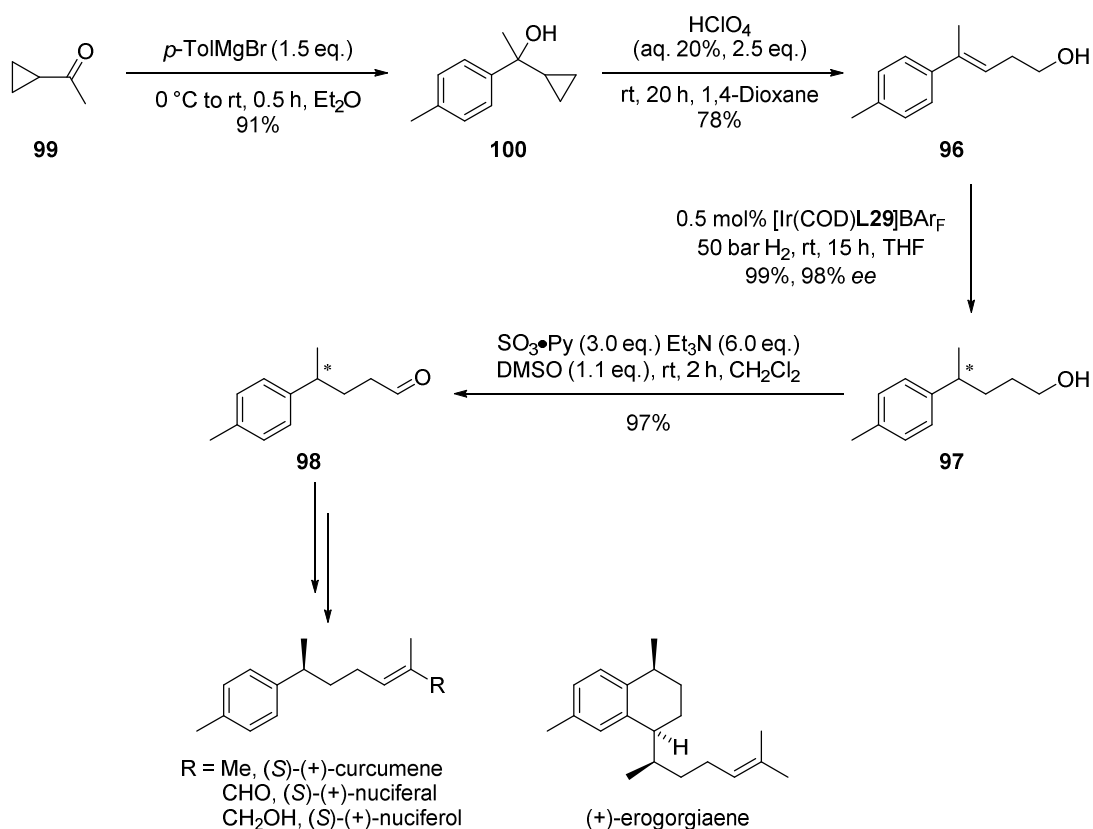
Furthermore, homoallylic alcohols **96a** and **96b** could be successfully reduced to give the saturated alcohols **97a** and **97b** with full conversion and excellent enantioselectivities (Scheme 46). The hydrogenation of this specific substrate class could not be explained

using Mazet's proposed catalytic cycle, since homoallylic alcohols cannot isomerize under these conditions to the corresponding aldehydes.



Scheme 46: Asymmetric hydrogenation of homoallylic alcohols achieved by Vincenzo Ramella and Paolo Tosatti.

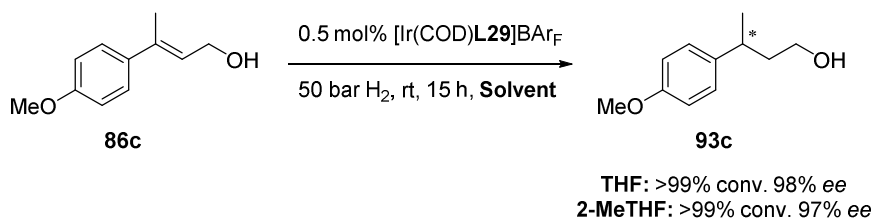
The asymmetric hydrogenation of homoallylic alcohols of this type bears considerable potential for application in organic synthesis. In fact, the reduction of **96b** to **97b** is a key step in the synthesis of four natural products, namely curcumene, nuciferal, nuciferol and erogorgiaene. All these bisabolane sesquiterpenes can be accessed starting from **97b** via the corresponding aldehyde **98**.^[140] Thus the sequence leading to highly enantioenriched aldehyde **98** shown in Scheme 47 represents a formal synthesis of these natural products.



Scheme 47: Formal total synthesis of natural products through alcohol **97b**.

Homoallylic alcohol **96b** was synthesized by Tosatti^[139] starting from commercially available cyclopropyl methyl ketone **99** and yielding the desired compound after a two-step transformation involving Grignard addition followed by acid-catalyzed rearrangement of the tertiary alcohol **100**. After iridium-catalyzed asymmetric hydrogenation of **96b**, the resulting chiral alcohol **97b** was converted to aldehyde **98** via Parikh–Doering oxidation^[141] in 97% yield. Compared to the most efficient published route to **98**, which is based on the enantioselective cyclopropanation of *para*-methylstyrene,^[142] the sequence shown in Scheme 47 was shorter and the overall yield of **98** was higher (68% vs. 30–36%).^[143]

In order to broaden the substrate scope of the asymmetric hydrogenation of allylic alcohols, Vincenzo Ramella synthesized, in the course of his master thesis,^[138] various aryl/alkyl and alkyl/alkyl 3,3-disubstituted allylic alcohols and tested them in the iridium-catalyzed asymmetric hydrogenation. During this study, following a suggestion by Tosatti, he found that similar results in the asymmetric hydrogenation of allylic alcohol **86c** were obtained using 2-MeTHF, a “greener” solvent alternative to THF (Scheme 48).



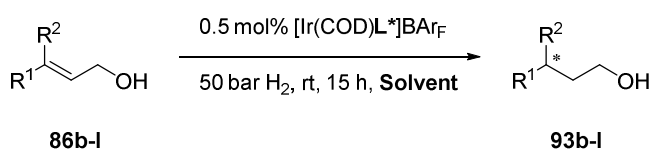
Scheme 48: Hydrogenation of allylic alcohol **86c** in THF and 2-MeTHF achieved by Vincenzo Ramella.^[138]

2-MeTHF is considered an ecofriendly solvent, as it can be obtained from renewable sources^[144] and has several advantages such as low miscibility with water, high stability under acid/basic conditions, formation of an effective azeotrope with water and a higher boiling point than THF, that render it particularly attractive for application in both industry and academia.^[145]

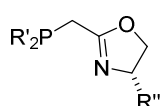
Consequently the hydrogenation of several allylic alcohols **86c–I** in THF and 2-MeTHF were examined. Table 39 summarizes the results obtained with [Ir(COD)**L29**]**BARF** and related catalysts derived from phosphinomethyloxazoline ligands. In general, slightly better results were observed in THF, although in most cases comparable levels of conversion and

enantioselectivity were achieved in the two solvents (entries 2-7). Yet in one case (entry 11) the reaction in 2-MeTHF gave significantly higher enantioselectivity than in THF. (*E*)-3-Methylcinnamyl alcohol **86b** and related aryl/methyl-substituted derivatives reacted with excellent enantioselectivities (*ee* 95-98%, entries 1-4) except for the 4-chlorophenyl derivative **86g**, which gave a slightly lower *ee* (entry 6).

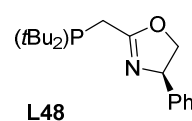
Table 39: Asymmetric hydrogenation of allylic alcohols **86** achieved by Vincenzo Ramella.^[138]



Entry	R ¹ , R ²	THF	2-MeTHF
		L*, Conv.(%), <i>ee</i> ^[a] (%)	L*, Conv.(%), <i>ee</i> ^[a] (%)
1	Ph, Me (b)	L51 , >99, 95, (–)-(R)	L51 , >99, 90
2	4-MeOC ₆ H ₄ , Me (c)	L29 , >99, 98, (–)-(R)	L29 , >99, 97
3	4-MeC ₆ H ₄ , Me (d)	L51 , >99, 95, (–)-(R)	L51 , >99, 95
4	2-MeC ₆ H ₄ , Me (e)	L51 , >99, 97, (–)	L51 , 41, 93 L51 , >99, 95 ^[b]
5	2-Naphthyl, Me (f)	L47 , 97, 95, (–)	L47 , 98, 93
6	4-ClC ₆ H ₄ , Me (g)	L48 , >99, 92, (+)	L48 , >99, 90
7	Ph, Cy (h)	L48 , 94, 92, (+)	L48 , >99, 90
8	<i>t</i> Bu, Ph (i)	L48 , 43, 96, (+)-(R)	L48 , 10, n.d. L48 , 68, 90 ^[c]
9	<i>t</i> Bu, Me (j)	L48 , >99, >99, ^[b] (–)-(S)	L48 , >99, 95 ^[b]
10	Cy, Me (k)	L53 , >99, 88, ^[b] (+)-(R)	L31 , >99, 60 ^[b]
11	<i>i</i> Bu, Me (l)	L48 , >99, 80, ^[b] (+)	L51 , >99, >99, ^[b] (–)



L29 (R' = R'' = *t*Bu)
L31 (R' = Ph, R'' = *t*Bu)
L47 (R' = *t*Bu, R'' = CH₂*t*Bu)
L51 (R' = *t*Bu, R'' = *i*Pr)
L53 (R' = Ph, R'' = *i*Pr)



[a] Conversions were determined by GC analysis of the crude reaction mixtures while enantioselectivities were determined by HPLC analysis on a chiral stationary phase; [b] 1 mol% of catalyst used; [c] Reaction carried out for 20 h with 2 mol% of catalyst.

The sterically hindered *ortho*-tolyl derivative **86e** required a higher catalyst loading of 1.0 mol% instead of 0.5 mol% to reach full conversion in 2-MeTHF. While high conversion and good enantioselectivity could be achieved for the phenyl/cyclohexyl-substituted substrate **86h** (entry 7), a substantial decrease of conversion but excellent *ee* (99% in THF) was observed for the phenyl/*tert*-butyl derivative **86i** (entry 8). The *tert*-butyl/methyl analog **86j**, on the other hand, gave full conversion at 1 mol% catalyst loading (entry 9). The dialkyl-substituted substrates **86k** and **86l** proved to be less reactive than the corresponding aryl/alkyl-substituted compounds, but at 1.0 mol% catalyst loading full conversion was achieved. While the enantioselectivity was only moderate for the cyclohexyl/methyl derivative **86k**, up to 99% *ee* was recorded for **86j** and **86l** using the appropriate catalyst and solvent (entries 9 and 11). Overall the results show that the proper choice of the phosphinomethyloxazoline ligand and the solvent (THF or 2-MeTHF) is crucial to obtain optimal results for a particular substrate.

4.3 Summary

In summary, the feasibility of a chemoselective asymmetric hydrogenation of α,β -unsaturated aldehydes was investigated using iridium catalysts developed in the Pfaltz group. This ambitious transformation, due to the similar reactivity of the C=C and C=O bonds, suffered from over-reduction yielding a mixture of the desired saturated aldehyde, the related allylic alcohol as well as the saturated alcohol. Nonetheless, the latter could be obtained in excellent enantiomeric excess in the reduction process of β,β -disubstituted enals using catalysts based on phosphinomethyloxazoline ligands.

Such ligands performed best also in the iridium-catalyzed asymmetric hydrogenation of the corresponding 3,3-disubstituted allylic alcohols, a type of substrate that cannot be efficiently hydrogenated in an enantioselective manner with current methodologies. In addition, the required ligands are structurally simple and readily accessible from enantiopure aminoalcohols *via* several short syntheses,^[29b,35-36,135] adding attractiveness to the reaction presented herein. Importantly, reactions could be carried out in either THF or 2-MeTHF, which are ecologically advantageous and better suited for industrial applications than the commonly used dichloromethane. In order to explore the scope of

Chapter 5

Chiral *N*-Heterocyclic Carbene/Pyridine Ligands for the Iridium-Catalyzed Asymmetric Hydrogenation of Olefins

5.1 Introduction: *N*-Heterocyclic Carbenes in Transition Metal Catalysis^[146]

Despite early work on *N*-heterocyclic carbenes carried out by Öfele^[51] and Wanzlick,^[50] in the 1960s, it was not until 1991 that these molecules started to attract the attention of several scientists. The turning point in this revived interest was represented by the discovery that some carbenes can be isolated and easily handled using classical inert atmosphere techniques.^[147] From this moment on, the number of reports dealing with the application of NHC carbenes as ligands in homogeneous catalysis grew significantly.^[148]

Nowadays the most common NHC ligands have five-membered scaffolds, namely imidazolylidenes, imidazolinylienes or a triazolylidenes (Figure 10). While the latter is widely used in organocatalysis,^[149] the first two structure classes are widely employed in transition metal catalysis, with elements of the d-block from group 7 to group 11.^[58d,146,150]

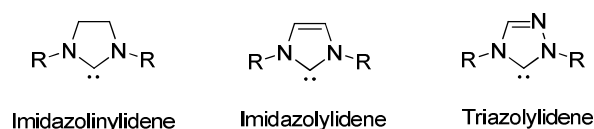


Figure 10: Structures of most common *N*-Heterocyclic Carbenes.^[146]

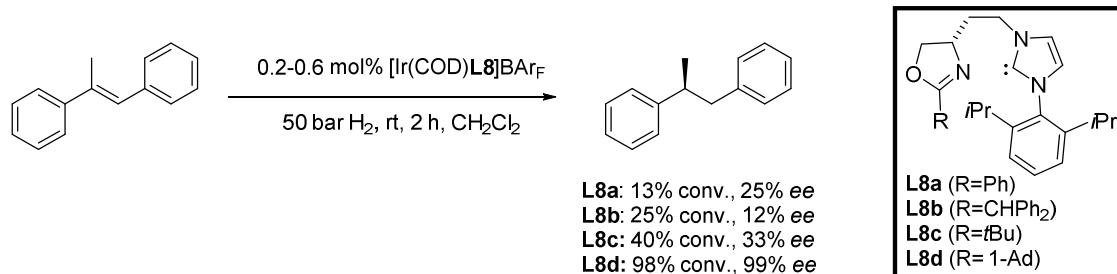
Classic applications of NHC-ligands in transition metal catalysis are represented by ruthenium-based olefin metathesis^[150] and palladium,^[151] nickel,^[152] copper^[153] or iron-catalyzed^[154] cross coupling reactions. In addition, a variety of other transformations like, for instance, cyclization,^[155] cycloaddition^[156] or cycloisomerization^[157] reactions have been shown to be catalyzed efficiently by NHC-metal complexes. Recently, this ligand class has also been deployed for reduction reactions, in particular, hydrosilylation,^[148b,158] borrowing hydrogen^[159] or more classical hydrogenation^[57b,61,160] reactions.

In general, the enhanced σ -electron-donating properties^[161] of the carbene ligands result

in strong carbene-metal bonds^[162] which render the catalyst structure robust, preventing complex decomposition.

5.1.1 *N*-Heterocyclic Carbenes in Asymmetric Hydrogenation Reactions

Although the first applications of NHC ligands to different asymmetric metal-catalyzed reactions were reported in the late 1990s and early 2000s,^[52,53b,60b] only poor to moderate enantioselectivities could be achieved. A breakthrough in this field is certainly represented by the work carried out in 2001 by Burgess *et al.*^[61] who found out that an iridium catalyst bearing a bulky bidentate imidazolyldine-oxazoline-based NHC ligand allowed for the enantioselective hydrogenation of various unfuctionalized olefins in very good yields and selectivities. In particular, excellent results in terms of activity and selectivity were obtained in the asymmetric hydrogenation of *trans*-methyl stilbene using ligand **L8d**, bearing a sterically demanding adamantyl-group on the imidazolyldine moiety and a 2,6-di-*isopropylphenyl* group on the oxazoline ring (Scheme 51).^[61]



Scheme 51: Asymmetric hydrogenation of *trans*-methyl stilbene using various NHC ligands **L8**.

After Burgess' initial investigations,^[61] other research groups,^[163] including our own,^[65,164] became interested in using bidentate NHC carbenes as ligands for iridium catalysts (Figure 11). Despite considerable efforts, none of the new complexes afforded better results than ligand **L8d**. Building on the success of their ligand in the hydrogenation of *trans*-methyl stilbene, the Burgess group^[165] broadened the substrate scope of the hydrogenation to functionalized olefins,^[165] demonstrating the versatility of NHC based ligands, that became valid alternatives to phosphines in iridium-catalyzed asymmetric hydrogenation in some cases.

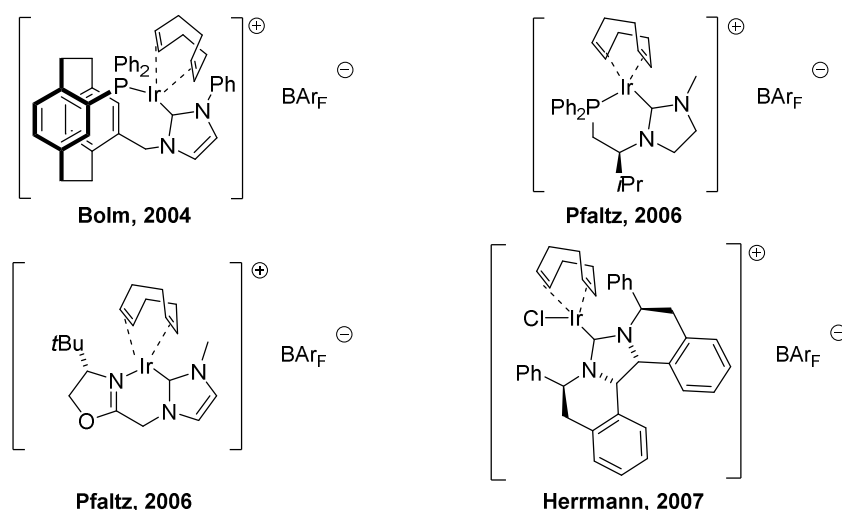


Figure 11: Iridium catalysts bearing NHC ligands applied to asymmetric hydrogenation.

Indeed, one advantage of iridium catalysts possessing a bidentate imidazolylidine-oxazoline-based NHC ligand is the lower acidity of the corresponding hydrides compared to their N,P-analogs,^[64] that renders these catalysts particularly suited for acid-sensitive substrates.^[64]

Given the utility of Burgess catalyst $[\text{Ir}(\text{COD})\text{L8d}]\text{BArF}$ and, on the other hand, the paucity of alternative ligands to **L8d** for iridium-catalyzed asymmetric hydrogenation, our group continued its efforts to find alternative NHC-based ligands which could be complementary to the Burgess system, so to broaden even more the current substrate scope of the hydrogenation.

In this context and considering the successful applications of pyridine phosphinite ligands,^[30g,166] Andreas Schumacher, prepared a series of NHC-pyridine analogs **L34a-c** to be tested as chiral ligands for iridium-catalyzed asymmetric hydrogenation (Figure 12).^[167]

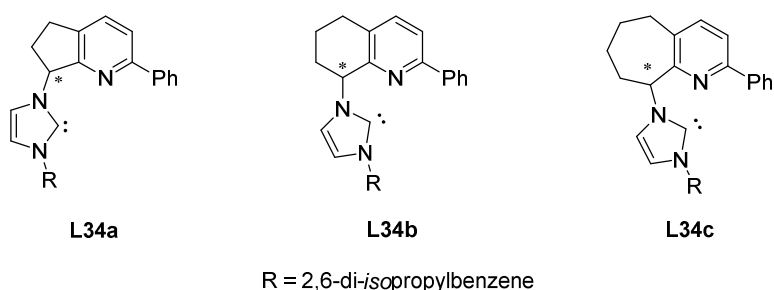
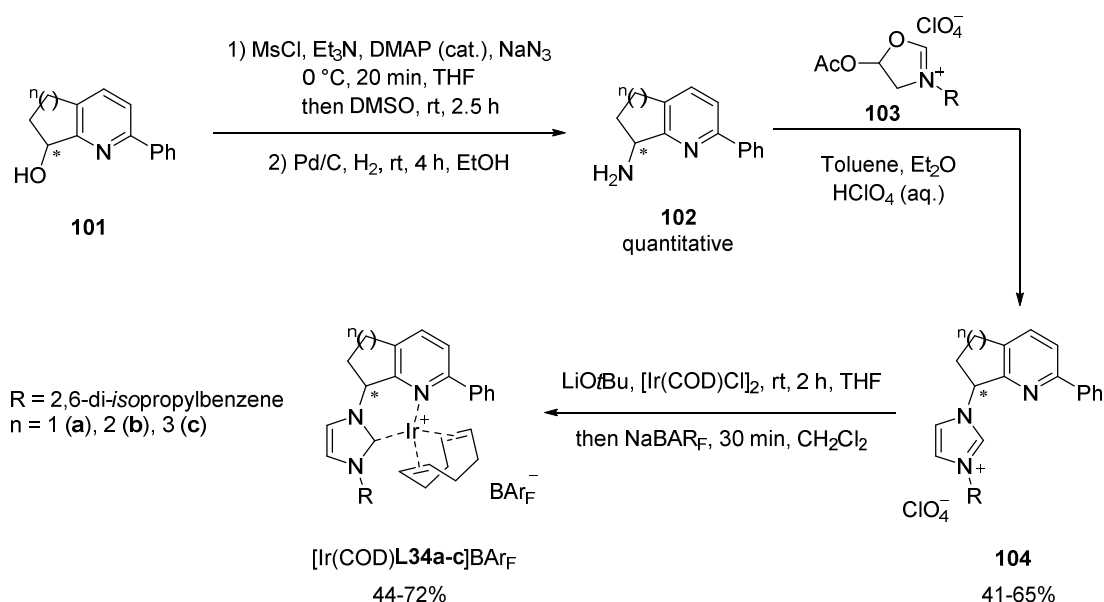


Figure 12: NHC-pyridine-based ligands synthesized by Schumacher for iridium-catalyzed asymmetric hydrogenation.

He started the preparation of ligands **L34a-c** from previously synthesized, enantiopure, bicyclic pyridyl alcohols having a five, six, or seven-membered carbocyclic ring. These alcohols were converted into the corresponding amines **102** by mesylation and subsequent reaction with sodium azide, followed by hydrogenation with Pd/C.^[168] The coupling of primary amines **102** with the imidazolium salt **103** was achieved following the method of Fürstner *et al.*,^[169] yielding the enantiomerically pure ligands **104** as perchlorate salts. Treatment with lithium *tert*-butoxide in THF and complexation with [Ir(COD)Cl]₂ in the presence of NaBAR_F resulted in the formation of the desired iridium complexes [Ir(COD)**L34a-c**]BAR_F in moderate to good yields (Scheme 52).^[167]

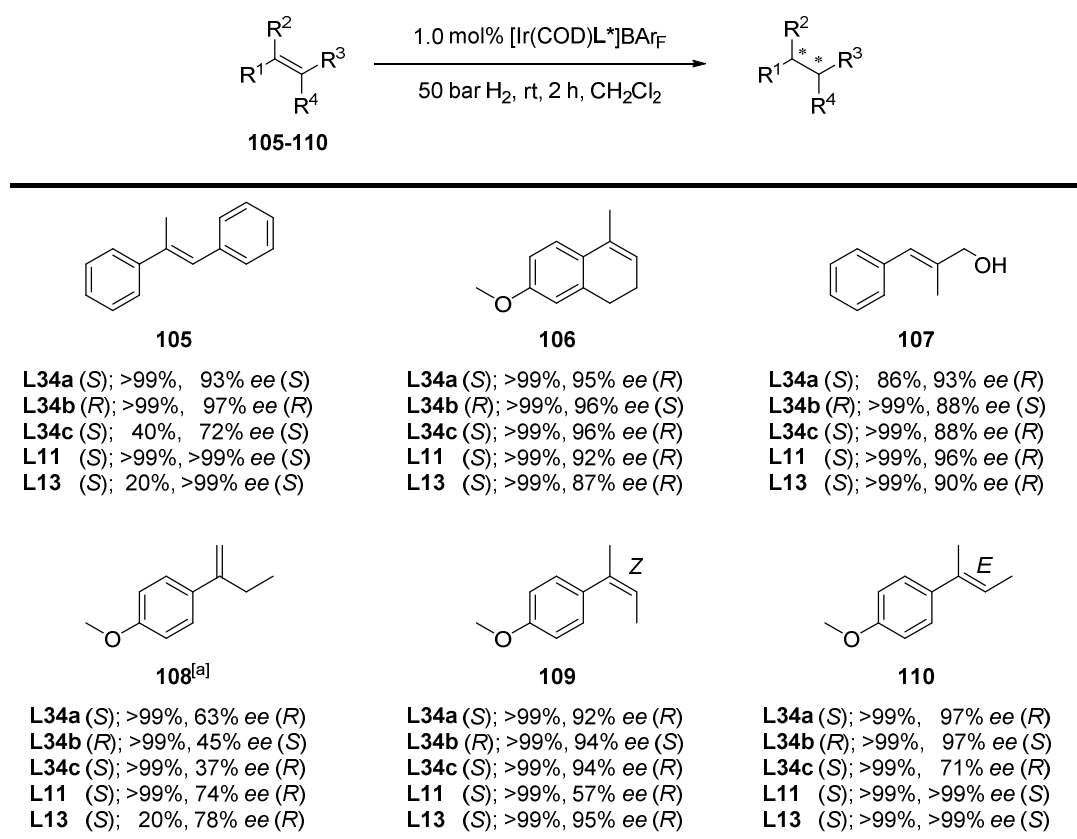


Scheme 52: Synthesis of catalysts [Ir(COD)**L34a-c**]BAR_F carried out by Andreas Schumacher.^[167]

Evaluation of the new NHC/pyridine ligands **L34a-c** in the iridium catalyzed asymmetric hydrogenation of six typical test substrates was started by Andreas Schumacher, who compared their results with those obtained with analogs pyridine phosphinite ligands **L11** and **L13** (Scheme 53).^[167] With two exceptions (**L34c** with substrate **105** and **L34a** with **107**), the new complexes showed high catalytic activity and led to full conversion within 2 hours at 50 bar hydrogen pressure and 1.0 mol% catalyst loading. In general, enantioselectivities were comparable to those obtained with analogs pyridine phosphinite ligands **L11** and **L13** or Burgess' oxazoline-NHC ligand **L8d**,^[61,170] with the exception of terminal alkene **108**. In this case ligand **L8d** yielded superior results compared to ligands **L34a-c** (89 vs. 63% *ee*).^[170a]

The opposite effect was observed in the reduction of (*Z*)-alkene **109**, with ligands **L34a-c** performing better than ligand **L30** (92-94 vs. 80% *ee*).^[170a] This result indicates that the pyridine-derived ligands **L34a-c** are a useful addition to the oxazoline derived ligand **L8**, and enhance the application range of NHC-based iridium catalysts.

Further to the success of the catalysts based on ligands **L34**, the next step was to test their performance in the reduction of acid-labile substrates. An example of such compounds is represented by protected allylic alcohols,^[64] which can be hydrogenated with only poor results with standard N,P-ligand-based iridium catalysts.^[36] In addition, the activity of these new iridium complexes at lower catalyst loading needed to be investigated.

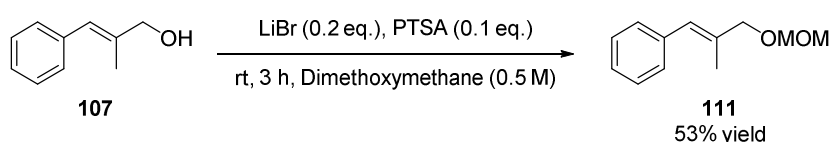


Scheme 53: Iridium-catalyzed asymmetric hydrogenation of substrates **105-110** performed by Schumacher;^[167] [a] Reaction carried out at 1.0 bar H₂.

5.2 Results and Discussion

5.2.1 Iridium-Catalyzed Asymmetric Hydrogenation of Acid-Labile Substrates

Methoxymethyl ether (MOM) protected allylic alcohol **111** was chosen as an initial test substrate for iridium-catalyzed asymmetric hydrogenation, since methoxymethyl ethers are known to be labile under acidic conditions^[171] and therefore represent an interesting substrate class for this investigation. Compound **111** was easily synthesized in moderate yield following Okahara's procedure^[172] starting from allylic alcohol **107** (Scheme 54).



Scheme 54: Synthesis of protected allylic alcohol **111**.

Despite the excellent enantiomeric excesses achieved using N,P-based ligands (Table 40, entries 1-2), the formation of an unidentified side product could not be avoided.

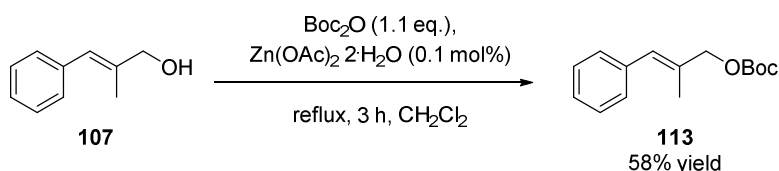
Table 40: Iridium-catalyzed asymmetric hydrogenation of **111**.

Entry	L*	Conversion to 112 ^[a] (%)	ee 112 ^[b] (%)
1 ^[c]	L11	83	93 (+)
2 ^[c]	L13	83	96 (+)
3	L34a	>99	30 (+)
4	L34b	>99	52 (–)

L11	L13	L34a	L34b

[a] Determined by GC analysis of the reaction mixture after removal of the catalyst; [b] Determined by HPLC analysis on a chiral stationary phase; [c] 17% of an unidentified product was observed.

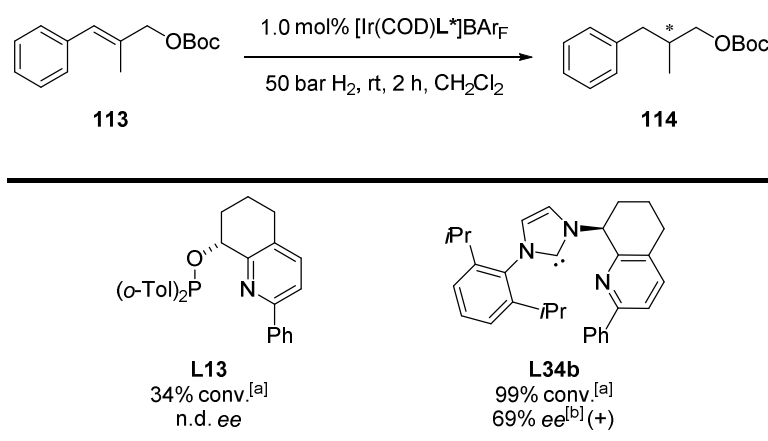
This undesired product did not form when the transformation was catalyzed by NHC ligands, although lower enantioselectivities were detected (*cf.* entries 1-2 with 3-4). Another acid-sensitive substrate that was used to test the performance of the catalyst based on ligand **34b**, was the *tert*-butoxycarbonyl (Boc) protected allylic alcohol **113**, synthesized in one step^[173] starting from allylic alcohol **107** (Scheme 55).



Scheme 55: Synthesis of protected allylic alcohol **113**.

As summarized in Table 41, the difference between the N,P-based and NHC-pyridine-based ligands was even more striking than in the previous example. Indeed, when the catalyst bearing ligand **L13** was applied to this transformation, in addition to the product, a mixture of many unidentified side products could be observed. In contrast, with ligands **L34b** substrate **113** underwent clean hydrogenation to afford the Boc-protected saturated alcohol **114** with 69% *ee* in essentially quantitative yield.

Table 41: Iridium-catalyzed asymmetric hydrogenation of **113**.



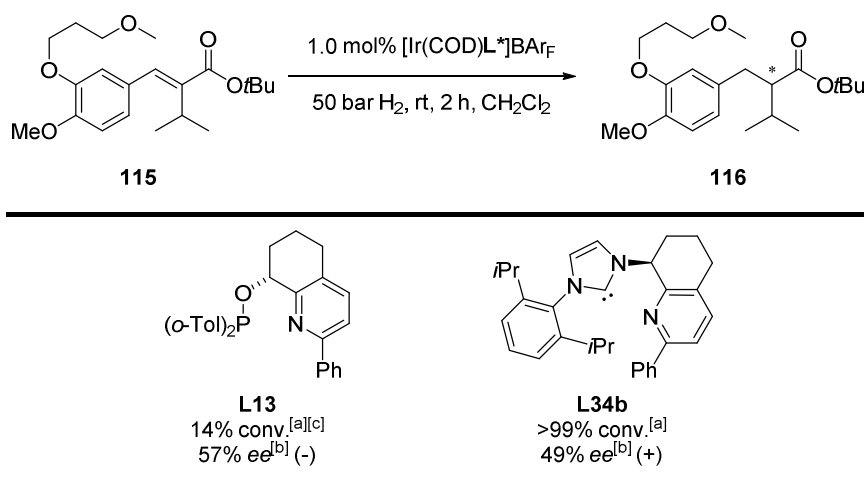
n.d.= not determined; [a] Conversion to compound **114**, determined by GC analysis of the reaction mixture after removal of the catalyst; [b] Determined by HPLC analysis on a chiral stationary phase.

Lastly, ester **115** was chosen as an additional test substrate to compare the performance of the NHC/pyridine ligands with the classic N,P-analogs. In previous investigations^[119] on the asymmetric hydrogenation of Aliskiren derivative **115**, the *tert*-butyl group on the

ester moiety was found to undergo cleavage in the presence of N,P-based iridium complexes, affording the corresponding saturated carboxylic acid as the major product. The high Brønsted acidity of the iridium hydrides formed in the course of the reaction is assumed to be responsible for the observed ester cleavage.^[64,119]

In order to avoid this undesired reaction, the novel, less acidic NHC/pyridine based ligand **L34b** was employed in the iridium-catalyzed hydrogenation of α,β -unsaturated ester **115** (Table 42). In the presence of [Ir(COD)**L13**] BAR_F the saturated carboxylic acid of **116** was formed in 86% yield.^[119] In contrast, the use of an iridium catalyst bearing the NHC/pyridine ligand **L34b**, allowed for the smooth hydrogenation of compound **115** to yield the desired *tert*-butyl ester **116** in full conversion and moderate enantioselectivity, confirming the reduced acidity of these new NHC/pyridine based complexes compared to the classical catalysts bearing N,P-ligands.

Table 42: Iridium-catalyzed asymmetric hydrogenation of **115**.



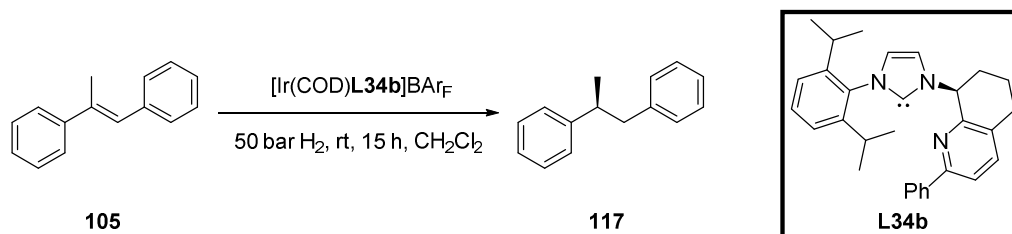
[a] Conversion to compound **116**, determined by GC analysis of the reaction mixture after removal of the catalyst; [b] Determined by HPLC analysis on a chiral stationary phase; [c] 86% conversion to the corresponding saturated carboxylic acid was detected.

5.2.2 Catalyst Loading Screening in the Asymmetric Hydrogenation of *trans*-Methyl Stilbene

Another goal of this project was to study the activity of the new iridium complexes by investigating the impact of lower catalyst loadings on the outcome of the hydrogenation

reaction. For this purpose *trans*-methyl stilbene **105** was chosen as the substrate of choice in combination with the most promising NHC/pyridine ligand, **L34b** (Table 43).

Table 43: Catalyst loading screening in the asymmetric hydrogenation of **105** using [Ir(COD)**L34b**]**BAR_F**.



Entry	Catalyst loading (mol%)	Conversion ^[a] (%)	ee ^[b] (%)
1	1.00	>99	97
2	0.75	>99	96
3	0.5	>99	96
4	0.25	28	83

[a] Determined by GC analysis of the reaction mixture after removal of the catalyst; [b] Determined by HPLC analysis on a chiral stationary phase.

As shown in Table 43, the catalyst loading could be reduced down to 0.5 mol% without affecting either the yield or the enantioselectivity of the transformation (entries 1-3). However, when the amount of catalyst was lowered to 0.25 mol%, a significant drop in activity and selectivity was observed (entry 4).

5.3 Summary^[167]

In summary, the newly synthesized NHC/pyridine based ligands developed by Andreas Schumacher showed that replacement of the phosphinite group in classical pyridine-based iridium complexes by a NHC unit leads to efficient and highly enantioselective hydrogenation catalysts. In the hydrogenation of various olefins the phosphinite- and the NHC-based catalysts showed similar selectivities. However, as a result of the lower acidity of the iridium hydride intermediates produced from the NHC-based complexes, these catalysts are better suited for the hydrogenation of acid-sensitive substrates like **111**, **113** and **115**. Moreover, the reaction proceeded with complete conversion even with reduced catalyst loadings (down to 0.5 mol%) confirming the high reactivity of this new ligand class.

Chapter 6

Experimental Section

6.1 General Information

6.1.1 Working techniques

Commercially available reagents were purchased from Acros, Aldrich, Alfa-Aesar and used as received. The solvents were collected from a purification column system (PureSolv, Innovative Technology Inc.)^[174] or purchased from Aldrich or Fluka in sure/sealedTM bottles over molecular sieves. Column chromatographic purifications were performed on Merck silica gel 60 (particle size 40–63 nm) according to the procedure published by *Still* and *Mitra*.^[175] The eluents were of technical grade and distilled prior to use. The hydrogenation experiments were prepared under air, unless otherwise specified.

6.2.1 Analytical methods

Thin Layer Chromatography (TLC): TLC plates were obtained from Merck (Silica gel 60 F₂₅₄). UV light (254 nm) or basic permanganate solution were used to visualize the respective compounds.

NMR Spectroscopy: NMR spectra were measured on either a Bruker DPX-NMR (400 MHz) or a Bruker Avance DRX-NMR (500 MHz) spectrometer equipped with BBO broadband probe heads. Chemical shifts (δ) are reported in parts per million (ppm) and coupling constants (J) are reported in Hertz (Hz). Deuterated NMR solvents were obtained from Cambridge Isotope Laboratories, Inc. (Andover, MA, USA). The measurements were performed at 25 °C. The chemical shift (δ) values were corrected to 7.26 ppm (¹H NMR) and 77.16 ppm (¹³C NMR) for CHCl₃, or to 2.54 ppm (¹H NMR) and 40.45 ppm (¹³C NMR) for DMSO. ¹³C and ¹⁹F spectra were recorded 1H-decoupled. Multiplicities are reported as follows: s=singlet, d=doublet, t=triplet, q=quartet, quin=quintet, sext=sextet, sept=septet, m=multiplet.

Infrared Spectroscopy (IR): IR spectra were recorded on a Shimadzu FTIR-8400S Fourier Transform spectrometer with ATR/Golden Gate technology. The absorption bands are given in wave numbers $\tilde{\nu}$ (cm^{-1}). The peak intensity is reported as follows s (strong), m (medium) and w (weak). The index br stands for broad.

Optical Rotations ($[\alpha]_D^{20}$): Optical rotations were measured on a Perkin Elmer Polarimeter 341 (1 dm cylindrical cell) or on a Jasco P-2000 Polarimeter (1 dm cylindrical cell) at 589 nm. The concentration (c) is given in g/100 mL.

High Resolution Mass Spectrometry (HRMS): High resolution mass spectra (ESI) were measured by Dr. H. Nadig (Department of Chemistry) on a Bruker MaXis 4G.

Elemental Analysis (EA): Elemental analyses were measured by Mr. Kirsch (Department of Chemistry, University of Basel) on a Leco CHN-900 (C-, H-, N-detection). The data are indicated in mass percent.

Melting Points (m.p.): Melting points were determined on a Büchi B-545 apparatus and were not corrected.

High Performance Liquid Chromatography (HPLC): HPLC analyses were performed with Shimadzu Class-VP Version 5.0 systems with SCL-10A system controller, LC-10AD pump system, SIL-10AD auto injector, CTO-10AC column oven, DGU-14A degasser and SPD-M10A diode array- or UV/VIS detector. Chiral columns *Chiralcel* IC, OJ and OD-H (4.6 mm \times 250 mm) from Daicel Chemical Industries were used. For enantioenriched samples, the retention time (t_R) of the major enantiomer is reported in boldface.

Gas Chromatography (GC): Gas chromatograms were recorded on Carlo Erba HRGC Mega2 Series 800 (HRGS Mega2) instruments. Achiral separations were performed on a *Restek* Rtx[®]-1701 column (30 m \times 0.25 mm \times 0.25 μm) using helium as carrier gas. For the separations of enantiomers *Chiraldex G-TA*, γ -cyclodextrin TFA column (30 m \times 0.25 mm \times 0.25 μm), *Brechbühler SE54* β -cyclodextrin DETButSil column (25 m \times 0.25 mm \times 0.25 μm) were used with H_2 as carrier gas. For enantioenriched samples, the retention

time (t_R) of the major enantiomer is reported in boldface.

Gas Chromatography-Mass Spectrometry (LRMS): A Shimadzu GCMS-QP2010 SE equipped with a *Restek* Rtx[®]-5MS column (30 m × 0.2 mm × 0.2 μm) was used. The carrier gas pressure (He) was set to 100 kPa with a 10:1 split ratio.

6.2 Iridium-Catalyzed Asymmetric Hydrogenation of Vinylsilyl Derivatives

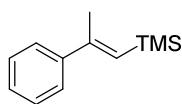
6.2.1 Synthesis and analytical data of trimethylsilyl- and dimethylphenyl- substituted vinylsilanes

6.2.1.1 Synthesis of Vinylsilanes 13, 24 and 25

Vinylsilanes **13**, **24** and **25** were synthesized *via* Pd-catalyzed coupling reaction of acetylenes, iodotrimethylsilane and an organozinc reagent according the procedure published by *Murai*.^[84]

In a flame-dried, argon flushed Schlenk tube a solution of the relevant alkyne (5 mmol, 1.0 eq.) in dioxane (10 mL) and Pd(PPh₃)₄ (0.1 mmol, 0.02 eq.) were added. After careful addition of the dialkylzinc reagent (5 mmol, 1.0 eq.), the solution was cooled down to 0 °C prior to dropwise addition of iodotrimethylsilane (10 mmol, 2.0 eq.). A very exothermic reaction was observed and the resulting mixture was allowed to stir at rt until no starting material could be detected anymore by TLC (1–6 h). After addition of H₂O (ca. 10 mL), the mixture was filtered through a plug of celite, extracted with *n*-hexane (2×10 mL), washed with brine, dried over Na₂SO₄, filtered and evaporated *in vacuo* to afford the crude product. Purification by column chromatography (SiO₂, pentane) or by Kugelrohr distillation yielded the pure product.

(*E*)-Trimethyl(2-phenylprop-1-en-1-yl)silane (**13**)



Purification: column chromatography (SiO₂, 2 cm × 18 cm, pentane);

Appearance: colorless liquid; **R_f**: 0.70 in pentane (visualization: UV,

KMnO₄); **Yield:** 46%; **¹H NMR** (400 MHz, CDCl₃) δ_H (ppm) = 7.47–7.44 (m,

2H), 7.41–7.20 (m, 3H), 5.92 (s, 1H), 2.22 (s, 3H), 0.19 (s, 9H); **¹³C NMR** (100 MHz, CDCl₃)

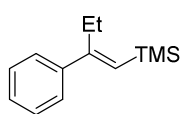
δ_C (ppm) = 151.8, 144.5, 128.2, 127.4, 126.5, 125.6, 21.1, 0.2; **LRMS** (EI, 70 eV) *m/z* (%)

190 (13) [M⁺], 176 (11), 175 (64), 159 (18), 135 (100); **IR** (neat): $\tilde{\nu}$ = 2954 (m), 2362 (w),

2345 (w), 1597 (w), 1441 (w), 1248 (s), 846 (s), 758 (s); **GC** (achiral phase), 60 kPa He, 100

°C, 2 min, 7 °C/min, 250 °C, 10 min: *t_R* = 13.1 min.

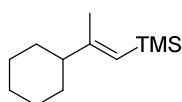
The ¹H and ¹³C NMR data were consistent with the literature data.^[176]

(E)-Trimethyl(2-phenylbut-1-en-1-yl)silane (24)

Purification: column chromatography (SiO₂, 2 cm × 19 cm, pentane);

Appearance: colorless oil; **R_f**: 0.65 in pentane (visualization: UV, KMnO₄);

Yield: 70%; **¹H NMR** (400 MHz, CDCl₃) δ_{H} (ppm) = 7.45–7.41 (m, 2H), 7.38–7.27 (m, 3H), 5.75 (s, 1H), 2.65 (q, J = 7.6 Hz, 2H), 1.00 (t, J = 7.6 Hz, 3H), 0.20 (s, 9H); **¹³C NMR** (100 MHz, CDCl₃) δ_{C} (ppm) = 159.4, 143.7, 128.5, 127.6, 127.6, 126.6, 28.3, 14.5, 0.6; **LRMS** (EI, 70 eV) m/z (%) 204 (11) [M⁺], 73 (100); **IR** (neat): $\tilde{\nu}$ = 2955 (m), 2896 (w), 2361 (w), 1594 (m), 1570 (m), 1493 (w), 1453 (w), 1247 (s), 929 (w), 853 (s), 834 (s), 759 (s), 693 (s); **GC** (achiral phase), 60 kPa He, 100 °C, 2 min, 7 °C/min, 250 °C, 10 min: t_{R} = 13.6 min. The ¹H and ¹³C NMR data were consistent with the literature data.^[176]

(E)-(2-Cyclohexylprop-1-en-1-yl)trimethylsilane (25)

Purification: Kugelrohr distillation (0.15 mbar at 90 °C); **Appearance:**

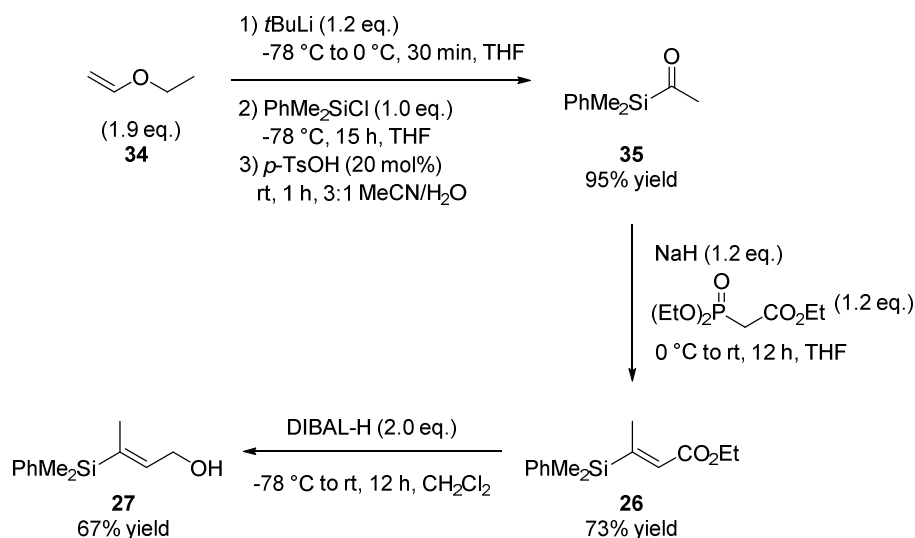
colorless liquid; **R_f**: 0.95 in pentane (visualization: UV, KMnO₄); **Yield:** 83%;

¹H NMR (400 MHz, CDCl₃) δ_{H} (ppm) = 5.16 (s, 1H), 1.85–1.77 (m, 1H), 1.76–1.65 (m, 7H), 1.28–1.13 (m, 6H), 0.09 (s, 9H); **¹³C NMR** (100 MHz, CDCl₃) δ_{C} (ppm) = 160.7, 120.3, 49.9, 32.2, 26.9, 26.6, 20.3, 0.3; **LRMS** (EI, 70 eV) m/z (%) 196 (12) [M⁺], 181 (32), 141 (13), 139 (20), 122 (43), 99 (12), 79 (14), 73 (100); **IR** (neat): $\tilde{\nu}$ = 2924 (m), 2852 (m), 2360 (w), 1611 (m), 1447 (m), 1246 (s), 835 (s); **GC** (achiral phase), 60 kPa He, 100 °C, 2 min, 7 °C/min, 250 °C, 10 min: t_{R} = 10.7 min.

The ¹H and ¹³C NMR data were consistent with the literature data.^[84]

6.2.1.2 Synthesis of Vinylsilanes 26 and 27

The synthesis of the title compounds was achieved according to the procedure published by Hoveyda.^[80k]



1-(Dimethyl(phenyl)silyl)ethan-1-one (**35**)

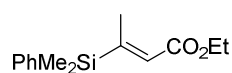
To a cold (-78 °C) solution of ethyl vinyl ether (**34**) (5 mL, 52.2 mmol, 1.9 eq.) in THF (40 mL), a *tert*-BuLi solution (1.6 M in heptane, 20 mL, 32.6 mmol, 1.2 eq.) was added dropwise. Upon addition, the reaction was allowed to warm up to 0 °C within 20 min and stirred for 30 min. The resulting yellow solution was cooled again to -78 °C prior to dropwise addition of dimethylphenylchlorosilane (4.6 mL, 27.1 mmol, 1.0 eq.). The reaction was then stirred for 15 h at room rt and then quenched by addition of a HCl (1 M aq., 30 mL). The layers were separated and the aqueous phase was extracted with Et₂O (2×30 mL). The combined organic layers were washed with brine, dried over Na₂SO₄, filtered and concentrated *in vacuo* to give a pale yellow liquid, which was dissolved in CH₃CN (120 mL) and H₂O (40 mL). To this solution *p*-TsOH (1.0 g, 5.1 mmol, 0.2 eq.) was added and the reaction stirred for 1 h at rt. The mixture was then extracted with EtOAc (2×30 mL) and the combined organic layers were washed with brine, dried over Na₂SO₄, filtered and concentrated *in vacuo* to give a pale yellow liquid which was purified by column chromatography (SiO₂, 4 cm × 17 cm, pentane/EtOAc, 40:1) to afford 4.5 g (93% yield) of the title compound as a pale yellow liquid.

R_f: 0.42 in pentane/EtOAc 30:1 (visualization: UV, KMnO₄); **¹H NMR** (400 MHz, CDCl₃) δ_H (ppm) = 7.57–7.54 (m, 2H), 7.43–7.35 (m, 3H), 2.24 (s, 3H), 0.50 (s, 6H); **¹³C NMR** (100 MHz, CDCl₃) δ_C (ppm) = 245.6, 134.4, 134.1, 130.1, 128.3, 36.1, -4.8; **LRMS** (EI, 70 eV) *m/z* (%) 177 (16) [M⁺], 136 (15), 135 (100), 105 (12); **IR** (neat): $\tilde{\nu}$ = 3065 (w), 2962 (w), 2361

(m), 2333 (m), 1742 (w), 1643 (s), 1425 (w), 1340 (w), 1252 (m), 1111 (m), 835 (w), 814 (m), 737 (m).

The ^1H and ^{13}C NMR data were consistent with the literature data.^[177]

Ethyl (*E*)-3-(dimethyl(phenyl)silyl)but-2-enoate (**26**)

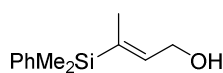


To a cold (0 °C) solution of NaH (288 mg, 12.0 mmol, 1.2 eq.) in THF (25 mL), triethylphosphonoacetate (2.3 mL, 11.5 mmol, 1.2 eq.) was added dropwise. The mixture was stirred at 0 °C for 30 min before adding dropwise acylsilane **35** (1.78 g, 10.0 mmol, 1.0 eq.). The reaction was allowed to warm up to rt within 20 min, stirred for 12 h and subsequently quenched by the addition of NH_4Cl (sat. aq., 20 mL). The layers were separated and the aqueous phase was extracted with Et_2O (2×20 mL). The combined organic layers were washed with brine, dried over Na_2SO_4 , filtered and concentrated *in vacuo* to give a colorless liquid which was purified by column chromatography (SiO_2 , 3 cm × 23 cm, pentane/ EtOAc , 60:1) to afford 1.8 g (73% yield) of the title compound as a colorless liquid.

R_f: 0.35 in pentane/ EtOAc , 50:1 (visualization: UV, KMnO_4); **^1H NMR** (400 MHz, CDCl_3) δ_{H} (ppm) = 7.50–7.36 (m, 5H), 6.09 (q, J = 1.2 Hz, 1H), 4.16 (q, J = 5.6 Hz, 2H), 2.18 (d, J = 1.2 Hz, 3H), 1.29 (t, J = 5.6 Hz, 3H), 0.41 (s, 6H); **^{13}C NMR** (100 MHz, CDCl_3) δ_{C} (ppm) = 165.8, 160.0, 136.3, 134.2, 129.6, 128.1, 127.9, 59.9, 17.6, 14.5, −3.8; **LRMS** (EI, 70 eV) m/z (%) 233 (8) [(M−Me)⁺], 205 (15), 203 (19), 171 (11), 170 (70), 143 (14), 142 (69), 137 (20), 136 (14), 135 (100), 127 (10), 121 (10), 107 (14), 105 (29), 77 (13); **EA**: calc. (%) for $\text{C}_{14}\text{H}_{20}\text{O}_2\text{Si}$, C 67.70, H 8.12; found C 67.70, H 8.29; **IR** (neat): $\tilde{\nu}$ = 2959 (w), 2361 (m), 2336 (m), 1715 (s), 1254 (w), 1182 (s), 1115 (w); **GC** (achiral phase), 60 kPa He, 100 °C, 2 min, 7 °C/min, 250 °C, 10 min: t_{R} = 20.5 min.

The ^1H and ^{13}C NMR data were consistent with the literature data.^[80k]

(*E*)-3-(Dimethyl(phenyl)silyl)but-2-en-1-ol (**27**)



A solution of ester **26** (1.4 g, 5.6 mmol, 1.0 eq.) in CH_2Cl_2 (15 mL) was added dropwise to DIBAL-H (1.7 M in toluene, 7.0 mL, 11.8 mmol, 2.1 eq.) in CH_2Cl_2 (10 mL) at −78 °C. After 4 h the reaction mixture was allowed to warm to rt,

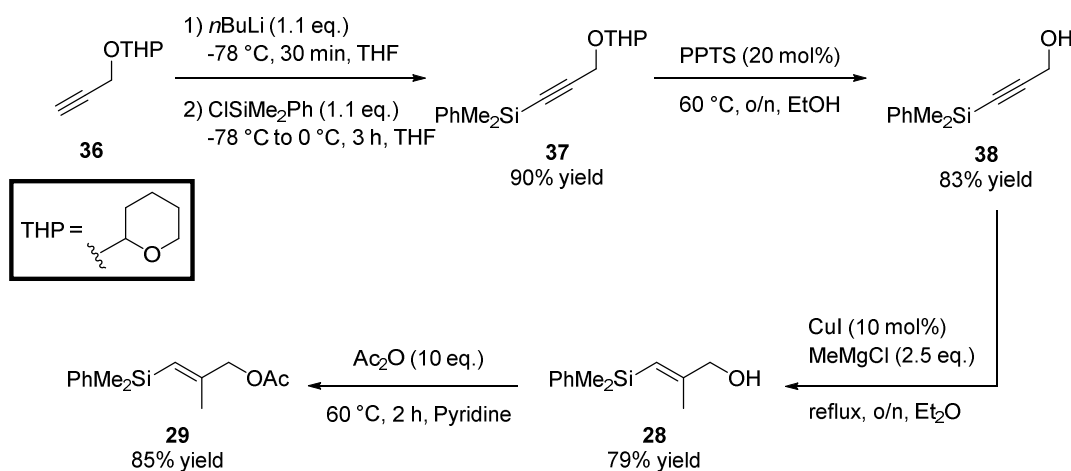
stirred for 13 h and quenched by addition of a NaHCO_3 (sat. aq. 20 mL) at -78°C . The mixture was stirred at rt for 15 min and filtered through a plug of celite. The combined organic layers were dried over Na_2SO_4 , filtered and concentrated *in vacuo* to give a pale yellow liquid which was purified by column chromatography (SiO_2 , 2 cm \times 20 cm, pentane/EtOAc, 7:1) to afford 775 mg (67% yield) of the title compound as a colorless liquid.

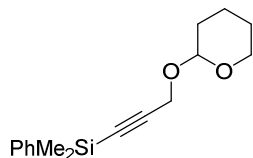
R_f: 0.35 in pentane/EtOAc, 7:1 (visualization: UV, KMnO_4); **^1H NMR** (400 MHz, CDCl_3) δ_{H} (ppm) = 7.53–7.47 (m, 2H), 7.38–7.32 (m, 3H), 6.01–5.90 (m, 1H), 4.30 (d, J = 5.8 Hz, 2H), 1.74–1.66 (m, 3H), 1.31 (s, 1H), 0.36 (s, 6H); **^{13}C NMR** (100 MHz, CDCl_3) δ_{C} (ppm) = 139.8, 138.0, 137.7, 134.1, 129.2, 127.9, 60.0, 15.2, -3.5 ; **LRMS** (EI, 70 eV) m/z (%) 206 (1) [M^+], 170 (43), 145 (11), 142 (45), 137 (29), 136 (17), 135 (100), 121 (12), 107 (15), 105 (30), 77 (17); **EA**: calc. (%) for $\text{C}_{12}\text{H}_{18}\text{O}_1\text{Si}$, C 69.85, H 8.79; found C 69.65, H 8.73; **IR** (neat): $\tilde{\nu}$ = 3304 (brs), 2957 (w), 2531 (w), 2154 (w), 1249 (m), 1109 (w), 825 (m), 672 (s); **GC** (achiral phase), 60 kPa He, 100 $^\circ\text{C}$, 2 min, 7 $^\circ\text{C}/\text{min}$, 250 $^\circ\text{C}$, 10 min: t_{R} = 19.4 min.

The ^1H and ^{13}C NMR data were consistent with the literature data.^[80k]

6.2.1.3 Synthesis of Vinylsilanes 28 and 29

Alkyne **36** has been synthesized by Larissa Pauli from the corresponding propargylic alcohol.

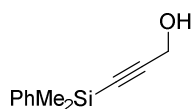


Dimethyl(phenyl)(3-((tetrahydro-2H-pyran-2-yl)oxy)prop-1-yn-1-yl)silane (37)

*n*BuLi (1.6 M in hexane, 55.4 mmol, 1.05 eq.) was added dropwise to a cold (−78 °C) solution of alkyne **36** (7.4 g, 52.7 mmol, 1.0 eq.) in THF (50 mL). The resulting mixture was stirred for 30 min and dimethylphenylchlorosilane (9.7 mL, 57.8 mmol, 1.1 eq.) was added. The reaction mixture was stirred for additional 30 min at −78 °C and then warmed to rt and stirred for 3 h. The solution was quenched by addition of H₂O (40 mL) and the aqueous phase extracted with pentane (2×35 mL). The combined organic layers were washed with brine, dried over Na₂SO₄, filtered and concentrated *in vacuo* to afford 13.0 g (90% yield) of the title compound as an orange liquid that was used without further purification.

R_f: 0.80 in pentane/EtOAc, 10:1 (visualization: UV, KMnO₄); **¹H NMR** (400 MHz, CDCl₃) δ_H (ppm) = 7.66–7.59 (m, 2H), 7.42–7.33 (m, 3H), 4.84 (t, *J* = 3.4 Hz, 1H), 4.31 (d, *J* = 6.8 Hz, 2H), 3.90–3.80 (m, 1H), 3.57–3.49 (m, 1H), 1.90–1.47 (m, 6H), 0.43 (s, 6H); **¹³C NMR** (100 MHz, CDCl₃) δ_C (ppm) = 136.9, 133.8, 129.6, 128.0, 103.5, 96.9, 89.0, 62.1, 55.0, 30.4, 25.5, 19.2, −0.8; **IR** (neat): $\tilde{\nu}$ = 2943 (m), 2919 (m), 2849 (m), 2176 (w), 1430 (w), 1343 (w), 1253 (m), 1203 (w), 1118 (s), 1061 (w), 1028 (s), 902 (w), 838 (w), 817 (s), 781 (w), 702 (m).

The ¹H and ¹³C NMR data were consistent with the literature data.^[178]

3-(Dimethyl(phenyl)silyl)prop-2-yn-1-ol (38)

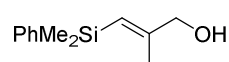
To a solution of alkyne **37** (4.0 g, 14.6 mmol, 1.0 eq.) in ethanol (20 mL), was added pyridinium *p*-toluenesulfonate (550 mg, 2.2 mmol, 0.15 eq.). After stirring the solution overnight at 60 °C, solid NaHCO₃ (ca. 1 g) was added, ethanol was removed *in vacuo* and the resulting mixture partitioned between Et₂O (20 mL) and H₂O (15 mL). The aqueous phase was extracted with Et₂O (2×15 mL). The combined organic layers were washed with brine, dried over Na₂SO₄, filtered and concentrated *in vacuo* to give a pale yellow liquid which was purified by column chromatography (SiO₂, 3 cm × 25 cm, pentane/EtOAc, 12:1) to afford 2.3 g (83% yield) of the title compound as a colorless liquid.

R_f: 0.27 in pentane/EtOAc, 10:1 (visualization: UV, KMnO₄); **¹H NMR** (400 MHz, CDCl₃) δ_H

(ppm) = 7.67–7.60 (m, 2H), 7.43–7.35 (m, 3H), 4.31 (d, J = 6.1 Hz, 2H), 1.86–1.73 (m, 1H), 0.44 (s, 6H); ^{13}C NMR (100 MHz, CDCl_3) δ_{C} (ppm) = 136.6, 133.8, 129.7, 128.1, 105.6, 88.9, 51.8, –0.9; LRMS (EI, 70 eV) m/z (%) 190 (1) [M^+], 175 (21), 147 (24), 135 (12), 131 (11), 115 (26), 105 (12), 91 (22); IR (neat): $\tilde{\nu}$ = 3301 (brs), 2961 (m), 2361 (m), 2176 (m), 1426 (w), 1253 (m), 1114 (m), 1041 (s), 982 (m), 820 (s), 781 (m), 733 (s), 701 (w).

The ^1H and ^{13}C NMR data were consistent with the literature data.^[80k]

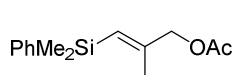
Ethyl (*E*)-3-(dimethyl(phenyl)silyl)but-2-enoate (**28**)



The synthesis of the title compound was performed according to the procedure published by Spino.^[179] In a flame-dried, argon flushed two-neck round bottom flask a solution of 3-(dimethyl(phenyl)silyl)prop-2-yn-1-ol **38** (1.5 g, 7.8 mmol, 1.0 eq.) in Et_2O (25 mL) was added to CuI (150 mg, 0.78 mmol, 0.1 eq.). After dropwise addition of methylmagnesium chloride (3.0 M in THF, 6.5 mL, 19.5 mmol, 2.5 eq.) the mixture was stirred at reflux overnight.

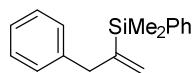
The solution was quenched by addition of NH_4Cl (sat. aq., ca. 10 mL) and the aqueous layer extracted with Et_2O (2×15 mL). The combined organic layers were washed with brine, dried over Na_2SO_4 , filtered and the solvent was evaporated *in vacuo* to yield the crude product, which was purified by column chromatography (SiO_2 , 2 cm × 25 cm, pentane/ EtOAc , 10:1) to afford 1.27 g (79 % yield) of the title compound as a pale yellow liquid.

R_f: 0.37 in pentane/ EtOAc , 8:1 (visualization: UV, KMnO_4); ^1H NMR (400 MHz, CDCl_3) δ_{H} (ppm) = 7.56–7.54 (m, 2H), 7.36–7.32 (m, 3H), 5.69 (s, 1H), 4.06 (s, 2H), 1.70 (s, 3H), 1.60 (brs, 1H), 0.42 (s, 6H); ^{13}C NMR (100 MHz, CDCl_3) δ_{C} (ppm) = 155.1, 139.7, 133.9, 129.0, 127.9, 118.8, 69.0, 18.8, –0.9; LRMS (EI, 70 eV) m/z (%) 191 (9) [($\text{M}-\text{Me}$) $^+$], 173 (13), 145 (18), 137 (31), 135 (34), 129 (11), 113 (25), 105 (17), 91 (11), 75 (100); EA: calc. (%) for $\text{C}_{12}\text{H}_{18}\text{O}_1\text{Si}$, C 69.85, H 8.79; found C 69.38, H 8.71; IR (neat): $\tilde{\nu}$ = 3281 (brs), 2955 (m), 2365 (w), 1628 (m), 1427 (w), 1250 (s), 1111 (m), 826 (s); GC (achiral phase), 60 kPa He, 100 °C, 2 min, 7 °C/min, 250 °C, 10 min: t_{R} = 19.3 min.

(E)-3-(Dimethyl(phenyl)silyl)-2-methylallyl acetate (29)

To a solution of (E)-3-(dimethyl(phenyl)silyl)-2-methylprop-2-en-1-ol **28** (516 mg, 2.5 mmol, 1.0 eq.) in pyridine (5 mL) was added acetic anhydride (2.4 mL, 25 mmol, 10 eq.). After stirring the solution during 2 h at 60 °C, the solution was quenched by addition of HCl (1 M aq., ca. 5 mL) and the aqueous layer extracted with Et₂O (2×15 mL). The combined organic layers were washed with brine, dried over Na₂SO₄, filtered and concentrated *in vacuo* to yield the crude product, which was purified by column chromatography (SiO₂, 1 cm × 19 cm, pentane/EtOAc, 20:1) to afford 530 mg (85% yield) of the title compound as a pale yellow liquid.

R_f: 0.50 in pentane/EtOAc, 25:1 (visualization: UV, KMnO₄); **¹H NMR** (400 MHz, CDCl₃) δ_H (ppm) = 7.60–7.48 (m, 2H), 7.40–7.31 (m, 3H), 5.64 (d, *J* = 0.8 Hz, 1H), 4.52 (s, 2H), 2.12 (s, 3H), 1.71 (s, 3H), 0.39 (s, 6H); **¹³C NMR** (100 MHz, CDCl₃) δ_C (ppm) = 170.8, 149.8, 139.4, 133.9, 129.0, 128.0, 122.9, 70.1, 21.1, 19.1, –1.0; **LRMS** (EI, 70 eV) *m/z* (%) 248 (1) [M⁺], 173 (35), 145 (28), 137 (25), 135 (41), 129 (13), 117 (53), 113 (13), 105 (16), 91 (14), 75 (72), 61 (15), 43 (100); **EA**: calc. (%) for C₁₄H₂₀O₂Si, C 67.70, H 8.12; found C 67.61, H 8.11; **IR** (neat): $\tilde{\nu}$ = 2958 (brs), 1744 (s), 1629 (w), 1247 (m), 1227 (m), 832 (w); **GC** (achiral phase), 60 kPa He, 100 °C, 2 min, 7 °C/min, 250 °C, 10 min: *t_R* = 20.0 min.

6.2.1.4 Synthesis of vinylsilane 30**Dimethyl(phenyl)(3-phenylprop-1-en-2-yl)silane (30)**

The title compound was synthesized *via* regioselective silycupration of terminal alkynes according to the procedure published by Loh.^[88] Inside a glovebox, a flame-dried, argon flushed Schlenk tube was charged with CuCl (20 mg, 0.2 mmol, 0.1 eq.), NaOtBu (21 mg, 0.2 mmol, 0.1 eq.), Johnphos (60 mg, 0.2 mmol, 0.1 eq.) and THF (8 mL). The resulting mixture was stirred for 20 min and Ph(Me)₂SiBpin (0.6 mL, 2.2 mmol, 1.1 eq.) was added. The reaction mixture was removed from the glovebox and cooled to 0 °C. After 30 min the corresponding terminal alkyne (0.25 mL, 2 mmol, 1.0 eq.) and methanol (0.16 mL, 4 mmol, 2.0 eq.) were added to the reaction mixture. The reaction was stirred overnight at 0 °C prior to be diluted with CH₂Cl₂, filtered over a plug of Celite

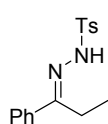
and concentrated *in vacuo*. Purification by column chromatography (SiO₂, 1 cm × 26 cm, pentane) to afford 340 mg (68 % yield) of the title compound as a colorless liquid.

R_f: 0.41 in pentane (visualization: UV/KMnO₄); **¹H NMR** (400 MHz, CDCl₃) δ_H (ppm) = 7.50–7.44 (m, 2H), 7.38–7.29 (m, 3H), 7.24–7.20 (m, 2H), 7.20–7.13 (m, 1H), 7.10–7.04 (m, 2H), 5.58–5.54 (m, 1H), 5.51–5.48 (m, 1H), 3.42 (s, 2H), 0.26 (s, 6H); **¹³C NMR** (100 MHz, CDCl₃) δ_C (ppm) = 149.8, 140.0, 138.1, 134.1, 129.5, 129.1, 128.3, 127.9, 127.9, 126.1, 42.7, –2.8; **LRMS** (EI, 70 eV) *m/z* (%) 252 (1) [M⁺], 237 (19), 175 (12), 174 (69), 159 (85), 136 (15), 135 (100), 121 (31), 107 (10), 105 (21), 91 (12); **EA**: calc. (%) for C₁₇H₂₀Si, C 80.89 H 7.99; found C 80.52, H 8.02; **IR** (neat): $\tilde{\nu}$ = 2955 (m), 2362 (w), 1428 (m), 1250 (m), 1111 (m), 929 (w), 831 (s), 816 (s), 776 (m), 738 (m), 700 (s); **GC** (achiral phase), 60 kPa He, 100 °C, 2 min, 7 °C/min, 250 °C, 10 min: *t_R* = 22.1 min.

The ¹H and ¹³C NMR data were consistent with the literature data.^[88]

6.2.1.5 Synthesis of vinylsilane 31

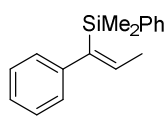
(*E*)-4-Methyl-N'-(1-phenylpropylidene)benzenesulfonohydrazide (41)



To a solution of benzenesulfonyl hydrazide (5.4 g, 31 mmol, 1.0 eq.) in ethanol (40 mL), propiophenone (4.0 mL, 30 mmol, 1.0 eq.) and *p*-toluenesulfonic acid (ca. 50 mg) were added and the resulting mixture was stirred at 55 °C for 5 h. After this time the solution was concentrated *in vacuo* to half its volume and stored in the fridge (4 °C) overnight. A white precipitate was formed, filtered off and dried under high vacuum overnight to afford 6.28 g (69% yield) of the title compound as a white crystalline solid as a 8:1 mixture of *trans* and *cis* isomers.

m.p.: 111–114 °C; **R_f**: 0.18 in pentane/EtOAc, 6:1 (visualization: UV, KMnO₄); **¹H NMR** (400 MHz, CDCl₃) δ_H (ppm) = 7.95–7.88 (m, 2H), 7.69 (s, 1H), 7.67–7.61 (m, 2H), 7.39–7.32 (m, 4H), 7.31 (s, 1H), 2.58 (q, *J* = 7.8 Hz, 2H), 2.42 (s, 3H), 1.10 (t, *J* = 7.7 Hz, 3H).

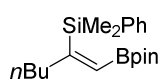
The ¹H NMR data were consistent with the literature data.^[180]

(Z)-Dimethyl(phenyl)(1-phenylprop-1-en-1-yl)silane (31)

The title compound was synthesized *via* Shapiro reaction according to the procedure published by Chan.^[90] In a flame-dried, argon flushed two-neck round bottom flask TMEDA (10 mL) was added to **41** (800 mg, 2.75 mmol, 1.0 eq.) and the resulting mixture was cooled to $-78\text{ }^{\circ}\text{C}$. *n*-BuLi (1.6 M in hexane, 6.8 mL, 11 mmol, 4.0 eq.) was added dropwise and the mixture gently allowed to warm up to rt. Strong gas evolution was observed. The mixture was stirred for 45 min before addition of dimethylphenylchlorosilane (0.5 mL, 3.1 mmol, 1.1 eq.). After 4 h the mixture was quenched by careful addition of HCl (6% aq., ca. 10 mL). The aqueous layer was extracted with pentane (2×20 mL), washed with brine, dried over Na_2SO_4 , filtered and concentrated *in vacuo* to afford the crude product. Purification by column chromatography (SiO_2 , 1 cm × 19 cm, pentane) afforded 493 mg (72% yield) of the title compound as a colorless liquid.

R_f: 0.93 in pentane (visualization: UV, KMnO_4); **¹H NMR** (400 MHz, CDCl_3) δ_{H} (ppm) = 7.53–7.48 (m, 2H), 7.39–7.33 (m, 3H), 7.26–7.21 (m, 2H), 7.19–7.12 (m, 1H), 6.89–6.83 (m, 2H), 6.12 (q, J = 6.6 Hz, 1H), 1.58 (dd, J = 6.5, 1.2 Hz, 3H), 0.31 (d, J = 1.2 Hz, 6H); **¹³C NMR** (100 MHz, CDCl_3) δ_{C} (ppm) = 144.0, 142.1, 138.5, 137.9, 134.3, 129.0, 128.2, 128.1, 127.8, 125.5, 16.2, -2.8 ; **LRMS** (EI, 70 eV) m/z (%) 252 (32) [M^+], 238 (10), 237 (39), 197 (33), 159 (13), 136 (15), 135 (100), 121 (23), 107 (13), 105 (21), 91 (12); **IR** (neat): $\tilde{\nu}$ = 3014 (w), 2957 (m), 2361 (m), 1489 (w), 1250 (s), 1111 (m), 702 (s); **GC** (achiral phase), 60 kPa He, 100 $^{\circ}\text{C}$, 2 min, 7 $^{\circ}\text{C}/\text{min}$, 250 $^{\circ}\text{C}$, 10 min: t_{R} = 20.8 min.

The ¹H and ¹³C NMR data were consistent with the literature data.^[181]

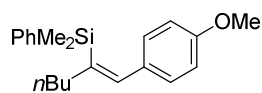
6.2.1.6 Synthesis of vinylsilanes 32 and 33**(Z)-Dimethyl(phenyl)(1-(4,4,5,5-tetramethyl-1,3,2-dioxaborolan-2-yl)hex-1-en-2-yl)silane (32)**

The title compound was synthesized according to the procedure published by Ito^[91] and Suginome.^[182] A flame-dried, argon flushed Young tube was charged with $\text{Pd}(\text{OAc})_2$ (18 mg, 0.08 mmol, 0.04 eq.) and 1,1,3,3-

tetramethylbutylisocyanide (0.25 mL, 1.2 mmol, 0.6 eq.). The color of the reaction mixture turned red. Toluene (1.0 mL) and 1-hexyne (0.7 mL, 6 mmol, 3.0 eq.) were added and the mixture was heated at reflux for 2 h. The solvent was then removed *in vacuo* and the crude product was purified by column chromatography (SiO₂, 1 cm × 16 cm, pentane/EtOAc, 50:1) to afford 1.15 g (88% yield) of the title compound as a red liquid.

R_f: 0.44 in pentane/EtOAc, 50:1 (visualization: UV, KMnO₄); **¹H NMR** (400 MHz, CDCl₃) δ_H (ppm) = 7.57–7.48 (m, 2H), 7.34–7.27 (m, 3H), 6.18 (s, 1H), 2.22 (td, *J* = 7.4, 1.0 Hz, 2H), 1.40–1.19 (m, 4H), 1.06 (s, 12H), 0.82 (t, *J* = 7.2 Hz, 3H), 0.49–0.38 (m, 6H); **¹³C NMR** (100 MHz, CDCl₃) δ_C (ppm) = 166.7, 140.6, 134.2, 128.5, 127.5, 121.4, 83.2, 42.4, 32.0, 24.8, 22.7, 14.1, –0.7; **LRMS** (EI, 70 eV) *m/z* (%) 329 (6) [(M–Me)⁺], 287 (29), 202 (25), 145 (14), 137 (15), 135 (100), 121 (15), 119 (10), 107 (14), 85 (13), 84 (70), 83 (49); **IR** (neat): $\tilde{\nu}$ = 2977 (w), 2956 (w), 2927 (m), 2856 (w), 1585 (m), 1459 (w), 1428 (w), 1371 (s), 1352 (s), 1333 (s), 1245 (s), 1144 (s), 1110 (m), 968 (w), 835 (s), 816 (s), 775 (s), 700 (s); **GC** (achiral phase), 60 kPa He, 100 °C, 2 min, 7 °C/min, 250 °C, 10 min: *t_R* = 28.8 min.

(*Z*)-(1-(4-Methoxyphenyl)hex-1-en-2-yl)dimethyl(phenyl)silane (**33**)



(*Z*)-Dimethyl(phenyl)(1-(4,4,5,5-tetramethyl-1,3,2-dioxaborolan-2-yl)hex-1-en-2-yl)silane **32** (517 mg, 1.5 mmol, 1.0 eq.) and *p*-

bromoanisole (0.21 mL, 1.65 mmol, 1.1 eq.) were added to a suspension of PdCl₂(dppf) (25 mg, 0.03 mmol, 0.02 eq.) and K₃PO₄ (955 mg, 4.5 mmol, 3.0 eq.) in THF (10 mL). Degassed H₂O (0.29 mL, 16 mmol, 10 eq.) was added and the resulting mixture was stirred at 80 °C for 15 h. After extraction with CH₂Cl₂, the organic phase was dried over Na₂SO₄. Filtration, *in vacuo* removal of the solvent and subsequent purification by column chromatography (SiO₂, 2 cm × 25 cm, pentane/EtOAc, 50:1) afforded 400 mg (82% yield) of the title compound as an orange liquid.

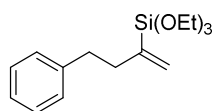
R_f: 0.39 in pentane/EtOAc, 50:1 (visualization: UV, KMnO₄); **¹H NMR** (400 MHz, CDCl₃) δ_H (ppm) = 7.50–7.45 (m, 2H), 7.34–7.27 (m, 3H), 7.22 (s, 1H), 7.02 (d, *J* = 8.6 Hz, 2H), 6.68 (d, *J* = 8.6 Hz, 2H), 3.76 (s, 3H), 2.29–2.21 (m, 2H), 1.49–1.39 (m, 2H), 1.39–1.28 (m, 2H), 0.89 (t, *J* = 7.3 Hz, 3H), 0.18 (s, 6H); **¹³C NMR** (100 MHz, CDCl₃) δ_C (ppm) = 158.6, 143.1, 141.3, 140.4, 134.0, 132.4, 130.0, 128.7, 127.8, 113.2, 55.3, 39.1, 33.0, 22.7, 14.1, –0.7; **LRMS** (EI,

70 eV) m/z (%) 324 (26) [M^+], 232 (12), 231 (55), 165 (13), 136 (15), 135 (100), 121 (13); **EA**: calc. (%) for $C_{21}H_{28}OSi$, C 77.72, H 8.70; found C 77.45, H 8.76; **IR** (neat): $\tilde{\nu}$ = 2954 (m), 2926 (w), 2372 (w), 1609 (w), 1506 (s), 1246 (s), 1175 (w), 1108 (w), 1036 (w), 818 (m); **GC** (achiral phase), 60 kPa He, 100 °C, 2 min, 7 °C/min, 250 °C, 10 min: t_R = 31.5 min.

6.2.2 Synthesis and analytical data of vinylsiloxanes

Vinylsiloxanes were synthesized *via* hydrosilylation of the corresponding terminal alkynes according to the procedure published by Trost.^[183] In a flame-dried, argon flushed Schlenk tube a solution of the alkyne (5 mmol, 1.0 eq.) and $RuCp^*(MeCN)_3$ (0.005 mmol, 0.01 eq.) were dissolved in CH_2Cl_2 (10 mL). To the resulting black solution the corresponding siloxane (6 mmol, 1.2 eq.) was added dropwise and the mixture was allowed to stir at rt for 2 h. The solvent was then evaporated *in vacuo* and the desired compound was purified by column chromatography (SiO_2 , pentane/EtOAc) or Kugelrohr distillation.

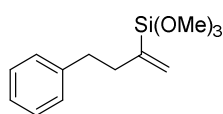
Triethoxy(4-phenylbut-1-en-2-yl)silane (54)



Purification: column chromatography (SiO_2 , 2 cm \times 29 cm, pentane);

Appearance: colorless liquid; **R_f**: 0.41 in pentane/EtOAc, 25:1 (visualization: UV, $KMnO_4$); **Yield**: 57%; **1H NMR** (400 MHz, $CDCl_3$) δ_H

(ppm) = 7.32–7.27 (m, 2H), 7.24–7.15 (m, 3H), 5.79–5.74 (m, 1H), 5.70–5.65 (m, 1H), 3.85 (q, J = 7.0 Hz, 6H), 2.83–2.74 (m, 2H), 2.50–2.41 (m, 2H), 1.25 (t, J = 7.0 Hz, 9H); **^{13}C NMR** (100 MHz, $CDCl_3$) δ_C (ppm) = 143.3, 142.6, 129.7, 128.6, 128.4, 125.8, 58.7, 38.2, 35.5, 18.4; **LRMS** (EI, 70 eV) m/z (%) 294 (12) [M^+], 265 (12), 203 (13), 164 (12), 163 (98), 159 (21), 135 (33), 130 (31), 129 (12), 128 (14), 119 (51), 115 (10), 107 (20), 103 (11), 91 (100), 79 (70), 77 (13); **HRMS** (ESI) exact mass calculated for $C_{16}H_{26}O_3SiNa$ [$(M+Na)^+$], 317.1543, found 317.1542; **IR** (neat): $\tilde{\nu}$ = 2972 (s), 2922 (w), 2357 (m), 1549 (w), 1447 (w), 1387 (w), 1163 (w), 1072 (s), 949 (s), 781 (m), 737 (m); **GC** (achiral phase), 60 kPa He, 100 °C, 2 min, 7 °C/min, 250 °C, 10 min: t_R = 19.7 min.

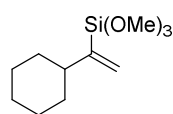
Trimethoxy(4-phenylbut-1-en-2-yl)silane (55)

Purification: column chromatography (SiO₂, 2 cm × 24 cm, pentane);

Appearance: colorless liquid; **R_f**: 0.36 in pentane/EtOAc, 30:1

(visualization: UV, KMnO₄); **Yield:** 70%; **¹H NMR** (400 MHz, CDCl₃) δ_{H}

(ppm) = 7.31–7.26 (m, 2H), 7.23–7.14 (m, 3H), 5.83–5.76 (m, 1H), 5.69–5.63 (m, 1H), 3.60 (s, 9H), 2.82–2.72 (m, 2H), 2.51–2.41 (m, 2H); **¹³C NMR** (100 MHz, CDCl₃) δ_{C} (ppm) = 142.3, 141.9, 130.3, 128.6, 128.4, 125.9, 50.8, 38.0, 35.4; **LRMS** (EI, 70 eV) m/z (%) 252 (10) [M⁺], 220 (16), 130 (41), 121 (96), 117 (12), 91 (100); **EA:** calc. (%) for C₁₃H₂₀O₃Si, C 61.87, H 7.99; found C 62.01, H 7.93; **IR** (neat): $\tilde{\nu}$ = 2941 (brs), 2839 (m), 2361 (m), 2338 (w), 1603 (w), 1452 (m), 1188 (m), 1074 (s), 939 (m), 804 (s), 737 (s), 698 (m); **GC** (achiral phase), 60 kPa He, 100 °C, 2 min, 7 °C/min, 250 °C, 10 min: t_{R} = 18.0 min.

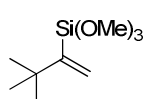
(1-Cyclohexylvinyl)trimethoxysilane (56)

Purification: column chromatography (SiO₂, 2 cm × 30 cm, pentane/EtOAc,

60:1); **Appearance:** yellow liquid; **R_f**: 0.45 in pentane/EtOAc, 40:1

(visualization: UV, KMnO₄); **Yield:** 38%; **¹H NMR** (400 MHz, CDCl₃) δ_{H}

(ppm) = 5.77 (dd, J = 2.7, 1.2 Hz, 1H), 5.62 (d, J = 2.8 Hz, 1H), 3.56 (s, 9H), 2.13–2.00 (m, 1H), 1.83–1.71 (m, 4H), 1.71–1.61 (m, 1H), 1.37–1.05 (m, 5H); **¹³C NMR** (100 MHz, CDCl₃) δ_{C} (ppm) = 148.17, 128.07, 50.69, 43.84, 32.82, 26.92, 26.36; **LRMS** (EI, 70 eV) m/z (%) 230 (4) [M⁺], 198 (22), 122 (10), 121 (100), 108 (17), 91 (52), 79 (10); **EA:** calc. (%) for C₁₁H₂₂O₃Si, C 57.35, H 9.62; found C 57.05, H 9.46; **IR** (neat): $\tilde{\nu}$ = 2923 (m), 2842 (m), 1450 (w), 1190 (m), 1077 (s), 940 (m), 798 (s), 770 (m); **GC** (achiral phase), 60 kPa He, 100 °C, 2 min, 7 °C/min, 250 °C, 10 min: t_{R} = 13.2 min.

(3,3-Dimethylbut-1-en-2-yl)trimethoxysilane (57)

Purification: column chromatography (SiO₂, 2 cm × 25 cm, pentane/EtOAc,

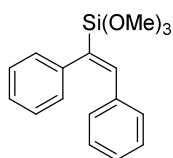
90:1); **Appearance:** colorless liquid; **R_f**: 0.46 in 60:1 pentane/EtOAc

(visualization: KMnO₄); **Yield:** 53%; **¹H NMR** (400 MHz, CDCl₃) δ_{H} (ppm) = 5.82 (d, J = 2.0

Hz, 1H), 5.64 (d, J = 2.1 Hz, 1H), 3.56 (s, 9H), 1.10 (s, 9H); **¹³C NMR** (100 MHz, CDCl₃) δ_{C} (ppm) = 152.2, 127.0, 50.6, 36.0, 30.1; **LRMS** (EI, 70 eV) m/z (%) 204 (5) [M⁺], 121 (100),

91 (37); **GC** (achiral phase), 60 kPa He, 100 °C, 2 min, 7 °C/min, 250 °C, 10 min: t_R = 7.2 min; **EA**: calc. (%) for $C_9H_{20}O_3Si$, C 52.90, H 9.86; found C 53.10, H 9.61; **IR** (neat): $\tilde{\nu}$ = 2945 (m), 2840 (m), 1461 (w), 1362 (w), 1190 (m), 1078 (s), 925 (m), 794 (s), 703 (s).

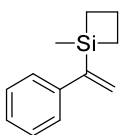
(*E*)-(1,2-Diphenylvinyl)trimethoxysilane (66)



Purification: Kugelrohr distillation (0.12 mbar at 230°C); **Appearance:** pale yellow liquid; **R_f**: 0.83 in pentane/EtOAc, 10:1 (visualization: UV, $KMnO_4$); **Yield:** 95%; **¹H NMR** (400 MHz, $CDCl_3$) δ_H (ppm) = 7.32–7.11 (m, 9H), 7.06–7.02 (m, 2H), 3.58 (s, 9H); **¹³C NMR** (100 MHz, $CDCl_3$) δ_C (ppm) = 143.0, 140.6, 136.8, 135.8, 130.0, 128.8, 128.3, 128.1, 127.8, 126.4, 51.1; **LRMS** (EI, 70 eV) m/z (%) 300 (56) [M^+], 238 (11), 180 (16), 179 (22), 178 (60), 177 (13), 152 (10), 121 (100), 107 (18), 91 (88); **HRMS** (ESI) exact mass calculated for $C_{17}H_{20}O_3SiNa$ [$(M+Na)^+$], 323.1074, found 323.1074; **IR** (neat): $\tilde{\nu}$ = 2943 (m), 2841 (m), 2363 (m), 2334 (m), 1742 (w), 1450 (w), 1192 (m), 1084 (s), 968 (w), 806 (m), 700 (m).

6.2.3 Synthesis and analytical data of vinylsiletane 63

1-Methyl-1-(1-phenylvinyl)siletane (63)



The title compound was synthesized according the procedure published by Dudley.^[96] A solution of α -styrenylmagnesium bromide (1 M in Et_2O , 10.0 mL, 10 mmol, 1.0 eq.) was added to a solution of 1-chloro-1-methylsilacyclobutane (1.35 mL, 11 mmol, 1.1 eq.) in Et_2O (6 mL). The reaction mixture was then heated at reflux for 15 h. The solution was then allowed to cool down to rt and quenched by addition of NH_4Cl (sat. aq., ca. 10 mL). The aqueous layer was extracted with pentane (2×10 mL) and the combined organic layers were then washed with brine, dried over Na_2SO_4 , filtered and evaporated *in vacuo*. Purification by column chromatography (SiO_2 , pentane, 50:1) afforded 800 mg (43% yield) of the title compound as an orange liquid.

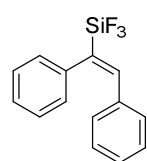
Purification: column chromatography (SiO_2 , 2 cm × 22 cm, pentane); **R_f**: 0.96 in pentane (visualization: UV, $KMnO_4$); **¹H NMR** (400 MHz, $CDCl_3$) δ_H (ppm) = 7.32–7.26 (m, 2H), 7.26–7.16 (m, 3H), 6.02 (d, J = 2.6 Hz, 1H), 5.69 (d, J = 2.6 Hz, 1H), 2.17–2.02 (m, 2H), 1.30–1.16

(m, 2H), 1.16–1.04 (m, 2H), 0.34 (s, 3H); ^{13}C NMR (100 MHz, CDCl_3) δ_{C} (ppm) = 151.2, 143.1, 128.5, 127.2, 126.9, 126.6, 18.2, 14.8, -1.2; LRMS (EI, 70 eV) m/z (%) 188 (16) [M^+], 160 (30), 159 (17), 147 (11), 146 (25), 145 (100), 143 (10), 131 (10), 121 (12), 105 (15); IR (neat): $\tilde{\nu}$ = 3051 (m), 2968 (w), 1939 (m), 1501 (s), 1406 (s), 1173 (w), 1088 (w), 818 (m).

The ^1H and ^{13}C NMR data were consistent with the literature data.^[96]

6.2.4 Synthesis and analytical data of trifluorovinylsilane 67

(E)-(1,2-Diphenylvinyl)trifluorosilane (67)



The title compound was synthesized from the corresponding vinylsiloxane according to the procedure published by Young.^[98] A solution of boron trifluoride etherate (0.4 mL, 3.2 mmol, 1.05 eq.) in Et_2O (3 mL) was added dropwise to vinylsiloxane **66** (900 mg, 3 mmol, 1.0 eq.) in Et_2O (3 mL) at rt. After 12 h the solvent was evaporated *in vacuo* and the resulting black oil purified by Kugelrohr distillation (0.40 mbar at 160 °C) to afford 327 mg (41% yield) of the title compound as a yellow liquid.

^1H NMR (400 MHz, CDCl_3) δ_{H} (ppm) = 7.51–7.22 (m, 11H); ^{13}C NMR (100 MHz, CDCl_3) δ_{C} (ppm) = 147.9, 136.4, 135.0, 130.4, 129.5, 129.4, 128.4, 128.3, 128.0, 126.7 (q, J_{CF} = 22.6 Hz); ^{19}F NMR (376 MHz, CDCl_3) δ_{F} (ppm) = -143.4; LRMS (EI, 70 eV) m/z (%) 264 (53) [M^+], 180 (15), 179 (100), 178 (74), 177 (13), 176 (12), 165 (11), 152 (13), 89 (12); IR (neat): $\tilde{\nu}$ = 3055 (w), 3022 (w), 2359 (w), 1603 (m), 1572 (w), 1491 (m), 1445 (s), 1150 (s), 1030 (w), 982 (s), 922 (s), 885 (m), 864 (s), 847 (s), 810 (w), 760 (s), 717 (w), 690 (s), 662 (m).

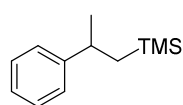
6.2.5 Analytical data for hydrogenation compounds

General procedure for the iridium-catalyzed hydrogenation

A 2 mL glass vial was charged with a cylindrical stirring bar (0.7 cm in length), the relevant iridium catalyst (0.5–1.0 mol%) and the substrate (100 μmol). The mixture was dissolved in CH_2Cl_2 (0.5 mL, 0.2 M) and placed in an autoclave.

The autoclave was attached to a high pressure hydrogen line and purged with H₂ three times before being sealed under the appropriate H₂ pressure. The mixture was stirred for the appropriate reaction time at rt. After release of H₂, the solution was concentrated under a stream of nitrogen and the catalyst was removed by filtration of the crude mixture through a plug of SiO₂ in a Pasteur pipette. After washing with ca. 5 mL of a 4:1 *n*-hexane:MTBE mixture, the solvent was concentrated *in vacuo* to yield the hydrogenation product.

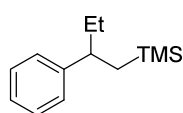
(–)-Trimethyl(2-phenylpropyl)silane (43)



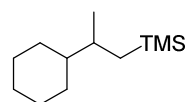
Appearance: colorless liquid; **¹H NMR** (400 MHz, CDCl₃) δ_{H} (ppm) = 7.29–7.14 (m, 5H), 2.88 (sext, J = 8.0 Hz, 1H), 1.28 (d, J = 8.0 Hz, 3H), 0.99 (dd, J = 14.4, 7.8 Hz, 1H), 0.90 (dd, J = 14.4, 7.8 Hz, 1H), –0.11 (s, 9H); **¹³C NMR** (100 MHz, CDCl₃) δ_{C} (ppm) = 150.0, 128.4, 126.8, 125.9, 36.6, 27.1, 26.5, –0.9; **LRMS** (EI, 70 eV) m/z (%) 192 (3) [M^+], 177 (32), 135 (57), 118 (10), 105 (11), 73 (100); **IR** (neat): $\tilde{\nu}$ = 3027 (w), 2954 (m), 2897 (w), 2359 (w), 1451 (w), 1247 (s), 834 (s); **GC** (achiral phase), 60 kPa He, 100 °C, 2 min, 7 °C/min, 250 °C, 10 min: t_{R} = 10.6 min; **GC** (chiral phase, *ChiralDEX G-TA*, Gamma CD-trifluoroacetyl column (30 m \times 0.25 mm \times 0.25 μm), 50 kPa He, 50 °C, 50 min, 0.5 °C/min, 70 °C, 0 min, 10 °C/min, 160 °C, 5 min): t_{R} = **80.2 min (–)**, t_{R} = 81.0 min (+), 98% *ee*; $[\alpha]_{\text{D}}^{20}$ = –5.2 (c = 1.00, CHCl₃).

The ¹H and ¹³C NMR data were consistent with the literature data.^[184]

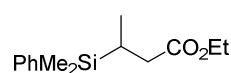
(–)-Trimethyl(2-phenylbutyl)silane (44)



Appearance: colorless oil; **¹H NMR** (400 MHz, CDCl₃) δ_{H} (ppm) = 7.28–7.25 (m, 2H), 7.18–7.15 (m, 3H), 2.60–2.47 (m, 1H), 1.69–1.53 (m, 2H), 0.96–0.93 (m, 2H), 0.74 (t, J = 7.4 Hz, 3H), –0.18 (s, 9H); **¹³C NMR** (100 MHz, CDCl₃) δ_{C} (ppm) = 147.9, 128.5, 128.0, 126.2, 44.3, 34.0, 25.3, 12.6, –0.7; **LRMS** (EI, 70 eV) m/z (%) 206 (1) [M^+], 73 (100); **EA:** calc. (%) for C₁₃H₂₂Si, C 75.65, H 10.74; found C 75.50, H 10.62; **GC** (achiral phase), 60 kPa He, 100 °C, 2 min, 7 °C/min, 250 °C, 10 min: t_{R} = 11.8 min; **GC** (chiral phase, *ChiralDEX G-TA*, Gamma CD-trifluoroacetyl column (30 m \times 0.25 mm \times 0.25 μm), 90 kPa He, 60 °C, 35 min, 10 °C/min, 160 °C, 5 min): t_{R} = 38.1 min (+), t_{R} = **38.3 min (–)**, 99% *ee*; $[\alpha]_{\text{D}}^{20}$ = –7.2 (c = 1.50, CHCl₃).

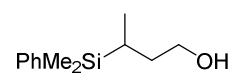
(+)-(2-Cyclohexylbutyl)trimethylsilane (45)

Appearance: colorless oil; $^1\text{H NMR}$ (400 MHz, CDCl_3) δ_{H} (ppm) = 1.79–1.55 (m, 6H), 1.51–1.40 (m, 1H), 1.28–1.05 (m, 5H), 0.83 (t, J = 6.9 Hz, 3H), 0.62 (dd, J = 14.6, 4.0 Hz, 1H), 0.34 (dd, J = 14.8, 9.8 Hz, 1H), -0.01 (s, 9H); $^{13}\text{C NMR}$ (100 MHz, CDCl_3) δ_{C} (ppm) = 45.7, 34.7, 30.3, 27.1, 27.0, 21.9, 19.4, -0.5 ; **LRMS** (EI, 70 eV) m/z (%) 198 (1) [$(\text{M})^+$], 115 (30), 74 (10), 73 (100); **IR** (neat): $\tilde{\nu}$ = 2953 (m), 2923 (m), 2852 (m), 1610 (w), 1246 (s), 834 (s); **GC** (achiral phase), 60 kPa He, 100 °C, 2 min, 7 °C/min, 250 °C, 10 min: t_{R} = 11.2 min; **GC** (chiral phase, *Chiraldex G-TA*, Gamma CD-6-Methyl-2,3-pentyl PS086 column (30 m \times 0.25 mm \times 0.25 μm), 50 kPa He, 50 °C, 80 min, 10 °C/min, 180 °C, 5 min): t_{R} = **68.8 min (+)**, t_{R} = 69.9 min (–), 98% *ee*; $[\alpha]_{\text{D}}^{20}$ = +8.8 (c = 0.60, CHCl_3).

(+)-Ethyl 3-(dimethyl(phenyl)silyl)butanoate (46)

Appearance: colorless liquid; $^1\text{H NMR}$ (400 MHz, CDCl_3) δ_{H} (ppm) = 7.53–7.47 (m, 2H), 7.39–7.32 (m, 3H), 4.11 (q, J = 7.1 Hz, 2H), 2.38 (dd, J = 15.2, 4.1 Hz, 1H), 2.04 (dd, J = 15.2, 11.3 Hz, 1H), 1.51–1.37 (m, 1H), 1.23 (t, J = 7.1 Hz, 3H), 0.97 (d, J = 7.3 Hz, 3H), 0.28 (s, 6H); $^{13}\text{C NMR}$ (100 MHz, CDCl_3) δ_{C} (ppm) = 174.1, 137.5, 134.1, 129.2, 127.9, 60.3, 37.0, 16.6, 14.6, 14.4, -4.9 , -5.2 ; **LRMS** (EI, 70 eV) m/z (%) 250 (1) [M^+], 235 (11), 163 (12), 145 (24), 137 (22), 136 (15), 135 (100), 129 (11), 107 (10), 105 (19); **EA**: calc. (%) for $\text{C}_{14}\text{H}_{22}\text{O}_2\text{Si}$, C 67.15, H 8.85; found C 67.20, H 8.76; **IR** (neat): $\tilde{\nu}$ = 3254 (m), 2904 (s), 1732 (s), 1254 (m), 1208 (m), 1151 (w), 815 (m); **GC** (achiral phase), 60 kPa He, 100 °C, 2 min, 7 °C/min, 250 °C, 10 min: t_{R} = 19.7 min; **HPLC** (chiral, Daicel Chiracel OD-H, 0.46 cm \times 25 cm, *n*-heptane/isopropanol 99:1, 0.5 mL/min, 20 °C): t_{R} = **11.9 min (+)**, t_{R} = 13.3 (–), 89% *ee*; $[\alpha]_{\text{D}}^{20}$ = +4.2 (c = 0.50, CHCl_3).

The ^1H and ^{13}C NMR data were consistent with the literature data.^[185]

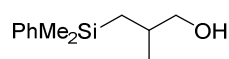
(–)-3-(Dimethyl(phenyl)silyl)butan-1-ol (47)

Appearance: colorless liquid; $^1\text{H NMR}$ (400 MHz, CDCl_3) δ_{H} (ppm) = 7.54–7.47 (m, 2H), 7.40–7.32 (m, 3H), 3.75–3.65 (m, 1H), 3.64–3.54 (m, 1H), 1.82–1.68 (m, 1H), 1.43–1.29 (m, 1H), 1.17 (s, 1H), 1.07–0.99 (m, 1H), 0.96 (d, J = 6.0 Hz, 3H), 0.27 (d, J = 1.9 Hz, 6H); $^{13}\text{C NMR}$ (100 MHz, CDCl_3) δ_{C} (ppm) = 138.3, 134.1, 129.1,

127.9, 61.9, 34.7, 15.4, 14.0, -4.7, -5.1; **LRMS** (EI, 70 eV) m/z (%) 193 (22) [(M-Me)⁺], 152 (10), 137 (100), 136 (11), 135 (55), 105 (15), 43 (14); **EA**: calc. (%) for C₁₂H₂₀OSi, C 69.17, H 9.67 found C 68.90, H 9.39; **IR** (neat): $\tilde{\nu}$ = 3370 (brs), 2953 (m), 2867 (w), 1723 (m), 1426 (w), 1249 (s), 1111 (s), 1047 (m), 831 (s), 813 (s), 770 (m), 733 (s), 701 (s); **GC** (achiral phase), 60 kPa He, 100 °C, 2 min, 7 °C/min, 250 °C, 10 min: t_R = 19.0 min; **HPLC** (chiral, Daicel Chiracel AD-H, 0.46 cm × 25 cm, *n*-heptane/isopropanol 99:1, 0.5 mL/min, 20 °C): t_R = 41.4 min (+), t_R = **44.1** (-), 37% *ee*; $[\alpha]_D^{20}$ = -1.8 (c = 1.00, CHCl₃).

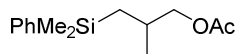
The ¹H and ¹³C NMR data were consistent with the literature data. [80n]

(-)-3-(Dimethyl(phenyl)silyl)-2-methylpropan-1-ol (48)



Appearance: colorless liquid; **¹H NMR** (400 MHz, CDCl₃) δ_H (ppm) = 7.55–7.49 (m, 2H), 7.37–7.33 (m, 3H), 3.40 (dd, J = 10.4, 5.8 Hz, 1H), 3.33 (dd, J = 10.4, 6.8 Hz, 1H), 1.87–1.72 (m, 1H), 1.27 (s, 1H), 0.91 (d, J = 6.7 Hz, 4H), 0.60 (dd, J = 14.8, 9.1 Hz, 1H), 0.31 (d, J = 0.9 Hz, 6H); **¹³C NMR** (100 MHz, CDCl₃) δ_C (ppm) = 139.8, 133.6, 129.0, 127.9, 70.8, 32.5, 20.2, 19.7, -1.8, -2.1; **LRMS** (EI, 70 eV) m/z (%) 193 (10) [(M-Me)⁺], 138 (18), 137 (100), 136 (13), 135 (82), 131 (13), 105 (11); **EA**: calc. (%) for C₁₂H₂₀OSi, C 69.17, H 9.67; found C 68.90, H 9.58; **IR** (neat): $\tilde{\nu}$ = 3301 (brs), 2953 (m), 2871 (m), 1426 (m), 1248 (m), 1112 (s), 1032 (s), 829 (s), 700 (s); **GC** (achiral phase), 60 kPa He, 100 °C, 2 min, 7 °C/min, 250 °C, 10 min: t_R = 18.3 min; **GC** (chiral phase, Brechbühler, β -cyclodextrin dimethyl-tertbutylsilyl SE54 column (30 m × 0.25 mm × 0.25 μ m), 80 kPa He, 95 °C, 80 min, 10 °C/min, 180 °C, 5 min): t_R = 62.9 min (+); t_R = **66.3** min (-), 96% *ee*; $[\alpha]_D^{20}$ = -9.5 (c = 0.60, CHCl₃).

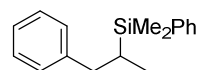
(-)-3-(Dimethyl(phenyl)silyl)-2-methylpropyl acetate (49)



Appearance: pale yellow liquid; **¹H NMR** (400 MHz, CDCl₃) δ_H (ppm) = 7.54–7.49 (m, 2H), 7.38–7.33 (m, 3H), 3.86 (dd, J = 10.6, 5.9 Hz, 1H), 3.78 (dd, J = 10.6, 7.1 Hz, 1H), 2.02 (s, 3H), 1.99–1.87 (m, 1H), 0.91 (d, J = 6.7 Hz, 4H), 0.65 (dd, J = 14.9, 9.2 Hz, 1H), 0.31 (d, J = 0.7 Hz, 6H); **¹³C NMR** (100 MHz, CDCl₃) δ_C (ppm) = 171.3, 139.5, 133.6, 129.1, 127.9, 71.6, 29.3, 21.1, 20.4, 20.0, -1.9, -2.1; **LRMS** (EI, 70 eV) m/z (%) 235 (17) [(M-Me)⁺], 193 (11), 180 (12), 179 (72), 173 (19), 137 (80), 136 (18), 135 (100), 117 (43), 105 (15), 75 (18); **EA**: calc. (%) for C₁₄H₂₂O₂Si, C 67.15, H 8.85; found C

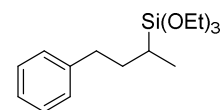
67.00, H 8.73; **IR** (neat): $\tilde{\nu}$ = 2957 (brs), 2877 (w), 1742 (s), 1247 (m), 1237 (m), 831 (w), 673 (s); **GC** (achiral phase), 60 kPa He, 100 °C, 2 min, 7 °C/min, 250 °C, 10 min: t_R = 19.7 min; **HPLC** (chiral, Daicel Chiracel OD-H, 0.46 cm \times 25 cm, *n*-heptane/isopropanol 100:0, 0.5 mL/min, 20 °C): t_R = 60.2 min (+), t_R = **64.0** (–), 58% *ee*; $[\alpha]_D^{20}$ = –4.4 (c = 1.00, CHCl₃).

(+)-Dimethyl(phenyl)(1-phenylpropan-2-yl)silane (50)

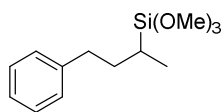


Appearance: colorless liquid; **¹H NMR** (400 MHz, CDCl₃) δ_H (ppm) = 7.59–7.51 (m, 2H), 7.41–7.34 (m, 3H), 7.29–7.21 (m, 2H), 7.19–7.07 (m, 3H), 2.87 (dd, J = 13.7, 3.6 Hz, 1H), 2.22 (dd, J = 13.6, 11.8 Hz, 1H), 1.29–1.14 (m, 1H), 0.84 (d, J = 7.3 Hz, 3H), 0.30 (s, 6H); **¹³C NMR** (100 MHz, CDCl₃) δ_C (ppm) = 142.6, 138.4, 134.1, 129.0 ($\times 2$), 128.2, 127.9, 125.7, 38.0, 21.8, 13.8, –4.76, –4.84; **LRMS** (EI, 70 eV) m/z (%) 254 (1) [M^+], 176 (23), 136 (16), 135 (100), 121 (10), 118 (16), 105 (10), 91 (11); **EA:** calc. (%) for C₁₇H₂₂Si, C 80.25, H 8.71 found C 79.94, H 8.57; **IR** (neat): $\tilde{\nu}$ = 3023 (w), 2952 (w), 2862 (w), 1495 (w), 1249 (s), 1111 (s), 979 (w), 828 (s), 811 (s), 769 (m), 699 (s); **GC** (achiral phase), 60 kPa He, 100 °C, 2 min, 7 °C/min, 250 °C, 10 min: t_R = 23.1 min; **HPLC** (chiral, Daicel Chiracel OJ, 0.46 cm \times 25 cm, *n*-heptane/isopropanol 99:1, 0.5 mL/min, 20 °C): t_R = 13.4 min (–), t_R = **16.0** (+), 42% *ee*; $[\alpha]_D^{20}$ = +5.4 (c = 0.60, CHCl₃).

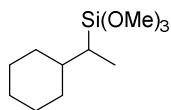
(+)-Triethoxy(4-phenylbutan-2-yl)silane (58)



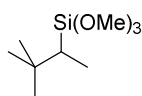
Appearance: colorless liquid; **¹H NMR** (400 MHz, CDCl₃) δ_H (ppm) = 7.31–7.26 (m, 2H), 7.22–7.08 (m, 3H), 3.83 (q, J = 7.0 Hz, 6H), 2.83–2.68 (m, 1H), 2.67–2.51 (m, 1H), 1.99–1.84 (m, 1H), 1.65–1.49 (m, 1H), 1.23 (t, J = 7.0 Hz, 9H), 1.09 (d, J = 7.4 Hz, 3H), 0.96–0.84 (m, 1H); **¹³C NMR** (100 MHz, CDCl₃) δ_C (ppm) = 143.1, 128.6, 128.4, 125.7, 58.6, 34.8, 33.6, 18.5, 16.4, 14.0; **LRMS** (EI, 70 eV) m/z (%) 296 (2) [M^+], 205 (30), 164 (17), 163 (100), 119 (28), 91 (22), 79 (17); **HRMS** (ESI) exact mass calculated for C₁₆H₂₈O₃SiNa [(M +Na)⁺], 319.1700, found 319.1701; **IR** (neat): $\tilde{\nu}$ = 2972 (m), 2925 (w), 1389 (w), 1164 (w), 1101 (s), 1075 (s), 954 (s), 778 (m); **GC** (achiral phase), 60 kPa He, 100 °C, 2 min, 7 °C/min, 250 °C, 10 min: t_R = 19.6 min; **HPLC** (chiral, Daicel Chiracel OJ, 0.46 cm \times 25 cm, *n*-heptane/isopropanol 100:0, 0.2 mL/min, 20 °C): t_R = 23.4 min (–), t_R = **27.9** (+), 70% *ee*; $[\alpha]_D^{20}$ = +9.2 (c = 1.00, CHCl₃).

(-)-Trimethoxy(4-phenylbutan-2-yl)silane (60)

Appearance: colorless liquid; $^1\text{H NMR}$ (400 MHz, CDCl_3) δ_{H} (ppm) = 7.31–7.22 (m, 2H), 7.21–7.09 (m, 3H), 3.58 (s, 9H), 2.85–2.68 (m, 1H), 2.65–2.47 (m, 1H), 1.97–1.80 (m, 1H), 1.65–1.47 (m, 1H), 1.10 (d, J = 7.3 Hz, 3H), 1.02–0.74 (m, 1H); $^{13}\text{C NMR}$ (100 MHz, CDCl_3) δ_{C} (ppm) = 142.9, 128.6, 128.4, 125.8, 51.0, 34.7, 33.5, 15.8, 13.8; **LRMS** (EI, 70 eV) m/z (%) 254 (1) [M^+], 163 (24), 122 (11), 121 (100), 91 (43); **EA:** calc. (%) for $\text{C}_{13}\text{H}_{22}\text{O}_3\text{Si}$, C 61.38, H 8.72 found C 61.34, H 8.59; **IR** (neat): $\tilde{\nu}$ = 2939 (brs), 2841 (m), 2363 (m), 2356 (w), 1601 (w), 1456 (m), 1188 (m), 1078 (s), 798 (s), 748 (s), 698 (m); **GC** (achiral phase), 60 kPa He, 100 °C, 2 min, 7 °C/min, 250 °C, 10 min: t_{R} = 18.1 min; **HPLC** (chiral, Daicel Chiracel OB-H, 0.46 cm \times 25 cm, *n*-heptane/isopropanol 100:0, 0.2 mL/min, 20 °C): t_{R} = **36.1 min (-)**, t_{R} = 40.6 (+), 77% *ee*; $[\alpha]_{\text{D}}^{20}$ = -4.9 (c = 0.50, CHCl_3).

(-)-(1-Cyclohexylethyl)trimethoxysilane (61)

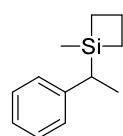
Appearance: colorless liquid; $^1\text{H NMR}$ (400 MHz, CDCl_3) δ_{H} (ppm) = 3.58 (s, 9H), 1.71 (d, J = 11.7 Hz, 2H), 1.63 (d, J = 12.8 Hz, 2H), 1.50–1.35 (m, 1H), 1.32–1.02 (m, 6H), 1.00 (d, J = 7.5 Hz, 3H), 0.91–0.81 (m, 1H); $^{13}\text{C NMR}$ (100 MHz, CDCl_3) δ_{C} (ppm) = 50.8, 39.4, 32.6, 31.2, 27.4, 27.1, 26.7, 23.2, 10.8; **LRMS** (EI, 70 eV) m/z (%) 232 (1) [M^+], 122 (10), 121 (100), 110 (45), 91 (38); **HRMS** (ESI) exact mass calculated for $\text{C}_{11}\text{H}_{24}\text{O}_3\text{SiNa}$ [$(\text{M}+\text{Na})^+$], 255.1387, found 255.1387; **IR** (neat): $\tilde{\nu}$ = 2920 (s), 2838 (m), 1447 (w), 1189 (w), 1080 (s), 796 (s); **GC** (achiral phase), 60 kPa He, 100 °C, 2 min, 7 °C/min, 250 °C, 10 min: t_{R} = 13.4 min; **GC** (chiral phase, *Hydrodex*, β -3P column (30 m \times 0.25 mm \times 0.25 μm), 60 kPa He, 50 °C, 0 min, 0.5 °C/min, 100 °C, 0 min, 10 °C/min, 180 °C, 5 min): t_{R} = 99.2 (+), t_{R} = **102.3 (-)**, 88% *ee*; $[\alpha]_{\text{D}}^{20}$ = -7.3 (c = 0.50, CHCl_3).

(-)-(3,3-Dimethylbutan-2-yl)trimethoxysilane (62)

Appearance: colorless liquid; $^1\text{H NMR}$ (400 MHz, CDCl_3) δ_{H} (ppm) = 3.58 (s, 9H), 1.02 (d, J = 7.7 Hz, 3H), 0.97 (s, 9H), 0.82 (dd, J = 15.4, 7.7 Hz, 1H); $^{13}\text{C NMR}$ (100 MHz, CDCl_3) δ_{C} (ppm) = 50.7, 32.0, 29.6, 29.0, 10.6; **LRMS** (EI, 70 eV) m/z (%) 191 (25) [$(\text{M}-\text{Me})^+$], 150 (34), 122 (13), 121 (100), 118 (19), 91 (32); **HRMS** (ESI) exact mass

calculated for $C_9H_{20}O_3SiNa [(M+Na)^+]$, 229.1230, found 229.1233; **GC** (achiral phase), 60 kPa He, 100 °C, 2 min, 7 °C/min, 250 °C, 10 min: $t_R = 7.5$ min; **GC** (chiral phase, *Chiraldex*, γ -cyclodextrin 6-Methyl-2,3-pentyl PS 086 column (30 m \times 0.25 mm \times 0.25 μ m), 120 kPa He, 35 °C, 50 min, 10 °C/min, 180 °C, 5 min): $t_R = 25.7$ min (+), $t_R = 27.3$ min (–), 53% *ee*; $[\alpha]_D^{20} = -7.2$ ($c = 0.40$, $CHCl_3$).

(–)-1-Methyl-1-(1-phenylethyl)siletane (64)



Appearance: colorless liquid; 1H NMR (400 MHz, $CDCl_3$) δ_H (ppm) = 7.30–7.22 (m, 2H), 7.14–7.06 (m, 3H), 2.41 (q, $J = 7.5$ Hz, 1H), 2.07–1.81 (m, 2H), 1.44 (d, $J = 7.5$ Hz, 3H), 1.15–0.98 (m, 2H), 0.98–0.92 (m, 2H), 0.15 (s, 3H); ^{13}C NMR (100 MHz, $CDCl_3$) δ_C (ppm) = 144.8, 128.2, 126.9, 124.5, 29.6, 17.6, 14.2, 12.9, 12.8, –3.6; **LRMS** (EI, 70 eV) m/z (%) 190 (27) [M^+], 162 (41), 149 (10), 148 (20), 147 (56), 145 (16), 121 (12), 105 (17), 86 (10), 85 (100); **IR** (neat): $\tilde{\nu} = 3048$ (w), 2972 (w), 1495 (w), 1237 (m); **GC** (achiral phase), 60 kPa He, 100 °C, 2 min, 7 °C/min, 250 °C, 10 min: $t_R = 14.0$ min; **HPLC** (chiral, Daicel Chiracel OJ, 0.46 cm \times 25 cm, *n*-heptane/isopropanol 99:1, 0.5 mL/min, 20 °C): $t_R = 7.8$ min (–), $t_R = 8.6$ (+), 96% *ee*; $[\alpha]_D^{20} = -13.6$ ($c = 0.50$, $CHCl_3$).

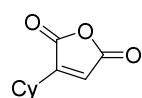
The 1H and ^{13}C NMR data were consistent with the literature data.^[96]

6.3 Iridium-Catalyzed Asymmetric Hydrogenation of Maleic Acid Dimethyldiester

6.3.1 Synthesis and analytical data of maleic anhydrides

6.3.2.1 General procedure for the synthesis of maleic anhydrides

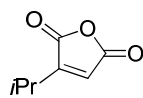
3-Cyclohexylfuran-2,5-dione (73b)



The title compound was prepared according to the procedure followed for the synthesis of 3-isopropylfuran-2,5-dione (see above). The crude material was purified by crystallization (CH_2Cl_2) to afford 1.04 g (70% yield) of the title compound as a white solid.

m.p. 109–111 °C; **¹H NMR** (400 MHz, DMSO-*d*₆) δ_{H} (ppm) 5.85 (s, 1H), 2.41 (tt, J = 10.9, 3.2 Hz, 1H), 1.98–1.87 (m, 4H), 1.85–1.71 (m, 1H), 1.63–1.19 (m, 5H); **¹³C NMR** (100 MHz, DMSO-*d*₆) δ_{C} (ppm) 169.6, 166.2, 165.5, 116.9, 41.7, 30.8, 25.6, 25.4; **LRMS** (EI, 70 eV) m/z (%) 180 (18) [M^+], 153 (22), 152 (100), 139 (16), 135 (21), 134 (22), 124 (20), 112 (48), 107 (54); **HRMS** (EI) exact mass calculated for $\text{C}_{10}\text{H}_{12}\text{O}_3$ [M^+], 180.0786, found 180.0777; **IR** (neat): $\tilde{\nu}$ = 2924 (w), 2853 (w), 1694 (s), 1638 (s), 1419 (s), 1276 (s), 1246 (s), 1217 (s), 906.4 (m), 880 (m); **GC** (achiral phase), 60 kPa He, 50 °C, 0 min, 2 °C/min, 120 °C, 0 min, 10 °C/min, 250 °C, 5 min: t_{R} = 46.7 min.

3-Isopropylfuran-2,5-dione (73c)

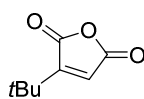


To a mixture of dimethyl 2-isopropylmaleate (1.2 g, 6.4 mmol, 1.0 eq.) in THF/H₂O (1:1 mixture, 15 mL) a LiOH solution (4 M in water, 25.8 mmol, 6.4 mL) was added. The reaction was heated at 50 °C and stirred overnight at the same temperature. After cooling the mixture to 0 °C, the reaction was quenched with HCl (1 M aq., ca. 10 mL) and extracted with MTBE (3×25 mL), washed with brine, dried over Na₂SO₄, filtered and concentrated *in vacuo* to yield a pale yellow liquid, which was purified by Kugelrohr distillation (5 mbar at 110 °C) to afford 352 mg (40% yield) of the title compound as a colorless liquid.

¹H NMR (400 MHz, CDCl₃) δ_{H} (ppm) 6.55 (d, J = 1.6 Hz, 1H), 2.90 (septd, J = 6.9, 1.6 Hz, 1H), 1.28 (d, J = 6.9 Hz, 6H); **¹³C NMR** (100 MHz, CDCl₃) δ_{C} (ppm) 165.4, 164.1, 159.4, 127.1, 26.8, 20.6; **LRMS** (EI, 70 eV) m/z (%) 125 (3) [($\text{M}-\text{Me}$)⁺], 112 (87), 111 (11), 97 (26), 95 (12), 94 (13), 81 (28), 69 (16), 68 (16), 67 (100), 66 (13), 53 (51); **IR** (neat): $\tilde{\nu}$ = 2974 (w), 1837 (w), 1761 (s), 1635 (w), 1269 (m), 1231 (s), 967 (s), 891 (s), 772 (m); **GC** (achiral phase), 60 kPa He, 50 °C, 0 min, 2 °C/min, 120 °C, 0 min, 10 °C/min, 250 °C, 5 min: t_{R} = 34.6 min.

The ¹H and ¹³C NMR data were consistent with the literature data.^[186]

3-(*tert*-Butyl)furan-2,5-dione (73d)



The title compound was prepared according to the procedure followed for the synthesis of 3-isopropylfuran-2,5-dione (see above). The crude material

was purified by Kugelrohr distillation (5 mbar at 140 °C) to afford 390 mg (54% yield) of the title compound as a white solid.

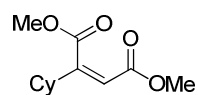
m.p.: 60–62 °C; **¹H NMR** (400 MHz, CDCl₃) δ_{H} (ppm) 6.52 (1H, s), 1.34 (9H, s); **¹³C NMR** (100 MHz, CDCl₃) δ_{C} (ppm) 164.3, 163.8, 161.7, 127.1, 33.5, 28.2; **LRMS** (EI, 70 eV) m/z (%) 139 (10) [(M–Me)⁺], 126 (88), 125 (10), 111 (59), 110 (31), 109 (19), 108 (25), 95 (59), 83 (62), 67 (100); **IR** (neat): $\tilde{\nu}$ = 2974 (m), 1829 (m), 1765 (s), 1616 (m), 1508 (s), 1472 (m), 1246 (m), 1192 (m), 959 (s), 744 (w); **GC** (achiral phase), 60 kPa He, 100 °C, 2 min, 7 °C/min, 250 °C, 10 min: t_{R} = 11.5 min.

The ¹H and ¹³C NMR data were consistent with the literature data.^[187]

6.3.2 Synthesis and analytical data of maleic acid dimethylesters

6.3.2.1 General procedure for the synthesis of maleic acid dimethylesters

Dimethyl 2-cyclohexylmaleate (76b)



The title compound was prepared according to the procedure published by Li.^[107] To a cold (–40 °C) solution of cuprous bromide-dimethylsulfide complex (4.1 g, 20 mmol, 1.0 eq.) in THF (50 mL) was added dropwise a solution of cyclohexylmagnesium chloride (1.3 M in THF/toluene 1:1, 20 mL, 26 mmol, 1.3 eq.). The resulting yellow solution was stirred at –40 °C for 2 h and then cooled at –78 °C prior to dropwise addition of dimethyl acetylenedicarboxylate (2.45 mL, 20 mmol, 1.0 eq.) in THF (15 mL). The resulting dark mixture was stirred at –78 °C for 2 h, quenched with NH₄Cl (sat. aq., 10 mL) and allowed to warm to rt. The layers were separated and the aqueous phase was extracted with MTBE (3×40 mL). The combined organic layers were washed with brine, dried over Na₂SO₄, filtered and concentrated *in vacuo* to give a black oil as a 24:1 *Z/E* isomers mixture. Purification by column chromatography (SiO₂, 2 cm × 23 cm, pentane/EtOAc, 15:1) afforded 2.2 g (50% yield) of the title compound as a pale yellow oil.

R_f: 0.33 in pentane/EtOAc, 15:1 (visualization: KMnO₄); **¹H NMR** (400 MHz, CDCl₃) δ_{H} (ppm) = 5.76 (d, J = 1.3 Hz, 1H), 3.83 (s, 3H), 3.71 (s, 3H), 2.32–2.27 (m, 1H), 1.88–1.64 (m, 5H), 1.22–1.08 (m, 5H); **¹³C NMR** (100 MHz, CDCl₃) δ_{C} (ppm) = 169.6, 165.9, 156.5, 117.1, 52.4, 51.9, 42.6, 31.2, 26.2, 25.9; **LRMS** (EI, 70 eV) m/z (%) 226 (4) [M⁺], 194 (47), 167 (80), 135 (100), 107 (51), 79 (42); **EA**: calc. (%) for C₁₂H₁₈O₄, C 63.70, H 8.02; found C 63.72, H 8.18; **IR** (neat): $\tilde{\nu}$ = 2931 (m), 2345 (w), 1722 (s), 1643 (m), 1444 (m), 1255 (s), 1202 (m), 1163 (s); **GC** (achiral phase), 60 kPa He, 50 °C, 0 min, 2 °C/min, 120 °C, 0 min, 10 °C/min, 250 °C, 5 min: t_{R} = 47.6 min.

The ¹H and ¹³C NMR data were consistent with the literature data.^[188]

6.3.2.2 Synthesis of Grignard reagents

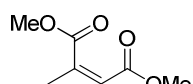
Grignard reagents that were not commercially available were synthesized according to the following procedure:

Procedure for the synthesis of Grignard reagents:

In a flame-dried argon flushed two-neck round bottom flask were added freshly grounded magnesium turnings (312 mg, 13 mmol, 1.3 eq.) and Et₂O (15 mL). To this mixture a solution of the relevant arylbromide (12 mmol, 1.2 eq.) in Et₂O (5 mL) was added. To the mixture a crystal of iodine was added and the reaction was refluxed for 90 min. After cooling to rt, the Grignard solution was used directly as described above in the synthesis of dimethyl 2-cyclohexylmaleate.

6.3.2.3 Analytical data

Dimethyl 2-methylbut-2-enedioate ((*Z*)- and (*E*)-76a)



The title compound was prepared according to the procedure followed for the synthesis of dimethyl 2-cyclohexylmaleate (see above) using methylmagnesium bromide (3 M in diethyl ether, 4.2 mL, 25 mmol, 1.25 eq.) as reagent. The crude material consisted of a 6:1 *Z/E* isomers mixture, which were separated by column chromatography (SiO₂, 2 cm × 29 cm, pentane/EtOAc, 25:1) to afford 2.1 g (76%

yield) of the title compound (**Z**)-**76a** and 540 mg (17% yield) of dimethyl 2-methylfumarate (**E**)-**76a** both as pale yellow liquids.

(Z)-76a:

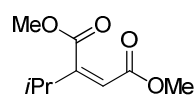
R_f: 0.43 in pentane/EtOAc, 15:1 (visualization: KMnO₄); **¹H NMR** (400 MHz, CDCl₃) δ_{H} (ppm) = 5.85 (q, J = 3.2, 1.6 Hz, 1H), 3.82 (s, 3H), 3.81 (s, 3H), 2.05 (d, J = 1.6 Hz, 3H); **¹³C NMR** (100 MHz, CDCl₃) δ_{C} (ppm) = 169.5, 165.5, 145.8, 120.7, 52.5, 51.9, 20.6; **LRMS** (EI, 70 eV) m/z (%) 158 (5) [M⁺], 128 (26), 127 (100), 126 (17), 99 (42); **GC** (achiral phase), 60 kPa He, 50 °C, 0 min, 4 °C/min, 150 °C, 0 min, 10 °C/min, 250 °C, 5 min: t_{R} = 18.1 min.

(E)-76a:

R_f: 0.47 in pentane/EtOAc, 15:1 (visualization: KMnO₄); **¹H NMR** (400 MHz, CDCl₃) δ_{H} (ppm) = 6.78 (dd, J = 1.4, 1.0 Hz, 1H), 3.80 (s, 3H), 3.76 (s, 3H), 2.28 (m, 3H); **¹³C NMR** (100 MHz, CDCl₃) δ_{C} (ppm) = 167.7, 166.4, 143.9, 126.6, 52.7, 51.8, 14.4; **LRMS** (EI, 70 eV) m/z (%) 158 (5) [M⁺], 128 (26), 127 (100), 126 (17), 99 (42); **GC** (achiral phase), 60 kPa He, 50 °C, 0 min, 4 °C/min, 150 °C, 0 min, 10 °C/min, 250 °C, 5 min: t_{R} = 17.6 min.

The ¹H and ¹³C NMR data of both isomers were consistent with the literature data.^[189]

(Z)-Dimethyl 2-isopropylmaleate (76c)

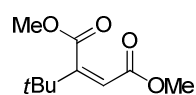


The title compound was prepared according to the procedure followed for the synthesis of dimethyl 2-cyclohexylmaleate (see above) using isopropylmagnesium bromide (2 M in THF, 13.0 mL, 26 mmol, 1.3 eq.) as reagent. The crude material consisted of a 20:1 *Z/E* isomers mixture, which were separated by column chromatography (SiO₂, 3 cm × 24 cm, pentane/EtOAc, 5:1) to afford 2.85 g (77% yield) of the title compound as a pale yellow liquid.

R_f: 0.65 in pentane/EtOAc, 5:1 (visualization: KMnO₄); **¹H NMR** (400 MHz, CDCl₃) δ_{H} (ppm) = 5.79 (m, 1H), 3.84 (s, 3H), 3.73 (s, 3H), 2.69–2.62 (m, 1H), 1.16 (d, J = 6.9 Hz, 6H); **¹³C NMR** (100 MHz, CDCl₃) δ_{C} (ppm) = 169.3, 165.7, 157.0, 116.9, 52.2, 51.8, 32.9, 20.7; **LRMS** (EI, 70 eV) m/z (%) 155 (29) [(M–MeO)⁺], 154 (92), 127 (27), 126 (100), 125 (20), 111 (37), 96 (15), 95 (41), 94 (15); **HRMS** (ESI) exact mass calculated for C₉H₁₄O₄Na [(M+Na)⁺], 209.0784, found 209.0785; **IR** (neat): $\tilde{\nu}$ = 2968 (w), 2955 (w), 1723 (s), 1647 (m), 1435 (m),

1374 (w), 1258 (s), 1196 (m), 1166 (s), 1054 (m), 877 (m); **GC** (achiral phase), 60 kPa He, 50 °C, 0 min, 4 °C/min, 150 °C, 0 min, 10 °C/min, 250 °C, 5 min: t_R = 25.3 min.

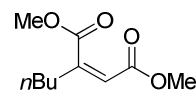
(Z)-Dimethyl 2-(*tert*-butyl)maleate (76d)



The title compound was prepared according to the procedure followed for the synthesis of dimethyl 2-cyclohexylmaleate (see above) using *tert*-butylmagnesium chloride (1 M in diethyl ether, 26.0 mL, 26 mmol, 1.3 eq.) as reagent. The crude material showed no trace of the corresponding fumarate. Purification by column chromatography (SiO₂, 3 cm × 29 cm, pentane/EtOAc, 30:1) afforded 1.5 g (38% yield) of the title compound as a colorless liquid.

R_f: 0.36 in pentane/EtOAc, 15:1 (visualization: KMnO₄); **¹H NMR** (400 MHz, CDCl₃) δ_H (ppm) = 5.84 (m, 1H), 3.84 (s, 3H), 3.71 (s, 3H), 1.18 (s, 9H); **¹³C NMR** (100 MHz, CDCl₃) δ_C (ppm) = 169.2, 165.9, 161.0, 116.0, 52.2, 51.9, 35.8, 29.0; **LRMS** (EI, 70 eV) m/z (%) 185 (8) [(M–Me)⁺], 169 (29), 153 (22), 141 (100), 140 (18), 125 (25), 109 (78), 81 (40); **HRMS** (ESI) exact mass calculated for C₁₀H₁₆O₄Na [(M+Na)⁺], 223.0941, found 223.0945; **IR** (neat): $\tilde{\nu}$ = 2955 (w), 1724 (s), 1688 (m), 1640 (m), 1434 (m), 1348 (m), 1260 (m), 1236 (m), 1193 (m), 1165 (s), 1161 (m), 1028 (w), 874 (w); **GC** (achiral phase), 60 kPa He, 50 °C, 0 min, 2 °C/min, 120 °C, 0 min, 10 °C/min, 250 °C, 5 min: t_R = 40.0 min.

(Z)-Dimethyl 2-butylmaleate (76e)

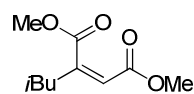


The title compound was prepared according to the procedure followed for the synthesis of dimethyl 2-cyclohexylmaleate (see above) using *n*-butylmagnesium chloride (14.6 mL of a 20% wt solution in THF/toluene, 25 mmol, 1.25 eq.) as reagent. The crude material consisted of a 12:1 *Z/E* isomers mixture, which were separated by column chromatography (SiO₂, 3 cm × 26 cm, pentane/EtOAc, 30:1) to afford 3.5 g (88% yield) of the title compound as a yellow oil.

R_f: 0.30 in pentane/EtOAc, 15:1 (visualization: KMnO₄); **¹H NMR** (400 MHz, CDCl₃) δ_H (ppm) = 5.80 (m, 1H), 3.83 (d, J = 0.7 Hz, 3H), 3.72 (d, J = 0.7 Hz, 3H), 2.38–2.29 (m, 2H), 1.53–1.42 (m, 2H), 1.42–1.30 (m, 2H), 0.91 (t, J = 7.3 Hz, 3H); **¹³C NMR** (100 MHz, CDCl₃) δ_C (ppm)

169.6, 165.9, 151.2, 119.1, 52.5, 51.9, 34.2, 29.2, 22.2, 13.9; **LRMS** (EI, 70 eV) m/z (%) 200 (2) [M^+], 185 (6), 169 (100), 153 (9), 141 (40), 140 (46), 126 (83), 125 (34), 113 (20), 109 (24), 98 (30), 81 (55); **EA**: calc. (%) for $C_{10}H_{16}O_4$, C 59.98, H 8.05; found C 59.46, H 7.96; **IR** (neat): $\tilde{\nu}$ = 2931 (m), 2345 (w), 1722 (s), 1643 (m), 1444 (m), 1255 (s), 1202 (m), 1163 (s); **GC** (achiral phase), 60 kPa He, 50 °C, 0 min, 2 °C/min, 120 °C, 0 min, 10 °C/min, 250 °C, 5 min: t_R = 42.5 min.

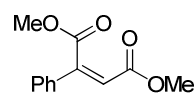
(Z)-Dimethyl 2-isobutylmaleate (76f)



The title compound was prepared according to the procedure followed for the synthesis of dimethyl 2-cyclohexylmaleate (see above) using isobutylmagnesium chloride (2 M in diethyl ether, 13.0 mL, 26 mmol, 1.3 eq.) as reagent. The crude material showed no trace of the corresponding fumarate. Purification by column chromatography (SiO_2 , 2 cm \times 24 cm, pentane/EtOAc, 40:1) afforded 1.25 g (31% yield) of the title compound as a pale yellow liquid.

R_f: 0.19 in pentane/EtOAc, 25:1 (visualization: $KMnO_4$); **1H NMR** (400 MHz, $CDCl_3$) δ_H (ppm) = 5.79 (t, J = 1.2 Hz, 1H), 3.82 (s, 3H), 3.72 (s, 3H), 2.22 (dd, J = 7.2, 1.3 Hz, 2H), 1.89–1.70 (m, 1H), 0.93 (d, J = 6.6 Hz, 6H); **^{13}C NMR** (100 MHz, $CDCl_3$) = δ_C (ppm) 169.5, 165.5, 150.2, 120.4, 52.4, 51.9, 44.1, 26.6, 22.3; **LRMS** (EI, 70 eV) m/z (%) 185 (2) [($M-Me$) $^+$], 169 (16), 127 (11), 126 (100), 98 (36), 69 (11); **EA**: calc. (%) for $C_{10}H_{16}O_4$, C 59.98, H 8.05; found C 59.68, H 8.05; **IR** (neat): $\tilde{\nu}$ = 2956 (m), 2339 (w), 1722 (s), 1645 (w), 1369 (w), 1262 (m), 1165 (s); **GC** (achiral phase), 60 kPa He, 50 °C, 0 min, 4 °C/min, 150 °C, 0 min, 10 °C/min, 250 °C, 5 min: t_R = 27.5 min.

(Z)-Dimethyl 2-(phenyl)maleate (76g)

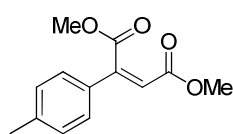


The title compound was prepared according to the procedure followed for the synthesis of dimethyl 2-cyclohexylmaleate (see above) using phenylmagnesium bromide (2.8 M in diethyl ether, 2.25 mL, 6.25 mmol, 1.25 eq.) as reagent. The crude material consisted of a 4.6:1 *Z/E* isomers mixture, which were separated by column chromatography (SiO_2 , 2 cm \times 33 cm, pentane/EtOAc, 23:1) to afford 248 mg (24% yield) of the title compound as a colorless liquid.

R_f: 0.24 in pentane/EtOAc, 10:1 (visualization: UV, KMnO₄); **¹H NMR** (400 MHz, CDCl₃) δ_{H} (ppm) = 7.52–7.49 (m, 2H), 7.44–7.38 (m, 3H), 6.34 (s, 1H), 3.97 (s, 3H), 3.81 (s, 3H); **¹³C NMR** (100 MHz, CDCl₃) δ_{C} (ppm) = 168.5, 165.6, 149.1, 133.3, 130.8, 129.2, 126.9, 117.2, 52.9, 52.2; **LRMS** (EI, 70 eV) m/z (%) 220 (67) [M⁺], 219 (26), 205 (68), 189 (50), 161 (100), 118 (12), 115 (51), 102 (50); **GC** (achiral phase), 60 kPa He, 50 °C, 0 min, 4 °C/min, 150 °C, 0 min, 10 °C/min, 250 °C, 5 min: t_{R} = 35.6 min.

The ¹H and ¹³C NMR data were consistent with the literature data. ^[190]

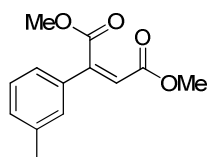
(Z)-Dimethyl 2-(*p*-tolyl)maleate (76h)



The title compound was prepared according to the procedure followed for the synthesis of dimethyl 2-cyclohexylmaleate (see above) using *p*-tolylmagnesium bromide (0.5 M in diethyl ether, 24 mL, 12 mmol, 1.2 eq.) as reagent. The crude material consisted of a 3:1 *Z/E* isomers mixture, which were separated by column chromatography (SiO₂, 2 cm × 29 cm, pentane/EtOAc, 12:1) to afford 330 mg (14% yield) of the title compound as a yellow solid.

m.p.: 35–37 °C; **R_f**: 0.36 in pentane/EtOAc, 8:1 (visualization: UV, KMnO₄); **¹H NMR** (400 MHz, CDCl₃) δ_{H} (ppm) = 7.38–7.36 (2H, d, J = 8.2 Hz), 7.21–7.19 (2H, d, J = 8.2 Hz), 6.29 (1H, s), 3.95 (3H, s), 3.78 (3H, s), 2.37 (3H, s); **¹³C NMR** (100 MHz, CDCl₃) δ_{C} (ppm) = 168.7, 165.7, 149.1, 141.3, 130.4, 130.0, 126.8, 116.0, 52.8, 52.2, 21.5; **LRMS** (EI, 70 eV) m/z (%) 234 (90) [M⁺], 219 (62), 203 (27), 176 (17), 175 (100), 132 (18), 119 (21), 116 (46), 115 (76), 91 (29); **HRMS** (ESI) exact mass calculated for C₁₃H₁₄O₄Na [(M+Na)⁺], 257.0784, found 257.0784; **IR** (neat): $\tilde{\nu}$ = 2953 (w), 2361 (w), 1725 (s), 1512 (w), 1433 (m), 1302 (m), 1149 (s), 955 (m), 868 (m), 783 (m); **GC** (achiral phase), 60 kPa He, 50 °C, 0 min, 4 °C/min, 150 °C, 0 min, 10 °C/min, 250 °C, 5 min: t_{R} = 37.6 min.

(Z)-Dimethyl 2-(*m*-tolyl)maleate (76i)

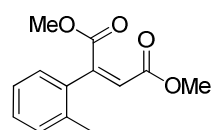


The title compound was prepared according to the procedure followed for the synthesis of dimethyl 2-cyclohexylmaleate (see above) using *m*-tolylmagnesium bromide (12.5 mmol, 1.25 eq.) as reagent, which was synthesized according to the procedure for the synthesis of Grignard reagents. The crude

material consisted of a 6:1 *Z/E* isomers mixture, which were separated by column chromatography (SiO₂, 3 cm × 28 cm, pentane/EtOAc, 19:1) to afford 360 mg (15% yield) of the title compound as a yellow oil.

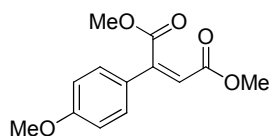
R_f: 0.43 in pentane/EtOAc, 8:1 (visualization: UV, KMnO₄); **¹H NMR** (400 MHz, CDCl₃) δ_{H} (ppm) = 7.31–7.21 (m, 4H), 6.30 (s, 1H), 3.95 (s, 3H), 3.79 (s, 3H), 2.37 (s, 3H); **¹³C NMR** (100 MHz, CDCl₃) δ_{C} (ppm) = 168.6, 165.6, 149.3, 139.0, 133.2, 131.6, 129.0, 127.5, 124.1, 117.0, 52.9, 52.2, 21.6; **LRMS** (EI, 70 eV) m/z (%) 234 (70) [M⁺], 233 (22), 220 (13), 219 (100), 203 (34), 176 (13), 175 (85), 132 (15), 119 (15), 116 (45), 115 (72), 91 (30); **HRMS** (ESI) exact mass calculated for C₁₃H₁₄O₄Na [(M+Na)⁺], 257.0784, found 257.0787; **IR** (neat): $\tilde{\nu}$ = 2951 (w), 2361 (w), 1734 (s), 1718 (s), 1621 (m), 1433 (m), 1347 (m), 1294 (m), 1230 (m), 1160 (s), 1036 (m), 790 (m); **GC** (achiral phase), 60 kPa He, 50 °C, 0 min, 4 °C/min, 150 °C, 0 min, 10 °C/min, 250 °C, 5 min: t_{R} = 37.0 min.

(*Z*)-Dimethyl 2-(*o*-tolyl)maleate (76j)



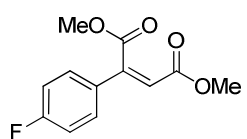
The title compound was prepared according to the procedure followed for the synthesis of dimethyl 2-cyclohexylmaleate (see above) using *o*-tolylmagnesium bromide (12.5 mmol, 1.25 eq.) as reagent, which was synthesized according to the Procedure for the synthesis of Grignard reagents. The crude material consisted of a 4:1 *Z/E* isomers mixture, which were separated by column chromatography (SiO₂, 2 cm × 34 cm, pentane/EtOAc, 15:1) to afford 210 mg (9% yield) of the title compound as pale yellow liquid.

R_f: 0.40 in pentane/EtOAc, 10:1 (visualization: UV, KMnO₄); **¹H NMR** (400 MHz, CDCl₃) δ_{H} (ppm) = 7.22–7.18 (m, 2H), 7.15–7.12 (m, 2H), 5.94 (s, 1H), 3.76 (s, 3H), 3.72 (s, 3H), 2.29 (s, 3H); **¹³C NMR** (100 MHz, CDCl₃) δ_{C} (ppm) = 168.0, 165.4, 148.3, 136.1, 134.8, 131.0, 129.4, 128.7, 126.1, 123.4, 52.7, 52.2, 20.2; **LRMS** (EI, 70 eV) m/z (%) 234 (9) [M⁺], 204 (14), 202 (25), 175 (23), 174 (64), 129 (24), 116 (27), 115 (100), 91 (13); **HRMS** (ESI) exact mass calculated for C₁₃H₁₄O₄Na [(M+Na)⁺], 257.0784, found 257.0789; **IR** (neat): $\tilde{\nu}$ = 2952 (w), 2920 (w), 2852 (w), 2362 (w), 1722 (s), 1635 (w), 1434 (mw), 1345 (w), 1271 (w), 1196 (m), 1165 (m), 888 (w); **GC** (achiral phase) 60 kPa He, 50 °C, 0 min, 4 °C/min, 150 °C, 0 min, 10 °C/min, 250 °C, 5 min: t_{R} = 35.2 min.

(Z)-Dimethyl 2-(4-methoxyphenyl)maleate (76k)

The title compound was prepared according to the procedure followed for the synthesis of dimethyl 2-cyclohexylmaleate (see above,) using 4-methoxyphenylmagnesium bromide (1 M in THF, 12.5 mL, 12.5 mmol, 1.25 eq.) as reagent. The crude material consisted of a 4.6:1 *Z/E* isomers mixture, which were separated by column chromatography (SiO₂, 3 cm × 30 cm, pentane/EtOAc, 15:1) to afford 248 mg (24% yield) of the title compound as a colorless liquid.

R_f: 0.24 in pentane/EtOAc, 10:1 (visualization: UV, KMnO₄); **¹H NMR** (400 MHz, CDCl₃) δ_H (ppm) = 7.43–7.41 (m, 2H), 6.93–6.88 (m, 2H), 6.23 (s, 1H), 3.95 (s, 3H), 3.83 (s, 3H), 3.77 (s, 3H); **¹³C NMR** (100 MHz, CDCl₃) δ_C (ppm) = 168.8, 165.8, 161.8, 148.8, 128.6, 125.6, 114.6, 114.5, 55.6, 52.8, 52.1; **LRMS** (EI, 70 eV) *m/z* (%) 250 (100) [M⁺], 219 (18), 192 (19), 191 (78), 135 (25), 132 (29), 117 (14), 89 (18); **HRMS** (ESI) exact mass calculated for C₁₃H₁₄O₅Na [(M+Na)⁺], 273.0733, found 273.0735; **IR** (neat): $\tilde{\nu}$ = 2952 (w), 2361 (w), 1734 (s), 1715 (s), 1598 (s), 1513 (m), 1435 (w), 1356 (m), 1289 (m), 1254 (m), 1164 (s), 1031 (m), 997 (m), 833 (m); **GC** (achiral phase), 60 kPa He, 50 °C, 0 min, 4 °C/min, 150 °C, 0 min, 10 °C/min, 250 °C, 5 min: *t_R* = 28.7 min.

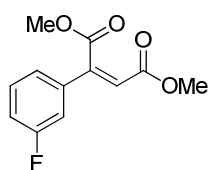
(Z)-Dimethyl 2-(4-fluorophenyl)maleate (76l)

The title compound was prepared according to the procedure followed for the synthesis of dimethyl 2-cyclohexylmaleate (see above) using 4-fluorophenylmagnesium bromide (0.8 M in THF, 15 mL, 12 mmol, 1.2 eq.) as reagent. The crude material consisted of a 4:1 *Z/E* isomers mixture, which were separated by column chromatography (SiO₂, 2 cm × 35 cm, pentane/EtOAc, 15:1) to afford 680 mg (28% yield) of the title compound as a white solid.

m.p.: 50–51 °C; **R_f**: 0.47 in pentane/EtOAc, 5:1 (visualization: UV, KMnO₄); **¹H NMR** (400 MHz, CDCl₃) δ_H (ppm) = 7.49–7.45 (m, 2H), 7.11–7.07 (m, 2H), 6.26 (s, 1H), 3.94 (s, 3H), 3.78 (s, 3H); **¹³C NMR** (100 MHz, CDCl₃) δ_C (ppm) = 168.3, 165.4, 164.3 (d, *J_{CF}* = 252 Hz), 148.0, 129.5 (d, *J_{CF}* = 3.4 Hz), 129.0 (d, *J_{CF}* = 8.6 Hz), 117.2 (d, *J_{CF}* = 1.8 Hz), 116.4 (d, *J_{CF}* =

22.0 Hz), 53.0, 52.2; **¹⁹F NMR** (376 MHz, CDCl₃) δ_F (ppm) = -109.1; **LRMS** (EI, 70 eV) m/z (%) 238 (86) [M⁺], 210 (22), 207 (48), 180 (15), 179 (100), 133 (19), 123 (14), 120 (47), 115 (24), 109 (17); **EA**: calc. (%) for C₁₂H₁₁FO₄, C 60.50, H 4.65; found C 60.89, H 4.87; **IR** (neat): $\tilde{\nu}$ = 2968 (w), 2371 (w), 1724 (s), 1718 (s), 1627 (w), 1601 (w), 1508 (m), 1430 (m), 1352 (m), 1164 (s), 1025 (m), 995 (m), 837 (s), 808 (s); **GC** (achiral phase), 60 kPa He, 50 °C, 0 min, 4 °C/min, 150 °C, 0 min, 10 °C/min, 250 °C, 5 min: t_R = 35.3 min.

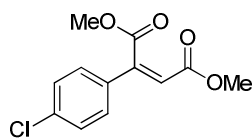
(Z)-Dimethyl 2-(3-fluorophenyl)maleate (76m)



The title compound was prepared according to the procedure followed for the synthesis of dimethyl 2-cyclohexylmaleate (see above) using 3-fluorophenylmagnesium bromide (1 M in THF, 12.5 mL, 12.5 mmol, 1.25 eq.) as reagent. The crude material consisted of a 10:1 Z/E isomers mixture, which were separated by column chromatography (SiO₂, 2 cm × 30 cm, pentane/EtOAc, 15:1) to afford 298 mg (13% yield) of the title compound as a colorless liquid.

R_f: 0.40 in pentane/EtOAc, 8:1 (visualization: UV, KMnO₄); **¹H NMR** (400 MHz, CDCl₃) δ_H (ppm) = 7.42–7.34 (m, 1H), 7.29–7.24 (m, 1H), 7.22–7.16 (m, 1H), 7.16–7.10 (m, 1H), 6.31 (s, 1H), 3.94 (s, 3H), 3.79 (s, 3H); **¹³C NMR** (100 MHz, CDCl₃) δ_C (ppm) = 168.0, 165.3, 163.1 (d, J_{CF} = 248 Hz), 147.7 (d, J_{CF} = 2.5 Hz), 135.5 (d, J_{CF} = 7.9 Hz), 130.8 (d, J_{CF} = 8.3 Hz), 122.7 (d, J_{CF} = 3.0 Hz), 118.6, 117.6 (d, J_{CF} = 21.3 Hz), 113.9 (d, J_{CF} = 23.2 Hz), 53.0, 52.3; **¹⁹F NMR** (376 MHz, CDCl₃) δ_F (ppm) = -111.6; **LRMS** (EI, 70 eV) m/z (%) 238 (89) [M⁺], 207 (55), 180 (15), 179 (100), 136 (15), 120 (50), 115 (29), 109 (19); **EA**: calc. (%) for C₁₂H₁₁FO₄, C 60.50, H 4.65; found C 60.45, H 4.69; **IR** (neat): $\tilde{\nu}$ = 2963 (w), 2379 (w), 1718 (s), 1626 (w), 1583 (m), 1351 (m), 1196 (s), 1160 (s); **GC** (achiral phase), 60 kPa He, 50 °C, 0 min, 4 °C/min, 150 °C, 0 min, 10 °C/min, 250 °C, 5 min: t_R = 33.5 min.

(Z)-Dimethyl 2-(4-chlorophenyl)maleate (76n)

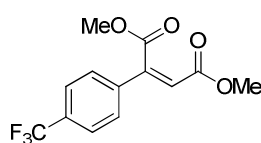


The title compound was prepared according to the procedure followed for the synthesis of dimethyl 2-cyclohexylmaleate (see above) using 4-chlorophenylmagnesium bromide (1 M in diethyl

ether, 12.5 mL, 12.5 mmol, 1.25 eq.) as reagent. The crude material consisted of a 5:1 *Z/E* isomers mixture, which were separated by column chromatography (SiO₂, 3 cm × 33 cm, pentane/EtOAc, 20:1) to afford 205 mg (8% yield) of the title compound as a white solid.

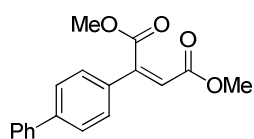
m.p.: 54–57 °C; **R_f**: 0.28 in pentane/EtOAc, 10:1 (visualization: UV, KMnO₄); **¹H NMR** (400 MHz, CDCl₃) δ_{H} (ppm) = 7.42–7.36 (m, 4H), 6.29 (s, 1H), 3.95 (s, 3H), 3.79 (s, 3H); **¹³C NMR** (100 MHz, CDCl₃) δ_{C} (ppm) = 168.1, 165.4, 147.8, 137.0, 131.8, 129.5, 128.2, 117.8, 53.0, 52.3; **LRMS** (EI, 70 eV) m/z (%) 254 (88) [M⁺], 226 (25), 225 (17), 223 (51), 197 (34), 195 (100), 152 (11), 137 (12), 136 (49), 116 (37), 115 (41); **HRMS** (ESI) exact mass calculated for C₁₂H₁₁ClO₄Na [(M+Na)⁺], 277.0238, found 277.0240; **IR** (neat): $\tilde{\nu}$ = 2965 (w), 2371 (w), 1725 (s), 1710 (s), 1624 (m), 1435 (m), 1347 (m), 1196 (s), 1169 (s), 1090 (m), 844 (m), 821 (m); **GC** (achiral phase), 60 kPa He, 50 °C, 0 min, 4 °C/min, 150 °C, 0 min, 10 °C/min, 250 °C, 5 min: t_{R} = 38.3 min.

(*Z*)-Dimethyl 2-(4-(trifluoromethyl)phenyl)maleate (**76o**)



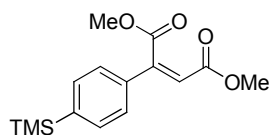
The title compound was prepared according to the procedure followed for the synthesis of dimethyl 2-cyclohexylmaleate (see above) using (4-(trifluoromethyl)phenyl)magnesium bromide (12.5 mmol, 1.25 eq.) as reagent, which was synthesized according to procedure **A**. The crude material consisted of a 5:1 *Z/E* isomers mixture, which were separated by column chromatography (SiO₂, 3 cm × 30 cm, pentane/EtOAc, 19:1) to afford 110 mg (4% yield) of the title compound as a yellow oil.

R_f: 0.47 in pentane/EtOAc, 5:1 (visualization: UV, KMnO₄); **¹H NMR** (400 MHz, CDCl₃) δ_{H} (ppm) = 7.69–7.53 (m, 4H), 6.36 (s, 1H), 3.95 (s, 3H), 3.81 (s, 3H); **¹³C NMR** (100 MHz, CDCl₃) δ_{C} (ppm) = 167.7, 165.1, 147.4, 136.9, 132.4 (q, J_{CF} = 32.9 Hz), 127.3, 126.1 (q, J_{CF} = 3.8 Hz), 123.8 (d, J_{CF} = 272.4 Hz), 119.8, 53.0, 52.4; **¹⁹F NMR** (376 MHz, CDCl₃) = –63.0; **LRMS** (EI, 70 eV) m/z (%) 288 (62) [M⁺], 287 (26), 257 (76), 230 (14), 229 (98), 219 (23), 170 (23), 165 (16), 151 (27), 120 (14); **HRMS** (ESI) exact mass calculated for C₁₃H₁₁O₄F₃Na [(M+Na)⁺], 311.0502, found 311.0506; **IR** (neat): $\tilde{\nu}$ = 2955 (w), 2361 (w), 1722 (s), 1630 (w), 1436 (m), 1322 (s), 1285 (m), 1167 (s), 1115 (s), 1068 (s), 844 (m); **GC** (achiral phase), 60 kPa He, 50 °C, 0 min, 4 °C/min, 150 °C, 0 min, 10 °C/min, 250 °C, 5 min: t_{R} = 34.6 min.

(Z)-Dimethyl 2-[(1,1'-biphenyl)-4-yl]maleate (76p)

The title compound was prepared according to the procedure followed for the synthesis of dimethyl 2-cyclohexylmaleate (see above) using 4-biphenylmagnesium bromide (0.5 M in THF, 24 mL, 12 mmol, 1.2 eq.) as reagent. The crude material consisted of a 6:1 *Z/E* isomers mixture, which were separated by column chromatography (SiO₂, 2 cm × 32 cm, pentane/EtOAc, 12:1) to afford 350 mg (12% yield) of the title compound as a crystalline white solid.

m.p.: 106–110 °C; **R_f:** 0.32 in pentane/EtOAc, 8:1 (visualization: UV, KMnO₄); **¹H NMR** (400 MHz, CDCl₃) δ_{H} (ppm) = 7.66–7.54 (m, 6H), 7.48–7.44 (m, 2H), 7.41–7.37 (m, 1H), 6.37 (s, 1H), 3.98 (s, 3H), 3.81 (s, 3H); **¹³C NMR** (100 MHz, CDCl₃) δ_{C} (ppm) = 168.5, 165.6, 148.7, 143.7, 140.0, 132.1, 129.1, 128.2, 127.8, 127.4, 127.2, 116.8, 52.9, 52.2; **LRMS** (EI, 70 eV) *m/z* (%) 296 (100) [M⁺], 281 (15), 265 (13), 237 (41), 179 (11), 178 (42), 176 (12); **EA:** calc. (%) for C₁₈H₁₆O₄, C 72.96, H 5.44; found C 72.70, H 5.25; **IR** (neat): $\tilde{\nu}$ = 2950 (w), 2361 (w), 1718 (s), 1622 (w), 1431 (w), 1350 (w), 1291 (w), 1196 (s), 1171 (s), 769 (m); **GC** (achiral phase), 100 kPa He, 100 °C, 0 min, 6 °C/min, 250 °C, 10 min: *t_R* = 36.8 min.

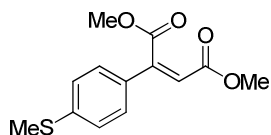
(Z)-Dimethyl 2-(4-(trimethylsilyl)phenyl)maleate (76q)

The title compound was prepared according to the procedure followed for the synthesis of dimethyl 2-cyclohexylmaleate (see above) using (4-(trimethylsilyl)phenyl)magnesium bromide (12.5 mmol, 1.25 eq.) as reagent, which was synthesized according to procedure **A**. The crude material consisted of a 4:1 *Z/E* isomers mixture, which were separated by column chromatography (SiO₂, 2 cm × 33 cm, pentane/EtOAc, 25:1) to afford 155 mg (5% yield) of the title compound as a white solid.

m.p.: 40–42 °C; **R_f:** 0.47 in pentane/EtOAc, 10:1 (visualization: UV, KMnO₄); **¹H NMR** (400 MHz, CDCl₃) δ_{H} (ppm) = 7.57–7.53 (m, 2H), 7.46–7.44 (m, 2H), 6.33 (s, 1H), 3.94 (s, 3H), 3.79 (s, 3H), 0.30 (s, 3H); **¹³C NMR** (100 MHz, CDCl₃) δ_{C} (ppm) = 168.5, 165.6, 149.3, 144.3, 134.1, 133.5, 126.0, 117.1, 52.8, 52.2, –1.2; **LRMS** (EI, 70 eV) *m/z* (%) 292 (12) [M⁺], 278 (20), 277 (100), 230 (14), 229 (98), 219 (23), 170 (23), 165 (16), 151 (27), 120 (14); **HRMS**

(ESI) exact mass calculated for $C_{15}H_{20}O_4SiNa [(M+Na)^+]$, 315.1023, found 315.1024; **IR** (neat): $\tilde{\nu}$ = 2953 (w), 2358 (w), 1721 (s), 1624 (m), 1434 (m), 1353 (m), 1289 (s), 1168 (brs), 991 (m), 842 (s), 818 (s), 760 (m); **GC** (achiral phase), 100 kPa He, 100 °C, 0 min, 6 °C/min, 250 °C, 15 min: t_R = 24.0 min.

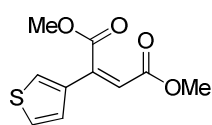
(Z)-Dimethyl 2-(4-(methylthio)phenyl)maleate (76r)



The title compound was prepared according to the procedure followed for the synthesis of dimethyl 2-cyclohexylmaleate (see above) using 4-(methylthio)phenylmagnesium bromide (0.5 M in THF, 24 mL, 12 mmol, 1.2 eq.) as reagent. The crude material consisted of a 10:1 *Z/E* isomers mixture, which were separated by column chromatography (SiO_2 , 3 cm \times 29 cm, pentane/EtOAc, 12:1) to afford 401 mg (15% yield) of the title compound as a pink solid.

m.p.: 63–65 °C; **R_f**: 0.35 in pentane/EtOAc, 5:1 (visualization: UV, $KMnO_4$); **¹H NMR** (400 MHz, $CDCl_3$) δ_H (ppm) = 7.39–7.37 (m, 2H), 7.24–7.21 (m, 2H), 6.28 (s, 1H), 3.94 (s, 3H), 3.78 (s, 3H), 2.49 (s, 3H); **¹³C NMR** (100 MHz, $CDCl_3$) δ_C (ppm) = 168.5, 165.7, 148.6, 142.9, 129.4, 127.2, 126.1, 115.8, 52.9, 52.1, 15.2; **LRMS** (EI, 70 eV) m/z (%) 266 (100) [M^+], 208 (12), 207 (37), 148 (23), 147 (11), 133 (11), 115 (12), 89 (14); **EA:** calc. (%) for $C_{13}H_{14}O_4S$, C 58.63, H 5.30; found C 58.65, H 5.34; **IR** (neat): $\tilde{\nu}$ = 2956 (w), 2349 (w), 1727 (m), 1708 (s), 1587 (m), 1434 (w), 1354 (w), 1169 (m), 1091 (m), 993 (w), 843 (w), 817 (w); **GC** (achiral phase), 60 kPa He, 50 °C, 0 min, 4 °C/min, 150 °C, 0 min, 10 °C/min, 250 °C, 5 min: t_R = 36.7 min.

(Z)-Dimethyl 2-(thiophen-3-yl)maleate (76s)



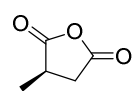
In a flame-dried argon flushed two-neck round bottom flask a solution of 3-bromothiophene (0.62 mL, 6.6 mmol, 1.1 eq.) in THF (6 mL) and isopropylmagnesium chloride-lithium chloride complex solution (1.3 M in THF, 4.6 mL, 6 mmol, 1.0 eq.) were added. After stirring for 2 h at rt, the reaction mixture was cooled at –40 °C, and a solution of cuprous bromide-dimethylsulfide complex (1.23 g, 6 mmol, 1.0 eq.) in THF (6 mL) was added, causing the mixture's color to turn from white to dark brown. The reaction mixture was allowed to stir for 2 h, prior to addition of

a solution of dimethylacetylenedicarboxylate (0.74 mL, 6 mmol, 1.0 eq.) in THF (4 mL) at $-78\text{ }^{\circ}\text{C}$. The resulting black mixture was then allowed to warm up to rt overnight. The reaction was then quenched with NH_4Cl (sat. aq., 10 mL) the layers were separated and the aqueous phase was extracted with MTBE (3×15 mL). The combined organic layers were washed with brine, dried over Na_2SO_4 , filtered and concentrated *in vacuo*. The crude material consisted of a 7.5:1 *Z/E* isomers mixture, which were separated by column chromatography (SiO_2 , 3 cm × 30 cm, pentane/EtOAc, 15:1) to afford 190 mg (13% yield) of the title compound as a pale yellow solid.

m.p.: 40–42 $^{\circ}\text{C}$; **R_f:** 0.22 in pentane/EtOAc, 10:1 (visualization: UV, KMnO_4); **^1H NMR** (400 MHz, CDCl_3) δ_{H} (ppm) = 7.47–7.44 (m, 1H) 7.38–7.34 (m, 1H), 7.26–7.22 (m, 1H), 6.24 (s, 1H), 3.95 (s, 3H), 3.77 (s, 3H); **^{13}C NMR** (100 MHz, CDCl_3) δ_{C} (ppm) = 168.4, 165.8, 143.6, 135.3, 127.4, 127.1, 125.1, 115.6, 52.9, 52.2; **LRMS** (EI, 70 eV) m/z (%) 226 (33) [M^+], 195 (16), 168 (12), 167 (100), 108 (18); **HRMS** (ESI) exact mass calculated for $\text{C}_{10}\text{H}_{10}\text{O}_4\text{SNa}$ [$(\text{M}+\text{Na})^+$], 249.0192 found 249.0195; **IR** (neat): $\tilde{\nu}$ = 3116 (s), 3089 (s), 2946 (w), 2360 (w), 1724 (s), 1710 (s), 1617 (m), 1432 (m), 1328 (m), 1279 (m), 1234 (m), 1194 (m), 1164 (s), 1012 (m), 963 (w), 923 (w), 879 (w), 857 (m), 804 (s), 681 (s); **GC** (achiral phase), 60 kPa He, 50 $^{\circ}\text{C}$, 0 min, 4 $^{\circ}\text{C}/\text{min}$, 150 $^{\circ}\text{C}$, 0 min, 10 $^{\circ}\text{C}/\text{min}$, 250 $^{\circ}\text{C}$, 5 min: t_{R} = 36.4 min.

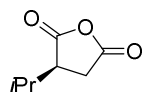
6.3.3 Analytical data of the hydrogenation products

(*R*)-(+)-3-Methyldihydrofuran-2,5-dione (74a)



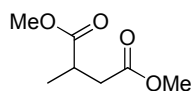
Appearance: colorless liquid; **m.p.:** 38–39 $^{\circ}\text{C}$; **^1H NMR** (400 MHz, CDCl_3) 3.24–3.10 (m, 2H), 2.70–2.53 (m, 1H), 1.46 (d, J = 7.0 Hz, 3H); **^{13}C NMR** (100 MHz, CDCl_3) δ_{C} (ppm) 174.4, 169.9, 36.2, 35.7, 16.4; **IR** (neat): $\tilde{\nu}$ = 2961 (w), 2365 (w), 1771 (m), 1693 (m), 1405 (m), 1219 (bm), 1062 (w); **GC** (achiral phase), 60 kPa He, 50 $^{\circ}\text{C}$, 0 min, 1 $^{\circ}\text{C}/\text{min}$, 150 $^{\circ}\text{C}$, 0 min, 10 $^{\circ}\text{C}/\text{min}$, 250 $^{\circ}\text{C}$, 5 min: t_{R} = 58.2 min; **GC** (chiral phase, *Macherey-Nagel*, Capillary column, Lipodex E (25 m × 0.25 mm × 0.25 μm), 60 kPa H_2 , 70 $^{\circ}\text{C}$, 0 min, 1 $^{\circ}\text{C}/\text{min}$, 145 $^{\circ}\text{C}$, 0 min, 20 $^{\circ}\text{C}/\text{min}$, 180 $^{\circ}\text{C}$, 5 min): t_{R} = **41.5 min (*R*, +)**, t_{R} = 44.4 min (*S*, –), 90% *ee*; **$[\alpha]_{\text{D}}^{20}$** +25.2 (c = 0.40, CHCl_3).

The ^1H and ^{13}C NMR data were consistent with the literature data.^[103]

(R)-(+)-3-Isopropylidihydrofuran-2,5-dione (74c)

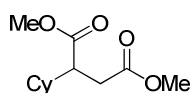
Appearance: colorless liquid; $^1\text{H NMR}$ (400 MHz, CDCl_3) 3.07 (1H, ddd, $J = 10.2, 5.5, 4.8$ Hz), 2.97 (1H, dd, $J = 18.7, 10.0$ Hz), 2.73 (1H, dd, $J = 18.7, 5.6$ Hz), 2.37–2.25 (1H, m), 1.05 (3H, d, $J = 6.9$ Hz), 0.99 (3H, t, $J = 7.9$ Hz); $^{13}\text{C NMR}$ (100 MHz, CDCl_3) δ_{C} (ppm) 173.0, 170.4, 46.9, 30.8, 29.4, 19.9, 18.2; **LRMS** (EI, 70 eV) m/z (%) 127 (2) [(M–Me) $^+$], 100 (34), 97 (14), 70 (77), 55 (100), 43 (17), 42 (29), 41 (24); **IR** (neat): $\tilde{\nu} = 2966$ (w), 1859 (w), 1773 (s), 1690 (m), 1469 (w), 1258 (w), 1190 (w), 1061 (m), 913 (s), 895 (s), 728 (m); **GC** (achiral phase), 60 kPa He, 50 °C, 0 min, 2 °C/min, 120 °C, 0 min, 10 °C/min, 250 °C, 5 min: $t_{\text{R}} = 41.3$ min; **GC** (chiral phase, *Macherey-Nagel*, Capillary column, Lipodex E (25 m \times 0.25 mm \times 0.25 μm), 80 kPa He, 70 °C, 0 min, 0.2 °C/min, 110 °C, 0 min, 10 °C/min, 180 °C, 5 min): $t_{\text{R}} = 145.1$ min (**R, +**), $t_{\text{R}} = 151.8$ min (**S, –**), 90% *ee*; $[\alpha]_{\text{D}}^{20} +15.8$ ($c = 0.80$, CHCl_3).

The ^1H and ^{13}C NMR data were consistent with the literature data.^[191]

(+)-Dimethyl 2-methylsuccinate (77a)

Appearance: colorless liquid; $^1\text{H NMR}$ (400 MHz, CDCl_3) δ_{H} (ppm) = 3.70 (s, 3H), 3.68 (s, 3H), 2.99–2.87 (m, 1H), 2.74 (dd, $J = 16.5, 8.1$ Hz, 1H), 2.41 (dd, $J = 16.5, 6.1$ Hz, 1H), 1.22 (d, $J = 7.2$ Hz, 3H); $^{13}\text{C NMR}$ (100 MHz, CDCl_3) δ_{C} (ppm) 175.9, 172.5, 52.1, 51.9, 37.6, 35.9, 17.2; **LRMS** (EI, 70 eV) m/z (%) 129 (63) [(M–MeO) $^+$], 128 (41), 101 (35), 100 (31), 87 (18), 69 (20); **IR** (neat): $\tilde{\nu} = 2960$ (w), 2358 (w), 1718 (s), 1370 (w), 1204 (w), 1150 (s), 1004 (w); **GC** (achiral phase), 60 kPa He, 50 °C, 0 min, 4 °C/min, 150 °C, 0 min, 10 °C/min, 250 °C, 5 min: $t_{\text{R}} = 18.8$ min; **GC** (chiral phase, *Chiraldex G-TA*, γ -cyclodextrin TFA column (30 m \times 0.25 mm \times 0.25 μm), 80 kPa He, 50 °C, 0 min, 1 °C/min, 90 °C, 0 min, 10 °C/min, 160 °C, 5 min): $t_{\text{R}} = 34.2$ min (–), $t_{\text{R}} = 35.3$ min (+), 98% *ee*; $[\alpha]_{\text{D}}^{20} = +5.8$ ($c = 1.00$, CHCl_3).

The ^1H and ^{13}C NMR data were consistent with the literature data.^[189,192]

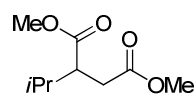
(+)-Dimethyl 2-cyclohexylsuccinate (77b)

Appearance: colorless liquid; $^1\text{H NMR}$ (400 MHz, CDCl_3) δ_{H} (ppm) = 3.69 (s, 3H) 3.66 (s, 3H), 2.68–2.77 (m, 2H), 2.44–2.49 (m, 1H), 1.75–1.56 (m,

6H), 1.25–1.00 (m, 5H); **¹³C NMR** (100 MHz, CDCl₃) δ_c (ppm) = 175.1, 173.2, 51.9, 51.8, 47.2, 40.1, 33.4, 30.8, 30.3, 26.4, 26.3; **LRMS** (EI, 70 eV) m/z (%) 197 (14) [(M–MeO)⁺], 155 (20), 146 (91), 137 (13), 114 (100), 95 (15), 87 (12); **IR** (neat): $\tilde{\nu}$ = 2926 (m), 2853 (w), 2360 (s), 1728 (s), 1435 (w), 1159 (s); **GC** (achiral phase), 60 kPa He, 50 °C, 0 min, 2 °C/min, 120 °C, 0 min, 10 °C/min, 250 °C, 5 min: t_R = 46.7 min; **GC** (chiral phase, *Brexbühler SE54* β -cyclodextrin DETButSil (25 m \times 0.25 mm \times 0.25 μ m)) 80 kPa H₂, 60 °C, 0 min, 1 °C/min, 130 °C, 0 min, 20 °C/min, 160 °C, 5 min: t_R = **63.4 min (+)**, t_R = 63.8 min (–), 99% *ee*; $[\alpha]_D^{20}$ = +22.9 (c = 1.00, CHCl₃).

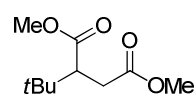
The ¹H and ¹³C NMR data were consistent with the literature data.^[193]

(+)-Dimethyl 2-isopropylsuccinate (76c)



Appearance: colorless liquid; **¹H NMR** (400 MHz, CDCl₃) δ_H (ppm) = 3.70 (s, 3H), 3.67 (s, 3H), 2.76–2.71 (m, 2H), 2.46–2.38 (m, 1H), 2.03–1.93 (m, 1H), 0.93 (d, J = 5.8 Hz, 3H), 0.92 (d, J = 5.8 Hz, 3H); **¹³C NMR** (100 MHz, CDCl₃) δ_c (ppm) = 175.1, 173.1, 51.9, 51.8, 47.6, 33.1, 30.3, 20.2, 19.7; **LRMS** (EI, 70 eV) m/z (%) 157 (34) [(M–MeO)⁺], 146 (40), 128 (12), 115 (46), 114 (100), 113 (14), 97 (33), 87 (27), 83 (15); **HRMS** (ESI) exact mass calculated for C₉H₁₆O₄Na [(M+Na)⁺], 211.0941, found 211.0941; **IR** (neat): $\tilde{\nu}$ = 2960 (w), 1731 (s), 1463 (w), 1437 (m), 1371 (w), 1253 (m), 1160 (s), 1000 (w), 846 (w); **GC** (achiral phase), 60 kPa He, 50 °C, 0 min, 4 °C/min, 150 °C, 0 min, 10 °C/min, 250 °C, 5 min: t_R = 24.1 min; **GC** (chiral phase, *Chiraldex G-TA*, γ -cyclodextrin TFA column (30 m \times 0.25 mm \times 0.25 μ m), 80 kPa He, 50 °C, 0 min, 1 °C/min, 105 °C, 0 min, 10 °C/min, 160 °C, 5 min): t_R = 47.0 min (–), t_R = **48.2 min (+)**, 99% *ee*; $[\alpha]_D^{20}$ = +13.7 (c = 0.80, CHCl₃).

(+)-Dimethyl 2-(*tert*-butyl)succinate (76d)

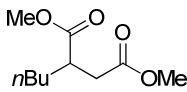


Appearance: colorless oil; **¹H NMR** (400 MHz, CDCl₃) δ_H (ppm) = 3.69 (s, 3H), 3.66 (s, 3H), 2.79 (dd, J = 16.5, 11.8 Hz, 1H), 2.64 (dd, J = 11.8, 3.0 Hz, 1H), 2.48 (dd, J = 16.5, 3.0 Hz, 1H), 0.96 (s, 9H); **¹³C NMR** (100 MHz, CDCl₃) δ_c (ppm) = 174.9, 173.3, 51.9, 51.5, 51.4, 32.8 (2C), 27.9; **LRMS** (EI, 70 eV) m/z (%) 171 (18) [(M–MeO)⁺], 155 (22), 146 (55), 114 (100), 95 (10), 87 (11), 85 (15), 83 (14); **IR** (neat): $\tilde{\nu}$ = 2955 (w), 2362 (w), 1728 (s), 1370 (w), 1207 (w), 1155 (s), 1004 (w); **GC** (achiral phase), 60 kPa He, 50 °C, 0 min, 2 °C/min, 120 °C, 0 min, 10 °C/min, 250 °C, 5 min: t_R = 39.1 min; **GC** (chiral

phase, *Brechbühler SE54* β -cyclodextrin DETButSil (25 m \times 0.25 mm \times 0.25 μ m)) 80 kPa H_2 , 60 $^{\circ}C$, 0 min, 1 $^{\circ}C/min$, 90 $^{\circ}C$, 0 min, 10 $^{\circ}C/min$, 160 $^{\circ}C$, 5 min): t_R = **26.4 min (+)**, t_R = 26.6 min (–), 98% *ee*; $[\alpha]_D^{20}$ = +13.8 (c = 1.00, $CHCl_3$).

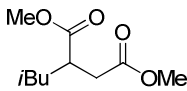
The 1H and ^{13}C NMR data were consistent with the literature data.^[192]

(+)-Dimethyl 2-butylsuccinate (76e)

 **Appearance:** pale yellow liquid; 1H NMR (400 MHz, $CDCl_3$) δ_H (ppm) = 3.72 (s, 3H), 3.70 (s, 3H), 2.92–2.81 (m, 1H), 2.74 (dd, J = 16.4, 9.3 Hz, 1H), 2.46 (dd, J = 16.4, 5.1 Hz, 1H), 1.74–1.61 (m, 1H), 1.61–1.47 (m, 1H), 1.41–1.21 (m, 4H), 0.91 (t, J = 7.0 Hz, 3H); ^{13}C NMR (100 MHz, $CDCl_3$) δ_C (ppm) = 175.7, 172.6, 51.9, 51.9, 41.3, 36.0, 31.8, 29.2, 22.6, 14.0; **LRMS** (EI, 70 eV) m/z (%) 171 (33) $[(M-MeO)^+]$, 146 (46), 138 (20), 129 (71), 127 (13), 114 (100), 111 (34), 110 (24), 101 (10), 97 (11), 87 (18), 83 (27); **IR** (neat): $\tilde{\nu}$ = 2954 (w), 2862 (w), 1730 (s), 1437 (w), 1160 (brs); **GC** (achiral phase), 60 kPa He , 50 $^{\circ}C$, 0 min, 2 $^{\circ}C/min$, 120 $^{\circ}C$, 0 min, 10 $^{\circ}C/min$, 250 $^{\circ}C$, 5 min: t_R = 41.2 min; **GC** (chiral phase, *Chiraldex G-TA*, γ -cyclodextrin TFA column (30 m \times 0.25 mm \times 0.25 μ m), 60 kPa He , 50 $^{\circ}C$, 0 min, 1 $^{\circ}C/min$, 120 $^{\circ}C$, 0 min, 10 $^{\circ}C/min$, 160 $^{\circ}C$, 5 min): t_R = **62.1 min (–)**, t_R = 62.9 min (+), 95% *ee*; $[\alpha]_D^{20}$ = +13.2 (c = 1.00, $CHCl_3$).

The 1H and ^{13}C NMR data were consistent with the literature data.^[192]

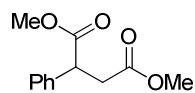
(+)-Dimethyl 2-isobutylsuccinate (76f)

 **Appearance:** colorless liquid; 1H NMR (400 MHz, $CDCl_3$) δ_H (ppm) = 3.69 (s, 3H), 3.67 (s, 3H), 2.96–2.84 (m, 1H), 2.69 (dd, J = 16.5, 9.4 Hz, 1H), 2.42 (dd, J = 16.5, 5.0 Hz, 1H), 1.65–1.50 (m, 2H), 1.37–1.20 (m, 1H), 0.92 (d, J = 6.2 Hz, 3H), 0.89 (d, J = 6.2 Hz, 3H); ^{13}C NMR (100 MHz, $CDCl_3$) δ_C (ppm) = 176.0, 172.6, 52.0, 51.9, 41.4, 39.6, 36.5, 26.0, 22.7, 22.4; **LRMS** (EI, 70 eV) m/z (%) 171 (26) $[(M-OMe)^+]$, 146 (42), 129 (53), 127 (34), 114 (100), 111 (24), 87 (15), 85 (16); **EA:** calc. (%) for $C_{10}H_{18}O_4$, C 59.39, H 8.97; found C 59.05, H 8.89; **IR** (neat): $\tilde{\nu}$ = 2956 (w), 2356 (w), 1733 (s), 1440 (w), 1239 (w), 1161 (s), 1045 (w); **GC** (achiral phase), 60 kPa He , 50 $^{\circ}C$, 0 min, 4 $^{\circ}C/min$, 150 $^{\circ}C$, 0 min, 10 $^{\circ}C/min$, 250 $^{\circ}C$, 5 min: t_R = 26.2 min; **GC** (chiral phase, *Chiraldex G-TA*, γ -cyclodextrin TFA column (30 m \times 0.25 mm \times 0.25 μ m), 60 kPa He , 50 $^{\circ}C$, 0 min, 1 $^{\circ}C/min$,

135 °C, 0 min, 10 °C/min, 160 °C, 5 min): t_R = 56.1 min (–), t_R = **57.0 min (+)**, 94% *ee*; $[\alpha]_D^{20}$ = +17.3 (c = 1.00, CHCl₃).

The ¹H and ¹³C NMR data were consistent with the literature data.^[192]

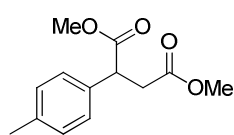
(+)-Dimethyl 2-phenylsuccinate (77g)



Appearance: white crystalline solid; **m.p.:** 53–55 °C; **¹H NMR** (400 MHz, CDCl₃) δ_H (ppm) = 7.35–7.25 (m, 5H), 4.09 (dd, J = 10.1, 5.2 Hz, 1H), 3.68 (s, 3H), 3.67 (s, 3H), 3.21 (dd, J = 17.0, 10.1 Hz, 1H), 2.67 (dd, J = 17.0, 5.3 Hz, 1H); **¹³C NMR** (100 MHz, CDCl₃) δ_C (ppm) = 173.6, 172.1, 137.8, 129.0, 127.9, 127.8, 52.5, 52.0, 47.2, 37.8; **LRMS** (EI, 70 eV) m/z (%) 191 (17) [(M–OMe)⁺], 190 (72), 163 (23), 162 (80), 131 (13), 121 (100), 104 (22), 103 (34), 91 (14); **IR** (neat): $\tilde{\nu}$ = 2958 (w), 2362 (w), 1724 (s), 1434 (m), 1307 (m), 1150 (m), 994 (m), 868 (w), 726 (w); **GC** (achiral phase), 60 kPa He, 50 °C, 0 min, 4 °C/min, 150 °C, 0 min, 10 °C/min, 250 °C, 5 min: t_R = 33.4 min; **GC** (chiral phase, *Brechbühler SE54* β -cyclodextrin DETButSil (25 m \times 0.25 mm \times 0.25 μ m)) 80 kPa He, 60 °C, 0 min, 1 °C/min, 150 °C, 0 min, 20 °C/min, 160 °C, 5 min): t_R = **63.0 min (+)**, t_R = 63.6 min (–), 95% *ee*; $[\alpha]_D^{20}$ = +110.7 (c = 1.00, CHCl₃).

The ¹H and ¹³C NMR data were consistent with the literature data.^[192,194]

(+)-Dimethyl 2-(*p*-tolyl)succinate (77h)

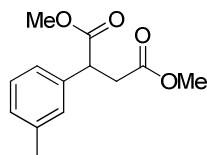


Appearance: white crystalline solid; **m.p.:** 29–31 °C; **¹H NMR** (400 MHz, CDCl₃) δ_H (ppm) = 7.20–7.10 (m, 4H), 4.06 (dd, J = 10.1, 5.3 Hz, 1H), 3.67 (6H, s), 3.19 (dd, J = 16.9, 10.1 Hz, 1H), 2.65 (dd, J = 16.9, 5.3 Hz, 1H), 2.32 (3H, s); **¹³C NMR** (100 MHz, CDCl₃) δ_C (ppm) = 173.7, 172.2, 137.6, 134.8, 129.7, 127.7, 52.5, 52.0, 46.8, 37.8, 21.2; **LRMS** (EI, 70 eV) m/z (%) 236 (1) [M⁺], 205 (12), 204 (65), 177 (28), 176 (90), 136 (11), 135 (100), 118 (16), 117 (42), 115 (14), 91 (17); **HRMS** (ESI) exact mass calculated for C₁₃H₁₆O₄Na [(M+Na)⁺], 259.0941, found 259.0943; **IR** (neat): $\tilde{\nu}$ = 2953 (w), 2361 (w), 1725 (s), 1512 (w), 1433 (m), 1302 (s), 1196 (w), 1149 (s), 995 (m), 868 (m), 783 (m); **GC** (achiral phase), 60 kPa He, 50 °C, 0 min, 4 °C/min, 150 °C, 0 min, 10 °C/min, 250 °C, 5 min: t_R = 34.9 min; **GC** (chiral phase, *ChiralDEX G-TA*, γ -cyclodextrin TFA column (30 m \times 0.25 mm \times 0.25 μ m), 90 kPa He, 60 °C, 0 min, 1 °C/min,

150 °C, 0 min, 10 °C/min, 160 °C, 5 min): t_R = 86.7 min (–), t_R = **87.2 min (+)**, 96% *ee*; $[\alpha]_D^{20}$ = +136.3 (c = 1.00, CHCl₃).

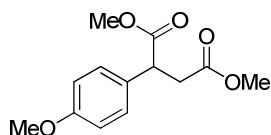
The ¹H and ¹³C NMR data were consistent with the literature data.^[194]

(+)-Dimethyl 2-(*m*-tolyl)succinate (**77i**)



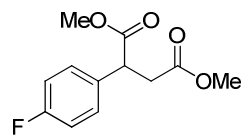
Appearance: colorless liquid; ¹H NMR (400 MHz, CDCl₃) δ_H (ppm) = 7.24–7.18 (m, 1H), 7.12–7.02 (m, 3H), 4.05 (dd, J = 10.2, 5.1 Hz, 1H), 3.679 (s, 3H), 3.676 (s, 3H), 3.20 (1H, dd, J = 17.0, 10.2 Hz), 2.65 (1H, dd, J = 17.0, 5.1 Hz), 2.34 (3H, s); ¹³C NMR (100 MHz, CDCl₃) δ_C (ppm) = 173.7, 172.2, 138.8, 137.7, 128.9, 128.6, 128.5, 124.9, 52.5, 52.0, 47.2, 37.8, 21.5; **LRMS** (EI, 70 eV) m/z (%) 236 (2) [M⁺], 205 (26), 204 (83), 177 (21), 176 (98), 145 (11), 136 (11), 135 (100), 118 (18), 117 (44), 115 (16), 91 (18); **HRMS** (ESI) exact mass calculated for C₁₃H₁₆O₄Na [(M+Na)⁺], 259.0941, found 259.0941; **IR** (neat): $\tilde{\nu}$ = 2952 (w), 1731 (s), 1607 (w), 1435 (m), 1260 (m), 1152 (brs), 1004 (w), 886 (w), 785 (w); **GC** (achiral phase), 60 kPa He, 50 °C, 0 min, 4 °C/min, 150 °C, 0 min, 10 °C/min, 250 °C, 5 min: t_R = 34.7 min; **HPLC** (chiral, Daicel Chiracel OD-H, 0.46 cm × 25 cm, *n*-heptane/isopropanol 92:8, 1.0 mL/min, 20 °C): t_R = **8.5 min (+)**, t_R = 12.5 min (–), 96% *ee*; $[\alpha]_D^{20}$ = +123.2 (c = 1.00, CHCl₃).

(+)-Dimethyl 2-(4-methoxyphenyl)succinate (**77k**)



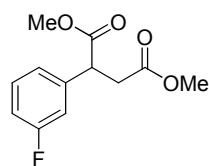
Appearance: colorless liquid; ¹H NMR (400 MHz, CDCl₃) δ_H (ppm) = 7.23–7.17 (m, 2H), 6.88–6.82 (m, 2H), 4.04 (dd, J = 9.9, 5.5 Hz, 1H), 3.79 (s, 3H), 3.670 (s, 3H), 3.666 (s, 3H), 3.17 (dd, J = 16.9, 10.0 Hz, 1H), 2.65 (dd, J = 16.9, 5.5 Hz, 1H); ¹³C NMR (100 MHz, CDCl₃) δ_C (ppm) = 173.8, 172.2, 159.2, 129.9, 128.9, 114.4, 55.4, 52.5, 52.0, 46.4, 37.9; **LRMS** (EI, 70 eV) m/z (%) 252 (5) [M⁺], 220 (41), 193 (36), 192 (100), 134 (21), 133 (22), 119 (10), 91 (15); **IR** (neat): $\tilde{\nu}$ = 2953 (w), 2361 (w), 1728 (s), 1513 (m), 1245 (m), 1156 (brs), 1031 (m); **GC** (achiral phase), 60 kPa He, 50 °C, 0 min, 4 °C/min, 150 °C, 0 min, 10 °C/min, 250 °C, 5 min: t_R = 37.6 min; **HPLC** (chiral, Daicel Chiracel OJ, 0.46 cm × 25 cm, *n*-heptane/isopropanol 92:8, 1.0 mL/min, 20 °C): t_R = 36.8 min (–), t_R = **42.4 min (+)**, 95% *ee*; $[\alpha]_D^{20}$ = +112.3 (c = 0.50, CHCl₃).

The ¹H and ¹³C NMR data were consistent with the literature data.^[194]

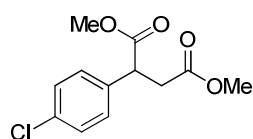
(+)-Dimethyl 2-(4-fluorophenyl)succinate (77l)

Appearance: colorless oil; $^1\text{H NMR}$ (400 MHz, CDCl_3) δ_{H} (ppm) = 7.31–7.26 (m, 2H), 7.07–7.00 (m, 2H), 4.10 (dd, J = 9.7, 5.6 Hz, 1H), 3.71 (s, 3H), 3.69 (s, 3H), 3.20 (dd, J = 16.9, 9.8 Hz, 1H), 2.69 (dd, J = 16.9, 5.6 Hz, 1H); $^{13}\text{C NMR}$ (100 MHz, CDCl_3) δ_{C} (ppm) = 173.4, 171.9, 162.4 (d, J_{CF} = 246.4 Hz), 133.5 (d, J_{CF} = 3.3 Hz), 129.5 (d, J_{CF} = 8.1 Hz), 115.8 (d, J_{CF} = 21.5 Hz), 52.6, 52.1, 46.5, 37.8; $^{19}\text{F NMR}$ (376 MHz, CDCl_3) δ_{F} (ppm) = –114.6; **LRMS** (EI, 70 eV) m/z (%) 209 (13) [(M–OMe) $^+$], 208 (71), 181 (29), 180 (80), 140 (11), 139 (100), 122 (23), 121 (29), 109 (11), 101 (13); **IR** (neat): $\tilde{\nu}$ = 2954 (w), 1730 (s), 1605 (w), 1508 (s), 1437 (m), 1224 (m), 1156 (brs), 1006 (m), 836 (m), 807 (m); **GC** (achiral phase), 60 kPa He, 50 °C, 0 min, 4 °C/min, 150 °C, 0 min, 10 °C/min, 250 °C, 5 min: t_{R} = 33.3 min; **GC** (chiral phase, *ChiralDEX G-TA*, γ -cyclodextrin TFA column (30 m \times 0.25 mm \times 0.25 μm), 80 kPa He, 80 °C, 0 min, 1 °C/min, 145 °C, 0 min, 10 °C/min, 160 °C, 5 min): t_{R} = 58.7 min (–), t_{R} = **59.1 min (+)**, 95% *ee*; $[\alpha]_{\text{D}}^{20}$ = +103.0 (c = 1.00, CHCl_3).

The ^1H and ^{13}C NMR data were consistent with the literature data.^[194]

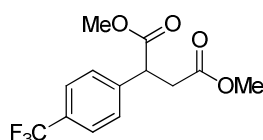
(+)-Dimethyl 2-(3-fluorophenyl)succinate (77m)

Appearance: white crystalline solid; **m.p.:** 31–32 °C; $^1\text{H NMR}$ (400 MHz, CDCl_3) δ_{H} (ppm) = 7.33–7.26 (m, 1H), 7.08–6.94 (m, 3H), 4.09 (dd, J = 9.9, 5.5 Hz, 1H), 3.69 (s, 3H), 3.68 (s, 3H), 3.18 (dd, J = 17.0, 9.9 Hz, 1H), 2.67 (dd, J = 17.0, 10.0 Hz, 1H); $^{13}\text{C NMR}$ (100 MHz, CDCl_3) δ_{C} (ppm) = 173.0, 171.8, 163.1 (d, J_{CF} = 246.8 Hz), 140.1 (d, J_{CF} = 7.4 Hz), 130.5 (d, J_{CF} = 8.3 Hz), 123.6 (d, J_{CF} = 3.0 Hz), 115.0 (d, J_{CF} = 14.1 Hz), 114.8 (d, J_{CF} = 13.1 Hz), 52.7, 52.1, 46.9, 37.6; $^{19}\text{F NMR}$ (376 MHz, CDCl_3) δ_{F} (ppm) = –112.2; **LRMS** (EI, 70 eV) m/z (%) 209 (23) [(M–OMe) $^+$], 208 (41), 180 (69), 139 (100), 122 (23), 121 (24), 109 (11), 101 (14); **EA:** calc. (%) for $\text{C}_{12}\text{H}_{13}\text{FO}_4$, C 60.00, H 5.45; found C 59.64, H 5.56; **IR** (neat): $\tilde{\nu}$ = 2951 (w), 2360 (w), 1729 (s), 1590 (m), 1437 (m), 1158 (brs), 1007 (w); **GC** (achiral phase), 60 kPa He, 50 °C, 0 min, 4 °C/min, 150 °C, 0 min, 10 °C/min, 250 °C, 5 min: t_{R} = 33.3 min; **GC** (chiral phase, *Brechbühler SE54* β -cyclodextrinDEtTButSil (25 m \times 0.25 mm \times 0.25 μm)) 80 kPa H_2 , 80 °C, 0 min, 1 °C/min, 130 °C, 0 min, 20 °C/min, 180 °C, 5 min): t_{R} = **47.4 min (+)**, t_{R} = 48.2 min (–), 95% *ee*; $[\alpha]_{\text{D}}^{20}$ = +119.0 (c = 1.00, CHCl_3).

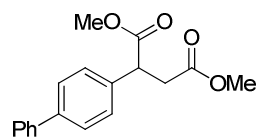
(+)-Dimethyl 2-(4-chlorophenyl)succinate (77n)

Appearance: colorless oil; $^1\text{H NMR}$ (400 MHz, CDCl_3) δ_{H} (ppm) = 7.33–7.27 (m, 2H), 7.24–7.19 (m, 2H), 4.07 (dd, $J = 9.7, 5.6$ Hz, 1H), 3.68 (s, 3H), 3.67 (s, 3H), 3.17 (dd, $J = 16.9, 9.7$ Hz, 1H), 2.66 (dd, $J = 16.9, 5.6$ Hz, 1H); $^{13}\text{C NMR}$ (100 MHz, CDCl_3) δ_{C} (ppm) = 173.2, 171.8, 136.3, 133.8, 129.3, 129.2, 52.6, 52.1, 46.6, 37.6; **LRMS** (EI, 70 eV) m/z (%) 256 (1) [M^+], 226 (21), 225 (12), 224 (63), 199 (11), 198 (36), 197 (33), 196 (100), 157 (28), 155 (87), 139 (12), 138 (22), 137 (23), 103 (22), 102 (12); **IR** (neat): $\tilde{\nu} = 2952$ (w), 1730 (s), 1491 (m), 1436 (m), 1156 (brs), 1090 (m), 1010 (m), 847 (m), 764 (m); **GC** (achiral phase), 60 kPa He, 50 °C, 0 min, 4 °C/min, 150 °C, 0 min, 10 °C/min 250 °C, 5 min: $t_{\text{R}} = 36.4$ min; **HPLC** (chiral, Daicel Chiracel OD-H, 0.46 cm \times 25 cm, *n*-heptane/isopropanol 98:2, 1.0 mL/min, 20 °C): $t_{\text{R}} = 9.1$ min (+), $t_{\text{R}} = 12.3$ min (–), 93% *ee*; $[\alpha]_{\text{D}}^{20} = +114.1$ ($c = 1.00$, CHCl_3).

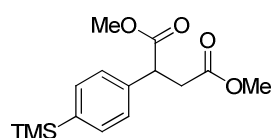
The ^1H and ^{13}C NMR data were consistent with the literature data.^[194]

(+)-Dimethyl 2-(4-(trifluoromethyl)phenyl)succinate (77o)

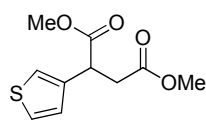
Appearance: white crystalline solid; **m.p.:** 32–33 °C; $^1\text{H NMR}$ (400 MHz, CDCl_3) δ_{H} (ppm) = 7.59 (d, $J = 8.1$ Hz, 2H), 7.41 (d, $J = 8.1$ Hz, 2H), 4.16 (dd, $J = 9.6, 5.7$ Hz, 1H), 3.69 (s, 3H), 3.68 (s, 3H), 3.21 (dd, $J = 17.0, 9.6$ Hz, 1H), 2.69 (dd, $J = 17.0, 5.7$ Hz, 1H); $^{13}\text{C NMR}$ (100 MHz, CDCl_3) δ_{C} (ppm) = 172.7, 171.5, 141.6 (q, $J_{\text{CF}} = 1.3$ Hz), 130.1 (q, $J_{\text{CF}} = 32.6$ Hz), 128.3, 125.9 (q, $J_{\text{CF}} = 3.8$ Hz), 125.4, 52.7, 52.2, 47.1, 37.5; $^{19}\text{F NMR}$ (376 MHz, CDCl_3) δ_{F} (ppm) = –62.7; **LRMS** (EI, 70 eV) m/z (%) 259 (21) [($\text{M}-\text{OMe}$) $^+$], 258 (75), 231 (18), 230 (76), 199 (16), 189 (100), 172 (19), 171 (21), 151 (12), 103 (11); **HRMS** (ESI) exact mass calculated for $\text{C}_{13}\text{H}_{13}\text{O}_4\text{F}_3\text{Na}$ [($\text{M}+\text{Na}$) $^+$], 313.0658, found 313.0662; **IR** (neat): $\tilde{\nu} = 2962$ (w), 2360 (w), 1730 (s), 1618 (w), 1438 (m), 1327 (brs), 1304 (s), 1151 (s), 1108 (s), 1068 (m), 991 (m), 869 (m), 843 (m), 815 (w); **GC** (achiral phase), 60 kPa He, 50 °C, 0 min, 4 °C/min, 150 °C, 0 min, 10 °C/min, 250 °C, 5 min: $t_{\text{R}} = 33.0$ min; **HPLC** (chiral, Daicel Chiracel OD-H, 0.46 cm \times 25 cm, *n*-heptane/isopropanol 99:1, 1.0 mL/min, 20 °C): $t_{\text{R}} = 11.3$ min (+), $t_{\text{R}} = 13.8$ min (–), 93% *ee*; $[\alpha]_{\text{D}}^{20} = +108.5$ ($c = 1.00$, CHCl_3).

(+)-Dimethyl 2-[(1,1'-biphenyl)-4-yl]succinate (77p)

Appearance: white crystalline solid; **m.p.** = 97–99 °C; **¹H NMR** (400 MHz, CDCl₃) δ_{H} (ppm) = 7.61–7.52 (m, 4H), 7.47–7.40 (m, 2H), 7.39–7.30 (m, 3H), 4.15 (dd, J = 10.0, 5.3 Hz, 1H), 3.71 (s, 3H), 3.69 (s, 3H), 3.25 (dd, J = 17.0, 10.0 Hz, 1H), 2.72 (dd, J = 17.0, 5.3 Hz, 1H); **¹³C NMR** (100 MHz, CDCl₃) δ_{C} (ppm) = 173.5, 172.1, 140.8, 140.7, 136.8, 128.9, 128.3, 127.8, 127.5, 127.2, 52.6, 52.1, 46.9, 37.7; **LRMS** (EI, 70 eV) m/z (%) 298 (5) [M^+], 267 (10), 266 (47), 239 (29), 238 (100), 197 (45), 180 (17), 179 (22), 178 (14), 165 (11); **HRMS** (ESI) exact mass calculated for C₁₈H₁₈O₄Na [($\text{M}+\text{Na}$)⁺], 321.1097, found 321.1096; **IR** (neat): $\tilde{\nu}$ = 2950 (w), 2361 (w), 1720 (s), 1487 (w), 1437 (m), 1407 (w), 1377 (w), 1326 (m), 1194 (m), 1160 (brs), 1001 (w), 851 (w), 832 (m), 756 (m), 699 (m); **GC** (achiral phase), 100 kPa He, 100 °C, 0 min, 6 °C/min, 250 °C, 15 min: t_{R} = 30.8 min; **HPLC** (chiral, Daicel Chiracel IC, 0.46 cm × 25 cm, *n*-heptane/isopropanol 95:5, 1.0 mL/min, 20 °C): t_{R} = 46.1 min (–), t_{R} = **50.5 min (+)**, 97% *ee*; **$[\alpha]_{\text{D}}^{20}$** = +141.1 (c = 1.00, CHCl₃).

(+)-Dimethyl 2-(4-(trimethylsilyl)phenyl)succinate (77q)

Appearance: colorless oil; **¹H NMR** (400 MHz, CDCl₃) δ_{H} (ppm) = 7.48 (d, J = 8.1 Hz, 2H), 7.26 (d, J = 8.0 Hz, 2H), 4.09 (dd, J = 10.3, 5.1 Hz, 1H), 3.68 (s, 6H), 3.21 (dd, J = 17.0, 10.3 Hz, 1H), 2.66 (dd, J = 17.0, 5.1 Hz, 1H), 0.25 (s, 9H); **¹³C NMR** (100 MHz, CDCl₃) δ_{C} (ppm) = 173.6, 172.2, 140.0, 138.2, 134.1, 127.2, 52.5, 52.0, 47.2, 37.7, –1.0; **LRMS** (EI, 70 eV) m/z (%) 279 (39) [($\text{M}-\text{Me}$)⁺], 263 (25), 262 (92), 235 (17), 234 (37), 220 (10), 219 (49), 210 (18), 209 (100), 193 (28), 161 (27), 89 (30); **HRMS** (ESI) exact mass calculated for C₁₅H₂₂O₄SiNa [($\text{M}+\text{Na}$)⁺], 317.1185, found 317.1188; **IR** (neat): $\tilde{\nu}$ = 2953 (w), 2360 (w), 1735 (s), 1436 (w), 1246 (m), 1158 (brs), 1006 (w), 837 (s), 735 (w), 638 (w); **GC** (achiral phase), 100 kPa He, 100 °C, 0 min, 6 °C/min, 250 °C, 15 min: t_{R} = 22.9 min; **HPLC** (chiral, Daicel Chiracel OD-H, 0.46 cm × 25 cm, *n*-heptane/isopropanol 99.5:0.5, 1.0 mL/min, 20 °C): t_{R} = **23.4 min (+)**, t_{R} = 31.9 min (–), 96% *ee*; **$[\alpha]_{\text{D}}^{20}$** = +90.4 (c = 0.90, CHCl₃).

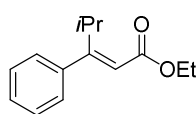
(+)-Dimethyl 2-(thiophen-3-yl)succinate (77s)

Appearance: colorless oil; $^1\text{H NMR}$ (400 MHz, CDCl_3) δ_{H} (ppm) = 7.28 (dd, J = 5.0, 3.0 Hz, 1H), 7.16–7.13 (m, 1H), 7.03 (d, J = 5.0 Hz, 1H), 4.22 (dd, J = 10.0, 5.3 Hz, 1H), 3.70 (s, 3H), 3.68 (s, 3H), 3.17 (dd, J = 16.9, 10.0 Hz, 1H), 2.71 (dd, J = 16.9, 5.4 Hz, 1H); $^{13}\text{C NMR}$ (100 MHz, CDCl_3) δ_{C} (ppm) = 173.2, 172.0, 137.7, 127.0, 126.4, 122.3, 52.5, 52.1, 42.6, 37.4; **LRMS** (EI, 70 eV) m/z (%) 228 (2) $[\text{M}^+]$, 197 (12), 196 (60), 169 (29), 168 (88), 127 (100), 110 (27), 109 (26); **HRMS** (ESI) exact mass calculated for $\text{C}_{10}\text{H}_{12}\text{O}_4\text{SNa}$ $[(\text{M}+\text{Na})^+]$, 251.0349, found 251.0351; **IR** (neat): $\tilde{\nu}$ = 2952 (w), 1729 (s), 1436 (m), 1337 (s), 1263 (m), 1154 (brs), 1002 (m), 778 (m); **GC** (achiral phase), 60 kPa He, 50 °C, 0 min, 4 °C/min, 150 °C, 0 min, 10 °C/min, 250 °C, 5 min: t_{R} = 36.5 min; **GC** (chiral phase, *ChiralDEX G-TA*, γ -cyclodextrin TFA column (30 m \times 0.25 mm \times 0.25 μm), 80 kPa He, 80 °C, 0 min, 1 °C/min, 145 °C, 0 min, 10 °C/min, 160 °C, 5 min): t_{R} = 61.6 min (–), t_{R} = **62.2 min (+)**, 80% *ee*; $[\alpha]_{\text{D}}^{20}$ = +71.8 (c = 0.90, CHCl_3).

6.4 Iridium-Catalyzed Asymmetric Hydrogenation of 3,3-Disubstituted Allylic Alcohols

6.4.1 Synthesis and analytical data of 3,3-disubstituted α,β -unsaturated esters

Ethyl (*E*)-4-methyl-3-phenylpent-2-enoate (85b)



To a cold (0 °C) solution of triethylphosphonoacetate (2.0 mL, 10 mmol, 1.0 eq.) in CH_2Cl_2 (10 mL) was added dropwise a solution of *n*BuLi (1.6 M in hexane, 5.0 mL, 8 mmol, 0.8 eq.). The mixture was stirred at 0 °C for 45 min prior to addition of isobutyrophenone (1.5 mL, 10 mmol, 1.0 eq.) at 0 °C. The reaction was refluxed overnight and quenched with NaHCO_3 (sat. aq., 10 mL). The layers were separated and the aqueous phase was extracted with methyl-*tert*-butylether (2 \times 15 mL). The combined organic layers were washed with brine, dried over Na_2SO_4 , filtered and concentrated *in vacuo* to give a pale yellow liquid. Purification by column chromatography

(SiO₂, 3 cm × 30 cm, pentane/EtOAc, 50:1) afforded 1.41 g (65% yield) of the title compound as a colorless liquid.

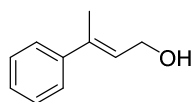
R_f: 0.51 in pentane/EtOAc, 30:1 (visualization: UV, KMnO₄); **¹H NMR** (500 MHz, CDCl₃) δ_H (ppm) = 7.35–7.29 (m, 3H), 7.22–7.18 (m, 2H), 5.70 (s, 1H), 4.20 (q, *J* = 7.1 Hz, 2H), 4.11 (sept, *J* = 7.0 Hz, 1H), 1.30 (t, *J* = 7.1 Hz, 3H), 1.09 (d, *J* = 7.0 Hz, 6H); **¹³C NMR** (125 MHz, CDCl₃) δ_C (ppm) = 167.3, 166.4, 140.9, 127.9, 127.8, 127.7, 118.7, 60.0, 29.7, 21.5, 14.4; **LRMS** (EI, 70 eV) *m/z* (%) 218 (100) [M⁺], 173 (40), 172 (55), 171 (23), 157 (31), 145 (87), 143 (35), 131 (25), 130 (20), 129 (57), 128 (45), 117 (20), 115 (23), 103 (18), 91 (35).

The ¹H and ¹³C NMR data were consistent with the literature data^[195]

6.4.2 Synthesis and analytical data of 3,3-disubstituted allylic alcohols

The general procedure for the synthesis of 3,3-disubstituted primary allylic alcohols by DIBAL-H reduction of the corresponding α,β-unsaturated esters using a work up procedure developed by Nelson,^[196] is described for the synthesis of (*E*)-3-phenylbut-2-en-1-ol (**86a**).

(*E*)-3-Phenylbut-2-en-1-ol (86a)



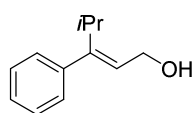
To a cold (0 °C) solution of 3,3-disubstituted ester **85a** (1.2 g, 6.3 mmol, 1.0 eq.) in CH₂Cl₂ (30 mL) was added dropwise a solution of DIBAL-H (1.0 M in CH₂Cl₂, 14 mL, 14 mmol, 2.3 eq.). The mixture was stirred at 0 °C for 30 min, and then for 2 h at rt. After this time the reaction mixture was cooled again to 0 °C and the excess of DIBAL-H quenched with sequential addition of H₂O (2.06 mL), NaOH (10% aq., 2.06 mL) and H₂O (4.14 mL). The ice bath was removed and the suspension stirred for 1 h at rt. Afterwards, the suspension was filtered, dried over Na₂SO₄, filtered and concentrated *in vacuo* to give an oil that was purified by column chromatography (SiO₂, 2 cm × 25 cm, pentane/EtOAc, 3:1) to afford 888 mg (95% yield) of the title compound as a colourless liquid.

R_f: 0.59 in pentane/EtOAc, 30:1 (visualization: UV, KMnO₄); **¹H NMR** (400 MHz, CDCl₃) δ_H (ppm) = 7.44–7.39 (m, 2H), 7.36–7.31 (m, 2H), 7.29–7.22 (m, 1H), 5.98 (td, *J* = 6.8, 1.4 Hz,

1H), 4.37 (d, $J = 6.7$ Hz, 2H), 2.09 (d, $J = 1.3$ Hz, 3H), 1.42 (s, 1H); ^{13}C NMR (100 MHz, CDCl_3) δ_{C} (ppm) = 143.0, 138.1, 128.4, 127.4, 126.6, 125.9, 60.1, 16.2; LRMS (EI, 70 eV) m/z (%) 148 (65) [M^+], 147 (22), 145 (22), 134 (10), 133 (100), 130 (57), 129 (46), 128 (26), 127 (11), 117 (12), 116 (16), 115 (89), 106 (48), 105 (78), 103 (31), 91 (81), 79 (28), 78 (28), 77 (40); EA: calc. (%) for $\text{C}_{10}\text{H}_{12}\text{O}$, C 81.04, H 8.16; found C 80.65, H 8.15; IR (neat): $\tilde{\nu} = 3362$ (brs), 2927 (w), 2876 (w), 1715 (s), 1675 (s), 1654 (s), 1445 (m), 1369 (m), 1266 (m), 1153 (m), 1015 (m), 1003 (s), 757 (s); GC (achiral phase), 60 kPa He, 100 °C, 2 min, 7 °C/min, 250 °C, 10 min): $t_{\text{R}} = 16.9$ min.

The ^1H and ^{13}C NMR data were consistent with the literature data.^[197]

(*E*)-4-methyl-3-phenylpent-2-en-1-ol (86b)

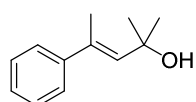


The title compound was prepared according to the procedure followed for the synthesis of (*E*)-3-phenylbut-2-en-1-ol (**86a**) starting from 3,3-disubstituted unsaturated ester **85b**. The crude material was purified by column chromatography (SiO_2 , 1 cm \times 16 cm, pentane/EtOAc, 4:1) to afford 202 mg (93% yield) of the title compound as a colorless liquid.

R_f: 0.38 in pentane/EtOAc, 5:1 (visualization: UV, KMnO_4); ^1H NMR (400 MHz, CDCl_3) δ_{H} (ppm) = 7.32–7.23 (m, 3H), 7.19–7.14 (m, 2H), 5.48 (t, $J = 6.7$ Hz, 1H), 4.36 (d, $J = 6.7$ Hz, 2H), 3.02 (quin, $J = 7.0$ Hz, 1H), 1.36 (s, 1H), 1.05 (d, $J = 7.0$ Hz, 6H); ^{13}C NMR (100 MHz, CDCl_3) δ_{C} (ppm) = 150.2, 142.4, 128.5, 127.8, 127.5, 126.8, 59.1, 29.9, 22.1; LRMS (EI, 70 eV) m/z (%) 176 (19) [M^+], 158 (11), 145 (14), 143 (37), 134 (19), 133 (100), 132 (38), 131 (11), 129 (15), 128 (27), 117 (34), 116 (16), 115 (55), 105 (45), 103 (18), 92 (15), 91 (41), 77 (20); IR (neat): $\tilde{\nu} = 3337$ (brs), 2924 (s), 1851 (m), 1651 (w), 1597 (w), 1491 (w), 1447 (m), 1011 (m), 891 (w), 766 (w), 702 (s); GC (achiral phase), 60 kPa He, 100 °C, 2 min, 7 °C/min, 250 °C, 10 min): $t_{\text{R}} = 17.2$ min.

The ^1H and ^{13}C NMR data were consistent with the literature data.^[198]

(*E*)-2-Methyl-4-phenylpent-3-en-2-ol (88)



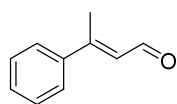
This compound was synthesized using the procedure described by Weinreb.^[134] To a cold (−78 °C) solution of 3,3-disubstituted ester **85a**

(0.55 mL, 3.0 mmol, 1.0 eq.) in THF (15 mL) was added dropwise a solution of methyllithium (1.6 M in Et₂O, 15 mL, 24 mmol, 8.0 eq.). The reaction was stirred at –78 °C for 3 h and then for 12 h at rt. After this time the mixture was cooled again to –78 °C and quenched with NaHCO₃ (sat. aq., 10 mL) and allowed to warm to rt. The layers were separated and the aqueous phase was extracted with EtOAc (2×15 mL). The combined organic layers were washed with brine, dried over Na₂SO₄, filtered and concentrated *in vacuo* to give a pale yellow liquid. Purification by column chromatography (SiO₂, 2 cm × 23 cm, pentane/EtOAc, 15:1) afforded 443 mg (84% yield) of the title compound as a colorless liquid.

R_f: 0.23 in pentane/EtOAc, 12:1 (visualization: UV, KMnO₄); **¹H NMR** (400 MHz, CDCl₃) δ_H (ppm) = 7.39–7.34 (m, 2H), 7.34–7.28 (m, 2H), 7.26–7.21 (m, 1H), 5.86 (q, *J* = 1.4 Hz, 1H), 2.29 (d, *J* = 1.4 Hz, 3H), 1.54 (s, 1H), 1.48 (s, 6H); **¹³C NMR** (100 MHz, CDCl₃) δ_C (ppm) = 144.8, 137.4, 135.4, 128.3, 127.1, 126.0, 71.5, 31.4, 17.0; **LRMS** (EI, 70 eV) *m/z* (%) 159 (2) [(M–OH)⁺], 258 (18), 144 (11), 143 (97), 142 (23), 141 (22), 129 (26), 128 (100), 127 (23), 115 (53), 102 (13), 91 (12); **EA**: calc. (%) for C₁₂H₁₆O, C 81.77, H 9.15; found C 81.50, H 9.09; **IR** (neat): $\tilde{\nu}$ = 3365 (brs), 2971 (m), 2373 (w), 1378 (w), 1139 (w), 951 (w); **GC** (achiral phase), 60 kPa He, 100 °C, 2 min, 7 °C/min, 250 °C, 10 min): *t_R* = 17.1 min.

6.4.3 Synthesis and analytical data of 3,3-disubstituted unsaturated aldehydes

(*E*)-3-Phenylbut-2-enal (87a)



The title compound was prepared according to the procedure published by Swern *et al.*^[133] To a cold (–60 °C) solution of oxalyl chloride (0.81 mL, 9.3 mmol, 1.1 eq.) in CH₂Cl₂ (20 mL) was added dropwise a solution of dimethylsulfoxide (1.3 mL, 19 mmol, 2.2 eq.) in CH₂Cl₂ (5 mL). The reaction was stirred at –60 °C for 10 min prior to dropwise addition of a solution of allylic alcohol **86a** (1.26 g, 8.5 mmol, 1.0 eq.) in CH₂Cl₂ (9 mL). Upon addition the mixture was stirred for 45 min and triethylamine (5.9 mL, 43 mmol, 5.0 eq.) was added. The reaction was allowed to warm up to 0 °C in 2 h. After this time the solvent was removed *in vacuo* and the resulting mixture partitioned between H₂O (15 mL) and CH₂Cl₂ (15 mL). The layers were separated

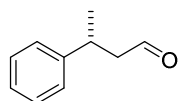
and the aqueous phase was extracted with CH_2Cl_2 (2×15 mL). The combined organic layers were washed with brine, dried over Na_2SO_4 , filtered and concentrated *in vacuo* to give a pale yellow liquid. Purification by column chromatography (SiO_2 , 3 cm × 20 cm, pentane/EtOAc, 10:1) afforded 960 mg (78% yield) of the title compound as a colorless liquid.

R_f: 0.42 in pentane/EtOAc, 10:1 (visualization: UV, KMnO_4); **^1H NMR** (250 MHz, CDCl_3) δ_{H} (ppm) = 10.19 (d, J = 7.8 Hz, 1H), 7.61–7.49 (m, 2H), 7.47–7.34 (m, 3H), 6.40 (d, J = 7.9 Hz, 1H), 2.58 (s, 3H); **^{13}C NMR** (125 MHz, CDCl_3) δ_{C} (ppm) = 191.4, 157.8, 140.7, 130.2, 128.9, 127.4, 126.4, 16.5; **GC** (achiral phase), 60 kPa He, 100 °C, 2 min, 7 °C/min, 250 °C, 10 min: t_{R} = 16.4 min.

The ^1H and ^{13}C NMR data were consistent with the literature data.^[199]

6.4.3 Analytical data of the hydrogenation products

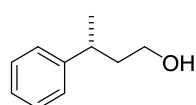
(R)-(-)-3-phenylbutanal (92a)



Appearance: colorless liquid; **^1H NMR** (400 MHz, CDCl_3) δ_{H} (ppm) = 9.63 (s, 1H), 7.29–7.13 (m, 5H), 3.33–3.24 (m, 1H), 2.70 (m, 1H), 2.58 (m, 1H), 1.23 (d, J = 7.0 Hz, 3H); **^{13}C NMR** (100 MHz, CDCl_3) δ_{C} (ppm) = 201.8, 145.3, 128.9, 127.1, 126.8, 52.0, 34.3, 22.5; **LRMS** (EI, 70 eV) m/z (%) 148 (35) [M^+], 133 (30), 115 (11), 106 (28), 105 (100), 91 (56), 79 (37), 78 (34), 77 (49); **GC** (achiral phase), 60 kPa He, 100 °C, 2 min, 7 °C/min, 250 °C, 10 min: t_{R} = 17.2 min; **GC** (chiral phase, Gamma CD-Trifluoroacetyl GTA, 60 KPa, 90 °C, 35 min, 10 °C/min, 160 °C, 5 min): t_{R} = 30.7 min (*S*, +), t_{R} = **31.7 min** (*R*, -).

The ^1H and ^{13}C NMR data were consistent with the literature data.^[198]

(R)-(-)-3-Phenylbutan-1-ol (93a)

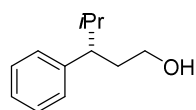


Appearance: colorless liquid; **^1H NMR** (400 MHz, CDCl_3) δ_{H} (ppm) = 7.34–7.27 (m, 2H), 7.24–7.17 (m, 3H), 3.56 (qt, J = 10.6, 6.6 Hz, 2H), 2.89 (sext, J = 7.1 Hz, 1H), 1.86 (dt, J = 7.9, 6.5 Hz, 2H), 1.34 (brs, 1H), 1.28 (d, J = 7.0 Hz, 3H); **^{13}C NMR** (100 MHz, CDCl_3) δ_{C} (ppm) = 147.0, 128.6, 127.1, 126.3, 61.4, 41.1, 36.6,

22.6; **LRMS** (EI, 70 eV) m/z (%) 150 (11) [M^+], 117 (51), 105 (100); **EA**: calc. (%) for $C_{10}H_{14}O$, C 79.96, H 9.39; found C 79.71, H 9.44; **GC** (achiral phase), 60 kPa He, 100 °C, 2 min, 7 °C/min, 250 °C, 10 min): t_R = 15.6 min; **GC** (chiral phase, Chiraldex (Gamma CD-6-Methyl-2,3-pentyl PS086, 60 KPa, 110 °C, 20 min, 10 °C/min, 180 °C, 10 min): t_R = 14.3 min (*S*, +), t_R = **15.9 min** (*R*, -).

The 1H and ^{13}C NMR data were consistent with the literature data.^[200]

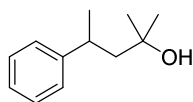
(*S*)-(-)-3-Phenylbutan-1-ol (93b)



Appearance: colorless liquid; 1H NMR (400 MHz, $CDCl_3$) δ_H (ppm) = 7.32–7.25 (m, 2H), 7.22–7.16 (m, 1H), 7.15–7.11 (m, 2H), 3.48 (ddd, J = 10.5, 7.4, 4.9 Hz, 1H), 3.39 (ddd, J = 10.5, 7.7, 6.7 Hz, 1H), 2.41 (ddd, J = 11.6, 7.8, 3.9 Hz, 1H), 2.13–2.05 (m, 1H), 1.91–1.75 (m, 2H), 1.28 (brs, 1H), 0.97 (d, J = 6.7 Hz, 3H), 0.73 (d, J = 6.7 Hz, 3H); ^{13}C NMR (100 MHz, $CDCl_3$) δ_C (ppm) = 144.0, 128.6, 128.4, 126.3, 61.8, 49.8, 36.1, 33.7, 21.1, 20.9; **LRMS** (EI, 70 eV) m/z (%) 178 (10) [M^+], 135 (25), 118 (10), 117 (25), 106 (10), 105 (100), 92 (10), 91 (68); **EA**: calc. (%) for $C_{12}H_{18}O$, C 80.85, H 10.18; found C 80.54, H 10.12; **GC** (achiral phase), 60 kPa He, 100 °C, 2 min, 7 °C/min, 250 °C, 10 min): t_R = 16.4 min; **HPLC** (chiral phase, Daicel Chiracel OD-H, 0.46 cm \times 25 cm, *n*-heptane/isopropanol 97:3, 0.5 mL/min, 20 °C): t_R = **23.2 min** (*S*, -), t_R = 25.9 min (*R*, +); $[\alpha]_D^{20}$ = -13 (c = 0.3, $CHCl_3$).

The 1H and ^{13}C NMR data were consistent with the literature data.^[201]

(-)-2-Methyl-4-phenylpentan-2-ol (94)



Appearance: colorless oil; 1H NMR (400 MHz, $CDCl_3$) δ_H (ppm) = 7.34–7.27 (m, 2H), 7.27–7.22 (m, 2H), 7.21–7.15 (m, 1H), 2.97 (dq, J = 9.0, 7.0, 4.6 Hz, 1H), 1.99 (dd, J = 14.3, 8.9 Hz, 1H), 1.78 (dd, J = 14.3, 4.6 Hz, 1H), 1.28 (d, J = 7.0 Hz, 3H), 1.16 (s, 3H), 1.14 (s, 3H), 1.08 (s, 1H); ^{13}C NMR (100 MHz, $CDCl_3$) δ_C (ppm) = 148.2, 128.8, 127.2, 126.3, 71.6, 51.4, 36.6, 30.1, 30.1, 25.3; **LRMS** (EI, 70 eV) m/z (%) 161 (1) [($M-OH$) $^+$], 160 (10), 145 (26), 143 (20), 118 (12), 117 (9), 105 (100), 103 (10); **HRMS** (ESI) exact mass calculated for $C_{12}H_{18}ONa$ [($M+Na$) $^+$], 201.1250 found 201.1252; **GC** (achiral phase), 60 kPa He, 100 °C, 2 min, 7 °C/min, 250 °C, 10 min: t_R = 14.1

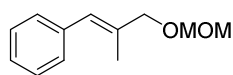
min; **GC** (chiral phase, Gamma CD-Trifluoroacetyl GTA), 60 kPa, 50 °C, 1 °C/min, 105 °C, 10 °C/min, 180 °C, 10 min): t_R = 56.2 min (+), t_R = **57.0 min (-)**.

The ^1H and ^{13}C NMR data were consistent with the literature data.^[202]

6.5 Chiral N-Heterocyclic Carbene/Pyridine Ligands for the Iridium-Catalyzed Asymmetric Hydrogenation of Olefins

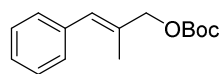
6.5.1 Synthesis and analytical data of the substrates

(E)-(3-(Methoxymethoxy)-2-methylprop-1-en-1-yl)benzene (111)



In a two-necked round bottom flask equipped with a magnetic stirring bar, allylic alcohol **107** (445 mg, 3.00 mmol, 1.00 eq.), lithium bromide (52.0 mg, 0.60 mmol, 0.2 eq.) and PTSA (51.0 mg, 0.30 mmol, 0.10 eq.) were dissolved in dimethoxyethane (6.00 mL, 67.8 mmol, 22.6 eq.). The mixture was stirred at rt for 3 h and after this time it was diluted with H_2O (5 mL), and extracted with MTBE (2×5 mL). The combined organic layers were washed with brine, dried over Na_2SO_4 , filtered and concentrated *in vacuo*. Purification by column chromatography (SiO_2 , 2 cm × 22 cm, pentane/EtOAc, 40:1) afforded 300 mg (53% yield) of the title compound as a colorless liquid.

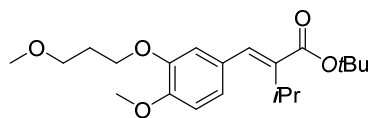
R_f: 0.65 in pentane/EtOAc, 40:1 (visualization: UV, KMnO_4); **^1H NMR** (400 MHz, CDCl_3) δ_{H} (ppm) = 7.36–7.29 (m, 4H), 7.26–7.23 (m, 1H), 6.55 (s, 1H), 4.71 (s, 2H), 4.12 (s, 2H), 3.43 (s, 3H), 1.92 (s, 3H); **^{13}C NMR** (100 MHz, CDCl_3) δ_{C} (ppm) = 137.6, 134.8, 129.0, 128.2, 127.3, 126.6, 95.7, 73.5, 55.5, 15.8; **LRMS** (EI, 70 eV) m/z (%) 192 (10) [M^+], 134 (42), 132 (31), 131 (49), 130 (28), 129 (25), 119 (16), 118 (10), 117 (38), 116 (14), 115 (36), 91 (98); **HRMS** (EI) exact mass calculated for $\text{C}_{12}\text{H}_{16}\text{O}_2$ [M^+], 192.1150, found 192.1149; **IR** (neat): $\tilde{\nu}$ = 2931 (w), 2884 (w), 1599 (w), 1491 (w), 1444 (w), 1212 (w), 1149 (s), 1101 (s), 1039 (s), 917 (s), 745 (m), 698 (s); **GC** (achiral phase), 60 kPa He, 100 °C, 2 min, 7 °C/min, 250 °C, 10 min: t_R = 16.9 min.

(E)-tert-Butyl(2-methyl-3-phenylallyl)carbonate (113)

In a two-necked round bottom flask equipped with a magnetic stirring bar, allylic alcohol **107** (445 mg, 3.00 mmol, 1.00 eq.), di-*tert*-butyl dicarbonate (0.76 mL, 3.30 mmol, 1.10 eq.) and $\text{Zn}(\text{OAc})_2$ (55 mg, 0.30 mmol, 0.10 eq.) were dissolved in CH_2Cl_2 (4 mL). The mixture was stirred and refluxed for 3 h and after this time it was diluted with H_2O (5 mL) and extracted with CH_2Cl_2 (2×5 mL). The combined organic layers were washed with brine, dried over Na_2SO_4 , filtered and concentrated *in vacuo* to give a colorless liquid. Purification by column chromatography (SiO_2 , 2 cm × 25 cm, pentane/EtOAc, 70:1) afforded 430 mg (58% yield) of the title compound as a colorless liquid.

R_f: 0.42 in pentane/EtOAc, 40:1 (visualization: UV, KMnO_4); **¹H NMR** (400 MHz, CDCl_3) δ_{H} (ppm) = 7.34–7.29 (m, 2H), 7.28–7.18 (m, 3H), 6.53 (s, 1H), 4.61 (s, 2H), 1.90 (d, J = 1.3 Hz, 3H), 1.50 (s, 9H); **¹³C NMR** (100 MHz, CDCl_3) δ_{C} (ppm) = 153.6, 137.2, 132.6, 129.1, 128.7, 128.3, 126.9, 82.3, 72.8, 27.9, 15.7; **IR** (neat): $\tilde{\nu}$ = 2980 (w), 2934 (w), 1736 (s), 1368 (m), 1273 (s), 1250 (s), 1156 (s), 1088 (m), 845 (m), 699 (m); **GC** (achiral phase), 60 kPa He, 100 °C, 2 min, 7 °C/min, 250 °C, 10 min: t_{R} = 21.5 min.

The ¹H and ¹³C NMR data were consistent with the literature data.^[173]

tert-Butyl (E)-2-(4-methoxy-3-(3-methoxypropoxy)benzylidene)-3-methylbutanoate (115)

The title compound was obtained by column chromatography (SiO_2 , pentane/EtOAc, 15:1) of a batch containing both stereoisomers of compound **115** which was previously synthesized by Esther Hörmann.^[119]

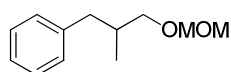
Appearance: colorless oil; **R_f**: 0.31 in pentane/EtOAc, 8:1 (visualization: UV, KMnO_4); **¹H NMR** (400 MHz, CDCl_3) δ_{H} (ppm) = 7.34 (s, 1H), 6.94–6.80 (m, 3H), 4.11 (d, J = 6.5 Hz, 2H), 3.88 (s, 3H), 3.57 (t, J = 6.2 Hz, 2H), 3.35 (s, 3H), 3.15 (sept, J = 6.9 Hz, 1H), 2.10 (quin, J = 6.3 Hz, 2H), 1.55 (s, 9H), 1.24 (d, J = 6.9 Hz, 6H); **¹³C NMR** (100 MHz, CDCl_3) δ_{C} (ppm) = 167.8, 149.3, 148.2, 139.7, 136.6, 129.1, 122.1, 114.4, 111.5, 80.7, 69.4, 66.2, 58.9, 56.1,

29.7, 28.5, 27.7, 21.4; **LRMS** (EI, 70 eV) m/z (%) 364 (35) [M^+], 308 (46), 290 (14), 217 (15), 190 (10), 73 (100); **HRMS** (ESI) exact mass calculated for $C_{21}H_{32}O_5Na$ [$(M+Na)^+$], 387.2142, found 387.2144; **GC** (achiral phase), 100 kPa He, 100 °C, 0 min, 6 °C/min, 250 °C, 15 min): t_R = 30.5 min.

The 1H and ^{13}C NMR data were consistent with the literature data.^[119]

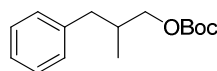
6.5.2 Analytical data of the hydrogenation products

(-)-(3-(Methoxymethoxy)-2-methylpropyl)benzene (111)



Appearance: colorless liquid; 1H NMR (400 MHz, $CDCl_3$) δ_H (ppm) = 7.32–7.27 (m, 2H), 7.23–7.18 (m, 3H), 4.64 (s, 2H), 3.46–3.37 (m, 5H), 2.81 (dd, J = 13.4, 6.0 Hz, 1H), 2.41 (dd, J = 13.5, 8.3 Hz, 1H), 2.13–1.95 (m, 1H), 0.92 (d, J = 6.8 Hz, 3H); ^{13}C NMR (100 MHz, $CDCl_3$) δ_C (ppm) = 140.8, 129.3, 128.3, 126.0, 96.8, 72.7, 55.3, 40.1, 35.7, 17.0; **LRMS** (EI, 70 eV) m/z (%) 163 (5) [$(M-OMe)^+$], 162 (32), 132 (31), 131 (18), 117 (44), 105 (12), 92 (32), 91 (100); **GC** (achiral phase), 60 kPa He, 100 °C, 2 min, 7 °C/min, 250 °C, 10 min: t_R = 15.0 min; **HPLC** (chiral phase, Daicel Chiracel OJ, 0.46 cm \times 25 cm, n -heptane/isopropanol 99:1, 0.5 mL/min, 20 °C): t_R = 15.2 min (+), t_R = **16.9 min (-)**, 70% *ee*; $[\alpha]_D^{20}$ = -4 (c = 0.20, $CHCl_3$).

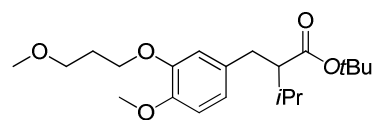
(+)-*tert*-Butyl (2-methyl-3-phenylpropyl)carbonate (114)



Appearance: colorless liquid; 1H NMR (400 MHz, $CDCl_3$) δ_H (ppm) = 7.31–7.27 (m, 2H), 7.23–7.12 (m, 3H), 3.97 (dd, J = 10.5, 6.1 Hz, 1H), 3.90 (dd, J = 10.5, 6.5 Hz, 1H), 2.77 (dd, J = 13.5, 6.1 Hz, 1H), 2.44 (dd, J = 13.5, 8.3 Hz, 1H), 2.22–2.07 (m, 1H), 1.50 (s, 9H), 0.93 (d, J = 6.7 Hz, 3H); ^{13}C NMR (100 MHz, $CDCl_3$) δ_C (ppm) = 153.9, 140.0, 129.3, 128.4, 126.2, 82.0, 71.5, 39.8, 34.8, 28.0, 16.6; **LRMS** (EI, 70 eV) m/z (%) 150 (2) [M^+], 133 (26), 132 (100), 131 (23), 117 (85), 92 (14), 91 (84); **HRMS** (ESI) exact mass calculated for $C_{15}H_{22}O_3Na$ [$(M+Na)^+$], 273.1461, found 273.1462; **IR** (neat): $\tilde{\nu}$ = 2975 (w), 2931 (w), 1737 (s), 1455 (w), 1369 (w), 1275 (s), 1252 (s), 1159 (s), 1094 (w), 862 (w), 701 (m); **GC** (achiral phase), 60 kPa He, 100 °C, 2 min, 7 °C/min, 250 °C, 10 min: t_R = 20.0 min; **HPLC** (chiral phase, Daicel Chiracel OJ, 0.46 cm \times 25 cm, n -heptane/isopropanol 99:1,

0.5 mL/min, 20 °C): t_R = **14.6 min (+)**, t_R = 16.9 min (–), 70% *ee*; $[\alpha]_D^{20}$ = +9.1 (c = 0.20, CHCl_3).

(+)-*tert*-Butyl 2-(4-methoxy-3-(3-methoxypropoxy)benzyl)-3-methylbutanoate (116)



Appearance: colorless oil; ^1H NMR (400 MHz, CDCl_3) δ_{H} (ppm) = 6.86–6.64 (m, 3H), 4.08 (t, J = 6.5 Hz, 2H), 3.82 (s, 3H), 3.56 (t, J = 6.2 Hz, 2H), 3.35 (s, 3H), 2.92–2.63 (m, 2H), 2.31 (ddd, J = 9.7, 7.2, 5.8 Hz, 1H), 2.09 (quin, J = 6.3 Hz, 2H), 1.87 (dq, J = 13.7, 6.9 Hz, 1H), 1.29 (s, 9H), 0.94 (d, J = 6.8 Hz, 3H), 0.91 (d, J = 6.7 Hz, 3H); ^{13}C NMR (100 MHz, CDCl_3) δ_{C} (ppm) = 173.4, 148.3, 148.9, 133.0, 121.4, 114.4, 111.8, 80.1, 69.6, 66.2, 58.8, 56.2, 55.4, 35.8, 31.0, 29.8, 28.2, 20.7, 20.3; **LRMS** (EI, 70 eV) m/z (%) 366 (37) [M^+], 311 (14), 293 (14), 210 (16), 209 (88), 177 (20), 151 (13), 138 (17), 137 (57), 73 (100); **HRMS** (ESI) exact mass calculated for $\text{C}_{21}\text{H}_{34}\text{O}_5\text{Na}$ [$(\text{M}+\text{Na})^+$], 389.2298, found 389.2301; **GC** (achiral phase), 100 kPa He, 100 °C, 0 min, 6 °C/min, 250 °C, 15 min: t_R = 28.2 min; **HPLC** (chiral phase, Daicel Chiracel AD-H, 0.46 cm \times 25 cm, *n*-heptane/isopropanol 99:1, 0.6 mL/min, 20 °C): t_R = 18.2 min (–), t_R = **19.3 min (+)**, 49% *ee*; $[\alpha]_D^{20}$ = +3.5 (c = 0.30, CHCl_3).

The ^1H and ^{13}C NMR data were consistent with the literature data.^[119]

References

- [1] a) W. Tang, X. Zhang, *Chem. Rev.* **2003**, *103*, 3029-3070; b) X. Cui, K. Burgess, *Chem. Rev.* **2005**, *105*, 3272-3296.
- [2] a) J. A. Osborn, F. H. Jardine, J. F. Young, G. Wilkinson, *J. Chem. Soc. A* **1966**, 1711-1732; b) R. S. Coffey, Imperial Chemical Industries, *Brit. Pat. I*, 121, 642, **1965**.
- [3] W. S. Knowles, M. J. Sabacky, B. D. Vineyard, *Chem. Commun.* **1972**, 10-11.
- [4] a) T. P. Dang, H. B. Kagan, *Chem. Commun.* **1971**, 481; b) H. B. Kagan, P. Dang Tuan, *J. Am. Chem. Soc.* **1972**, *94*, 6429-6433; c) B. D. Vineyard, W. S. Knowles, M. J. Sabacky, G. L. Bachman, D. J. Weinkauff, *J. Am. Chem. Soc.* **1977**, *99*, 5946-5952; d) W. S. Knowles, *Acc. Chem. Res.* **1983**, *16*, 106-112.
- [5] a) K. Achiwa, *J. Am. Chem. Soc.* **1976**, *98*, 8265-8266; b) M. D. Fryzuk, B. Bosnich, *J. Am. Chem. Soc.* **1977**, *99*, 6262-6267; c) M. D. Fryzuk, B. Bosnich, *J. Am. Chem. Soc.* **1978**, *100*, 5491-5494; d) M. Fiorini, G. M. Giongo, *J. Mol. Catal.* **1979**, *5*, 303-310; e) T. Hayashi, A. Katsumura, M. Konishi, M. Kumada, *Tetrahedron Lett.* **1979**, *20*, 425-428; f) W. A. Nugent, T. V. RajanBabu, M. J. Burk, *Science* **1993**, *259*, 479-483; g) M. J. Burk, *Acc. Chem. Res.* **2000**, *33*, 363-372.
- [6] a) R. Noyori, *Chem. Soc. Rev.* **1989**, *18*, 187-208; b) R. Noyori, *Science* **1990**, *248*, 1194-1199; c) R. Noyori, H. Takaya, *Acc. Chem. Res.* **1990**, *23*, 345-350; d) R. Noyori, *Angew. Chem. Int. Ed.* **2002**, *41*, 2008-2022.
- [7] W. S. Knowles, *Angew. Chem. Int. Ed.* **2002**, *41*, 1998-2007.
- [8] a) J. R. Shapley, R. R. Schrock, J. A. Osborn, *J. Am. Chem. Soc.* **1969**, *91*, 2816-2817; b) R. R. Schrock, J. A. Osborn, *J. Am. Chem. Soc.* **1976**, *98*, 2134-2143.
- [9] R. Crabtree, *Acc. Chem. Res.* **1979**, *12*, 331-337.
- [10] W. S. Knowles, *J. Chem. Educ.* **1986**, *63*, 222.
- [11] M. Kitamura, I. Kasahara, K. Manabe, R. Noyori, H. Takaya, *J. Org. Chem.* **1988**, *53*, 708-710.
- [12] a) T. Hayashi, M. Tanaka, I. Ogata, *Tetrahedron Lett.* **1977**, *18*, 295-296; b) T. Ohta, H. Ikegami, T. Miyake, H. Takaya, *J. Organomet. Chem.* **1995**, *502*, 169-176; c) K. Inagaki, T. Ohta, K. Nozaki, H. Takaya, *J. Organomet. Chem.* **1997**, *531*, 159-163.
- [13] S. Bhaduri, K. R. Sharma, W. Clegg, G. M. Sheldrick, D. Stalke, *J. Chem. Soc., Dalton Trans.* **1984**, 2851-2853.
- [14] E. Cesarotti, R. Ugo, H. B. Kagan, *Angew. Chem. Int. Ed.* **1979**, *18*, 779-780.
- [15] a) R. L. Halterman, K. P. C. Vollhardt, M. E. Welker, D. Blaesus, R. Boese, *J. Am. Chem. Soc.* **1987**, *109*, 8105-8107; b) R. L. Halterman, K. P. C. Vollhardt, *Organometallics* **1988**, *7*, 883-892.
- [16] a) L. A. Paquette, J. A. McKinney, M. L. McLaughlin, A. L. Rheingold, *Tetrahedron Lett.* **1986**, *27*, 5599-5602; b) L. A. Paquette, M. R. Sivik, E. I. Bzowej, K. J. Stanton, *Organometallics* **1995**, *14*, 4865-4878.
- [17] R. D. Broene, S. L. Buchwald, *J. Am. Chem. Soc.* **1993**, *115*, 12569-12570.
- [18] M. V. Troutman, D. H. Appella, S. L. Buchwald, *J. Am. Chem. Soc.* **1999**, *121*, 4916-4917.
- [19] S. J. Roseblade, A. Pfaltz, *Acc. Chem. Res.* **2007**, *40*, 1402-1411.
- [20] R. H. Crabtree, G. E. Morris, *J. Organomet. Chem.* **1977**, *135*, 395-403.

- [21] a) P. S. Hallman, B. R. McGarvey, G. Wilkinson, *J. Chem. Soc. A* **1968**, 3143-3150; b) R. H. Crabtree, A. Gautier, G. Giordano, T. Khan, *J. Organomet. Chem.* **1977**, *141*, 113-121.
- [22] a) R. H. Crabtree, H. Felkin, G. E. Morris, T. J. King, J. A. Richards, *J. Organomet. Chem.* **1976**, *113*, C7-C9; b) R. H. Crabtree, H. Felkin, G. E. Morris, *J. Organomet. Chem.* **1977**, *141*, 205-215.
- [23] P. Schnider, G. Koch, R. Prétôt, G. Wang, F. M. Bohnen, C. Krüger, A. Pfaltz, *Chem. Eur. J.* **1997**, *3*, 887-892.
- [24] a) O. Reiser, *Angew. Chem. Int. Ed.* **1993**, *32*, 547-549; b) P. von Matt, A. Pfaltz, *Angew. Chem. Int. Ed.* **1993**, *32*, 566-568; c) J. P. Janssen, G. Helmchen, *Tetrahedron Lett.* **1997**, *38*, 8025-8026; d) G. Helmchen, A. Pfaltz, *Acc. Chem. Res.* **2000**, *33*, 336-345.
- [25] A. Lightfoot, P. Schnider, A. Pfaltz, *Angew. Chem. Int. Ed.* **1998**, *37*, 2897-2899.
- [26] S. P. Smidt, A. Pfaltz, E. Martínez-Viviente, P. S. Pregosin, A. Albinati, *Organometallics* **2003**, *22*, 1000-1009.
- [27] H. Nishida, N. Takada, M. Yoshimura, T. Sonoda, H. Kobayashi, *Bull. Chem. Soc. Jpn.* **1984**, *57*, 2600-2604.
- [28] a) S. P. Smidt, N. Zimmermann, M. Studer, A. Pfaltz, *Chem. Eur. J.* **2004**, *10*, 4685-4693; b) K. Källström, I. Munslow, P. G. Andersson, *Chem. Eur. J.* **2006**, *12*, 3194-3200.
- [29] a) F. Menges, M. Neuburger, A. Pfaltz, *Org. Lett.* **2002**, *4*, 4713-4716; b) M. G. Schrems, E. Neumann, A. Pfaltz, *Angew. Chem. Int. Ed.* **2007**, *46*, 8274-8276; c) S. Li, S.-F. Zhu, C.-M. Zhang, S. Song, Q.-L. Zhou, *J. Am. Chem. Soc.* **2008**, *130*, 8584-8585; d) M. G. Schrems, A. Pfaltz, *Chem. Commun.* **2009**, 6210-6212; e) W.-J. Lu, X.-L. Hou, *Adv. Synth. Catal.* **2009**, *351*, 1224-1228.
- [30] a) J. Blankenstein, A. Pfaltz, *Angew. Chem. Int. Ed.* **2001**, *40*, 4445-4447; b) F. Menges, A. Pfaltz, *Adv. Synth. Catal.* **2002**, *344*, 40-44; c) S. P. Smidt, F. Menges, A. Pfaltz, *Org. Lett.* **2004**, *6*, 2023-2026; d) W. J. Drury, N. Zimmermann, M. Keenan, M. Hayashi, S. Kaiser, R. Goddard, A. Pfaltz, *Angew. Chem. Int. Ed.* **2004**, *43*, 70-74; e) K. Källström, C. Hedberg, P. Brandt, A. Bayer, P. G. Andersson, *J. Am. Chem. Soc.* **2004**, *126*, 14308-14309; f) F. Menges, A. Pfaltz, *Novel Organic Compounds and Metal Complexes*, WO 2005021562 A2, **2005**; g) S. Kaiser, S. P. Smidt, A. Pfaltz, *Angew. Chem. Int. Ed.* **2006**, *45*, 5194-5197.
- [31] a) R. Hilgraf, A. Pfaltz, *Synlett* **1999**, 1814-1816; b) R. Hilgraf, A. Pfaltz, *Adv. Synth. Catal.* **2005**, *347*, 61-77.
- [32] C. Valla, A. Baeza, F. Menges, A. Pfaltz, *Synlett* **2008**, 3167-3171.
- [33] A. Ganić, A. Pfaltz, *Chem. Eur. J.* **2012**, *18*, 6724-6728.
- [34] H. J. Jessen, A. Schumacher, T. Shaw, A. Pfaltz, K. Gademann, *Angew. Chem. Int. Ed.* **2011**, *50*, 4222-4226.
- [35] J. Sprinz, G. Helmchen, *Tetrahedron Lett.* **1993**, *34*, 1769-1772.
- [36] A. Schumacher, M. G. Schrems, A. Pfaltz, *Chem. Eur. J.* **2011**, *17*, 13502-13509.
- [37] D. Rageot, D. H. Woodmansee, B. Pugin, A. Pfaltz, *Angew. Chem. Int. Ed.* **2011**, *50*, 9598-9601.
- [38] D. H. Woodmansee, M.-A. Müller, M. Neuburger, A. Pfaltz, *Chem. Sci.* **2010**, *1*, 72-78.
- [39] a) G. G. Bianco, H. M. C. Ferraz, A. M. Costa, L. c. V. Costa-Lotufo, C. u. Pessoa, M. O. de Moraes, M. G. Schrems, A. Pfaltz, L. F. Silva, *J. Org. Chem.* **2009**, *74*, 2561-

- 2566; b) T. Yoshinari, K. Ohmori, M. G. Schrems, A. Pfaltz, K. Suzuki, *Angew. Chem. Int. Ed.* **2010**, *49*, 881-885; c) M. C. Pischl, C. F. Weise, M.-A. Müller, A. Pfaltz, C. Schneider, *Angew. Chem. Int. Ed.* **2013**, *52*, 8968-8972.
- [40] a) P. Cheruku, T. L. Church, A. Trifonova, T. Wartmann, P. G. Andersson, *Tetrahedron Lett.* **2008**, *49*, 7290-7293; b) P. Cheruku, J. Diesen, P. G. Andersson, *J. Am. Chem. Soc.* **2008**, *130*, 5595-5599; c) A. Paptchikhine, P. Cheruku, M. Engman, P. G. Andersson, *Chem. Commun.* **2009**, 5996-5998; d) J.-Q. Li, X. Quan, P. G. Andersson, *Chem. Eur. J.* **2012**, *18*, 10609-10616.
- [41] a) M. Diéguez, J. Mazuela, O. Pàmies, J. J. Verendel, P. G. Andersson, *J. Am. Chem. Soc.* **2008**, *130*, 7208-7209; b) P. i. Tolstoy, M. Engman, A. Paptchikhine, J. Bergquist, T. L. Church, A. W. M. Leung, P. G. Andersson, *J. Am. Chem. Soc.* **2009**, *131*, 8855-8860; c) J. Mazuela, J. J. Verendel, M. Coll, B. n. Schäffner, A. Börner, P. G. Andersson, O. Pàmies, M. Diéguez, *J. Am. Chem. Soc.* **2009**, *131*, 12344-12353.
- [42] A. Trifonova, J. S. Diesen, C. J. Chapman, P. G. Andersson, *Org. Lett.* **2004**, *6*, 3825-3827.
- [43] Z. Han, Z. Wang, X. Zhang, K. Ding, *Angew. Chem. Int. Ed.* **2009**, *48*, 5345-5349.
- [44] S. Li, S.-F. Zhu, C.-M. Zhang, S. Song, Q.-L. Zhou, *J. Am. Chem. Soc.* **2008**, *130*, 8584-8585.
- [45] Y. Zhang, Z. Han, F. Li, K. Ding, A. Zhang, *Chem. Commun.* **2010**, *46*, 156-158.
- [46] a) S.-M. Lu, X.-W. Han, Y.-G. Zhou, *Adv. Synth. Catal.* **2004**, *346*, 909-912; b) M. N. Cheemala, P. Knochel, *Org. Lett.* **2007**, *9*, 3089-3092.
- [47] G. Hou, F. Gosselin, W. Li, J. C. McWilliams, Y. Sun, M. Weisel, P. D. O'Shea, C.-y. Chen, I. W. Davies, X. Zhang, *J. Am. Chem. Soc.* **2009**, *131*, 9882-9883.
- [48] a) J.-B. Xie, J.-H. Xie, X.-Y. Liu, W.-L. Kong, S. Li, Q.-L. Zhou, *J. Am. Chem. Soc.* **2010**, *132*, 4538-4539; b) J.-H. Xie, X.-Y. Liu, J.-B. Xie, L.-X. Wang, Q.-L. Zhou, *Angew. Chem. Int. Ed.* **2011**, *50*, 7329-7332.
- [49] Q.-Q. Zhang, J.-H. Xie, X.-H. Yang, J.-B. Xie, Q.-L. Zhou, *Org. Lett.* **2012**, *14*, 6158-6161.
- [50] H. W. Wanzlick, H. J. Schönherr, *Angew. Chem. Int. Ed. Engl.* **1968**, *7*, 141-142.
- [51] K. Öfele, *J. Organomet. Chem.* **1968**, *12*, P42-P43.
- [52] D. Enders, H. Gielen, K. Breuer, *Tetrahedron: Asymmetry* **1997**, *8*, 3571-3574.
- [53] a) W. A. Herrmann, M. Elison, J. Fischer, C. Köcher, G. R. J. Artus, *Angew. Chem. Int. Ed. Engl.* **1995**, *34*, 2371-2374; b) W. A. Herrmann, L. J. Goossen, C. Köcher, G. R. J. Artus, *Angew. Chem. Int. Ed. Engl.* **1996**, *35*, 2805-2807.
- [54] a) J. Huang, H.-J. Schanz, E. D. Stevens, S. P. Nolan, *Organometallics* **1999**, *18*, 2370-2375; b) M. C. Perry, X. Cui, M. T. Powell, D.-R. Hou, J. H. Reibenspies, K. Burgess, *J. Am. Chem. Soc.* **2002**, *125*, 113-123.
- [55] M. G. Gardiner, W. A. Herrmann, C.-P. Reisinger, J. Schwarz, M. Spiegler, *J. Organomet. Chem.* **1999**, *572*, 239-247.
- [56] a) T. Weskamp, F. J. Kohl, W. Hieringer, D. Gleich, W. A. Herrmann, *Angew. Chem. Int. Ed.* **1999**, *38*, 2416-2419; b) T. M. Trnka, R. H. Grubbs, *Acc. Chem. Res.* **2000**, *34*, 18-29.
- [57] a) H. M. Lee, D. C. Smith, Z. He, E. D. Stevens, C. S. Yi, S. P. Nolan, *Organometallics* **2001**, *20*, 794-797; b) H. M. Lee, T. Jiang, E. D. Stevens, S. P. Nolan, *Organometallics* **2001**, *20*, 1255-1258; c) S. Urban, N. Ortega, F. Glorius, *Angew. Chem. Int. Ed.* **2011**, *50*, 3803-3806; d) S. Urban, B. Beiring, N. Ortega, D. Paul, F. Glorius, *J. Am. Chem.*

- Soc. **2012**, *134*, 15241-15244; e) N. Ortega, D.-T. D. Tang, S. Urban, D. Zhao, F. Glorius, *Angew. Chem. Int. Ed.* **2013**, *52*, 9500-9503.
- [58] a) W. A. Herrmann, C.-P. Reisinger, M. Spiegler, *J. Organomet. Chem.* **1998**, *557*, 93-96; b) T. Weskamp, V. P. W. Böhm, W. A. Herrmann, *J. Organomet. Chem.* **1999**, *585*, 348-352; c) J. Huang, S. P. Nolan, *J. Am. Chem. Soc.* **1999**, *121*, 9889-9890; d) S. Würtz, F. Glorius, *Acc. Chem. Res.* **2008**, *41*, 1523-1533; e) C. Valente, S. Çalimsiz, K. H. Hoi, D. Mallik, M. Sayah, M. G. Organ, *Angew. Chem. Int. Ed.* **2012**, *51*, 3314-3332.
- [59] J. Huang, G. Grasa, S. P. Nolan, *Org. Lett.* **1999**, *1*, 1307-1309.
- [60] a) D. Enders, H. Gielen, G. Raabe, J. Runsink, J. H. Teles, *Chem. Ber.* **1996**, *129*, 1483-1488; b) S. Lee, J. F. Hartwig, *J. Org. Chem.* **2001**, *66*, 3402-3415.
- [61] M. T. Powell, D.-R. Hou, M. C. Perry, X. Cui, K. Burgess, *J. Am. Chem. Soc.* **2001**, *123*, 8878-8879.
- [62] J. Zhao, K. Burgess, *J. Am. Chem. Soc.* **2009**, *131*, 13236-13237.
- [63] Y. Zhu, A. Loudet, K. Burgess, *Org. Lett.* **2010**, *12*, 4392-4395.
- [64] Y. Zhu, Y. Fan, K. Burgess, *J. Am. Chem. Soc.* **2010**, *132*, 6249-6253.
- [65] S. Nanchen, A. Pfaltz, *Chem. Eur. J.* **2006**, *12*, 4550-4558.
- [66] T. L. Church, P. G. Andersson, *Coord. Chem. Rev.* **2008**, *252*, 513-531.
- [67] a) R. H. Crabtree, H. Felkin, G. E. Morris, *J. Chem. Soc. Chem. Commun.* **1976**, 716-717; b) B. F. M. Kimmich, E. Somsook, C. R. Landis, *J. Am. Chem. Soc.* **1998**, *120*, 10115-10125.
- [68] a) P. Brandt, C. Hedberg, P. G. Andersson, *Chem. Eur. J.* **2003**, *9*, 339-347; b) Y. Fan, X. Cui, K. Burgess, M. B. Hall, *J. Am. Chem. Soc.* **2004**, *126*, 16688-16689; c) J. Mazuela, P.-O. Norrby, P. G. Andersson, O. Pàmies, M. Diéguez, *J. Am. Chem. Soc.* **2011**, *133*, 13634-13645.
- [69] a) J. Halpern, *Science* **1982**, *217*, 401-407; b) I. D. Gridnev, T. Imamoto, *Acc. Chem. Res.* **2004**, *37*, 633-644.
- [70] a) L. D. Vazquez-Serrano, B. T. Owens, J. M. Buriak, *Chem. Commun.* **2002**, 2518-2519; b) R. Dietiker, P. Chen, *Angew. Chem. Int. Ed.* **2004**, *43*, 5513-5516.
- [71] J. Bayardon, J. Holz, B. Schöffner, V. Andrushko, S. Verevkin, A. Preetz, A. Börner, *Angew. Chem. Int. Ed.* **2007**, *46*, 5971-5974.
- [72] J. S. Mills, G. A. Showell, *Exp. Opin. Invest. Drugs* **2004**, *13*, 1149-1157.
- [73] a) W. D. V., J. E. Christian, *Can. J. Pharm. Sci.* **1979**, *14*, 12-14; b) R. Tacke, J. Pikies, H. Linoh, R. Rohr-Ähle, S. Gönne, *Liebigs Ann. Chem.* **1987**, *1*, 51-57.
- [74] a) R. J. Fessenden, J. S. Fessenden, *Adv. Drug Res.* **1967**, *4*, 95-132; b) S. M. Sieburth, C. N. Langevine, D. M. Dardaris, *Pestic. Sci.* **1990**, *28*, 309-319; c) S. M. Sieburth, C. J. Manly, D. W. Gammon, *Pestic. Sci.* **1990**, *28*, 289-307; d) M. w. Mutahi, T. Nittoli, L. Guo, S. M. Sieburth, *J. Am. Chem. Soc.* **2002**, *124*, 7363-7375; e) J. Wang, C. Ma, Y. Wu, R. A. Lamb, L. H. Pinto, W. F. DeGrado, *J. Am. Chem. Soc.* **2011**, *133*, 13844-13847; f) A. K. Franz, S. O. Wilson, *J. Med. Chem.* **2012**, *56*, 388-405; g) G. K. Min, T. Skrydstrup, *J. Org. Chem.* **2012**, *77*, 5894-5906.
- [75] S. M. Sieburth, C.-A. Chen, *Eur. J. Org. Chem.* **2006**, 311-322.
- [76] a) W. Bains, R. Tacke, *Curr. Opin. Drug Discovery Dev.* **2003**, *6*, 526-543; b) G. A. Showell, J. S. Mills, *Drug Discov. Today* **2003**, *8*, 551-556; c) P. K. Pooni, G. A. Showell, *Mini-Rev. Med. Chem.* **2006**, *6*, 1169-1177.

- [77] M. J. Barnes, R. Conroy, D. J. Miller, J. S. Mills, J. G. Montana, P. K. Pooni, G. A. Showell, L. M. Walsh, J. B. H. Warneck, *Bioorg. Med. Chem. Lett.* **2007**, *17*, 354-357.
- [78] S. M. Sieburth, T. Nittoli, A. M. Mutahi, L. Guo, *Angew. Chem. Int. Ed.* **1998**, *37*, 812-814.
- [79] Y. Bo, S. Singh, H. Q. Duong, C. Cao, S. M. Sieburth, *Org. Lett.* **2011**, *13*, 1787-1789.
- [80] a) Y. Matsumoto, T. Hayashi, Y. Ito, *Tetrahedron* **1994**, *50*, 335-346; b) T. Hayashi, Y. Matsumoto, Y. Ito, *J. Am. Chem. Soc.* **1988**, *110*, 5579-5581; c) R. Shintani, K. Okamoto, T. Hayashi, *Org. Lett.* **2005**, *7*, 4757-4759; d) C. Walter, G. Auer, M. Oestreich, *Angew. Chem. Int. Ed.* **2006**, *45*, 5675-5677; e) C. Walter, M. Oestreich, *Angew. Chem. Int. Ed.* **2008**, *47*, 3818-3820; f) J. M. O'Brien, A. H. Hoveyda, *J. Am. Chem. Soc.* **2011**, *133*, 7712-7715; g) M. A. Kacprzynski, S. A. Kazane, T. L. May, A. H. Hoveyda, *Org. Lett.* **2007**, *9*, 3187-3190; h) K.-s. Lee, A. H. Hoveyda, *J. Am. Chem. Soc.* **2010**, *132*, 2898-2900; i) K.-s. Lee, H. Wu, F. Haeffner, A. H. Hoveyda, *Organometallics* **2012**, *31*, 7823-7826; j) V. Pace, J. P. Rae, H. Y. Harb, D. J. Procter, *Chem. Commun.* **2013**, *49*, 5150-5152; k) M. A. Kacprzynski, T. L. May, S. A. Kazane, A. H. Hoveyda, *Angew. Chem. Int. Ed.* **2007**, *46*, 4554-4558; l) Y. Shido, M. Yoshida, M. Tanabe, H. Ohmiya, M. Sawamura, *J. Am. Chem. Soc.* **2012**, *134*, 18573-18576; m) L. B. Delvos, D. J. Vyas, M. Oestreich, *Angew. Chem. Int. Ed.* **2013**, *52*, 4650-4653; n) M. Takeda, R. Shintani, T. Hayashi, *J. Org. Chem.* **2013**, *78*, 5007-5017; o) Y. Uozumi, T. Hayashi, *J. Am. Chem. Soc.* **1991**, *113*, 9887-9888; p) T. Ohmura, H. Taniguchi, M. Sugimoto, *J. Am. Chem. Soc.* **2006**, *128*, 13682-13683; q) B. H. Lipshutz, N. Tanaka, B. R. Taft, C.-T. Lee, *Org. Lett.* **2006**, *8*, 1963-1966; r) K. Källström, I. J. Munslow, C. Hedberg, P. G. Andersson, *Adv. Synth. Catal.* **2006**, *348*, 2575-2578; s) V. Cirriez, C. Rasson, T. Hermant, J. Petrignet, J. Díaz Álvarez, K. Robeyns, O. Riant, *Angew. Chem. Int. Ed.* **2013**, *52*, 1785-1788.
- [81] a) I. Fleming, R. Henning, D. C. Parker, H. E. Plaut, P. E. J. Sanderson, *J. Chem. Soc., Perkin Trans. 1* **1995**, 317-337; b) G. R. Jones, Y. Landais, *Tetrahedron* **1996**, *52*, 7599-7662; c) K. Itami, K. Mitsudo, J.-i. Yoshida, *J. Org. Chem.* **1999**, *64*, 8709-8714.
- [82] T. Naito, T. Yoneda, J.-i. Ito, H. Nishiyama, *Synlett* **2012**, *23*, 2957-2960.
- [83] A. Wang, unpublished results, University of Basel, **2009**.
- [84] N. Chatani, N. Amishiro, T. Morii, T. Yamashita, S. Murai, *J. Org. Chem.* **1995**, *60*, 1834-1840.
- [85] K. Miura, S. Okajima, T. Hondo, T. Nakagawa, T. Takahashi, A. Hosomi, *J. Am. Chem. Soc.* **2000**, *122*, 11348-11357.
- [86] D. C. Chauret, J. M. Chong, Q. Ye, *Tetrahedron: Asymmetry* **1999**, *10*, 3601-3614.
- [87] I. Fleming, M. Taddei, *Synthesis* **1985**, 899-900.
- [88] P. Wang, X.-L. Yeo, T.-P. Loh, *J. Am. Chem. Soc.* **2011**, *133*, 1254-1256.
- [89] a) R. H. Shapiro, M. J. Heath, *J. Am. Chem. Soc.* **1967**, *89*, 5734-5735; b) R. H. Shapiro, M. F. Lipton, K. J. Kolonko, R. L. Buswell, L. A. Capuano, *Tetrahedron Lett.* **1975**, *16*, 1811-1814.
- [90] T. H. Chan, A. Baldassarre, D. Massuda, *Synthesis* **1976**, 801-803.
- [91] M. Sugimoto, H. Nakamura, Y. Ito, *Chem. Commun.* **1996**, 2777-2778.
- [92] a) T. H. Chan, P. Pellon, *J. Am. Chem. Soc.* **1989**, *111*, 8737-8738; b) F. L. v. Delft, G. A. v. d. Marel, J. H. v. Boom, *Synlett* **1995**, 1069-1070; c) Y. Landais, D. Planchenault, V. Weber, *Tetrahedron Lett.* **1995**, *36*, 2987-2990.

- [93] H. Matsubashi, S. Asai, K. Hirabayashi, Y. Hatanaka, A. Mori, T. Hiyama, *Bull. Chem. Soc. Jpn.* **1997**, *70*, 437-444.
- [94] B. M. Trost, Z. T. Ball, *J. Am. Chem. Soc.* **2005**, *127*, 17644-17655.
- [95] a) A. G. Myers, S. E. Kephart, H. Chen, *J. Am. Chem. Soc.* **1992**, *114*, 7922-7923; b) K. Matsumoto, K. Oshima, K. Utimoto, *J. Org. Chem.* **1994**, *59*, 7152-7155; c) S. E. Denmark, B. D. Griedel, D. M. Coe, M. E. Schnute, *J. Am. Chem. Soc.* **1994**, *116*, 7026-7043.
- [96] J. D. Sunderhaus, H. Lam, G. B. Dudley, *Org. Lett.* **2003**, *5*, 4571-4573.
- [97] T. Sanada, T. Kato, M. Mitani, A. Mori, *Adv. Synth. Catal.* **2006**, *348*, 51-54.
- [98] J. Boyer, C. Breliere, F. Carre, R. J. P. Corriu, A. Kpoton, M. Poirier, G. Royo, J. C. Young, *J. Chem. Soc., Dalton Trans.* **1989**, 43-51.
- [99] a) M. C. Fournie-Zaluski, A. Coulaud, R. Bouboutou, P. Chaillet, J. Devin, G. Waksman, J. Costentin, B. P. Roques, *J. Med. Chem.* **1985**, *28*, 1158-1169; b) W. M. Moore, C. A. Spilburg, *Biochemistry* **1986**, *25*, 5189-5195; c) P. Buehlmayer, A. Caselli, W. Fuhrer, R. Goeschke, V. Rasetti, H. Rueger, J. L. Stanton, L. Criscione, J. M. Wood, *J. Med. Chem.* **1988**, *31*, 1839-1846; d) H. Harada, T. Yamaguchi, A. Iyobe, A. Tsubaki, T. Kamijo, K. Iizuka, K. Ogura, Y. Kiso, *J. Org. Chem.* **1990**, *55*, 1679-1682; e) H. Heitsch, R. Henning, H. W. Kleemann, W. Linz, W. U. Nickel, D. Ruppert, H. Urbach, A. Wagner, *J. Med. Chem.* **1993**, *36*, 2788-2800; f) M. Whittaker, C. D. Floyd, P. Brown, A. J. H. Gearing, *Chem. Rev.* **1999**, *99*, 2735-2776; g) V. Marcq, C. Mirand, M. Decarme, H. Emonard, W. Hornebeck, *Bioorg. Med. Chem. Lett.* **2003**, *13*, 2843-2846; h) G. Moroy, C. Denhez, H. El Mourabit, A. Toribio, A. Dassonville, M. Decarme, J.-H. Renault, C. Mirand, G. Bellon, J. Sapi, A. J. P. Alix, W. Hornebeck, E. Bourguet, *Bioorg. Med. Chem.* **2007**, *15*, 4753-4766.
- [100] a) H. Huang, Z. Zheng, H. Luo, C. Bai, X. Hu, H. Chen, *Org. Lett.* **2003**, *5*, 4137-4139; b) H. Fernández-Pérez, P. Etayo, A. Panossian, A. Vidal-Ferran, *Chem. Rev.* **2011**, *111*, 2119-2176; c) S. Song, S.-F. Zhu, Y. Li, Q.-L. Zhou, *Org. Lett.* **2013**, *15*, 3722-3725.
- [101] T. Ohta, T. Miyake, N. Seido, H. Kumobayashi, H. Takaya, *J. Org. Chem.* **1995**, *60*, 357-363.
- [102] M. J. Alcón, M. Iglesias, F. Sánchez, I. Viani, *J. Organomet. Chem.* **2001**, *634*, 25-33.
- [103] K. Shimoda, N. Kubota, *Tetrahedron: Asymmetry* **2004**, *15*, 3827-3829.
- [104] a) M. J. Burk, F. Bienewald, M. Harris, A. Zanotti-Gerosa, *Angew. Chem. Int. Ed.* **1998**, *37*, 1931-1933; b) D. Carmichael, H. Doucet, J. M. Brown, *Chem. Commun.* **1999**, 261-262; c) W. Tang, D. Liu, X. Zhang, *Org. Lett.* **2002**, *5*, 205-207; d) J. Almena, A. Monsees, R. Kadyrov, T. H. Riermeier, B. Gotov, J. Holz, A. Börner, *Adv. Synth. Catal.* **2004**, *346*, 1263-1266.
- [105] a) T. Ireland, G. Grossheimann, C. Wieser-Jeunesse, P. Knochel, *Angew. Chem. Int. Ed.* **1999**, *38*, 3212-3215; b) U. Berens, M. J. Burk, A. Gerlach, W. Hems, *Angew. Chem. Int. Ed.* **2000**, *39*, 1981-1984; c) Y. Liu, C. A. Sandoval, Y. Yamaguchi, X. Zhang, Z. Wang, K. Kato, K. Ding, *J. Am. Chem. Soc.* **2006**, *128*, 14212-14213.
- [106] Y. Chen, L. Deng, *J. Am. Chem. Soc.* **2001**, *123*, 11302-11303.
- [107] C.-C. Wang, W.-D. Z. Li, *J. Org. Chem.* **2012**, *77*, 4217-4225.
- [108] R. Liffert, student's report, University of Basel **2012**.
- [109] a) F. Neve, M. Ghedini, G. De Munno, A. Crispini, *Organometallics* **1991**, *10*, 1143-1148; b) M.-S. Eum, C. S. Chin, S. y. Kim, C. Kim, S. K. Kang, N. H. Hur, J. H. Seo, G. Y. Kim, Y. K. Kim, *Inorg. Chem.* **2008**, *47*, 6289-6295; c) P. Alam, M. Karanam, A.

- Roy Choudhury, I. Rahaman Laskar, *Dalton Trans.* **2012**, 41, 9276-9279; d) A. Schumacher, Ph.D thesis, University of Basel **2012**.
- [110] V. N. Kovalenko, O. G. Kulinkovich, *Tetrahedron: Asymmetry* **2011**, 22, 26-30.
- [111] a) R. Ballini, G. Bosica, D. Fiorini, P. Righi, *Synthesis* **2002**, 681-685; b) F. Manoni, C. Cornaggia, J. Murray, S. Tallon, S. J. Connon, *Chem. Commun.* **2012**, 48, 6502-6504.
- [112] P. L. Beaulieu, D. Wernic, Abraham, P. C. Anderson, T. Bogri, Y. Bousquet, G. Croteau, I. Guse, D. Lamarre, F. Liard, W. Paris, D. Thibeault, S. Pav, L. Tong, *J. Med. Chem.* **1997**, 40, 2164-2176.
- [113] a) R. E. Gawley, D. B. Eddings, M. Santiago, D. A. Vicic, *Org. Biomol. Chem.* **2006**, 4, 4285-4291; b) Y. Liu, W. Zhang, *Angew. Chem. Int. Ed.* **2013**, 52, 2203-2206.
- [114] a) H. Yoda, H. Kitayama, T. Katagiri, K. Takabe, *Tetrahedron* **1992**, 48, 3313-3322; b) H. Tomori, K. Shibutani, K. Ogura, *Bull. Chem. Soc. Jpn.* **1996**, 69, 207-215; c) S. Louwrier, M. Ostendorf, A. Boom, H. Hiemstra, W. Nico Speckamp, *Tetrahedron* **1996**, 52, 2603-2628.
- [115] M. Ostermeier, B. Brunner, C. Korff, G. Helmchen, *Eur. J. Org. Chem.* **2003**, 2003, 3453-3459.
- [116] a) I. Yamada, M. Yamaguchi, T. Yamagishi, *Tetrahedron: Asymmetry* **1996**, 7, 3339-3342; b) A. Scrivanti, S. Bovo, A. Ciappa, U. Matteoli, *Tetrahedron Lett.* **2006**, 47, 9261-9265; c) S.-F. Zhu, Y.-B. Yu, S. Li, L.-X. Wang, Q.-L. Zhou, *Angew. Chem. Int. Ed.* **2012**, 51, 8872-8875.
- [117] a) M. J. Burk, G. Casy, N. B. Johnson, *J. Org. Chem.* **1998**, 63, 6084-6085; b) R. Kuwano, K. Sato, T. Kurokawa, D. Karube, Y. Ito, *J. Am. Chem. Soc.* **2000**, 122, 7614-7615; c) I. D. Gridnev, M. Yasutake, N. Higashi, T. Imamoto, *J. Am. Chem. Soc.* **2001**, 123, 5268-5276; d) W. Tang, X. Zhang, *Angew. Chem. Int. Ed.* **2002**, 41, 1612-1614.
- [118] a) X. Cheng, Q. Zhang, J.-H. Xie, L.-X. Wang, Q.-L. Zhou, *Angew. Chem. Int. Ed.* **2005**, 44, 1118-1121; b) X. Cheng, J.-H. Xie, S. Li, Q.-L. Zhou, *Adv. Synth. Catal.* **2006**, 348, 1271-1276.
- [119] D. H. Woodmansee, M.-A. Müller, L. Tröndlin, E. Hörmann, A. Pfaltz, *Chem. Eur. J.* **2012**, 18, 13780-13786.
- [120] a) M. J. Fehr, G. Consiglio, M. Scalone, R. Schmid, *J. Org. Chem.* **1999**, 64, 5768-5776; b) D. A. Dobbs, K. P. M. Vanhessche, E. Brazi, V. Rautenstrauch, J.-Y. Lenoir, J.-P. Genêt, J. Wiles, S. H. Bergens, *Angew. Chem. Int. Ed.* **2000**, 39, 1992-1995; c) S.-M. Lu, C. Bolm, *Chem. Eur. J.* **2008**, 14, 7513-7516.
- [121] T. Ohkuma, R. Noyori in *Transition Metals for Organic Synthesis*, Wiley-VCH, Weinheim (Germany), **2004**, pp. 29-113.
- [122] K. Mashima, T. Akutagawa, X. Zhang, H. Takaya, T. Taketomi, H. Kumobayashi, S. Akutagawa, *J. Organomet. Chem.* **1992**, 428, 213-222.
- [123] a) T. Ohkuma, H. Ooka, T. Ikariya, R. Noyori, *J. Am. Chem. Soc.* **1995**, 117, 10417-10418; b) T. Ohkuma, H. Ikehira, T. Ikariya, R. Noyori, *Synlett* **1997**, 467-468; c) T. Ohkuma, M. Koizumi, H. Doucet, T. Pham, M. Kozawa, K. Murata, E. Katayama, T. Yokozawa, T. Ikariya, R. Noyori, *J. Am. Chem. Soc.* **1998**, 120, 13529-13530.
- [124] a) J. Teddy, A. Falqui, A. Corrias, D. Carta, P. Lecante, I. Gerber, P. Serp, *J. Catal.* **2011**, 278, 59-70; b) Y.-C. Hong, K.-Q. Sun, G.-R. Zhang, R.-Y. Zhong, B.-Q. Xu, *Chem. Commun.* **2011**, 47, 1300-1302.
- [125] a) J. W. Yang, M. T. Hechavarria Fonseca, B. List, *Angew. Chem. Int. Ed.* **2004**, 43, 6660-6662; b) S. G. Ouellet, J. B. Tuttle, D. W. C. MacMillan, *J. Am. Chem. Soc.* **2004**, 127, 32-33; c) J. W. Yang, M. T. Hechavarria Fonseca, N. Vignola, B. List, *Angew.*

- Chem. Int. Ed.* **2005**, *44*, 108-110; d) N. J. A. Martin, B. List, *J. Am. Chem. Soc.* **2006**, *128*, 13368-13369; e) J. B. Tuttle, S. G. Ouellet, D. W. C. MacMillan, *J. Am. Chem. Soc.* **2006**, *128*, 12662-12663; f) K. Akagawa, H. Akabane, S. Sakamoto, K. Kudo, *Org. Lett.* **2008**, *10*, 2035-2037; g) T. J. Hoffman, J. Dash, J. H. Rigby, S. Arseniyadis, J. Cossy, *Org. Lett.* **2009**, *11*, 2756-2759; h) C. Ebner, A. Pfaltz, *Tetrahedron* **2011**, *67*, 10287-10290.
- [126] T. Ohta, H. Takaya, M. Kitamura, K. Nagai, R. Noyori, *J. Org. Chem.* **1987**, *52*, 3174-3176.
- [127] L. A. Saudan, *Acc. Chem. Res.* **2007**, *40*, 1309-1319.
- [128] a) P. Bissel, R. Sablong, J.-P. Lepoittevin, *Tetrahedron: Asymmetry* **1995**, *6*, 835-838; b) P. Bissel, A. Nazih, R. Sablong, J.-P. Lepoittevin, *Org. Lett.* **1999**, *1*, 1283-1285.
- [129] J. F. Hartwig in *Organotransition Metal Chemistry: From Bonding to Catalysis*, University Science Books, Sausalito, California, **2010**, pp. 967-1014.
- [130] J.-X. Ji, A. S. C. Chan, in *Catalytic Asymmetric Synthesis, 3rd Edition* (Ed.: I. Ojima), John Wiley & Sons, Inc., **2010**, pp. 437-496.
- [131] a) L. Mantilli, D. Gérard, S. Torche, C. Besnard, C. Mazet, *Angew. Chem. Int. Ed.* **2009**, *48*, 5143-5147; b) L. Mantilli, C. Mazet, *Tetrahedron Lett.* **2009**, *50*, 4141-4144; c) L. Mantilli, D. Gérard, S. Torche, C. Besnard, C. Mazet, *Chem. Eur. J.* **2010**, *16*, 12736-12745; d) L. Mantilli, C. Mazet, *Chem. Commun.* **2010**, *46*, 445-447; e) A. Quintard, A. Alexakis, C. Mazet, *Angew. Chem. Int. Ed.* **2011**, *50*, 2354-2358.
- [132] S. Khumsubdee, K. Burgess, *ACS Catalysis* **2013**, *3*, 237-249.
- [133] A. J. Mancuso, S.-L. Huang, D. Swern, *J. Org. Chem.* **1978**, *43*, 2480-2482.
- [134] J. H. Seo, P. Liu, S. M. Weinreb, *J. Org. Chem.* **2010**, *75*, 2667-2680.
- [135] M. G. Schrems, E. Neumann, A. Pfaltz, *Heterocycles* **2008**, *76*, 771-781.
- [136] B. Zupančič, B. Mohar, M. Stephan, *Adv. Synth. Catal.* **2008**, *350*, 2024-2032.
- [137] M. Diéguez, O. Pàmies, C. Claver, in *Iridium Catalysis* (Ed.: P. G. Andersson), Springer Verlag, Heidelberg, **2011**, pp. 11-29.
- [138] V. Ramella, Master thesis, University of Basel **2012**.
- [139] P. Tosatti, University of Basel, **2012**.
- [140] a) Z. Du, G. Yue, Junying, X. She, T. Wu, X. Pan, *J. Chem. Res.* **2004**, 427-429; b) P. P. Mahulikar, R. B. Mane, *J. Chem. Res.* **2006**, 15-18; c) M. Harmata, X. Hong, P. R. Schreiner, *J. Org. Chem.* **2008**, *73*, 1290-1296.
- [141] J. R. Parikh, W. v. E. Doering, *J. Am. Chem. Soc.* **1967**, *89*, 5505-5507.
- [142] a) S. Sarel, J. Yovell, M. Sarel-Imber, *Angew. Chem. Int. Ed. Engl.* **1968**, *7*, 577-588; b) H. N. C. Wong, M. Y. Hon, C. W. Tse, Y. C. Yip, J. Tanko, T. Hudlicky, *Chem. Rev.* **1989**, *89*, 165-198.
- [143] D. Marcoux, S. b. R. Goudreau, A. B. Charette, *J. Org. Chem.* **2009**, *74*, 8939-8955.
- [144] a) A. Corma, S. Iborra, A. Velty, *Chem. Rev.* **2007**, *107*, 2411-2502; b) R. Palkovits, *Angew. Chem. Int. Ed.* **2010**, *49*, 4336-4338.
- [145] D. F. Aycok, *Org. Process Res. Dev.* **2006**, *11*, 156-159.
- [146] S. Díez-González, N. Marion, S. P. Nolan, *Chem. Rev.* **2009**, *109*, 3612-3676.
- [147] a) A. J. Arduengo, R. L. Harlow, M. Kline, *J. Am. Chem. Soc.* **1991**, *113*, 361-363; b) C. D. Abernethy, J. A. C. Clyburne, A. H. Cowley, R. A. Jones, *J. Am. Chem. Soc.* **1999**, *121*, 2329-2330; c) T. Weskamp, V. P. W. Böhm, W. A. Herrmann, *J. Organomet. Chem.* **2000**, *600*, 12-22.

- [148] a) W. A. Herrmann, C. Köcher, *Angew. Chem. Int. Ed. Engl.* **1997**, *36*, 2162-2187; b) W. A. Herrmann, *Angew. Chem. Int. Ed.* **2002**, *41*, 1290-1309.
- [149] a) N. Marion, S. Díez-González, S. P. Nolan, *Angew. Chem. Int. Ed.* **2007**, *46*, 2988-3000; b) D. Enders, O. Niemeier, A. Henseler, *Chem. Rev.* **2007**, *107*, 5606-5655.
- [150] C. Samojłowicz, M. Bieniek, K. Grela, *Chem. Rev.* **2009**, *109*, 3708-3742.
- [151] E. A. B. Kantchev, C. J. O'Brien, M. G. Organ, *Angew. Chem. Int. Ed.* **2007**, *46*, 2768-2813.
- [152] a) Z. Xi, B. Liu, W. Chen, *J. Org. Chem.* **2008**, *73*, 3954-3957; b) Z. Xi, Y. Zhou, W. Chen, *J. Org. Chem.* **2008**, *73*, 8497-8501; c) J. Berding, M. Lutz, A. L. Spek, E. Bouwman, *Organometallics* **2009**, *28*, 1845-1854.
- [153] a) J. Haider, K. Kunz, U. Scholz, *Adv. Synth. Catal.* **2004**, *346*, 717-722; b) C. Tubaro, A. Biffis, E. Scattolin, M. Basato, *Tetrahedron* **2008**, *64*, 4187-4195.
- [154] a) R. B. Bedford, M. Betham, D. W. Bruce, A. A. Danopoulos, R. M. Frost, M. Hird, *J. Org. Chem.* **2005**, *71*, 1104-1110; b) T. Hatakeyama, M. Nakamura, *J. Am. Chem. Soc.* **2007**, *129*, 9844-9845.
- [155] a) S. E. Gibson, C. Johnstone, J. A. Loch, J. W. Steed, A. Stevenazzi, *Organometallics* **2003**, *22*, 5374-5377; b) P. A. Evans, E. W. Baum, A. N. Fazal, M. Pink, *Chem. Commun.* **2005**, 63-65; c) A. Geny, S. Gaudrel, F. Slowinski, M. Amatore, G. Chouraqui, M. Malacria, C. Aubert, V. Gandon, *Adv. Synth. Catal.* **2009**, *351*, 271-275.
- [156] a) J. Louie, J. E. Gibby, M. V. Farnworth, T. N. Tekavec, *J. Am. Chem. Soc.* **2002**, *124*, 15188-15189; b) M. M. McCormick, H. A. Duong, G. Zuo, J. Louie, *J. Am. Chem. Soc.* **2005**, *127*, 5030-5031; c) S. Díez-González, A. Correa, L. Cavallo, S. P. Nolan, *Chem. Eur. J.* **2006**, *12*, 7558-7564; d) T. N. Tekavec, J. Louie, *J. Org. Chem.* **2008**, *73*, 2641-2648; e) S. Díez-González, S. P. Nolan, *Angew. Chem. Int. Ed.* **2008**, *47*, 8881-8884.
- [157] a) S. López, E. Herrero-Gómez, P. Pérez-Galán, C. Nieto-Oberhuber, A. M. Echavarren, *Angew. Chem. Int. Ed.* **2006**, *45*, 6029-6032; b) C. Mukai, R. Itoh, *Tetrahedron Lett.* **2006**, *47*, 3971-3974; c) Y.-J. Song, I. G. Jung, H. Lee, Y. T. Lee, Y. K. Chung, H.-Y. Jang, *Tetrahedron Lett.* **2007**, *48*, 6142-6146; d) G. Zhang, X. Huang, G. Li, L. Zhang, *J. Am. Chem. Soc.* **2008**, *130*, 1814-1815.
- [158] S. Díez-González, S. P. Nolan, *Org. Prep. Proc. Int.* **2007**, *39*, 523-559.
- [159] a) A. Prades, M. n. Viciano, M. Sanaú, E. Peris, *Organometallics* **2008**, *27*, 4254-4259; b) S. Liu, M. Rebros, G. Stephens, A. C. Marr, *Chem. Commun.* **2009**, 2308-2310.
- [160] D. Addis, S. Enthaler, K. Junge, B. Wendt, M. Beller, *Tetrahedron Lett.* **2009**, *50*, 3654-3656.
- [161] a) T. Strassner, *Top. Organomet. Chem.* **2004**, *13*, 1-20; b) S. Díez-González, S. P. Nolan, *Coord. Chem. Rev.* **2007**, *251*, 874-883.
- [162] a) H. Jacobsen, A. Correa, A. Poater, C. Costabile, L. Cavallo, *Coord. Chem. Rev.* **2009**, *253*, 687-703; b) U. Radius, F. M. Bickelhaupt, *Coord. Chem. Rev.* **2009**, *253*, 678-686.
- [163] a) T. Focken, G. Raabe, C. Bolm, *Tetrahedron: Asymmetry* **2004**, *15*, 1693-1706; b) D. Baskakov, W. A. Herrmann, E. Herdtweck, S. D. Hoffmann, *Organometallics* **2006**, *26*, 626-632; c) C. Metallinos, X. Du, *Organometallics* **2009**, *28*, 1233-1242.
- [164] S. Nanchen, A. Pfaltz, *Helv. Chim. Acta* **2006**, *89*, 1559-1573.
- [165] a) X. Cui, K. Burgess, *J. Am. Chem. Soc.* **2003**, *125*, 14212-14213; b) J. Zhou, Y. Zhu, K. Burgess, *Org. Lett.* **2007**, *9*, 1391-1393; c) J. Zhou, K. Burgess, *Angew. Chem. Int.*

-
- Ed. **2007**, 46, 1129-1131; d) J. Zhou, J. W. Ogle, Y. Fan, V. Banphavichit, Y. Zhu, K. Burgess, *Chem. Eur. J.* **2007**, 13, 7162-7170; e) Y. Zhu, K. Burgess, *J. Am. Chem. Soc.* **2008**, 130, 8894-8895; f) J. Zhao, K. Burgess, *Org. Lett.* **2009**, 11, 2053-2056.
- [166] a) S. Bell, B. Wüstenberg, S. Kaiser, F. Menges, T. Netscher, A. Pfaltz, *Science* **2006**, 311, 642-644; b) A. Wang, B. Wüstenberg, A. Pfaltz, *Angew. Chem. Int. Ed.* **2008**, 47, 2298-2300; c) A. Wang, R. P. A. Fraga, E. Hörmann, A. Pfaltz, *Chem. Asian J.* **2011**, 6, 599-606.
- [167] A. Schumacher, M. Bernasconi, A. Pfaltz, *Angew. Chem. Int. Ed.* **2013**, 52, 7422-7425.
- [168] J. Uenishi, M. Hamada, *Synthesis* **2002**, 625-630.
- [169] A. Furstner, M. Alcarazo, V. Cesar, C. W. Lehmann, *Chem. Commun.* **2006**, 2176-2178.
- [170] a) M. C. Perry, X. Cui, M. T. Powell, D.-R. Hou, J. H. Reibenspies, K. Burgess, *J. Am. Chem. Soc.* **2003**, 125, 113-123; b) M. C. Perry, K. Burgess, *Tetrahedron: Asymmetry* **2003**, 14, 951-961.
- [171] T. W. Green, P. G. M. Wuts, *Protective Groups in Organic Synthesis*, Wiley-Interscience, New York, **1999**.
- [172] T. Kikui, H. Maeda, Y. Nakatsuji, M. Okahara, *Synthesis* **1984**, 74-76.
- [173] G. Bartoli, M. Bosco, A. Carlone, R. Dalpozzo, M. Locatelli, P. Melchiorre, P. Palazzi, L. Sambri, *Synlett* **2006**, 2104-2108.
- [174] A. B. Pangborn, M. A. Giardello, R. H. Grubbs, R. K. Rosen, F. J. Timmers, *Organometallics* **1996**, 15, 1518-1520.
- [175] W. C. Still, M. Kahn, A. Mitra, *J. Org. Chem.* **1978**, 43, 2923-2925.
- [176] S. S. P. Chou, H. L. Kuo, C. J. Wang, C. Y. Tsai, C. M. Sun, *J. Org. Chem.* **1989**, 54, 868-872.
- [177] C. T. Clark, B. C. Milgram, K. A. Scheidt, *Org. Lett.* **2004**, 6, 3977-3980.
- [178] J. T. Lowe, J. S. Panek, *Org. Lett.* **2005**, 7, 3231-3234.
- [179] C. Spino, C. Gobdout, *J. Am. Chem. Soc.* **2003**, 125, 12106-12107.
- [180] S. Celebi, S. Leyva, D. A. Modarelli, M. S. Platz, *J. Am. Chem. Soc.* **1993**, 115, 8613-8620.
- [181] A. Chénédé, I. Fleming, R. Salmon, M. C. West, *J. Organomet. Chem.* **2003**, 686, 84-93.
- [182] N. Iwadate, M. Suginome, *J. Am. Chem. Soc.* **2010**, 132, 2548-2549.
- [183] B. M. Trost, Z. T. Ball, *J. Am. Chem. Soc.* **2001**, 123, 12726-12727.
- [184] K. Yamamoto, T. Hayashi, M. Zembayashi, M. Kumada, *J. Organomet. Chem.* **1976**, 118, 161-181.
- [185] J. Dambacher, M. Bergdahl, *J. Org. Chem.* **2004**, 70, 580-589.
- [186] G. A. Russel, D. Guo, W. Baik, S. J. Herron, *Heterocycles* **1989**, 28, 143-146.
- [187] T. Funabiki, A. Mizoguchi, T. Sugimoto, S. Tada, T. Mitsui, H. Sakamoto, S. Yoshida, *J. Am. Chem. Soc.* **1986**, 108, 2921-2932.
- [188] R. A. Doohan, J. J. Hannan, N. W. A. Geraghty, *Org. Biomol. Chem.* **2006**, 4, 942-952.
- [189] R. P. Herrera, D. Monge, E. Martín-Zamora, R. Fernández, J. M. Lassaletta, *Org. Lett.* **2007**, 9, 3303-3306.
- [190] H. Zeng, R. Hua, *J. Org. Chem.* **2008**, 73, 558-562.
- [191] C. H. R. King, C. D. Poulter, *J. Am. Chem. Soc.* **1982**, 104, 1413-1420.
- [192] D. E. James, J. K. Stille, *J. Org. Chem.* **1976**, 41, 1504-1511.

-
- [193] S. Protti, D. Ravelli, M. Fagnoni, A. Albini, *Chem. Commun.* **2009**, 7351-7353.
- [194] Y.-X. Gao, L. Chang, H. Shi, B. Liang, K. Wongkhan, D. Chaiyaveij, A. S. Batsanov, T. B. Marder, C.-C. Li, Z. Yang, Y. Huang, *Adv. Synth. Catal.* **2010**, 352, 1955-1966.
- [195] L. Jalander, M. Boms, *Acta Chem. Scand.* **1983**, B 37, 173-178.
- [196] L. H. Amundsen, L. S. Nelson, *J. Am. Chem. Soc.* **1951**, 73, 242-244.
- [197] W. Carruthers, N. Evans, R. Pooranamoorthy, *J. Chem. Soc., Perkin Trans. 1* **1975**, 76-79.
- [198] K. Tanaka, S. Qiao, M. Tobisu, M. M. C. Lo, G. C. Fu, *J. Am. Chem. Soc.* **2000**, 122, 9870-9871.
- [199] A. D. Fotiadou, A. L. Zografos, *Org. Lett.* **2012**, 14, 5664-5667.
- [200] G. Fronza, C. Fuganti, S. Serra, *Eur. J. Org. Chem.* **2009**, 6160-6171.
- [201] X. Cao, F. Liu, W. Lu, G. Chen, G.-A. Yu, S. H. Liu, *Tetrahedron* **2008**, 64, 5629-5636.
- [202] M. Murakami, H. Amii, K. Shigeto, Y. Ito, *J. Am. Chem. Soc.* **1996**, 118, 8285-8290.

Maurizio Bernasconi

Landskronstrasse 95, 4056 Basel, Switzerland • Tel.: + 41 (0)79 221 40 59

email: bernasconi.mauri@gmail.com • Date of Birth: 19 October 1985

Nationality: Swiss • Marital status: Married

Employment

Oct 2009 – Dec 2013: PhD research fellow in organic chemistry – University of Basel

PhD Advisor: Prof. A. Pfaltz; PhD Project: New Substrate Classes in Iridium-Catalyzed Asymmetric Hydrogenation

June 2009 – Sept 2009: Internship 100% in the Medicinal Chemistry laboratories (R&D) at F. Hoffmann-La Roche (Basel)

Responsible for the synthesis of new drug candidates in the team led by Dr. Alexander Mayweg

Education

Chemistry studies:

Oct 2007 – May 2009: Master of Science in Chemistry – Eidgenössische Technische Hochschule (ETHZ, Zürich)

Oct 2004 – Sept 2007: Bachelor of Science in Chemistry – Eidgenössische Technische Hochschule (ETHZ, Zürich)

International working experience:

Sept 2008 – Mar 2009: Master Thesis – University of California, Berkeley (Berkeley, CA, USA)

Supervisor: Prof. F. Dean Toste; Master Thesis: Asymmetric gold(I) catalyzed formal [3+2] cycloaddition of propargyl acetyl/ketals with aldehydes

Finance studies:

Jan 2011 – present: 2nd level CFA Candidate – Charlottesville (USA)/Zürich (Switzerland)

Oct 2011 – Feb 2012: Finance courses – University of Basel

Attended and passed the examination for the following finance lectures
"Strategische Unternehmensführung" and "Venture challenge "

Project management

Jan 2011 – Sept 2012: Supervisor and mentor of 3 Master students (Vincenzo Ramella, Annina Wehrle, Baptiste Barré) (**University of Basel**)

Award

SCNAT/SCS Chemistry Travel Award 2013 to present at the 17th OMCOS Conference in Fort Collins, CO, USA

Other Skills

Languages: Italian (native), English (fluent), German (fluent), French (intermediate)

IT: Highly proficient in Microsoft Office and several chemistry software programs including ChemDraw, SciFinder, and MestreNova

Publications

G. Wuitschik, M. Rogers-Evans, A. Buckl, **M. Bernasconi**, M. Märki, T. Godel, H. Fischer, B. Wagner, I. Parrilla, F. Schuler, J. Schneider, A. Alker, W. B. Schweizer, K. Müller and E. M. Carreira, "Spirocyclic Oxetanes: Synthesis and Properties" *Angew. Chem. Int. Ed.* **2008**, 47, 4512–4515

A. Schumacher, **M. Bernasconi** and A. Pfaltz, "Chiral N-Heterocyclic Carbene-Pyridine Ligands for the Iridium-Catalyzed Asymmetric Hydrogenation of Olefins" *Angew. Chem. Int. Ed.* **2013**, 52, 7422–7425

M. Bernasconi, V. Ramella, P. Tosatti and A. Pfaltz "Iridium-Catalyzed Asymmetric Hydrogenation of 3,3-Disubstituted Allylic Alcohols in Etheral Solvents" *Chem. Eur. J.* **2014**, accepted manuscript

F. Schmid, **M. Bernasconi**, H. J. Jessen, A. Pfaltz and K. Gademann, "Catalytic Enantioselective Total Synthesis of Pyridovericin" submitted manuscript

M. Bernasconi, M.-A. Müller and A. Pfaltz "Asymmetric Hydrogenation of Maleic Acid Diesters and Anhydrides" manuscript in preparation

Interests

Playing soccer, skiing, travelling, dancing salsa